Investigating the role of central nutrient-sensing neurones using adeno-associated viral manipulation of glucokinase

Thesis submitted for the degree of Doctor of Philosophy at Imperial College London
2011

Errol Richardson

Department of Diabetes, Endocrinology and Metabolism
Faculty of Medicine
Imperial College London

For

Emma

Abstract

The primary aim of the work described in this thesis was to investigate the physiological role of glucose sensing neurones within the arcuate nucleus of the hypothalamus (ARC). To this end, recombinant adeno-associated virus encoding glucokinase (rAAV-GKS) was delivered to the ARC of adult male Wistar rats. Glucokinase (GK) catalyses the first reaction in glycolysis and has been hypothesised to act as a regulator of hypothalamic glucose sensing. Furthermore, manipulation of GK has been shown to alter the sensitivity of glucose sensing neurones *in vitro*. I hypothesised that increasing GK expression in the ARC using rAAV-GKS would influence the sensitivity of glucose sensing neurones *in vivo* and provide insight into their physiological role.

Bilateral administration of rAAV-GKS to the ARC resulted in a 14-fold increase in hypothalamic GK mRNA expression compared to controls. Food intake and body weight gain were significantly increased in rAAV-GKS treated rats compared to controls on standard chow. The increased body weight of the rAAV-GKS group was attributed to a significant increase in adipose tissue with no difference in lean mass. Food intake and body weight gain were also significantly increased in rAAV-GKS treated animals maintained on a high calorie "western-style" diet.

Despite their increased adiposity, rAAV-GKS treated rats displayed significantly improved glucose tolerance compared to controls. The increased glucose tolerance of the rAAV-GKS group was associated with increased glucose-stimulated insulin secretion.

rAAV-GKS treated rats consumed a significantly greater volume of a 10% glucose solution compared to controls over a 16 hour period. In addition, rAAV-GKS animals showed a clear preference for glucose over standard chow compared to controls over 24 hours and during a 31 day longitudinal study.

The results of this work suggest that glucose sensing neurones in the ARC may be involved in the regulation of energy balance and glucose homeostasis. These results are of broader significance considering the proposed use of GK activating drugs in the treatment of type II diabetes mellitus.

Declaration of contributors

The research and work described in this thesis was performed by the author. All collaboration and assistance is declared below.

Chapter 2:

Recombinant adeno-associated viral particles were prepared by Dr James V Gardiner.

Glucokinase activity assay was performed with the assistance of Dr Tim Shipley.

Chapter 3:

Quantitative PCR was performed with the assistance of Dr Sufyan Hussain and Mr John Counsell.

Chapter 4:

Glucose and insulin tolerance tests were performed with the assistance of Mr Nikki Buckley, Mr John Counsell, Dr Sufyan Hussain and Ms Hannah Greenwood.

Acknowledgements

I would firstly like to thank my supervisors: Dr James Gardiner, Dr Gavin Bewick and Dr Kevin Murphy for their guidance and support throughout my PhD.

I am also extremely grateful to Professor Stephen Bloom for giving me the opportunity to work in his department.

I would like to thank the Biotechnology and Biological Sciences Research Council (BBSRC) and the Imperial College Centre for Integrative Mammalian Physiology & Pharmacology (CIMPP) for my training and funding.

Finally I would like to thank my family and friends for keeping my spirits up while I wrote this thesis. It never hurts to laugh out loud (LOL) and you have given me many opportunities to do so.

List of Abbreviations

2DG	2-Deoxyglucose
3OMG	3-O-methyl-N-acetylglucosamine
5TG	5-thio-d-glucose-6-phosphate
AAV	Adeno-associated virus
ACC	Acetyl-CoA carboxylase
aCSF	Artificial cerebrospinal fluid
ADP	Adenosine diphosphate
AgRP	Agouti related peptide
Amp	Ampicillin resistance gene
AMPK	Adenosine Monophosphate Activated Protein Kinase
ANOVA	Analysis of variance
ARC	Arcuate nucleus
AS	Antisense
ATP	Adenosine triphosphate
AV	Arteriovenous
BAT	Brown adipose tissue
BLAST	Basic Local Alignment Search Tool
Bp	Base pairs
cAMP	Cyclic adeno monophosphate
CART	Cocaine-and amphetamine-related transcript
CCK	Cholecystokinin
cDNA	Copy DNA

CLAMS	Comprehensive laboratory animals monitoring system
CNS	Central nervous system
CPT-1	Carnitine palmitoyltransferase 1
CRR	counter regulatory response
CSF	Cerebrospinal fluid
DIO	Diet induced obesity
DKA	Diabetic ketoacidosis
DMEM	Dubecco's modified eagle medium
DMN	Dorso medial nucleus
DNA	Deoxyribonucleic acid
dNTP	Deoxynucleotide triphosphate
DTT	Dithiothreitol
EDTA	Ethylenediaminetetraacetic acid
eGFP	Enhanced green fluorescent protein
ELISA	Enzyme-linked immune-sorbent assay
FAS	Fatty acid synthase
FBS	Foetal Bovine Serum
GDW	Glass distilled water
GE	Glucose-excited
GEE	General estimating equation
GFP	Green fluorescent protein
GI	Glucose-inhibited
GIP	Glucose-dependant insulinotropic peptide

GIPr	Glucose-dependant insulinotropic peptide receptor
GK	Glucokinase
GKAS	Glucokinase antisense
GKPF	Glucokinase pair-fed
GKS	Glucokinase sense
GLP-1	Glucagon-like peptide-1
GLP-1r	Glucoagon-like peptide 1 receptor
GOD	Glucose oxidase
G-P-6	Glucose-6-phosphate
GTE	Glucose tris EDTA
HBS	HEPES-buffered saline
HEK	Human embryonic kidney
HEPG2	Human hepatocellular carcinoma
HFD	High fat diet
HHS	Hyperosmolar hyperglycaemia syndrome
HX	Hexokinase
i.p.	Intraperitoneal
ICV	Intracerebroventricular
IP	Intraperitoneal
IR	Insulin receptor
ITRs	Inverted terminal repeats
ITT	Insulin tolerance test
kcal	Kilocalorie

Kj	Kilojoule
KO	Knock out
LCFA-CoA	Long chain fatty acyl-CoAs
LDH	Lactate dehydrogenase
LHA	Lateral hypothalamic area
MCH	Melanin-concentrating hormone
MCT-1	Monocarboxylate transporter
mRNA	Messenger Ribonucleic acid
MSH	Melanocyte stimulating hormone
NADPH	Nicotinamide adenine dinucleotide phosphate
NCBI	National Centre for Biotechnology Information
NPY	Neuropeptide Y
oGTT	Oral glucose tolerance test by gavage
PBS	Phosphate buffered saline
PCR	Polymerase chain reaction
PFK	Phosphofructokinase
POD	Peroxidise
POMC	Pro-opiomelanocortin
PVN	Paraventricular nucleus
QPCR	Quantitative polymerase chain reaction
rAAV	Recombinant adeno associated virus
rAAV-GKAS	rAAV glucokinase antisense
rAAV-GKS	rAAV glucokinase

RNA	Ribonucleic acid
RT	Reverse transcriptase
SAP	Shrimp alkaline phosphatase
SDS	Sodium dodecyl sulfate
SEM	Standard error of the mean
SGLT-1	Sodium-dependant glucose transporter 1
SSC	Saline sodium citrate
TAE	Tris-Acetate EDTA
TE	Tris EDTA
tRNA	transfer Ribonucleic acid
UCP-1	Uncoupling protein 1
UV	Ultraviolet
vGTT	voluntary Oral glucose tolerance test
VMH	Ventromedial hypothalamic area
VMN	Ventromedial hypothalamic nucleus
WAT	White adipose tissue
WPRE	Woodchuck hepatitis virus promoter response element

Table of Contents

1. Chapter 1 General Introduction 21

1.1 The importance of maintaining normoglycaemia 23

1.2 Glucose homeostasis and glucose sensing 25

1.2.1 The endocrine pancreas and insulin action 25

1.2.2 Insulin secretion 26

1.2.3 Insulin's actions 28

1.2.4 Glucagon and its actions 30

1.3 Extra pancreatic glucose sensing 31

1.3.1 Intestinal glucose-sensing 32

1.3.2 Portal glucose sensing 33

1.4 CNS regulation of glucose homeostasis and feeding 34

1.4.1 A brief history 34

1.4.2 Hypothalamic distribution 35

1.4.2.1 The arcuate nucleus (ARC) 36

1.4.2.2 Ventromedial hypothalamic nucleus 37

1.4.2.3 The lateral hypothalamic area (LHA) 37

1.4.3 Mechanism of glucose-sensing 38

1.4.3.1 Glucose uptake 38

1.4.3.2 GE neurones 39

1.4.3.3 GI neurones 41

1.4.4 Is GK the primary regulator of hypothalamic glucose sensing? 42

1.4.5 Glucose sensors or metabolic sensors? 44

1.5 Summary 47

2.1 Introduction 49

2.1.1 Studying appetite and neuroendocrinology using molecular approaches 49

2.1.2 Transgenic animals 50

2.1.3 Gene transfer 52

2.1.4 Choice of Gene Transfer Vector 52

2.1.4.1 Adenoviruses 53

2.1.4.2 Retroviruses and Lentiviruses 53

2.1.4.3 Herpesviruses 54

2.1.4.4 Adeno-associated virus 55
2.1.4.5 Recombinant adeno-associated virus 56

2.2 Aims and Objectives 58

2.3 Materials and methods 59
2.3.1 Production of GKAS using polymerase chain reaction (PCR) 59
2.3.1.1 Reverse transcription 59
2.3.1.2 PCR 60
2.3.1.3 Visualisation of PCR products 62
2.3.2 Insertion of GK and GKAS into pTR-CGW 62
2.3.2.1 Restriction endonuclease digestion of PCR products and pTR-CGW 63
2.3.2.2 Electroelution of DNA fragments 64
2.3.2.3 Ligation of PCR product into pTR-CGW 65
2.3.3 Preparation of GKS-pTR-CGW-plasmid and GKAS-pTR-CGW-plasmid 66
2.3.3.1 Transformation of competent bacteria by electroporation 66
2.3.3.2 Small scale preparation of plasmid 67
2.3.3.3 Large scale preparation of plasmid 68
2.3.3.4 Caesium chloride gradient purification 69
2.3.3.5 DNA sequencing 71
2.3.4 Cell Culture 72
2.3.4.1 Maintenance of cells 72
2.3.4.2 Transfection of cells with GKS and GKAS pTR-CGW plasmids 73
2.3.5 Glucokinase activity assays 75
2.3.5.1 Standard glucokinase activity assay 75
2.3.5.2 Optimized glucokinase activity assay 77
2.3.5.3 Comparison of GK assay methodologies 78
2.3.6 Production of rAAV-GKS, GKAS-rAAV and rAAV-eGFP particles 79
2.3.6.1 Production of rAAV 79
2.3.6.2 Calcium phosphate transfection 79
2.3.6.3 Recovery and purification of rAAV 80
2.3.7 Statistical analysis 81

2.4 Results 82
2.4.1 PCR products 82
2.4.1.1 GKS 82
2.4.1.2 GKAS 82
2.4.2 Restriction endonuclease digestion of small scale plasmid preparation 82
2.4.3 Restriction endonuclease digestion of large scale plasmid preparation 83

2.4.3.1 GKS 83
2.4.3.2 GKAS 84
2.4.4 DNA sequencing 85
2.4.4.1 GKS 85
2.4.4.2 GKAS 87
2.4.5 Comparison of GK assays methodologies 88
2.4.6 Effect of GKAS-pTR-CGW plasmid transfection on GK activity in HEK293T cells 89
2.4.7 Effect of GKAS-pTR-CGW plasmid transfection on GK activity in HEPG2 cells 90

2.5 Discussion 91

3. Chapter 3 Effect administration on food intake and body weight 93

3.1 Introduction 94
3.1.1 The Glucostatic hypothesis 94
3.1.2 Experimental evidence 94
3.1.3 Mechanism of glucose-induced regulation of feeding 95
3.1.4 Blood glucose and spontaneous feeding 96

3.2 Hypothesis and Aims 98
3.2.1 Hypothesis 98
3.2.2 Aims and Objectives 98

3.3 Methods 99
3.3.1 Animals 99
3.3.2 Isolation of specific hypothalamic nuclei by punch biopsy from coronal sections 99
3.3.3 Isolation of specific hypothalamic nuclei by punch biopsy from sagittal sections 100
3.3.4 Quantification of glucokinase activity in the hypothalamic nuclei of fed and fasted rats 100
3.3.5 Protein assay on punch biopsy samples 101
3.3.6 Injection of GKS-AAV in the rat brain 102
3.3.7 Confirmation of gene transfer by in situ hybridisation 103
3.3.7.1 Production of radiolabelled RNA probe for in situ hybridisation 103
3.3.7.2 In situ hybridisation 105
3.3.8 Cohort One 107
3.3.8.1 Effect of iARC rAAV-GKS on food intake and bodyweight 107
3.3.8.2 Effect of iARC rAAV-GKS on GK activity in the ARC and PVN 107
3.3.8.3 Effect of iARC rAAV-GKS on body composition 107
3.3.8.4 Glycerol assay 108
3.3.9 Cohort 2 109

3.3.9.1 Effect of iARC rAAV-GKS on food intake and bodyweight, effect of pair feeding 109
3.3.9.2 Effect of iARC rAAV-GKS on 24hr food intake following fast 109
3.3.9.3 Body composition 109
3.3.9.4 Glucose homeostasis 110
3.3.9.5 Glucose assay 110
3.3.9.6 Plasma insulin ELISA 111
3.3.9.7 Quantification of Hypothalamic mRNA by QPCR 112
3.3.9.7.1 RNA Extraction 112
3.3.9.7.2 RNA Purification 112
3.3.9.7.3 Reverse Transcription of Hypothalamic mRNA 113
3.3.9.7.4 QPCR Analysis of Hypothalamic cDNA 114
3.3.10 Cohort 3 115
3.3.10.1 Effect of iARC rAAV-GKS on food intake and bodyweight: High energy diet 115
3.3.11 Statistical analysis 115

3.4 Results 116
3.4.1 Glucokinase activity in the hypothalamic nuclei of fed and fasted rats 116
3.4.2 Cohort 1: Effect of iARC rAAV-GKS on food intake and bodyweight 118
3.4.2.1 Confirmation of gene transfer by in situ hybridisation 118
3.4.2.2 Effect on bodyweight and bodyweight gain 119
3.4.2.3 Effect on food intake 121
3.4.2.4 Body composition 122
3.4.2.5 Effect of iARC rAAV-GKS on GK activity in the ARC and PVN 124
3.4.3 Cohort 2: Effect of iARC rAAV-GKS on food intake and bodyweight, effect of pair feeding 125
3.4.3.1 Effect on bodyweight and weight gain 125
3.4.3.2 Effect on food intake 126
3.4.3.3 Effect of iARC rAAV-GKS on 24hr food intake and bodyweight following 24hr fast 127
3.4.3.3.1 Food intake 127
3.4.3.3.2 Bodyweight 129
3.4.3.4 Effect of iARC rAAV-GKS on body composition and plasma hormones 131
3.4.3.4.1 BAT weight 131
3.4.3.4.2 Epididymal WAT weight 132
3.4.3.4.3 Fed blood glucose 133
3.4.3.4.4 Fed plasma insulin 134
3.4.3.5 Hypothalamic gene expression 135
3.4.3.5.1 GK 135
3.4.3.5.2 AMPK 136

3.4.3.5.3 CART 137
3.4.3.5.4 FAS 138
3.4.3.5.5 NPY 139
3.4.3.5.6 POMC 140
3.4.4 Cohort 3: Effect of iARC rAAV-GKS on food intake and bodyweight: High energy diet 141
3.4.4.1 Effect on bodyweight gain 141
3.4.4.2 Effect on food intake 142

3.5 Discussion 143
3.5.1 Identifying a primary target for rAAV-GKS injection 143
3.5.2 *Ex-vivo* GK assay 144
3.5.3 Effect of iARC rAAV-GKS; Cohort one 145
3.5.4 Effect of iARC rAAV-GKS; Cohort two 146
3.5.5 Effect of iARC rAAV-GKS; High energy diet 148

4. Chapter 4 Effect GKS administration on intake of sugars and glucose homeostasis 150

4.1 Introduction 151
4.1.1 The role of sugars in the regulation of food intake 151
4.1.2 Fructose metabolism in the brain and food intake 152

4.2 Hypothesis and Aims 155
4.2.1 Hypothesis 155
4.2.2 Aims and Objectives 155

4.3 Methods 156
4.3.1 Cohort 4: Effect of iARC rAAV-GKS on food intake, intake of glucose and bodyweight gain 156
4.3.1.1 Energy intake calculation 156
4.3.1.2 Effect of iARC-GKS on intake sugars and standard chow 156
4.3.1.3 Effect of iARC rAAV-GKS on 24hr intake of standard chow and 2% glucose solution 157
4.3.1.4 Effect of iARC rAAV-GKS on 24hr intake of standard chow and 10% glucose solution 157
4.3.1.5 Effect of iARC rAAV-GKS on 24hr intake of standard chow and 20% glucose solution 157
4.3.1.6 Effect of iARC rAAV-GKS on 24hr intake of standard chow and 40% glucose solution 158
4.3.1.7 Effect of iARC rAAV-GKS on intake of standard chow and 10% glucose solution: long term study 158
4.3.1.8 Effect of iARC rAAV-GKS on plasma glucose following oral glucose challenge 158
4.3.2 Group 5 159
4.3.2.1 Oral glucose tolerance test by gavage (oGTT) 159

4.3.2.2 Tail vein cannulation 160
4.3.2.3 Insulin tolerance test 161
4.3.2.4 Voluntary oral glucose tolerance test (vGTT) 161
4.3.2.5 Effect of iARC rAAV-GKS on glucose stimulated insulin release 162
4.3.3 Statistical analysis 162

4.4 Results 163
4.4.1 Cohort 4 163
4.4.1.1 24 hour intake of 10% glucose 163
4.4.1.2 24 hour intake of 10% fructose 165
4.4.1.3 24 hour food intake without glucose solution 166
4.4.1.4 24 hour intake of standard chow and 2% glucose solution 167
4.4.1.5 24 hour intake of standard chow and 10% glucose solution 171
4.4.1.6 24 hour intake of standard chow and 20% glucose solution 174
4.4.1.7 24 hour intake of standard chow and 40% glucose solution 177
4.4.1.8 Effect of iARC rAAV-GKS on food intake, intake of glucose and bodyweight gain 180
4.4.1.9 Effect on intake of 10% glucose solution 183
4.4.1.10 Effect on total energy intake 184
4.4.1.11 Effect of iARC rAAV-GKS on plasma glucose following oral glucose challenge 185
4.4.2 Cohort 5: Glucose homeostasis 187
4.4.2.1 Oral glucose tolerance test 187
4.4.2.2 Insulin tolerance test 189
4.4.2.3 Voluntary oral glucose tolerance test group 5 190
4.4.2.4 Plasma insulin during voluntary oral glucose tolerance test 191

4.5 Discussion 192

5. Chapter 5 General discussion and plan of future work 198
5.1.1 Summary of rAAV results 200
5.1.2 Mechanism of action 201
5.1.3 The significance of this work 205
5.1.4 Future work 206

1. Appendix I – Solutions 226

2. Appendix II - Figures 230

3. Appendix III- Randomisation method and calculations 233

4. Appendix IV – List of suppliers 235

Table of figures

Figure 1.1 Glucose excited neurone 40

Figure 1.2 Glucose inhibited neurone 41

Figure 1.3 Hypothalamic Lipid Sensing 45

Figure 2.1 Schematic of wild-type AAV-2 serotype genome 56

Figure 2.2 PCR primers used for amplification of GK gene sequences 61

Figure 2.3 Gel electrophoresis of large scale plasmid production of GKS 83

Figure 2.4 Gel electrophoresis of large scale plasmid production of GKAS 84

Figure 2.5 BLAST analysis of sequencing result for GKS-pTR-CGW vs. pCMV4.GKB1 sequence 86

Figure 2.6 BLAST analysis of GKAS-pTR-CGW sequencing results vs. rat pancreatic GK sequence 87

Figure 2.7 Comparing GK assays 88

Figure 2.8 Effect of GKS-pTR-CGW plasmid transfection on GK activity in HEK293T cells 89

Figure 2.9 Effect of GKAS-pTR-CGW plasmid transfection on GK activity in HEPG2 cells 90

Figure 3.1 Glucokinase activity in ARC of fed and fasted rats 116

Figure 3.2 Glucokinase activity in the PVN of fed and fasted rats 117

Figure 3.3 Glucokinase activity in the VMN of fed and fasted rats 117

Figure 3.4 Confirmation of gene transfer by in situ hybridisation 118

Figure 3.5 Effect of iARC rAAV-GKS on bodyweight and bodyweight gain 120

Figure 3.6 Effect of iARC rAAV-GKS on food intake 121

Figure 3.7 Effect of iARC rAAV-GKS on glycerol concentration and adiposity 122

Figure 3.8 Effect of iARC rAAV-GKS on protein concentration and lean body mass123

Figure 3.9 Effect of iARC rAAV-GKS on GK activity in the ARC and PVN 124

Figure 3.10 Effect of iARC rAAV-GKS on bodyweight and weight gain; effect of pair feeding 125

Figure 3.11 Effect of iARC rAAV-GKS on food intake, effect of pair feeding 126

Figure 3.12 Effect of iARC rAAV-GKS on 24hr food intake following 24hr fast 128

Figure 3.13 Effect of iARC rAAV-GKS on 24hr bodyweight following 24hr fast and re-feed 130

Figure 3.14 Effect of iARC rAAV-GKS on BAT weight 131

Figure 3.15 Effect of iARC rAAV-GKS on epididymal WAT weight 132

Figure 3.16 Effect of iARC rAAV-GKS on fed blood glucose 133

Figure 3.17 Effect of iARC rAAV-GKS on fed plasma insulin 134

Figure 3.18 Effect of iARC rAAV-GKS on hypothalamic GK mRNA expression 135

Figure 3.19 Effect of iARC rAAV-GKS on hypothalamic AMPK mRNA expression 136

Figure 3.20 Effect of iARC rAAV-GKS on hypothalamic CART mRNA expression 137

Figure 3.21 Effect of iARC rAAV-GKS on hypothalamic FAS mRNA expression 138

Figure 3.22 Effect of iARC rAAV-GKS on hypothalamic NPY mRNA expression 139

Figure 3.23 Effect of iARC rAAV-GKS on hypothalamic POMC mRNA expression 140

Figure 3.24 Effect of iARC rAAV-GKS on bodyweight and weight gain; high energy diet 141

Figure 3.25 Effect of iARC rAAV-GKS on intake of high energy diet 142

Figure 4.1 Effect of iARC rAAV-GKS on 24hr intake of 10% glucose solution 164

Figure 4.2 Effect of iARC rAAV-GKS on 24hr intake of 10% fructose solution 165

Figure 4.3 Effect of iARC rAAV-GKS on 24hr food intake without glucose solution 166

Figure 4.4 Effect of iARC rAAV-GKS on 24hr food intake (with 2% glucose solution) 168

Figure 4.5 Effect of iARC rAAV-GKS on 24hr intake of a 2% glucose solution 169

Figure 4.6 Effect of iARC rAAV-GKS on total energy intake over a 24hr period (2% glucose) 170

Figure 4.7 Effect of iARC rAAV-GKS on 24hr food intake (with 10% glucose solution) 171

Figure 4.8 Effect of iARC rAAV-GKS on 24hr intake of a 10% glucose solution 172

Figure 4.9 Effect of iARC rAAV-GKS on total energy intake over a 24hr period (10% glucose) 173

Figure 4.10 Effect of iARC rAAV-GKS on 24hr food intake (with 20% glucose solution) 174

Figure 4.11 Effect of iARC rAAV-GKS on 24hr intake of a 20% glucose solution 175

Figure 4.12 Effect of iARC rAAV-GKS on total energy intake over a 24hr period (20% glucose) 176

Figure 4.13 Effect of iARC rAAV-GKS on 24hr food intake (with 40% glucose solution) 177

Figure 4.14 Effect of iARC rAAV-GKS on 24hr intake of a 40% glucose solution 178

Figure 4.15 Effect of iARC rAAV-GKS on total energy intake over a 24hr period (40% glucose) 179

Figure 4.16 Effect of iARC rAAV-GKS on bodyweight and bodyweight gain 181

Figure 4.17 Effect of iARC rAAV-GKS on food intake 182

Figure 4.18 Effect of iARC rAAV-GKS on intake of 10% glucose solution 183

Figure 4.19 Effect of iARC rAAV-GKS on total energy intake 184

Figure 4.20 Effect of iARC rAAV-GKS on plasma glucose response to oral glucose challenge 186

Figure 4.21 Oral glucose tolerance test via gavage 188

Figure 4.22 Insulin tolerance test 189

Figure 4.23 Voluntary oral glucose tolerance test 190

Figure 4.24 Plasma insulin during voluntary oral glucose tolerance test 191

Chapter 1

General Introduction

Glucose is the major product of photosynthesis in plants and most photosynthetic bacteria, and is the conduit by which solar energy is stored and utilized by most life on Earth. Within biology glycolysis is virtually universal, occurring in organisms as evolutionarily distant as haloarchaea (Falb & Muller, 2008) and man. In multicellular organisms glucose is utilized by all cells; in aerobic and fermentative tissues alike, and is vital for the function of a number of organs including the brain. Intracellular glucose levels must be tightly controlled, as both high and low levels of glucose can be cytotoxic (Bronk, 1999). Classically, glucose homeostasis is believed to be largely regulated by the autonomously functioning endocrine pancreas. However, it is becoming increasingly clear that glucose-sensing neurones in the other organs play an important role in glucose homeostasis (Bronk, 1999;Levin *et al*, 1999). Since glucose homeostasis represents a small, but integral, part of total energy balance it is unsurprising that glucose-sensing neurones are also sensitive to other nutrients and have been postulated to have additional roles in energy balance; including the regulation of food intake (Loftus *et al*, 2000). In the present work the physiological role of hypothalamic glucose-sensing neurones is investigated utilizing adeno-associated viral gene transfer of glucokinase; an enzyme vital to the glucose-sensing mechanism of some cell types.

1.1 The importance of maintaining normoglycaemia

In healthy humans, plasma glucose is usually maintained between 4-6mmol/l, regardless of changes in glucose uptake by peripheral tissues or dietary contribution. This is important, as hypo- and hyperglycaemia can result in ill health. Severe hypoglycaemia most frequently occurs as a result of intensive insulin therapy in the treatment of type I diabetes mellitus. In humans, hypoglycaemia presents with symptoms including perspiration, shaking and dizziness, confusion and hunger (McAulay *et al*, 2001). In healthy individuals hypoglycaemia is usually avoided by an increased urge to feed and by the counter regulatory response (CRR). The CRR is a hormonally and neurally mediated cascade, primarily involving a decrease in plasma insulin and an increase in plasma glucagon, which reduces peripheral glucose utilization whilst simultaneously

increasing endogenous glucose production and release by the liver (Evans *et al*, 2004). In type I diabetes intensive insulin therapy blunts the CRR, and masks the physical manifestations of hypoglycaemia resulting in potentially fatal hypoglycaemic events (Mokan *et al*, 1994). It has been estimated that 2-10% of all type I diabetes deaths are as a result of iatrogenic hypoglycaemia (Cryer, 1997;Skrivarhaug *et al*, 2006).

Hyperglycaemia is usually associated with type II diabetes mellitus but also occurs in conditions of acute stress such as myocardial infarction, stroke, burns and infection.

The early stage of type II diabetes is characterised by peripheral insulin resistance which results in persistent and moderate hyperglycemia. Type II diabetes is by far the most prevalent form of diabetes accounting for 90-95% of all cases of diabetes worldwide (American Diabetes Association, 2011). The pathogenesis of type II diabetes is closely related to obesity; in particular central adiposity. In fact, almost 80% of type II diabetes sufferers are obese (Bloomgarden, 2000).

Insulin resistance describes the state in which tissues (primarily the skeletal muscle, liver and adipose tissue) are resistant to the plasma glucose lowering effects of insulin. In addition to insulin resistance, type II diabetes is characterised by progressive β-cell dysfunction which, combine with the increased demand created by insulin resistance, can lead to β-cell burnout and the requirement for insulin therapy.

Hyperglycaemia may also occur in type I diabetes mellitus as part of diabetic ketoacidosis (DKA) or hyperosmolar hyperglycaemia syndrome (HHS). Both conditions are caused by relative lack of insulin action and both are potentially lethal (Rosenbloom & Hanas, 1996;Magee & Bhatt, 2001). Aside from DKA and HHS, hyperglycaemia is rarely acutely lethal. Rather, chronic hyperglycemia over a period of decades causes micro- and macrovascular injury. Microvascular complications include diabetic retinopathy, neuropathy and nephropathy. While macrovascular injury can result in cardiovascular-, cerebrovascular- and peripheral vascular disease (American Diabetes Association, 2011). Sufferers of type II diabetes are at a two- to fourfold increased risk of coronary heart disease (Haffner & Miettinen, 1997).

1.2 Glucose homeostasis and glucose sensing

In order to maintain glucose homeostasis, it is necessary that at some level the body is ‘aware’ of the concentration of glucose in bodily tissues and also ‘aware’ of the quantity of glucose entering the system. In mammals this is achieved via the combined effort of numerous cell types with glucose-sensing ability that are located both within the circulatory system and outside it.

Glucose-sensing cells convert changes in local glucose concentrations into signals (usually endocrine or neural) that inform and influence the function of other cells within the body. In the following sections, glucose-sensing cells will be described and considered in terms of their roles in glucose homeostasis and regulation of energy balance.

1.2.1 The endocrine pancreas and insulin action

In the classical textbook description of glucose homeostasis the pancreas is described as an autonomously functioning master regulator that controls plasma glucose levels through altered hormonal secretion. In this model, glucose homeostasis is maintained by pancreatic hormones modulating peripheral glucose utilization and hepatic glucose production. Although this is a vast over-simplification, it is still the case that the endocrine pancreas plays a central role in glucose homeostasis and that many extra-pancreatic glucose sensors mediate their effects via modulation of pancreatic endocrine signalling.

The Islets of Langerhans constitute the endocrine portion of the pancreas and make up approximately 1-2% of pancreatic mass. Pancreatic islets are composed of 4 endocrine cells types;

1) α-cells; containing glucagon granules

2) β-cells; containing insulin granules

3) δ cells; containing somatostatin granules

4) PP cells; containing pancreatic polypeptide granules

(Elayat, 1995)

Of the four cell types α and β cells are most important in glucose homeostasis. In humans and in rats β pancreatic cells are located in central regions of the islets while α-cells are located peripherally (Sacchi & Bani, 1985). Insulin, a 5800Da endocrine hormone consisting of an α and β chain linked by two disulphide bridges, is the primary secretory product of β-cells. It is produced from a single chain precursor, proinsulin, by proteolytic cleavage and is subsequently stored in cytoplasmic secretory vesicles. The secretion of mature insulin is regulated by numerous hormonal and non-hormonal extracellular signals. In the postprandial state, secretion of insulin occurs primarily in response to increases in plasma glucose although, nervous innervation plays an important role (Henquin, 2000).

1.2.2 Insulin secretion

The stimulation of insulin release by glucose is primarily mediated via an increased rate of glycolysis in β-cells in response to hyperglycaemia. This increases intracellular adenosine triphosphate (ATP) levels which inhibits ATP-sensitive K^+ channels, resulting in membrane depolarisation. Depolarisation of the membrane opens voltage gated Ca^{2+}channels causing a rapid influx of Ca^{2+}down its electrochemical gradient.

Increasing cytoplasmic Ca^{2+}levels facilitates the binding of secretory vesicles with the plasma membrane and subsequently the exocytosis of insulin (Henquin, 2000).

Insulin secretion by the β-cell is dependent on its ability to sense local glucose concentrations, for this to happen the rate of glycolysis within the cell must be tightly coupled to changes in local plasma glucose levels. This is only possible because the β-cell expresses both glucokinase (GK) and the glucose transporter type II (GLUT 2) (Matschinsky, 1990;Matschinsky *et al*, 1993).

The GLUT family facilitate the transport of sugars including glucose and fructose across the plasma membrane of most mammalian cells. Members of the GLUT family create aqueous pores in the plasma membrane through which sugars are transported in an energy-independent manner. Since transport via the GLUT family is passive, sugars will only move down their concentration gradient.

GLUT 2 has a high Km for glucose meaning that it does not become saturated in the normal physiological range. This ensures that glucose transport across the cell membrane increases in line with changes in plasma glucose (Thorens, 1992). However, this is only possible because the β-cell also express GK.

GK belongs to the hexokinase family of enzymes which is comprised of four members. Hexokinases catalyse the first reaction in glycolysis; glucose + ATP to glucose-6-phosphate (G-6-P) + ADP. The conversion of glucose to G-6-P creates the concentration gradient required for the passive transport of glucose across the cell membrane. The rate of transport is, therefore, at least partially dependent on the rate at which specific hexokinases convert glucose to G-6-P. Phosphorylation also prevents glucose from escaping the cell because mammalian cells do not possess a G-6-P transporter (Iynedjian, 2009).

Hexokinase I is the most widely expressed hexokinase in the mammalian biology. It is typical of the group in that it has a low Km for glucose (and is therefore saturated at physiological glucose concentrations) and is inhibited by its product G-6-P. Hexokinase I acts as a regulatory step in both glycolysis and glycogen synthesis.

GK is an atypical member of the hexokinase family. It is approximately half the molecular weight of the other hexokinases and shares only 54.4% homology with hexokinase I (Zhang *et al*, 2006). It also possess significant functional and kinetic differences; GK has a high Km for glucose (~8 mmol/l) and is not inhibited by its product G-6-P (Iynedjian, 1993).

Two isoforms of GK are expressed in mammals under the control of tissue specific promoters. The first promoter produces the neuroendocrine isoform of GK which is expressed in the pancreas, central nervous system (CNS) and intestine. The second promoter produces the hepatic isoform of GK which is expressed exclusively in the liver. The two isoforms are functionally and kinetically identical and differ only by 13-15 amino acids at their N-termini. The major difference between the isoforms occurs at the level of their expression (Iynedjian, 2009). Expression of the liver isoform but not the neuroendocrine is dependent on insulin. Hepatic GK expression is reduced by 90% in streptozotocin-induced diabetic rats (Iynedjian *et al*, 1988).

In the pancreas, the high Km of GK and lack of end product inhibition maintains the concentration gradient between intracellular and extracellular glucose as plasma glucose levels increase post prandially. This, combined with rapid glucose transport by GLUT 2, couples the post-prandial rise in plasma glucose with glycolysis and ultimately insulin secretion.

1.2.3 Insulin's actions

Insulin signals at target tissues via receptor-ligand interaction with the ubiquitously expressed plasma membrane insulin receptor (IR). The IR is a member of the receptor tyrosine kinase family of transmembrane receptors and is composed of two α- and two β-subunits. Binding of insulin to insulin-binding sites located on the extracellular α-subunits causes localized conformational change, which ultimately results in the autophosphorylation of specific tyrosine residues on the intracellular β-subunits. Autophosphorylation of the β-subunits induces further conformational changes and increases receptor kinase activity (Baron *et al*, 1992). Activation of IR kinase activity

regulates a variety of intracellular phosphorylation cascades involved in metabolic regulation and gene expression.

In skeletal muscle and adipose tissue, binding of insulin to the IR increases glucose uptake by initiating translocation of the GLUT 4 from cytoplasmic storage vesicles to the plasma membrane. GLUT 4 is the only member of the GLUT family that is insulin responsive. Translocation of GLUT 4 to the plasma membrane of myocytes and adipocytes is the most important mechanism involved in insulin-induced post prandial glucose clearance. Indeed, approximately two-thirds of all postprandial insulin-mediated glucose disposal occurs in skeletal muscle alone (Klip and Paquet 1990).

The other major site involved in insulin-induced post prandial glucose clearance is the liver. Hepatocytes express both the GLUT 2 and GK. GLUT 2 is not insulin-induced however its high Km and affinity for glucose allows glucose to be rapidly taken up by the liver when plasma glucose is high as it does in the pancreas. As previously discussed, hepatic GK expression is insulin dependent. At basal plasma insulin levels hepatic GK expression and glucose uptake is low. Insulin-induced increases in hepatic GK assists in postprandial glucose clearance by increasing the rate at which glucose is phosphorylated to G-6-P; thus creating the concentration gradient required for passive glucose transporter by GLUT2. Hepatic knockout of GK does not markedly influence plasma glucose levels in the basal state. However, glucose tolerance, hepatic glucose uptake and hepatic glycogen synthesis are impaired in hepatic GK knockout mice demonstrating the importance of hepatic GK in the post prandial state (Postic *et al*, 2001).

Insulin is also able to cross the blood brain barrier and the IR is expressed within the central nervous system, with particularly high expression in the hypothalamus and the olfactory bulb (Havrankova *et al*, 1978). Neurones do not express the insulin-dependent hepatic isoform of GK and insulin is not believed to play a major regulatory role in their glucose uptake or metabolism (Seaquist *et al*, 2001). Rather, insulin signalling in the CNS regulates peripheral glucose metabolism and energy balance. Infusion of insulin into the CNS inhibits feeding and stimulates the vagus nerve which increases pancreatic insulin secretion and inhibits hepatic glucose production (Obici *et al*, 2002;Szabo *et al*, 1983). This not only highlights the importance of insulin signalling in the CNS but also the importance of CNS-peripheral interactions in the regulation of glucose homeostasis.

Furthermore, the pancreas-insulin-CNS pathway provides an example of how glucose-sensing (in this case in the pancreas) indirectly influences feeding behaviour.

1.2.4 Glucagon and its actions

In the transition between the absorptive and post-absorptive states plasma glucose slowly falls as peripheral glucose uptake exceeds glucose appearance. This is accompanied by reduced insulin release by β-cells, increased secretion of glucagon by α-pancreatic cells, and increased plasma adrenaline (Evans *et al*, 2004). Glucagon is a 3500 Da peptide with essentially opposing metabolic actions to insulin. The pathways regulating glucagon secretion are complex and ill understood. What is known is that secretion of glucagon is inhibited by glucose, somatostatin and activation of β-cells, and is stimulated by pyruvate (Ishihara *et al*, 2003). Increased plasma glucagon-to-insulin ratio in the early post absorptive state promotes glycogenolysis and subsequent glucose release from the liver. Furthermore, glucagon promotes lipolysis and proteolysis in adipose tissue and skeletal muscle respectively, and thereby provides precursors for hepatic gluconeogenesis (Bronk, 1999).

Interestingly, in addition to its effects on glucose metabolism, glucagon has been shown to influence feeding behaviour. As is the case with insulin, there is a small increase in plasma glucagon within minutes of feeding (De Jong *et al*, 1977). Plasma glucagon also increases following sham feeding which suggests that this phenomenon may be regulated by cephalic stimulation (Nilsson & Uvnas Wallensten, 1977). Administration of glucagon to humans reduces meal size and it has been shown that glucagon elicits its effects on feeding via a pathway involving the liver, the vagus nerve and the CNS (Geary, 1990;Geary & Smith, 1983;Weatherford & Ritter, 1988).

1.3 Extra pancreatic glucose sensing

In addition to the pancreas, glucose sensing cells are located in the CNS, the mouth, the gut and the hepatic portal vein. Glucose sensing in each of these regions is required for proper regulation of glucose homeostasis.

Glucose-sensing begins within seconds of glucose entering the body, as evidenced by the preabsorptive or cephalic insulin response. In the mouth glucose interacts with the sweet taste receptor which is a member of the T1R family of taste receptors that include the receptors for bitter and umami taste modalities. The sweet taste receptor is a heteromeric g-protein coupled receptor formed of T1R2 and T1R3 proteins (Nelson *et al*, 2001). α-gustducin is a taste-specific g-protein that plays an important role in the transduction of both sweet and bitter taste. In mice, knock-out of α-gustducin results in reduced responsiveness to bitter and sweet taste modalities(Wong *et al*, 1996). Activation of the sweet taste receptor results in insulin release via parasympathetic stimulation of the pancreas by vagal efferents (Berthoud *et al*, 1980).

The ability to sense glucose in food as early in the digestive process as in the mouth is likely to offer a number of evolutionarily important advantages. Firstly, it allows the body to prepare for an imminent increase in plasma glucose and thus dampens the post-prandial hyperglycaemia associated with ingestion of carbohydrate rich foods. In addition, the ability to recognise sources of simple sugars or high calorie food stuffs would be advantageous to any mammal for which future food supply is uncertain (such as early man). Aversive feeding behaviour to bitter tasting compounds is believed to protect against the ingestions of toxins and it possible that activation of the sweet taste receptor would increase the drive to feed high calorie simple sugars that could be stored in adipose tissue and skeletal muscle and called upon in times of need.

1.3.1 Intestinal glucose-sensing

Following its ingestion, glucose is sensed in the intestine by K and L cells. K and L cells secrete the incretin hormones glucose-dependent insulinotropic peptide (GIP) and glucagon-like peptide 1 (GLP-1) respectively. As is the case with the taste receptors of the tongue, the primary function of GIP and GLP-1 is to prepare the body for the forthcoming post prandial increase in plasma glucose. The term 'incretin' describes the ability of these hormones to increase or augment insulin release.

GIP is released from K-cells in response to post prandial increases in both fats and carbohydrates. The exact mechanism of glucose sensing in K cells is poorly understood. However, glucose sensing in this cell type is dependent on the expression of the sodium-dependent glucose transporter 1 (SGLT-1) and ATP-sensitive K+ channels, suggesting that glycolysis may be involved as it is in the β-cell (Parker *et al*, 2009). GIP signals via the glucose-dependant insulinotropic peptide receptor (GIPr) and is believed to primarily exert its metabolic effects at the level of the adipose tissue and pancreas. In adipose tissue GIP has been shown to increase both uptake of glucose and conversion of glucose to fatty acids and thus aides post-prandial glucose clearance (Hauner *et al*, 1988). At the level of the pancreas GIP increases glucose-stimulated insulin release via interaction with its g-protein coupled receptor and subsequent increase of cytosolic cAMP and calcium (Siegel & Creutzfeldt, 1985;Lu *et al*, 1993).

GLP-1 secretion from L-cells is also believed to be dependent on the expression of SGLT-1 and ATP-sensitive K+ channels (Reimann *et al*, 2008).The glucagon-like peptide 1 receptor (GLP-1r) is expressed in numerous sites throughout the body including the pancreas, hepatic portal vein, vagus nerve and the central nervous system (including the hypothalamus) (Drucker, 2007). In the pancreas, the GLP-1r is expressed on both α and β-cells. GLP-1 increases glucose-stimulated insulin release while decreasing glucagon secretion.

In addition to its effects on glucose metabolism, GLP-1 has also been shown to influence feeding behaviour. In humans, intravenous GLP-1 infusion results in a dose dependent decrease in food intake (Gutzwiller *et al*, 1999). In rodents, intracerebroventricular (ICV) infusion of GLP-1 results in reduced intake of both food

and water (Tang-Christensen *et al*, 1996). Thus, as is the case in the pancreas, glucose sensing in the intestine influences both glucose homeostasis and feeding behaviour.

1.3.2 Portal glucose sensing

Following absorption, glucose enters the circulation at the hepatic portal vein, which transports blood from the gastrointestinal tract to the hepatic capillary beds. As well as being the conduit between the gastrointestinal tract and the liver, the hepatic portal vein is an important glucose sensor. Glucose is sensed in the hepatic portal vein by glucose-sensing neurones projecting from the nodose ganglia which express both the ATP sensitive K+ channel and GLUT 2 (Grabauskas *et al*, 2010;Burcelin *et al*, 2000b). Knockout of GLUT2 appears to abolish glucose sensing which suggests that glucose-sensing in the hepatic portal vein is dependent on glucose transport and metabolism (Burcelin *et al*, 2000b). This further suggests that the glucose-sensing mechanism in hepatic neurones is similar to that of the pancreatic β-cell.

Infusion of glucose into the hepatic portal vein activates a number of glucose-lowering mechanisms including increasing hepatic and peripheral glucose uptake, and decreasing food intake (Stempel & Jungermann, 1997;Burcelin *et al*, 2000a;Berthoud *et al*, 1980;Russek, 1970). The hepatic portal vein is also sensitive to GLP-1. Infusion of GLP-1 into the hepatic portal vein reduces plasma glucose by increasing hepatic glucose uptake and pancreatic insulin secretion (Nishizawa *et al*, 2003). Administration of chlorisondamine (a ganglionic blocker) prevents the augmentation of insulin release by hepatic portal GLP-1 administration, suggesting that its effects are mediated via a neural mechanism (Balkan & Li, 2000).

1.4 CNS regulation of glucose homeostasis and feeding

Within the central nervous system, glucose-sensing neurones are found in numerous regions including the hypothalamus, hindbrain, motor cortex, amygdala and septum (McCrimmon, 2008). Glucose-sensing neurones may be broadly divided in to two groups based on their electrophysiological response to glucose. Glucose-excited (GE) neurones increase their firing rate as ambient glucose levels increase while glucose-inhibited (GI) neurones decrease their firing rate in response to the same stimulus (Oomura *et al*, 1964). With regard to glucose homeostasis and feeding behaviour, it is those neurones located in the hypothalamus which have received the greatest attention.

1.4.1 A brief history

The earliest indication of the brains involvement in glucose homeostasis was provided by Claude Bernard in 1849. Bernard showed that punching holes in the floor of the fourth cerebral ventricle resulted in glycosuria in the dog (Pyke, 1979). In the early 1950's Jean Mayer proposed the 'Glucostatic Hypothesis', in which he suggested that food intake was regulated by alterations in plasma glucose. Mayer hypothesized that the hypothalamus contained glucose-sensitive neurones which acted as "glucoreceptors". He proposed that these glucoreceptors altered their electrical activity in response to changes in their rate of glucose utilisation; to produce feelings of hunger when glucose was limiting and satiety when plasma glucose was adequate (Mayer, 1952). Although this hypothesis has never been proven, and is almost certainly an over simplification, it correctly predicted the existence of glucose-sensitive neurons in the hypothalamus. In 1964 two groups, Omura et al and Anand et al, separately documented the presence of glucose-sensitive neurones in the hypothalamus using electrophysiological methods (Oomura *et al*, 1964;Anand *et al*, 1964).

With regard to the physiological function of glucose-sensing neurones, most evidence to date has been derived from manipulation of glucose supply or glucose metabolism. In 1989, Biggers et al, demonstrated the importance of CNS glucose-sensing by inducing

peripheral hypoglycaemia while maintaining euglycemia in the brain by infusing glucose bilaterally into the carotid and vertebral arteries. It was found that this treatment dramatically reduced release of the counter regulatory hormones glucagon and adrenaline and peripheral hypoglycaemia remained uncorrected (Biggers *et al*, 1989). The CRR to hypoglycaemia is also abolished if glucose is infused directly into the ventromedial hypothalamus (VMH) (Borg *et al*, 1997). Conversely, infusion of 2-deoxy-glucose (2DG) (a glucose anti-metabolite) into the VMH results in initiation of the CRR, even in the presence of peripheral euglycemia (Borg *et al*, 1995). Thus, central glucose-sensing appears to be the major mechanism regulating the CRR to hypoglycaemia.

In line with the Mayer "Glucostatic" hypothesis, both acute (Kurata *et al*, 1986) and chronic (Davis *et al*, 1981) central glucose infusion has been shown to reduce feeding in rodents. Again, the VMH appears to be involved, as chronic infusion of glucose into the VMH results in 27% reduction in feeding (Panksepp & Rossi III, 1981). Conversely administration of 2DG into the third cerebral ventricle results in a dose dependent increase in food intake, suggesting that inhibition of glucose metabolism therein is sufficient to induce feeding (Tsujii & Bray, 1990).

1.4.2 Hypothalamic distribution

Within the hypothalamus glucose-sensing neurones are found in the paraventricular nucleus (PVN), lateral hypothalamic area (LHA) and in the ventromedial hypothalamus (VMH); which includes the arcuate nucleus (ARC) and ventromedial nucleus (VMN) (Lynch *et al*, 2000). While the absolute role, and indeed neurotransmitter identity, of glucose-sensing neurones in each of these regions is currently unknown, suggestive experimental evidence is gathering, particularly with regard to neuronal populations in the VMH and LHA.

1.4.2.1 **The arcuate nucleus (ARC)**

The ARC is superior to the median eminence and extends from the optic chiasm to the mammillary bodies; encapsulating the third cerebral ventricle. The ARC has a semi permeable blood brain barrier, resulting from a highly fenestrated local capillary network, and thus is exposed to peripheral signals involved in energy homeostasis such as glucose, fatty acids, leptin and ghrelin. With regard to feeding, the ARC contains two neuronal populations which have been well characterised; one population which co-expresses the orexigenic peptides neuropeptide Y (NPY) and agouti related peptide (AgRP), and another which expresses the anorexic peptides pro-opiomelanocortin (POMC) and cocaine-and-amphetamine-related transcript (CART). NPY/AgRP neurones project to the LHA and the PVN and are activated by ghrelin and inhibited by leptin. POMC/CART neurones project to numerous hypothalamic and extra-hypothalamic regions and are activated by leptin and insulin, and in some cases glucose, resulting in reduced feeding (Cone *et al*, 2001).

The ARC also contains a large number of glucose-sensing neurones and evidence suggests that these populations partially overlap with both NPY/AgRP and POMC/CART neurones. Muroya et al (1999) found that 94% of GI neurones isolated from the rat ARC were immunoreactive for NPY (Muroya *et al*, 1999). While Ibrahim et al (2003) identified 80% of POMC neurones as glucose excited by taking electrical readings of transgenic POMC-eGFP neurones from mouse brain slices (Ibrahim *et al*, 2003). These results are consistent with glucose being a satiety signal. However, the GE nature of POMC neurones is controversial. Some investigators have reported no effect of glucose on POMC firing rate while others have reported a reduced firing rate with increasing glucose concentration (Fioramonti *et al*, 2007).The situation is further confused by a study showing no POMC immunoreactivity in 8/8 GE neurones from the mouse ARC (Wang *et al*, 2004). Further investigation is required to resolve these discrepancies.

1.4.2.2 **Ventromedial hypothalamic nucleus**

The VMN lies superior to the ARC and, was classically defined as the hypothalamic "satiety" centre after lesioning of the area was shown to induce hyperphagia (reviewed in (Schwartz *et al*, 2000). The VMN receives input from hypothalamic nuclei including the PVN, dorsomedial hypothalamic nucleus (DMN) and LHA and returns projections to the LHA and DMN. Unlike the ARC and LHA, the neuropeptide expression of the VMN, especially with regard to glucose sensitive neurones, is less well understood (Burdakov *et al*, 2005b). With regard to glucose-sensing the VMH remains the most well studied region of the hypothalamus and has been shown to be of importance in the regulation of glucose homeostasis and feeding. However, it should be remembered that the VMH, as opposed to the VMN, also contains the ARC. So it is difficult to extrapolate a specific function of VMN glucose-sensing neurones.

1.4.2.3 **The lateral hypothalamic area (LHA)**

The Lateral hypothalamic area (LHA) is a large, poorly defined region of the hypothalamus lying lateral to the VMN. The LHA was classically described as the "feeding centre" of the hypothalamus after lesioning of the area was shown to induce hypophagia (Anand & Brobeck, 1951). Two of the major neuronal population in the LHA are those expressing orexin (De Lecea *et al*, 1998) and melanin concentrating hormone (MCH) (Broberger *et al*,).

Activation of NPYergic neurones, which project from the ARC to the LHA, causes the release of orexin A and B from orexin neurones (Horvath *et al*, 1999). Orexins are orexigenic neuropeptides that increase arousal and food searching behaviour. The greater majority, ~95%, of orexin neurones in the mouse LHA are inhibited by glucose at physiologically relevant concentrations (0.2-5mmol/l) and have been classified as being GI (Burdakov *et al*, 2005a).

Evidence from mice with targeted deletion of either MCH or the MCH receptor, and intracerebroventricular injection of MCH suggest that MCH may play an opposing role to that of the orexins (i.e. promoting sleep and suppression of activity). Interestingly, it

has recently been shown that the majority of MCH neurones in the LHA, some 80%, are excited by glucose in a dose manner (Burdakov *et al*, 2005a).

The neuropeptide co-localisation of glucose-sensing neurones in the ARC and LHA suggests that their activation/inhibition may result in entirely different physiological outcomes. This is also likely to be the case for other hypothalamic and extra-hypothalamic regions.

1.4.3 Mechanism of glucose-sensing

1.4.3.1 Glucose uptake

For a cell to be capable of sensing glucose via metabolism, it must be able to take up glucose at a rate that allows intracellular glucose levels to closely reflect extracellular levels. In the β-cell this is facilitated by expression of the high capacity GLUT-2 transporter and GK; and glucose-sensing in the β-cell is dependent on their expression.

Although GLUT-2 is expressed in the hypothalamus, there is some controversy as to which glucose transporter is most important in hypothalamic glucose sensing. GLUT-2 does appear to be involved in the glucose-sensing of some hypothalamic neurones (Stolarczyk *et al*, 2010). However, in the hypothalamus GLUT-2 is primarily expressed on astrocytes rather than neurones (Leloup *et al*, 1994).

Some neurones in glucose-sensing regions co-express the insulin receptor and the insulin-sensitive GLUT-4 transporter (Vannucci *et al*, 1998). The Km for glucose of GLUT-4 is 4.6mmol/l (Nishimura *et al*, 1993), this is above the normal range of glucose within the brain so it is possible that GLUT-4 is involved in neuronal glucose-sensing. However, the majority of glucose-sensing neurones express GLUT-3.

Of the class I glucose transporters (1,2,3,4), GLUT-3 has the lowest Km. Despite this, the transport capacity of GLUT-3 is higher than that of GLUT-1 and GLUT-4 owing to its high affinity for glucose. The high affinity of GLUT-3 makes it well suited for rapid

uptake of glucose in the physiological range of the brain (usually ~1-2mmol/l) (Simpson *et al*, 2008).

Glucose levels in the VMH are higher than most other brain regions and have been shown to range from 0.73 to 4.23mmol/l (Mayer *et al*, 2006;de Vries *et al*, 2005). Since no single transporter is maximally active across this range it makes teleological sense that neurones in the VMH express a variety of transporters with varying kinetics.

1.4.3.2 **GE neurones**

After it is transported across the cell membrane, glucose is sensed in GE neurones in much the same way as in the β-cells of the pancreas. As intracellular glucose levels increase, glucose is rapidly converted to G-6-P and enters glycolysis leading to an increase in the ATP/ADP ratio. In some neurones this is facilitated by GK, which is expressed in 64% of GE neurones (Kang *et al*, 2004). High ATP/ADP ratio causes the closure of ATP sensitive K^+ channels resulting in membrane depolarisation, action potential and neurotransmitter release (Levin *et al*, 2004).

Glucose-sensing in GE neurones has been shown to be dependent on the expression and closure of ATP sensitive K^+. ATP levels within neurones are well buffered so changes in glucose utilization are unlikely to alter absolute cellular levels sufficiently to affect ATP sensitive K^+ channels. This suggests that the increase in ATP may be compartmentalised at the cell membrane and proximal to the ATP sensitive K^+ channel. However, to date this has not been demonstrated experimentally (Levin *et al*, 2004). (figure 1.1)

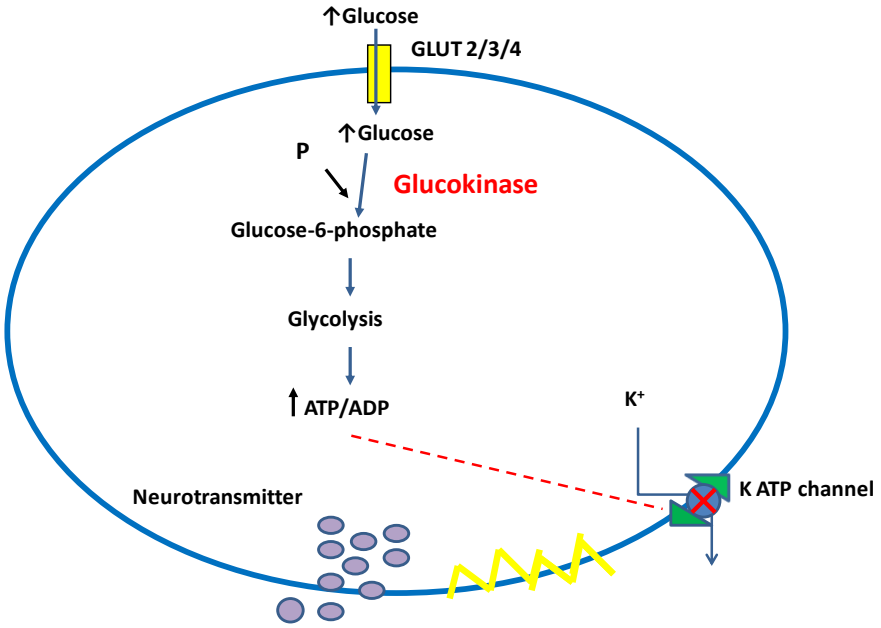


Figure 1.1 Glucose excited neurone: The potential mechanism of glucose-sensing in the GE neurones. Rate of glycolysis is translated to increased ATP/ADP ratio resulting in closure of ATP sensitive K+ channel and subsequent membrane depolarisation.

1.4.3.3 **GI neurones**

Compared to GE neurones, the glucose-sensing mechanisms of GI neurones are less well understood. Approximately 45% of GI neurones express GK (Kang *et al*, 2004) so it is possible that the sensing mechanism is directly related to glucose metabolism, as it is in the GE neurone. In the case of GI neurones it has been postulated that membrane depolarisation may occur at low glucose levels as a result of activation of Adenosine Monophosphate Activated Protein Kinase (AMPK) in response to low ATP/ADP ratio. It has been suggested that activation of AMPK may phosphorylate, and deactivate, membrane Cl^-channels, leading to depolarisation (Mountjoy & Rutter, 2007). (figure 1.2)

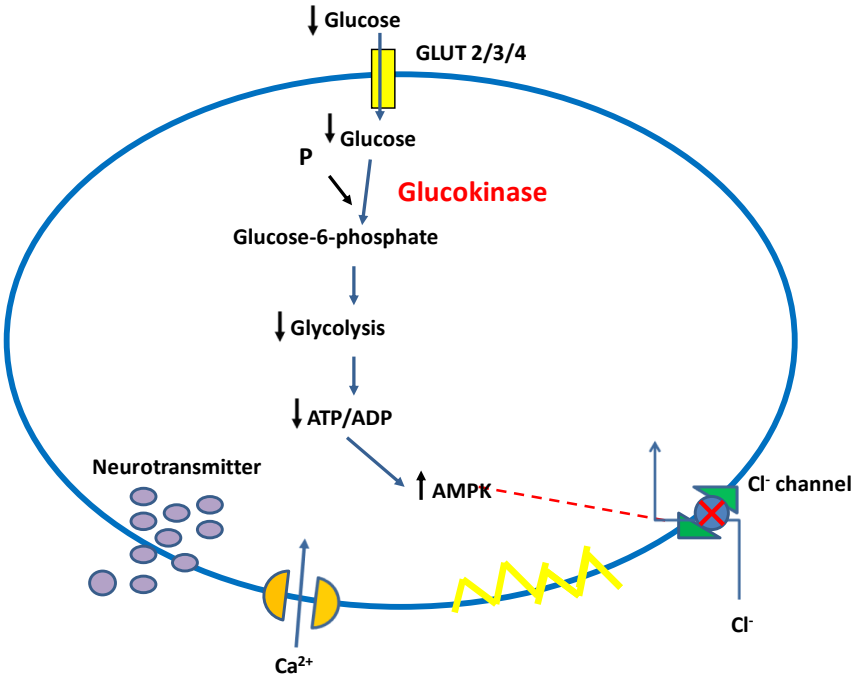


Figure 1.2 Glucose inhibited neurone: The potential mechanism of glucose sensing in the GI neurones. Reduced rate of glycolysis results in a decrease in cellular ATP and activation of AMPK which inhibits membrane Cl- channels causing membrane depolarisation.

1.4.4 Is GK the primary regulator of hypothalamic glucose sensing?

It has been stated, primarily by Levin *et al*, that GK acts as the primary regulator of neuronal glucose sensing, as it does in the β-cells of the pancreas (Levin *et al*, 2004;Kang *et al*, 2004). However, GK is not expressed in all GE and GI neurones. This observation has led some investigators to question the importance of GK in glucose-sensing in the hypothalamus.

In the hypothalamus, the neuroendocrine form of GK is expressed. Hypothalamic GK is expressed only in regions where glucose-sensing neurones are found, suggesting a specific role. In *ex vivo* VMH neurones, pharmacological activation of GK increases activity of GE neurones and inhibits the stimulatory effect of low glucose on GI neurones. Furthermore, a 90% reduction in GK mRNA in cultured VMH neurones results in total loss of glucose sensitivity in GI and GE neurones, suggesting that glucose-sensing is dependent on GK in both cell types (Kang *et al*, 2006).

A sticking point in the "GK as a glucose-sensor" hypothesis is that the Km of GK (~8mmol/l for glucose) is far higher than glucose levels observed in the brain (Kang *et al*, 2006; Roncero *et al*, 2000). It is therefore questionable as to whether it is GK which gives glucose-sensing neurones their sensitivity to changes in glucose concentration; especially as GE neurones have been shown to be most sensitive to changes in glucose concentration at <2mmol/l (Wang *et al*, 2004).

Considering the fact that GK is not expressed in all glucose-sensing neurones it is impossible to confidently state that it is the primary hypothalamic glucose sensor, and it is certain that other glucose sensors exist, including AMPK.

Interestingly, it also appears that at least some glucose-sensing neurones sense glucose via non-metabolic mechanisms. That is to say that glucose is sensed without being taken up by the neurone and without being metabolised. For example, in addition to its role as a glucose transporter, GLUT-2 also possesses receptor activity via an intracytoplasmic loop domain. Transgenic mice have been produced in which the receptor activity of the GLUT-2 loop domain is blocked but the transport function is maintained. Such mice display decreased c-Fos activation in the ARC following glucose infusion and increased

food intake as a result of increased meal size; demonstrating the importance of glucose-sensing via the cytoplasmic loop (Stolarczyk *et al*, 2010).

It has also been shown that T1R2/T1R3 sweet taste receptor and α-gustducin are expressed in the ARC and the PVN (Ren *et al*, 2009). This suggests that some glucose-sensing neurones may sense glucose using the same machinery as taste receptors of the tongue. Thus, non-metabolic glucose sensing in the hypothalamus appears to be important in the regulation of energy balance. Non-metabolic glucose-sensing might also explain how some neurones that do not express GK are able to sense changes in extracellular glucose.

1.4.5 Glucose sensors or metabolic sensors?

Finally, it is important to address the term "glucose-sensing" neurone, which may be something of a misnomer. While it is true that these cells respond to glucose, they also respond to a variety of other nutrients and nutrient-related hormones. For example, some neurones in the ARC are responsive to oleic acid. Wang *et al* found that 13% of ARC neurones are excited by oleic acid and 6% are inhibited when they are incubated with 2.5mmol/l glucose. When incubated in 0.1mmol/l glucose, oleic acid inhibits 30% of neurones and excites none (Wang *et al*, 2006). Therefore it is possible that there are interactions between fatty acid and glucose metabolism within glucose-sensing neurons which regulate their activity.

One hypothesis suggests that this occurs as a result of accumulation of long chain fatty acyl-CoAs (LCFA-CoA) in the cytoplasm. Briefly, the end product of glycolysis, acetyl-CoA, is converted to malonyl-CoA by acetyl-CoA carboxylase (ACC) when cellular ATP is high. Malonyl-CoA is a potent inhibitor of mitochondrial membrane transporter Carnitine palmitoyltransferase 1 (CPT-1). CPT-1 mediates transport of fatty acyl-CoAs across the outer mitochondrial membrane and in so doing regulates β-oxidation. Inhibition of CPT-1 results in the accumulation of lipid in the cytosol, which in turn activates Protein kinase C causing membrane depolarisation. When glucose is limiting, malonyl-CoA is low and CPT1 is active, thus lipids do not accumulate in the cytoplasm and the membrane remains polarised (figure 1.3).

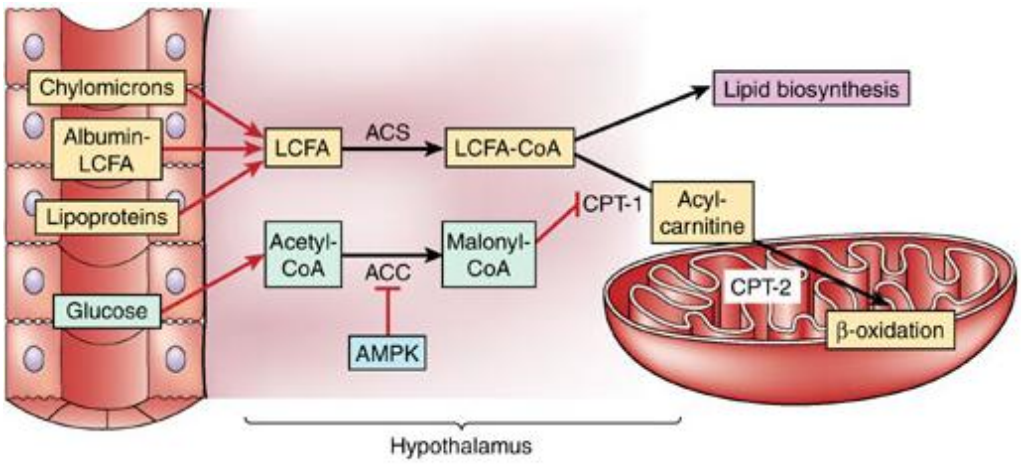


Figure 1.3 Hypothalamic Lipid Sensing: In the presence of glucose mitochondrial lipid transport is inhibited by malonyl-CoA, leading to accumulation of lipid in the cytoplasm. The causes membrane depolarisation and may signal the fed state. Adapted from Lam et al, 2005.

AMPK may also play an important role in this pathway. AMPK is the primary regulator of ACC, the enzyme responsible for the conversion of acetyl-CoA to malonly- CoA. Activation of AMPK, when the ratio of ATP-ADP is low, results in the inhibition of ACC and reduced malonyl-CoA, thus reducing CPT-1 inhibition and accumulation of LCFA-CoAs in the cytoplasm. In healthy individuals, high plasma glucose plus high plasma lipids will only occur in the fed state. Thus, depolarisation may signal the fed state. This concept is supported by the fact that lipid administration to the basomedial hypothalamus results in decreased feeding and decreased glucose production by the liver (Lam *et al*, 2005b).

Glucose sensing neurones are also sensitive to lactate. ICV lactate infusion results in hypoglycaemia due to reduced hepatic glucose output and lipid production (Lam *et al*, 2005a;Lam *et al*, 2007). This is believed to occur as a result of activation of GE neurones and possibly inhibition of GI neurones.

Astrocytes are a major endogenous source of lactate in the brain and it has been suggested that glucose-sensing in the brain is dependent on astrocytes as proposed in the "astrocyte-neurone shuttle hypothesis" (Pellerin *et al*, 2000). This hypothesis proposes that glucose is taken up by astrocytes where it is metabolised via glycolysis to pyruvate and next converted to lactate. Lactate is released by the astrocyte and taken up by the neurone via the monocarboxylate transporter (MCT1). Once transported across the cell membrane lactate is converted back to pyruvate by lactate dehydrogenase (LDH). Pyruvate is a late stage glycolytic intermediate and its metabolism results in an increase in ATP/ADP ratio, closing ATP-sensitive K+ channels (Penicaud *et al*, 2006). This idea is supported by the finding that specific pharmacological inhibition of astrocytes results in loss of ARC glucose-sensing following glucose infusion. However, it is not supported by the fact that manipulation of GK in neurones influences their glucose-sensing ability. The metabolism of lactate is downstream of GK. If glucose-sensing occurred purely via lactate, manipulation of GK would not be expected to influence it.

Some glucose-sensing neurones are also sensitive to leptin, insulin and ghrelin. In the hypothalamus, leptin and insulin suppress AMPK activity (Minokoshi *et al*, 2004) while ghrelin activates it (Andersson *et al*, 2004). Since AMPK regulates ACC this offers a potential mechanism by which glucose-sensing in neurones may interact with the response to endocrine hormones. Equally, since AMPK activity is affected by glucose,

fatty acids and a host of endocrine hormones, it suggests that integration between these factors may occur in intracellular signalling pathways and may be important in nutrient sensing (Penicaud *et al*, 2006).

While the term "glucose-sensing" may be something of a misnomer, it is the term used most frequently in the literature. For the sake of convention and clarity it will also be used in this thesis.

1.5 Summary

A considerable body of literature exists which suggests that glucose-sensing neurones of the hypothalamus play important physiological roles, particularly in feeding behaviour and glucose homeostasis. However, at present, their exact physiological role and their nutrient sensing mechanisms are not clear. Glycolysis appears to be important to glucose-sensing and may also be involved in lactate, fatty acid and leptin induced signalling via modulation of AMPK, especially in GE neurones. Since GK is central to the glucose-sensing mechanism, modulating its expression may help to elucidate the physiological role of glucose-sensing neurones. rAAV offers a safe and robust method of gene transfer which, by stereotaxic injection into adult animals, avoids problems associated with embryonic compensation. With stereotaxic injection of rAAV glucokinase (rAAV-GKS) and rAAV glucokinase antisense (rAAV-GKAS) it will be possible to modulate glucose sensing in specific hypothalamic nuclei, without reliance on nuclei specific promoters. This is attractive, since it is possible, if not probable, that glucose-sensing neurones perform different functions depending on location.

Chapter 2

rAAV: Production and testing

2.1 Introduction

2.1.1 Studying appetite and neuroendocrinology using molecular approaches

The fields of neuroendocrinology and appetite regulation have benefited greatly from advances in molecular biology. Transgenic methods allow the expression of endogenous genes to be increased, decreased or completely knocked out. It is also possible to introduce genes into species and areas of the body in which they are not normally expressed. Such methods offer insight into gene functions that were not previously possible.

Prior to these molecular advances the field of appetite regulation relied heavily on administration of compounds via cannulation of a desired location (e.g. the third cerebral ventricle or specific hypothalamic nuclei). CNS injection of substances, including neuropeptides and nutrients (such as glucose), have greatly increased the understanding of neuroendocrinology and appetite regulation (Zarjevski *et al*, 1993;Davis *et al*, 1981).

Daily ICV injections can be tolerated for a period of one to two weeks. However, ICV administrations of compounds can produce non-specific effects because the third cerebral ventricle bathes a number of hypothalamic and extra hypothalamic structures. Intranuclear injections increase specificity and localisation but daily injections are only tolerable for short periods (less than one week) due to destruction of tissue at the injection site. The presence of an indwelling cannula and repeated injection also increases the risk of infection. Finally, repeated injection protocols cause disruption to the normal behavioural patterns of research animals (including feeding behaviour) and increase stress.

2.1.2 Transgenic animals

In 1985, Gordon *et al* described a method in which purified plasmid DNA, containing segments of the herpes simplex virus and simian virus 40 genome, were microinjected into pronuceli of fertilized mouse oocytes. The fertilized oocytes were transferred to the oviducts of pseudopregnant host mice and allowed to develop to term. In the initial study, injection of several hundred embryos resulted in 78 viable young. Of these animals only two were positive for the plasmid DNA (Gordon *et al*, 1980). In the present day, the majority of transgenic animals are produced using similar methodology to that outlined by Gordon et al. Although the techniques have been refined the production of transgenic animals remains inefficient (Niemann & Kues, 2003).

A major limitation associated with knockout mice is the phenomenon of embryonic or developmental compensation. Embryonic compensation describes the ability of a fetus to adapt to the absence of a knocked out/in gene and develop phenotypically normal. An example of embryonic compensation is the AgRP/NPY double knockout mouse. NPY and AgRP are orexigenic neuropeptides. Knockout of NPY and AgRP would be expected to produce a phenotype displaying reduced energy intake and low bodyweight. Surprisingly, AgRP/NPY KO mice are normal with regard to food intake and bodyweight gain (Qian *et al*, 2002).

The developmental root of this phenotype is elegantly demonstrated by a transgenic mouse model in which AgRP/NPY neurones can be ablated in a temporally controlled manner using diphtheria toxin. Ablation of AgRP/NPY in neonatal mice has little effect on feeding behaviour. However, ablation of the same neurones in adult animals produces rapid starvation showing that early loss of certain pathways can be compensated for during development and early life (Luquet *et al*, 2005). There is a high degree of redundancy in the CNS pathways that regulate feeding behaviour, so embryonic knockout models are not ideal for the study of appetite circuits.

A further potential problem effecting KO animals is early life or embryonic lethality. Early life or embryonic lethality occurs when a gene is knocked out that is vital for pre or perinatal development. The glucokinase homozygote KO mouse is an example of an early life lethal KO. GK KO homozygotes die postnatally between days three and five, are markedly diabetic and do not feed (Yang *et al*, 2007). Replacing the pancreatic

form of glucokinase but not the hepatic form partially rescues the phenotype and animals survive into adulthood (Grupe *et al*, 1995). However, the pancreatic form of GK is expressed in the hypothalamus so this approach would not be applicable to the present work (Roncero *et al*, 2000).

Localising transgenesis to a specific region of the body is another hurdle associated with KO models. GK is expressed in various parts of the body including the central nervous system, liver and pancreas (Roncero *et al*, 2000 ;Iynedjian *et al*, 1986). Global GK KO heterozygotes have impaired β-cell response to glucose and are hypoglycaemic and hyperphagic (Yang *et al*, 2007). However, it is impossible to extrapolate the involvement of GK expressing cells in any one region of the body from this model.

By using tissue specific promoters it is possible to alter gene expression in distinct regions of the body or in a specific cell type. An example of this is the VMH specific leptin receptor KO mouse. These mice are produced by crossing two mouse lines. The first, the Sf1-Cre mouse expresses Cre recombinase only in cells that express Sf1. The second mouse is a Lepr flox/flox mouse in which the leptin receptor is flanked by lox-p sites. Cre recombinase excises DNA that is found between lox-p sites. Crossing these mouse lines produces mice in which Cre recombinase and lox-p are expressed together in Sf1 expressing cells. The result is a mouse with VMH specific KO of the leptin receptor because the VMH is the only region of the hypothalamus that expresses both the leptin receptor and Sf1 (Dhillon *et al*, 2006).

Unfortunately, this approach is not applicable to the present work because there is no ARC-specific promoter that would target all ARC neurones. The ARC is composed of a variety of cell populations and at present it is unclear exactly which cells express GK (Wang *et al*, 2004;Muroya *et al*, 1999;Ibrahim *et al*, 2003). For this reason and others discussed above, traditional transgenic methods do not lend themselves to the current project.

2.1.3 Gene transfer

Gene transfer offers a number of advantages over traditional transgenic approaches. Using stereotaxic injection of an appropriate vector it is possible to target specific hypothalamic nuclei in adult animals and a chosen gene of interest can be over or under expressed for the duration of the host's life. This negates the requirement for a site specific promoter and circumvents the problems associated with embryonic lethality and embryonic compensation. As such, gene transfer is a preferable method to traditional transgenic methods for this work.

2.1.4 Choice of Gene Transfer Vector

Desirable characteristics in a gene transfer vector include; ease of production, sustained transgene expression, unlimited insert size, the ability to target specific tissues and the ability to tranduce post-mitotic cells. It is also desirable that the vector of choice evokes a low host immune response and it may be desirable for transgene expression to be reversible (Park *et al*, 2008). At present, no single perfect gene transfer vector exists but there are a wide variety of vectors available each with desirable and undesirable attributes.

Gene transfer vectors may be broadly divided into two categories; viral and non-viral. In general, viral vectors are a more efficient method of gene transfer, especially *in vivo*. However, the introduction of viral proteins during gene transfer using viruses can activate innate and acquired immune responses which can limit gene expression and negatively affect the health of the host (Wells, 2004).

Recombinant viral vectors are extremely useful in animal research because they are; able to recognise host cells, are transported across cells membranes and transfer genetic material to the cell nucleus. They are also able to produce sustained transgene expression by effectively high-jacking cellular protein synthesising machinery. At present, their use in humans is limited due to toxicity and immunogenic reaction. However, a number of different viral vectors have been used successfully in animal

research and a great deal of effort is focused on creating gene vectors that will be better tolerated by humans.

2.1.4.1 **Adenoviruses**

Adenoviruses are double stranded DNA viruses with a 36kb genome. In nature, adenoviruses cause infections of the respiratory tract and most humans come into contact with various serotypes during early life. In laboratory settings most recombinant adenoviruses are derived from serotypes 2 and 5 (Snyder *et al*, 2010).

First generation replication-deficient adenoviruses were produced by deleting the E1a and E1b genes, leaving 90% of the viral genome intact. These viruses are capable of carrying large transgenes and produce high levels of infection. In organisms that have not previously been exposed to adenoviruses transgene expression is sustained. However, pre-existing immunity to adenoviruses severely limits duration of transgene expression (Kaplan *et al*, 1997).

High capacity, or gutless, adenoviruses have recently been developed which contain only the minimum proportion of the viral genome required for infection. Due to the removal of most of the viral genome high capacity adenoviruses are capable of producing sustained transgene expression in animals that have been previously immunized against adenovirus (Barcia *et al*, 2007).

2.1.4.2 **Retroviruses and Lentiviruses**

Retroviruses are small single stranded RNA viruses with a carrying capacity of approximately 7-12kb. Following infection of a host cell the viral genome must first be converted to double stranded DNA by reverse transcriptase. Next, the double stranded DNA integrates randomly into the host genome (Temin & Baltimore, 1972). The random integration of the newly formed double stranded DNA is problematic in both clinical and research settings because of the possibility of insertional mutagenesis of host genes. Retroviruses are also limited in their uses because they are only able to

tranduce dividing cells and transgene expression can only occur in cells that are actively replicating (Miller *et al*, 1990).

Lentiviruses are a subgroup of retroviruses which include human immunodeficiency virus type I and II. Unlike other retroviruses, they are able to tranduce non-dividing cells and produce sustained transgene expression. As such, they can be suitable vectors for gene transfer into tissues including the brain, eye, lungs and pancreas (Naldini *et al*, 1996;Miyoshi *et al*, 1997). Many lentiviruses are extremely pathogenic and cause a number of slow-progress disease states. For this reason, safety is an important concern when working with lentiviruses.

2.1.4.3 **Herpesviruses**

Herpes viruses are enveloped double-stranded DNA viruses. They are responsible for a number of human diseases including; herpes labialis and genitalis (Nishiyama, 2004). Herpes viruses are naturally neurotropic and have the capacity to carry large trangenes and infect a broad range of cell types. As such, they are an attractive vector for research and clinical trials involving the nervous system.

Replication-defective herpes vectors, which lack viral replication genes including thymidine kinase, have been shown to be effective in rodents when introduced into the CNS. Recently, herpes viral vectors have been tested in a phase I clinical trial in humans (Wolfe *et al*, 2009).

The large and complicated nature of the herpes genome makes the virus complicated and potentially dangerous to use. In addition, the virus can be strongly immunogenic and cytotoxic.

2.1.4.4 **Adeno-associated virus**

Adeno-associated virus (AAV) is a small non-enveloped dependovirus measuring approximately 20-25nm. The AAV genome comprises a single strand of linear DNA of approximately 4.7kb. Human infection with AAV is extremely common; 90% of humans produce antibodies against at least one AAV serotype. However, AAV is considered non-pathogenic because it has not been associated with any human disease. In addition, as a dependovirus, AAV viruses are replication deficient and do not possess innate lytic ability (Atchison & Casto, 1965). Because of these qualities, AAV is extremely safe to work with and with modification is a safe viral vector. In addition, AAV is very stable and is resistant to repeat freeze thawing, temperatures up to 65˚C and certain proteases.

An AAV viral particle is composed of 26% DNA and 74% protein. Each virion contains one copy of the viral genome which may be packaged as positive-sense (5'-3') or negative-sense (3'-5') (Berns & Adler, 1972). The AAV serotype 2 genome is comprised of two open reading frames that are flanked by inverted terminal repeats (ITRs) (Srivastava *et al*, 1983). ITRs are 145 base pair sequences that are required for viral DNA replication, viral packaging and host genome integration. Each ITR contains a 125 base pair palindromic sequence which forms a hairpin structure and acts as the origin of replication and as a primer for host-cell mediated second strand DNA synthesis (Lusby *et al*, 1980;Bohenzky *et al*, 1988).

In addition to the ITRs, the AAV genome contains the Rep and Cap genes. The Rep gene is under the control of two promoters (p5 and p19) and encodes four overlapping proteins Rep78, Rep68, Rep52 and Rep40 (Kyostio *et al*, 1994). Wild type AAV integrates in a site specific manner into human chromosome 19. In the absence of the Rep gene, AAV remains episomal or integrates into the host genome randomly (Weitzman *et al*, 1994). Rep proteins are also involved in viral DNA packaging and have endonuclease and helicase activity (Im & Muzyczka, 1990) (figure 2.1).

The Cap gene is under the control of the p40 promoter and encodes the structural proteins VP1, VP2 and VP3 which form the viral protein coat (figure 2.1). AAV possess an icosahedral protein coat that is formed of 60 capsid proteins with 85% of protein

mass being made up by the smallest of the coat proteins VP3 (Rose *et al*, 1971;Jay *et al*, 1981).

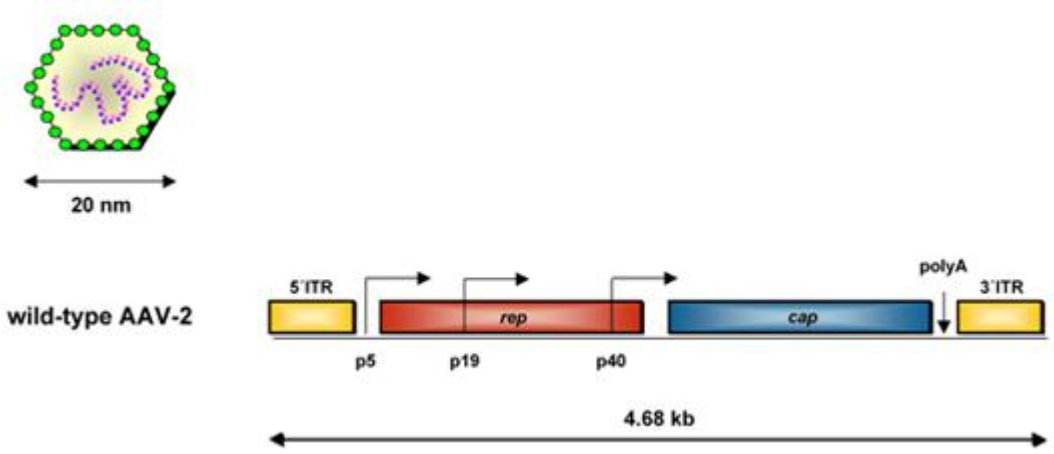


Figure 2.1: Schematic of wild-type AAV-2 serotype genome.

2.1.4.5 **Recombinant adeno-associated virus**

Recombinant adeno-associated viruses (rAAV) are a commonly used viral vector, Rep and Cap genes are removed from the packaged genome leaving only the ITRs. Since the ITRs are not translated rAAV does not produce any viral proteins (Samulski *et al*, 1989). This means that host immune response to rAAV is extremely low and trangene expression is sustained. Although rAAV administration does not result in inflammation it has been shown that antibodies are formed against the capsid proteins. This is not problematic if the virus is only introduced on a single occasion to a host that does not have pre-existing immunity. However, repeat administration or administration to an immune primed host can result in inflammatory responses and limited trangene expression (Zaiss & Muruve, 2005).

rAAV serotype 2 has a strong neurotropism. So, when injected into the brain, rAAV-2 infection is largely neurone specific (Mandel *et al*, 1998). The neurotropism of serotype 2 is dependent on specific cell surface proteins. Heparan sulphate proteoglycan, a member of the ubiquitously expressed protoglycan family, is necessary for efficient attachment and infection of neurones (Summerford & Samulski, 1998). In addition, it

has been shown that infection is further improved by the expression of the fibroblast growth receptor and the alphaVbeta5 integrin receptor which are both found on the neurone cell surface (Qing *et al*, 1999;Summerford *et al*, 1999). However, the role of the alphaVbeta5 integrin receptor has been disputed and the methods utilized in the work of Summerford *et al* have been criticised (Qiu & Brown, 1999).

Upon infection, rAAV travels to the cell nucleus where its single stranded viral genome is converted to double stranded DNA before gene transcription can occur. The production of the second DNA strand delays transcription and is considered a rate-limiting step in transgene expression (Afione *et al*, 2000;Ferrari *et al*, 1996). Within the nucleus, the rAAV genome can exist episomally or randomly integrated into the host genome (Duan *et al*, 1998).

rAAV has been used to investigate the role of a number of neuropeptides in the CNS of adult animals. Gardiner et al utilized a rAAV vector encoding antisense neuropeptide Y targeted at the ARC. Infection with rAAV antisense NPY resulted in decreased food intake and bodyweight weight compared to rAAV-eGFP injected controls (Gardiner *et al*, 2005). This study and others like it demonstrate the potential of rAAV as a tool for the study of hypothalamic energy regulation. To date, no studies have been published that utilize rAAV to chronically over express GK in the CNS.

2.2 Aims and Objectives

I aim to investigate the role of hypothalamic glucose-sensing in the regulation of energy balance and glucose homeostasis. In order to do this I will:

1. Modify pTR-CGW plasmid to contain GK (GKS) and antisense GK (GKAS) cassettes.
2. Test the efficacy of the GKS-pTR-CGW and GKAS-pTR-CGW plasmids by transfecting cultured cells and subsequently performing enzymatic GK activity assay.

2.3 Materials and methods

Unless stated otherwise all chemicals were purchased from Sigma, Poole, Dorset, UK.

2.3.1 Production of GKAS using polymerase chain reaction (PCR)

2.3.1.1 Reverse transcription

Materials

Rat hypothalamic RNA (5mg/ml)
10mM dNTPs (GE Healthcare, Buckinghamshire, UK)
5x Reverse transcriptase buffer (Promega, Madison, WI)
Avian myoblastoma virus reverse transcriptase (RT) 10U/µl (Promega)
Oligo $dT_{(12\text{-}18)}$ 200ng/µl (GE Healthcare)

Method

The reaction was set up in a final volume of 20µl containing the following: 1mg/ml RNA, 1x reverse transcriptase buffer, 1mM dNTPs and 10mg/ml oligo dT. The solution was heated to 65ºC for 5 minutes and allowed to cool at room temperature for 30 minutes, 10U RT were then added and the reaction was incubated at 42ºC for 1 hour. The reaction was then used in PCR.

2.3.1.2 **PCR**

Materials

10x Taq buffer

20µM oligonucleotide primers (Oswel DNA service, Southampton, UK)

Taq DNA polymerase (5U/µl)

10mM dNTPs (GE Healthcare)

Reverse Transcriptase Reaction (RTr)

pCMV4.GKB1 encoding full length GK (gift from M.Magnuson, Vanderbilt University)

Method

For glucokinase antisense (GKAS), cDNA fragments from the RT reaction were amplified using primers corresponding to sequences on the glucokinase gene (nucleotides 1-185, figure 2.2). Half of the reverse transcription reaction was added to a tube containing 1x taq buffer, 0.2mM dNTPs, 200nM oligonucleotide primers. The reaction was heated to 95ºC for 5 minutes and then 5U taq DNA polymerase were added. The reaction was then cycled thirty times through the following temperatures: 95ºC for thirty seconds, 55ºC for thirty seconds and 72ºC for thirty seconds. After completion of the reaction, 10µl of the PCR products were visualised by gel electrophoresis on a 1% TAE/agarose gel.

For glucokinase sense (GKS), the above method was repeated with the exception that 1ul pCMV4.GKB1 was added to the reaction in the place of the reverse transcriptase reaction and amplification was achieved using primers corresponding to sequences on the pCMV4.GKB1 plasmid (nucleotides 787-2247, figure 2.2).

Primer	Sequence
GKS forward	5’-ACGTACCGGTATTCACATCTGGTACCTGGG -3’
GKS reverse	5’-AGCTCGTACGTATTAGGACAAGGCTGGTGG-3’
GKAS forward	5’-AGCTTGTACAGGGGGTCCCAGTTCACCTGG-3’
GKAS reverse	5’-AGCTGGATCCTGGGTCTCCAGGCCCAGGCC-3’

Figure 2.2 PCR primers used for amplification of GK gene sequences.

2.3.1.3 **Visualisation of PCR products**

Materials

Agarose, type II-A medium EEO

50x TAE: (appendix I)

2M Tris-Acetate pH 8.5

0.05M EDTA pH 8.0

Ethidium Bromide (10mg/ml) (VWR International Ltd, Poole, UK)

DNA marker (BRL 1Kb plus ladder, Invitrogen , Paisley, UK)

Gel loading buffer (appendix I)

Method

A 1% (w/v) agarose gel was prepared by dissolving the agarose in 1x TAE using a microwave oven. The gel was cooled to 45ºC and ethidium bromide added to a final concentration of 0.5µg/ml. Once set the gel was placed into an electrophoresis tank containing 0.5 TAE with 0.5µg/ml ethidium bromide. Three microlitres of gel loading buffer was added to 10µl PCR product, 1µl of DNA marker was added to 9µl GDW and treated in the same way. The samples were loaded onto the gel and electrophoresed at 10V/cm. The DNA was visualised by illumination with UV light (300nm).

2.3.2 Insertion of GK and GKAS into pTR-CGW

One of the most important advances in the field of molecular biology was the ability to cut DNA at specific sites and to ligate the cut ends. Restriction endonucleases (isolated from bacteria) recognise specific target sites within double stranded DNA and cleave it. Ligating cut fragments relies on the use of a virus-derived enzyme that catalyses the formation of phosphodiester bonds between a free 5’ phosphate and a free 3’ hydroxyl group (Sambrook *et al,* 1989)

2.3.2.1 **Restriction endonuclease digestion of PCR products and pTR-CGW**

Materials

PCR products
pTR-CGW (rAAV plasmid) (gift from Dr. Verhaggen, Amsterdam)
Restriction endonucleases: BamHI, BsrGI, BsiWI, AgeI (New England Biolabs, Hitchin, Hertfordshire, UK)
10x Restriction buffer (as supplied) (appendix I)
10x Bovine serum albumin (BSA) (New England Biolabs)
Phenol/Chloroform pH8 (VWR)
5M Sodium acetate, pH 5.2 (appendix I)
Shrimp alkali phosphatase (SAP) 4U/µl (GE Healthcare)

Method

In separate reactions the PCR products and pTR-CGW were diluted in autoclaved glass distilled water (GDW), restriction buffer and BSA added to give a final concentration of 1x. Forty units of each restriction endonuclease (for GKAS BamHI and BsrGI. For GKS AgeI and BsiWI) were added; the total volume of enzyme added was kept below 10% of the final volume. The reaction was incubated for at least one hour at 37ºC. In the digestion of pTR-CGW, 8U SAP was added 30 minutes before the end of the incubation. SAP removes 5' phosphate groups preventing self-ligation of the plasmid. The reactions were extracted with an equal volume of phenol/chloroform and the phases separated by centrifugation for 3 minutes at 13,000xg. The DNA was ethanol precipitated with 0.1 volumes sodium acetate pH5.2 and 2.5 volumes absolute ethanol and was incubated at -20ºC for at least one hour. The DNA was recovered by centrifugation for 7 minutes at 13,000xg.

2.3.2.2 **Electroelution of DNA fragments**

Following restriction digestion it is advantageous to purify the DNA fragment of interest and remove any contaminating fragments. This is especially true for plasmids as restriction digests are not 100% efficient and a small amount of closed plasmid DNA can produce a high background during transformations. The DNA was therefore size fractionated by electrophoresis on an agarose gel and the bands of interest electroeluted.

Materials

50x TAE
Dialysis tubing (VWR)
Gel loading buffer (appendix I)
DNA marker (Invitrogen)

Method

A 1% agarose gel was prepared (as described in section 2.3.1.2). The precipitated DNA was dissolved in 20µl GDW and 6µl loading buffer added. One microlitre of DNA marker was added to 9µl GDW and 3µl loading buffer added. Samples were loaded onto the gel and electrophoresed at 10V/cm.

The DNA was visualised by illumination with UV light, the band of interest was cut out from the gel using a scalpel and placed into dialysis tubing sealed at one end with a clip. Four hundred microlitres of 0.5x TAE was added to the gel slice, air excluded from the end of the tubing and the other end sealed with a clip. The DNA was eluted from the gel by electrophoresis at 20V/cm for 20 minutes. The TAE was removed from the tubing, phenol/chloroform extracted and the DNA was recovered by ethanol precipitation (as described in section 2.3.2.1). The DNA was dissolved in GDW and quantified visually by running 1µl on a 1% agarose gel.

2.3.2.3 **Ligation of PCR product into pTR-CGW**

Materials

T4 DNA ligase, 6U/µl (New England Biolabs)
10x Ligase buffer (as supplied)
Digested PCR products
Digested pTR-CGW

Method

DNA ligation was used to insert the digested GKAS and GK into pTR-CGW plasmid. Twenty nanograms of plasmid DNA were dissolved in GDW and a fourfold molar excess of PCR product added. Ligase buffer was added to a final concentration of 1x and 6U T4 DNA ligase added to give a final volume of 10µl. The reaction was incubated at 16ºC overnight.

2.3.3 Preparation of GKS-pTR-CGW-plasmid and GKAS-pTR-CGW-plasmid

2.3.3.1 Transformation of competent bacteria by electroporation

Competent bacteria can be induced to take up DNA via the process of electroporation. Passing a voltage across a bacteria/plasmid mixture opens transient pores in the bacteria plasma membrane allowing the plasmid to move into the cell. pTR-GCW contains an ampillicin resistance gene. Subsequent incubation allows the expression of the resistance genes before exposure to antibiotic.

Materials

Ligation reaction
LB (appendix I)
$LB_{(amp)}$ plates
JC811 bacteria (ATCC, Middlesex, UK)
Glyercol (VWR)

Method

Prior to transformation, all salts must be removed from the reaction mixture to prevent arcing during electroporation. One microliter of glycogen was added to the ligation reaction to act as a carrier and the reaction ethanol precipitated for at least one hour (as described in section 2.3.2.1). DNA was recovered by centrifugation for 7 minutes at 13000xg. The DNA was then dissolved in 10 µl GDW.

An aliquot of frozen bacteria (JC811 cells) was thawed on ice, 10ng of plasmid (5µl ligation reaction) added and the mixture transferred to an electrocuvette with an intra-electrode distance of 1mm. A voltage of 1.4 kilovolts was then passed across the cuvette. Eight hundred microlitres of warmed LB was then added and the reaction incubated at 37ºC for an hour. Agar plates (supplemented with 100µg/ml ampicillin) were warmed and 150µl of the transformed bacteria added to the plate. The bacteria were spread over the surface of the agar, the plate inverted and incubated at 37ºC overnight.

2.3.3.2 **Small scale preparation of plasmid**

Plasmids are isolated on a small scale to allow several clones to be analysed simultaneously (Sambrook *et al*, 1989). To isolate the plasmids from bacteria it is necessary to disrupt the cell wall to release the plasmid and at the same time contaminants (proteins, genomic DNA and RNA) must be removed. Treatment with alkaline SDS disrupts the cell wall and bacterial debris is then precipitated using potassium acetate. This step also removes most of the genomic DNA, RNA is removed later by treatment with RNase A.

Materials

$LB_{(amp)}$
GTE (appendix I)
0.2M sodium hydroxide 1% SDS (v/v) (appendix I)
5M potassium acetate (appendix I)
5M sodium acetate (appendix I)
Phenol/Chloroform
Propan-2-ol (VWR)

Method

A single bacterial colony was placed in 2ml LB supplemented with ampicillin. This was incubated overnight at 37°C with vigorous shaking. From this 1.5ml was removed and centrifuged at 13,000xg for 3 minutes, the remainder was stored at 4°C for future use. The supernatant was removed and the bacterial pellet resuspended in 100µl GTE. Two hundred microliters of alkaline SDS were added to the bacteria and the mixture left on ice for 5 minutes, 150µl 5M KAc was then added and the mixture left on ice for a further 5 minutes. The mixture was centrifuged at 13,000xg for 5 minutes and 350µl supernatant was removed to a fresh tube. Phenol chloroform extraction was carried out and the DNA precipitated by the addition of 0.6 volume propan-2-ol and incubation at room temperature for 10 minutes. This was centrifuged at 13,000xg for 7 minutes to pellet the DNA. Following removal of the supernatant, DNA was dissolved in 100µl GDW. The DNA was recovered by ethanol precipitated with 0.1 volumes sodium

acetate pH5.2 and 2.5 volumes absolute ethanol and was incubated at -20ºC for at least one hour.

Restriction endonuclease digestion was carried out (as described in 2.3.2.1) to identify which clones contained an insert of the correct size. Purified DNA was dissolved in 10µl GDW; GKS plasmid was digested by AgeI and BsiWI and GKAS plasmid was digested by BamHI and BsrGI. Both plasmids were also digested by XmaI to check for presence of inverted terminal repeats (ITRs) and visualised by gel electrophoresis. Clones containing the correct insert and ITRs were selected for large scale preparation.

2.3.3.3 **Large scale preparation of plasmid**

Materials

$LB_{(amp)}$
GTE
Lysozyme
0.2M sodium hydroxide/1% (w/v) SDS
5M potassium acetate (KAc)
Propan-2-ol
100x TE (appendix I)
DNase free RNase A 10mg/ml in GDW (GE Healthcare)
Phenol/Chloroform (VWR)

Method

A small quantity of bacteria containing pTR-CGW with the correct size insert was inoculated into 500ml $LB_{(amp)}$ and incubated at 37ºC overnight with vigorous shaking. The bacteria were recovered by centrifugation for 8 minutes at 3000xg (4000rpm in HS-4 rotor in RC-5B superspeed centrifuge, Du Pont, Bristol, UK) at 4ºC. The pellet was resuspended in 25ml GTE supplemented with 2mg/ml lysozyme and the sample incubated at room temperature for 5 minutes. Fifty millilitres of SDS/NaOH were added, the sample mixed by inversion and incubated on ice for 5 minutes. Then 38ml 5M KAc were added, the sample mixed by inversion and incubated on ice for 10

minutes. Bacterial debris was removed by centrifugation for 15 minutes at 9000xg (7000rpm in HS-4 rotor in RC-5B superspeed centrifuge, Du Pont) at 4ºC. The supernatant was transferred to a clean tube and 0.6 volumes propan-2-ol added. The sample was incubated on ice for 15 minutes and the DNA recovered by centrifugation for 15 minutes at 9000xg at 4ºC. The pellet was dissolved in 10ml GDW to which 100µl 100x TE was added. RNase A was added at a concentration of 0.1mg/ml and the reaction incubated at 37ºC for 30 minutes. The reaction was extracted with an equal volume of phenol/chloroform and the phases separated by centrifugation for 20 minutes at 10000xg and 4ºC. The DNA was recovered by addition of 0.1 volumes 2M sodium acetate pH 5.2 and one volume propan-2-ol and incubation at -20ºC for at least one hour. The DNA was then purified by caesium chloride gradient.

2.3.3.4 **Caesium chloride gradient purification**

Large scale plasmid purification was carried out using a caesium chloride gradient (Sambrook *et al*, 1989). This purification method depends on the decrease in density of nucleic acids when bound to ethidium bromide. Because ethidium bromide binds by intercalation into the DNA, it causes unwinding of the helix. In closed circular DNA this increases supercoiling of the plasmid so binding of ethidium bromide is limited and the plasmid has a higher buoyant density than linear or nicked plasmids. The difference in buoyant density allows separation of the plasmid on a caesium chloride density gradient.

Materials

TES:

50mM Tris-HCL, pH 8.0 (appendix I)

50mM sodium chloride

5 mM EDTA

Caesium chloride (Boehringer, Berkshire, UK)

10mg/ml ethidium bromide

Caesium chloride-saturated propan-2-ol (appendix I)

Method

DNA obtained from large scale plasmid purification was recovered by centrifugation for 20 minutes at 24,000xg (12,000rpm in HBS rotor in RC5B superspeed centrifuge, Du Pont) and 4ºC. The DNA was then dissolved in 8.25ml TES. Eight point four grams of caesium chloride were dissolved in the DNA solution and 150µl of ethidium bromide added and the solution mixed. The sample was divided into two polyallomer tubes (Ultracrimp, Du Pont), balanced, and overlaid with mineral oil. The tubes were sealed and centrifuged for 16 hours at 20ºC and 216,518xg (60,000rpm in a T-8100 rotor in a Sorvall 100SE centrifuge, Fisher Scientific, Loughborough, UK).

After centrifugation, DNA bands were visualised by UV illumination and the band containing the closed pTR-CGW DNA removed using a 20-gauge needle and a 2ml syringe. Ethidium bromide was removed from the plasmid by repeated extraction with an equal volume of caesium chloride saturated propan-2-ol, until both phases were colourless. The DNA was precipitated by addition of two volumes of GDW and six volumes of room temperature absolute ethanol. DNA was recovered by centrifugation at 24,000xg and 20ºC for 15minutes. The DNA pellet was dissolved in 0.4ml GDW, ethanol precipitated and recovered by centrifugation for 7 minutes at 13,000xg. The DNA was then dissolved in 1ml GDW.

pTR-CGW was then quantified spectrophotometrically, 10µl DNA was diluted 1:100 and placed into a quartz cuvette. Absorbance was read at 260 and 280nm UV 1101 spectrophotometer (WPA, Cambridgeshire, UK). The reading at 280nm gives an indication of the purity of the sample as phenol absorbs more strongly at 280nm than DNA. The concentration of the DNA was calculated using the following formula:

Concentration (µg/ml) = (A_{260} x dilution factor) x 50

Samples were subjected to endonuclease digestion. GKAS-pTR-CGW was digested by BamHI and BsrGI. GKS-pTR-CGW was digested AgeI and BsiWI. Both plasmids were digested by XmaI to confirm the presence of ITRs.

Insert sequences were confirmed by DNA sequencing (Genomics Core Laboratory, Imperial College London, UK).

2.3.3.5 **DNA sequencing**

Sequencing of GKS-pTR-CGW and GKAS-pTR-CGW plasmids was performed by the Imperial College Genomics Core Laboratory. Prior to sequencing each plasmid was diluted and mixed with either the forward or reverse primer that was used during the PCR reaction (see figure 2.2). Each reaction was 10ul and contained 200ng of plasmid DNA and 3.2pmole of primer. In total four reactions were produced; GKS-pTR-CGW plus forward primer, GKS-pTR-CGW plus reverse primer, GKAS-pTR-CGW plus forward primer and GKAS-pTR-CGW plus reverse primer. Samples were cycle sequenced using BigDye v3.1 (Applied Biosystems Ltd, Warrington, UK).

Sequencing results were analysed for homology to known rat GK gene sequences using the Basic Local Alignment Search Tool (BLAST) on the National Centre for Biotechnology Information (NCBI) internet site.

2.3.4 Cell Culture

2.3.4.1 **Maintenance of cells**

Materials

Unless otherwise stated all cell-culture materials were purchased from Invitrogen

Human embryonic kidney cells (HEK293T. ATCC)

Human hepatocellular carcinoma (HEPG2. ATCC)

Dulbeccos modified eagle medium (DMEM)

Foetal Bovine Serum, heat inactivated (FBS)

2.5% Trypsin in hanks balanced salt solution

Versene: (appendix I)

0.14M sodium chloride

2.7mM potassium chloride

8mM di-sodium hydrogen orthophosphate

3mM EDTA

1.5mM potassium di-hydrogen orthophosphate

0.1%(v/v) phenol red

Method

Human embryonic kidney cells (HEK 293T) and human hepatocellular carcinoma cells (HEPG2) were cultured in DMEM containing 4.5mg/ml glucose and 1mM sodium pyruvate supplemented with 10% (v/v) FBS at 37^{o}C in a 5% carbon dioxide atmosphere. Medium was changed every three days and the cells sub-cultured when 70-80% confluent using 0.25% trypsin in versene. Briefly, the medium was aspirated and the cells incubated at 37^{o}C with fresh versene/trypsin until they detached from the flask. The trypsin was inactivated by the addition of 10ml of fresh medium and the cells recovered by centrifugation for 5 minutes at 100xg. The cells were resuspended in fresh medium and transferred to a new flask at a 1:10 dilution.

2.3.4.2 **Transfection of cells with GKS and GKAS pTR-CGW plasmids**

Untreated mammalian cells, in contrast to bacteria, absorb naked DNA from solution. However, the rate of absorption is slow and the proportion of cells transfected is low. Such transfection also requires the use of large quantities of the exogenous DNA. Several techniques have been developed to increase the efficiency of the process including chemical, membrane disruption (e.g. electroporation) and receptor mediated. In this work, calcium phosphate co-precipitation was used. HEK293T cells, which do not express GK, were transfected with GKS plasmid. HEPG2 cells, which express large quantities of GK, were transfected with GKAS plasmid. In both cases, pTR-CGW was transfected as a control.

Materials

2x HEPES-buffered saline (HBS) (appendix I)
- 280mM sodium chloride
- 10mM potassium chloride
- 1.5mM di-sodium hydrogen orthophosphate
- 12mM dextrose
- 50mM HEPES, pH7.05

2M calcium chloride (appendix I)

0.1xTE:
- 1mM Tris-HCl, pH 8.0
- 0.1mM EDTA, pH 8.0

DNA in 0.1 x TE:
- 40µg/ml plasmid DNA

DMEM

Method: transient transfection

Twenty four hours before transfection, cells at approximately 60% confluence were sub-cultured and plated at a density of $1x10^4$cells/cm in 90mm Petri dishes. The following day media was replaced with fresh media. A co-precipitate was formed by mixing 300µl 10xHBS with 28µg plasmid DNA in 2.5ml of GDW and then slowly adding 180µl 2M calcium chloride, while gently mixing using air expelled from a pipette

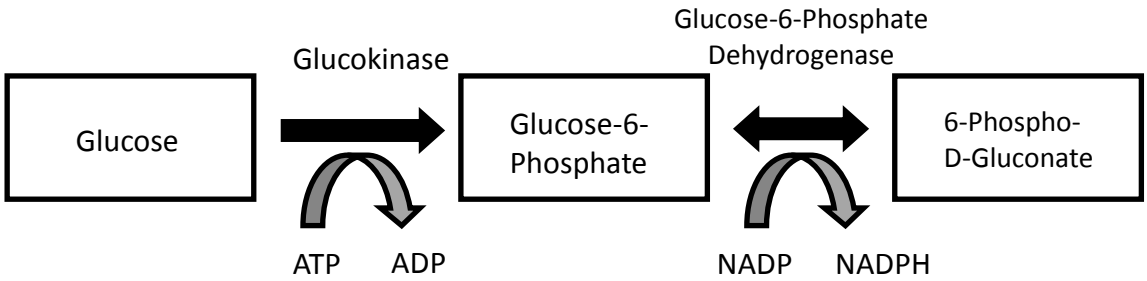
aid. The solution was incubated at room temperature for 5 minutes to allow formation of the precipitate. The precipitate was added to the cells and they were incubated at 37^{o}C in 5% carbon dioxide for 18 hours. The medium containing the precipitate was replaced with fresh media, cells were incubated for 48 hours after which time cells were lysed in GK extraction buffer and enzymatic assay was performed for GK activity as described in below.

2.3.5 Glucokinase activity assays

2.3.5.1 **Standard glucokinase activity assay**

The glucokinase assay is a coupled spectrophotometric assay. The first step is that catalysed by glucokinase in which glucose is phosphorylated to form glucose -6-phosphate (G-6-P) in the presence of ATP.

In the second step the G-6-P produced in step one is converted to 6–phospho-D-gluconate by glucose-6-phosphate dehydrogenase with a concomitant conversion of NADP to NADPH. The reactions are summarised below.



This increase in NADPH concentration can be quantified spectrophotometrically by a change in absorbance at 340nm. Thus the change in absorbance at 340nm can be used as an indirect measurement of GK activity.

Both GK and hexokinase (Hx) phosphorylate glucose, however GK has a relatively low affinity and high Km for glucose when compared to Hx. In order to differentiate GK from Hx activity the assay is performed in a reaction containing either 100mM or 0.5mM glucose as a substrate. At 0.5mM glucose GK activity should be low whereas Hx activity should be near maximal. At 100mM activity for both enzymes should be near maximal. Therefore GK activity for each sample can be calculated as:

$$A_{(100mM\ glucose)} - A_{(0.5mM\ glucose)} = GK\ activity$$

This figure can then be compared to a standard curve for GK activity (For calculations see appendix III).

Materials

GK extraction buffer (appendix I)
glucokinase (0.25µg/ml)
100mM adenosine 5'trisphosphate
2M and 0.01M D-glucose
100mM Gly-Gly, pH8 (appendix I)
12.5mM NADP
1M $MgCl_2$ (appendix I)
2U glucose-6-phosphate dehydrogenase

Method

Punch biopsies of various hypothalamic nuclei or HEK293T cells were homogenised in 200µl GK extraction buffer using a handheld homogeniser. The homogenate was centrifuged for 40 minutes at 13000xg at 4ºC. The supernatant was then removed. In order to calculate glucokinase activity in samples a standard curve for GK activity was used containing: 0.025µg GK, 0.02µg, 0.0175µg, 0.015µg, 0.01µg, 0.0075µg, 0.005µg and 0.001µg of glucokinase.

Assay reactions were set up in a total volume of 1ml, containing: 500µl 100mM Gly-Gly, 7.5µl 1M $MgCl_2$, 50µl 100mM ATP, 60µl 12.5mM NADP, 0.002µg glucose-6-phosphate dehydrogenase, and 50µl of either 2M or 10mM glucose. The reaction was initiated by the addition of either glucokinase standard or hypothalamus homogenate.

The reaction was incubated at 37˚C for 1 hour. Absorbance at 340nm was measured for each sample using a UV 1101 spectrophotometer (WPA, UK).

2.3.5.2 **Optimized glucokinase activity assay**

The optimized GK assay is similar to the standard assay with the exception of the addition of 5-thio-d-glucose-6-phosphate (5TG) (at a final concentration of 45 µM) and 3-O-methyl-N-acetylglucosamine (3OMG) (at a final concentration of 0.5mM). 5TG inhibits Hx activity without effecting GK, while 3OMG inhibits N-acetylglucosamine kinase, which phosphorylates glucose at high glucose concentrations. The addition of these agents is believed to increase the accuracy of the assay.

Materials

GK extraction buffer

glucokinase (0.25µg/ml)
100mM adenosine trisphosphate
2M D-glucose
100mM Gly-Gly, pH8
12.5mM NADP
1M $MgCl_2$
2U glucose-6-phosphate dehydrogenase
3-O-methyl-N-acetylglucosamine
5-thio-d-glucose-6-phosphate

Method

The assay is performed (as described in 2.3.5.1) except that 3-O-methyl-N-acetylglucosamine and 5-thio-d-glucose-6-phosphate are added to the reaction mixture prior to the addition of the GK standard or cell/hypothalamic homogenate. In addition, since Hx activity is inhibited there is no requirement for an assay carried out with 0.01M D-glucose as the substrate.

2.3.5.3 **Comparison of GK assay methodologies**

The two GK assay methodologies were compared using HEK293T cell which were maintained as described in 2.3.4.1. Prior to the assay, cells were washed twice in 1x PBS before being resuspended in GK extraction buffer. Cells were lysed using a handheld homogeniser and assay were performed as described in 2.3.5.1 and 2.3.5.2.

HEK293T cell do not express glucokinase but do express other hexokinases. Since both assays are expected to be specific for GK activity the NADPH production in both should be zero. Assays were performed via the standard method and the optimized method and where compared against an assay performed without HX inhibition. Assays were performed in triplicate and absorbance was read at 340nm.

NADPH production was calculated using the millimolar extinction coefficient 6.27 (ξ_{mM}) at 340nm using the following equation

$A_{340nm}/6.27\xi_{mM}$= mM concentration of NADPH

2.3.6 Production of rAAV-GKS, GKAS-rAAV and rAAV-eGFP particles

2.3.6.1 **Production of rAAV**

Adeno-associated virus was produced by Dr. J. Gardiner (Division for Diabetes, Endocrinology and Metabolism) using the two plasmid system. Briefly, host cells (HEK293) are co-transfected with the rAAV plasmid pTR-CGW and a helper plasmid pDG using calcium phosphate. There is no homology between the two plasmids so they cannot recombine and form wild-type virus. This results in the production of rAAV particles. To release the particles cells are lysed by freeze thawing and the rAAV produced is purified.

HEK293 cells were maintained in DMEM containing 4500µg/ml glucose and 1mM sodium pyruvate supplemented with 10% (v/v) FBS.

2.3.6.2 **Calcium phosphate transfection**

Materials

HEK293 cells
Plasmids
pTR-CGW (containing transgene)
pDG
10x HEBS buffer:
1.36M NaCl
0.05M KCl
0.007M $Na_2HPO_4.2H_20$
0.2M HEPES
0.125M glucose
2M $CaCl_2$

Methods

Cells were plated into a 10 chamber cell factory (L x W x H (mm): 335 x 205 x 190, culture area: 6320cm^2). Cells were incubated in 2000ml DMEM with 10% FBS. After 24 hours, when cells were 50% confluent, the culture medium was replaced (250ml culture medium was retained for transfection) and transfection performed 2 hours later.

Transfection mix was prepared for the cell factory, consisting of 560µg pTRCGW, 1.68mg pDG, 7.2ml 2M $CaCl_2$ and 52ml GDW. Immediately before transfection 12ml 10x HEBS buffer in 48ml GDW was added and mixed gently. After standing at room temperature for 1 minute the mixture was added slowly to 250ml DMEM supplemented with 10% FBS and added to the cell factory.

2.3.6.3 **Recovery and purification of rAAV**

Materials

0.01M PBS
DNaseI
Sepharoes column (GE Healthcare)
Iodixanol (Life Sciences Technology, Eggenstein, Germany)
0.3x PBS/0.1M NaCl
0.3x PBS/2mM EDTA
2M $MgCl_2$
Benzonase (Novagen, Nottingham, UK)
Lysis buffer (appendix I)

Methods

Forty-eight hours after transfection, cell medium was removed and cells were washed using 500ml PBS and then harvested using 1 L PBS/2mM EDTA. Cells were then recovered by centrifugation at 5000x*g* for 10 minutes, washed in 150ml PBS and recovered by centrifugation at 5000x*g* for 10 minutes. Cells were then resuspended in 60ml lysis buffer and aliquoted into four falcon tubes. Cells were subjected to three

cycles of 10 minutes in dry ice/ethanol followed by 10 minutes in a 37ºC waterbath. Seven point three microlitres of 2M $MgCl_2$ and 1.2µl Benzonase were then added to each falcon tube and incubated at 37ºC for 30 minutes. The reactions were then centrifuged at 2000x*g* for 10 minutes to pellet cell debris. The supernatant was removed and loaded into four 50ml polyallomer tubes (Beckman Coulter (U.K.), Buckinghamshire, UK) under layered with 100ml iodixanol gradient. The tubes were then topped up with lysis buffer, heat sealed and subjected to centrifugation at 69,000x*g* for 1 hour at 18ºC (in a Type 70 Ti rotor in a Sorvall 100SE centrifuge, Fisher Scientific). The top of each tube was punctured with an 18G needle and rAAV collected by puncturing the bottom of the tube and collecting 5ml of iodixanol gradient from the 60/40% interface. The fractions from the four tubes were pooled, added to 20ml PBS and loaded onto a Sepharose column which had been pre-washed with 25ml 0.1M NaCl/0.3x PBS and 50ml 0.3x PBS. The column was then washed with 50ml 0.3x PBS and the virus was eluted using 15ml 350mM NaCl/0.3xPBS. The elutant was transferred to an Apollo Concentrator containing 10ml PBS and subjected to centrifugation at 4000x*g* for 5 minutes. The flow through was discarded and 5ml PBS was added below the filter and 19.5ml PBS above. The tube was then subjected to centrifugation at 4000x*g* for 5 minutes and the 0.5ml remaining in the filter (which contained the rAAV) was aliquoted into eppendorf tubes. The viral titre was quantified by dot blot analysis.

2.3.7 Statistical analysis

Unpaired two tail t-test was used for experiments with two groups and analysis of variance (ANOVA) followed by Bonferroni *post hoc* analysis was used for experiments with more than two groups. $p<0.05$ was considered statistically significant throughout. Data analysis was performed using GraphPad Prism 4 software (CA, USA).

2.4 Results

2.4.1 PCR products

2.4.1.1 **GKS**

Following PCR, 10µl of GKS PCR product was visualised by gel electrophoresis. Comparison of the PCR product with a 1kb DNA ladder (Invitrogen) confirmed the presence of a band of between 1400-1600bp. The expected product size of this reaction was 1460bp.The presence of this band suggests that the reaction was successful.

2.4.1.2 **GKAS**

Following PCR, 10µl of GKAS PCR product was visualised by gel electrophoresis. Comparison of the PCR product with a 1kb DNA ladder confirmed the presence of a band of between 100-200bp. The expected product size of this reaction was 185bp. The presence of this band suggests that the reaction was successful.

2.4.2 Restriction endonuclease digestion of small scale plasmid preparation

DNA from small scale plasmid preparation was subjected to restriction endonuclease analysis to identify which clones contained the correct plasmid insert and retained their ITR's. GKS plasmid was digested by AgeI and BsiWI which should yield two bands; the cut plasmid of 4912bp and the GKS insert of 1460bp. GKAS plasmid was digested by BamHI and BsrGI and should yield two bands; the cut plasmid of 4892bp and the GKAS insert of 185bp. Both plasmids were also digested by XmaI to check for presence of ITR's. All products were visualised by gel electrophoresis. For both GKS and GKAS samples with the correct sized bands and strong ITRs were selected and used for large scale plasmid preparation.

2.4.3 Restriction endonuclease digestion of large scale plasmid preparation

2.4.3.1 **GKS**

Restriction endonuclease digestion of purified DNA from large scale GKS plasmid preparation using AgeI and BsiWI produced a band of between 1400-1600bp (figure 2.3, b). Digestion with XmaI showed strong ITR's (figure 2.3, a). Taken together this indicates that the plasmid contains the correct insert and the ITR's to allow expression of the viral DNA in host cells.

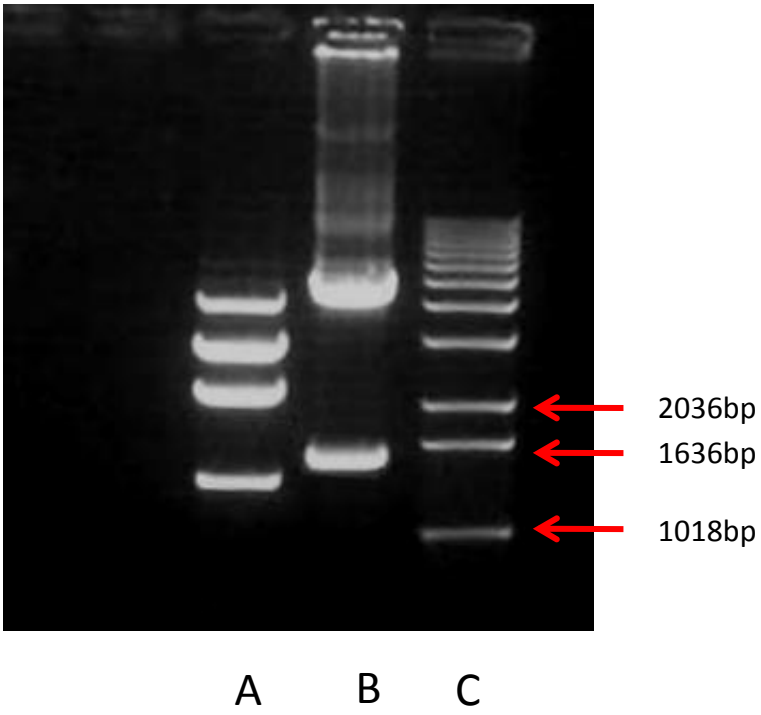


Figure 2.3 Gel electrophoresis of large scale plasmid production of GKS: *Purified DNA was digested by AgeI and BsiWI and produced a band of ~1450bp (b). Digestion with XmaI showed strong ITR's (a). Compared to Invitrogen 1kb ladder (c).*

2.4.3.2 **GKAS**

Restriction endonuclease digestion of purified DNA from large scale GKAS plasmid preparation using BamHI and BsrGI produced a band of between 100-200bp (figure 2.4, b). Digestion with XmaI showed strong ITR's (figure 2.4, a). Taken together this indicates that the plasmid contains the correct insert and the ITR's to allow expression of the viral DNA in host cells.

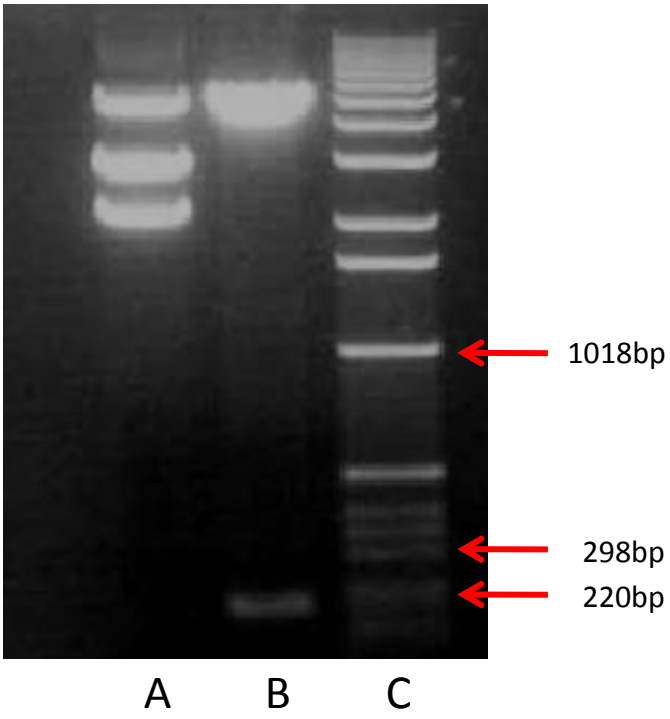


Figure 2.4 Gel electrophoresis of large scale plasmid production of GKAS: *Purified DNA was digested by BamHI and BsrG1 and produced a band of ~180bp (b). Digestion with XmaI showed strong ITR's (a).Compared to Invitrogen 1kb ladder (c).*

2.4.4 DNA sequencing

2.4.4.1 **GKS**

Sequencing results produced by the Imperial College Genomics Core laboratory were analysed using the nucleotide BLAST tool on the NCBI internet site. BLAST analysis of the GKS-pTR-CGW sequencing data revealed that the plasmid contained a full length copy of the glucokinase gene with 100% homology to pCMV4.GKB1 plasmid gifted from Vanderbilt University. As shown in figure 2.5.

```
Query  1     CTGGGCTGGTGGCTGCGCAGATGCTGGATGACAGAGCCAGGATGGAGGCCACCAAGAAGG  60
             ||||||||||||||||||||||||||||||||||||||||||||||||||||||||||||
Sbjct  1     CTGGGCTGGTGGCTGCGCAGATGCTGGATGACAGAGCCAGGATGGAGGCCACCAAGAAGG  60

Query  61    AAAAGGTCGAGCAGATCCTGGCAGAGTTCCAGCTGCAGGAGGAAGACCTGAAGAAGGTGA  120
             ||||||||||||||||||||||||||||||||||||||||||||||||||||||||||||
Sbjct  61    AAAAGGTCGAGCAGATCCTGGCAGAGTTCCAGCTGCAGGAGGAAGACCTGAAGAAGGTGA  120

Query  121   TGAGCCGGATGCAGAAGGAGATGGACCGTGGCCTGAGGCTGGAGACCCACGAGGAGGCCA  180
             ||||||||||||||||||||||||||||||||||||||||||||||||||||||||||||
Sbjct  121   TGAGCCGGATGCAGAAGGAGATGGACCGTGGCCTGAGGCTGGAGACCCACGAGGAGGCCA  180

Query  181   GTGTAAAGATGTTACCCACCTACGTGCGTTCCACCCCAGAAGGCTCAGAAGTCGGAGACT  240
             ||||||||||||||||||||||||||||||||||||||||||||||||||||||||||||
Sbjct  181   GTGTAAAGATGTTACCCACCTACGTGCGTTCCACCCCAGAAGGCTCAGAAGTCGGAGACT  240

Query  241   TTCTCTCCTTAGACCTGGGAGGAACCAACTTCAGRGTGATGCTGGTCAAAGTGGGAGAGG  300
             ||||||||||||||||||||||||||||||||||||||||||||||||||||||||||||
Sbjct  241   TTCTCTCCTTAGACCTGGGAGGAACCAACTTCAGRGTGATGCTGGTCAAAGTGGGAGAGG  300

Query  301   GGGAGGCAGGGCAGTGGAGCGTGAAGACAAAACACCAGATGTACTCCATCCCCGAGGACG  360
             ||||||||||||||||||||||||||||||||||||||||||||||||||||||||||||
Sbjct  301   GGGAGGCAGGGCAGTGGAGCGTGAAGACAAAACACCAGATGTACTCCATCCCCGAGGACG  360

Query  361   CCATGACGGGCACTGCCGAGATGCTCTTTGACTACATCTCTGAATGCATCTCTGACTTCC  420
             ||||||||||||||||||||||||||||||||||||||||||||||||||||||||||||
Sbjct  361   CCATGACGGGCACTGCCGAGATGCTCTTTGACTACATCTCTGAATGCATCTCTGACTTCC  420

Query  421   TTGACAAGCATCAGATGAAGCACAAGAAACTGCCCCTGGGCTTCACCTTCTCCTTCCCTG  480
             ||||||||||||||||||||||||||||||||||||||||||||||||||||||||||||
Sbjct  421   TTGACAAGCATCAGATGAAGCACAAGAAACTGCCCCTGGGCTTCACCTTCTCCTTCCCTG  480

Query  481   TGAGGCACGAAGACCTAGACAAGGGCATCCTCCTCAATTGGACCAAGGGCTTCAAGGCCT  540
             ||||||||||||||||||||||||||||||||||||||||||||||||||||||||||||
Sbjct  481   TGAGGCACGAAGACCTAGACAAGGGCATCCTCCTCAATTGGACCAAGGGCTTCAAGGCCT  540

Query  541   CTGGAGCAGAAGGGAACAACATCGTAGGACTTCTCCGAGATGCTATCAAGAGGAGAGGGG  600
             ||||||||||||||||||||||||||||||||||||||||||||||||||||||||||||
Sbjct  541   CTGGAGCAGAAGGGAACAACATCGTAGGACTTCTCCGAGATGCTATCAAGAGGAGAGGGG  600

Query  601   ACTTTGAGATGGATGTGGTGGCAATGGTGAACGACACAGTGGCCACAATGATCTCCTGCT  660
             ||||||||||||||||||||||||||||||||||||||||||||||||||||||||||||
Sbjct  601   ACTTTGAGATGGATGTGGTGGCAATGGTGAACGACACAGTGGCCACAATGATCTCCTGCT  660

Query  661   ACTATGAAGACCGCCAATGTGAGGTCGGCATGATTGTGGGCACTGGCTGCAATGCCTGCT  720
             ||||||||||||||||||||||||||||||||||||||||||||||||||||||||||||
Sbjct  661   ACTATGAAGACCGCCAATGTGAGGTCGGCATGATTGTGGGCACTGGCTGCAATGCCTGCT  720

Query  721   ACATGGAGGAAATGCAGAATGTGGAGCTGGTGGAAGGGGATGAGGGACGCATGTGCGTCA  780
             ||||||||||||||||||||||||||||||||||||||||||||||||||||||||||||
Sbjct  721   ACATGGAGGAAATGCAGAATGTGGAGCTGGTGGAAGGGGATGAGGGACGCATGTGCGTCA  780
```

```
Query  781   ACACGGAGTGGGGCGCCTTCGGGGACTCGGGCGAGCTGGATGAGTTCCTACTGGAGTATG  840
             ||||||||||||||||||||||||||||||||||||||||||||||||||||||||||||
Sbjct  781   ACACGGAGTGGGGCGCCTTCGGGGACTCGGGCGAGCTGGATGAGTTCCTACTGGAGTATG  840

Query  841   ACCGGATGGTGGATGAAAGCTCAGCGAACCCCGGTCAGCAGCTGTACGAGAAGATCATCG  900
             ||||||||||||||||||||||||||||||||||||||||||||||||||||||||||||
Sbjct  841   ACCGGATGGTGGATGAAAGCTCAGCGAACCCCGGTCAGCAGCTGTACGAGAAGATCATCG  900

Query  901   GTGGGAAGTATATGGGCGAGCTGGTACGACTTGTGCTGCTTAAGCTGGTGGACGAGAACC  960
             ||||||||||||||||||||||||||||||||||||||||||||||||||||||||||||
Sbjct  901   GTGGGAAGTATATGGGCGAGCTGGTACGACTTGTGCTGCTTAAGCTGGTGGACGAGAACC  960

Query  961   TTCTGTTCCACGGAGAGGCCTCGGAGCAGCTGCGCACGCGTGGTGCTTTTGAGACCCGTT  1020
             ||||||||||||||||||||||||||||||||||||||||||||||||||||||||||||
Sbjct  961   TTCTGTTCCACGGAGAGGCCTCGGAGCAGCTGCGCACGCGTGGTGCTTTTGAGACCCGTT  1020

Query  1021  TCGTGTCACAAGTGGAGAGCGACTCCGGGGACCGAAAGCAGATCCACAACATCCTAAGCA  1080
             ||||||||||||||||||||||||||||||||||||||||||||||||||||||||||||
Sbjct  1021  TCGTGTCACAAGTGGAGAGCGACTCCGGGGACCGAAAGCAGATCCACAACATCCTAAGCA  1080

Query  1081  CTCTGGGGCTTCGACCCTCTGTCACCGACTGCGACATTGTGCGCCGTGCCTGTGAAAGCG  1140
             ||||||||||||||||||||||||||||||||||||||||||||||||||||||||||||
Sbjct  1081  CTCTGGGGCTTCGACCCTCTGTCACCGACTGCGACATTGTGCGCCGTGCCTGTGAAAGCG  1140

Query  1141  TGTCCACTCGCGCCGCCCATATGTGCTCCGCAGGACTAGCTGGGGTCATAAATCGCATGC  1200
             ||||||||||||||||||||||||||||||||||||||||||||||||||||||||||||
Sbjct  1141  TGTCCACTCGCGCCGCCCATATGTGCTCCGCAGGACTAGCTGGGGTCATAAATCGCATGC  1200

Query  1201  GCGAAAGCCGCAGTGAGGACGTGATGCGCATCACTGTGGGCGTGGATGGCTCCGTGTACA  1260
             ||||||||||||||||||||||||||||||||||||||||||||||||||||||||||||
Sbjct  1201  GCGAAAGCCGCAGTGAGGACGTGATGCGCATCACTGTGGGCGTGGATGGCTCCGTGTACA  1260

Query  1261  AGCTGCACCCGAGCTTCAAGGAGCGGTTTCACGCCAGTGTGCGCAGGCTGACACCCAACT  1320
             ||||||||||||||||||||||||||||||||||||||||||||||||||||||||||||
Sbjct  1261  AGCTGCACCCGAGCTTCAAGGAGCGGTTTCACGCCAGTGTGCGCAGGCTGACACCCAACT  1320

Query  1321  GCGAAATCACCTTTCATCGAATCAGAGGAGGGCAGCGGCAGGGGAGCCGCRCTGGTCTCT  1380
             ||||||||||||||||||||||||||||||||||||||||||||||||||||||||||||
Sbjct  1321  GCGAAATCACCTTTCATCGAATCAGAGGAGGGCAGCGGCAGGGGAGCCGCRCTGGTCTCT  1380

Query  1381  GCGGTGGCCTGCAAGAAGGCTTGCATGCTGGCCCAGTGAAATCCAGGTCATATGGACCGG  1440
             ||||||||||||||||||||||||||||||||||||||||||||||||||||||||||||
Sbjct  1381  GCGGTGGCCTGCAAGAAGGCTTGCATGCTGGCCCAGTGAAATCCAGGTCATATGGACCGG  1440

Query  1441  GACCTCTAG  1449
             |||||||||
Sbjct  1441  GACCTCTAG  1449
```

Figure 2.5 BLAST analysis of sequencing results for GKS-pTR-CGW vs. pCMV4.GKB1 sequence: *Analysis of GKS-pTR-CGW compared to pCMV4.GKB1 revealed 100% homology and showed that the sequence contained start and stop codons (highlighted in red).*

2.4.4.2 **GKAS**

BLAST analysis of the GKAS-pTR-CGW sequencing data revealed that the plasmid contained a 185bp sequence with 100% homology to the rat pancreatic GK sequence (GenBank: M25807.1) as shown in figure 2.6.

```
Query  1    GGGGGTCCCAGTTCACCTGGGCTGGTGGCTGCGCAGATGCTGGATGACAGAGCCAGGATG  60
            ||||||||||||||||||||||||||||||||||||||||||||||||||||||||||||
Sbjct  1    GGGGGTCCCAGTTCACCTGGGCTGGTGGCTGCGCAGATGCTGGATGACAGAGCCAGGATG  60

Query  61   GAGGCCACCAAGAAGGAAAAGGTCGAGCAGATCCTGGCAGAGTTCCAGCTGCAGGAGGAA  120
            ||||||||||||||||||||||||||||||||||||||||||||||||||||||||||||
Sbjct  61   GAGGCCACCAAGAAGGAAAAGGTCGAGCAGATCCTGGCAGAGTTCCAGCTGCAGGAGGAA  120

Query  121  GACCTGAAGAAGGTGATGAGCCGGATGCAGAAGGAGATGGACCGTGGCCTGAGGCTGGAG  180
            ||||||||||||||||||||||||||||||||||||||||||||||||||||||||||||
Sbjct  121  GACCTGAAGAAGGTGATGAGCCGGATGCAGAAGGAGATGGACCGTGGCCTGAGGCTGGAG  180

Query  181  ACCCA  185
            |||||
Sbjct  181  ACCCA  185
```

Figure 2.6 BLAST analysis of GKAS-pTR-CGW sequencing results vs. rat pancreatic GK sequence: *Comparison of GKAS-pTR-CGW to published sequence revealed 100% homology.*

2.4.5 Comparison of GK assays methodologies

GK assays were performed on extracts of HEK 293T cells which express hexokinase (Hx) but not GK. In the standard and optimized assays HX activity and NADPH production should be zero.

In the standard GK assay NADPH production was reduced by 56% (0.057 +/-0.001 mM, n=3**)** compared to control (0.131 +/-0.002 mM, n=3, P<0.0001). The optimised assay reduced NADPH production by 81% (0.025 +/-0.0002 mM, n=3. P<0.0001) compared to controls**.** Compared to the standard assay the optimised assay reduced NADPH by 56% (P<0.0001) (figure 2.7). Therefore, the optimized assay was used in all subsequent analysis.

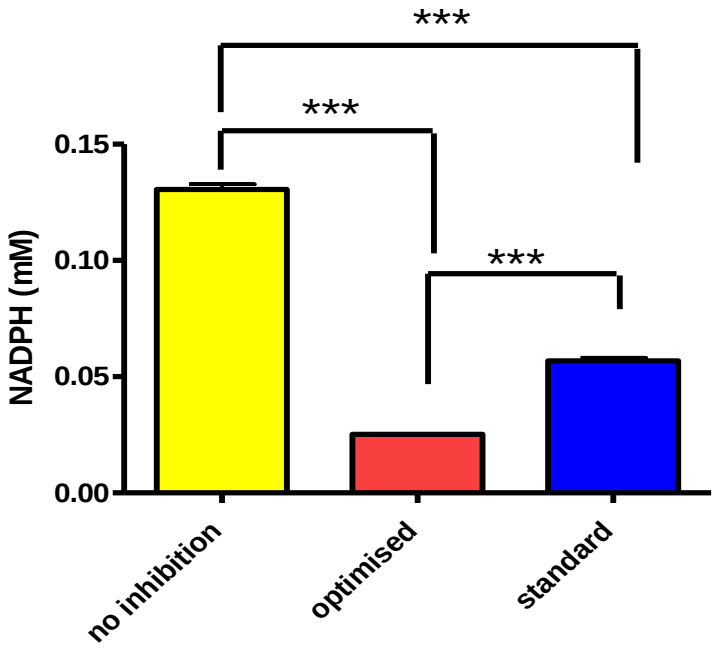


Figure 2.7 Comparing GK assays: *NADPH production in GK assays on HEK293T cell lysate using three different methodologies 1). No hexokinase inhibitor (yellow bar). 2) Optimised GK assay (red bar). 3) Standard GK assay (blue bar). Values are shown in mM, n=3. ***= P<0.001.*

2.4.6 Effect of GKAS-pTR-CGW plasmid transfection on GK activity in HEK293T cells

Transfection of HEK293T cells with GKS-pTR-CGW plasmid resulted in increased glucokinase activity compared to controls (controls 0.11 +/- 0.048 vs GKS 0.34 +/-0.02 units/mg protein, n=4, P<0.05) as shown in figure 2.8.

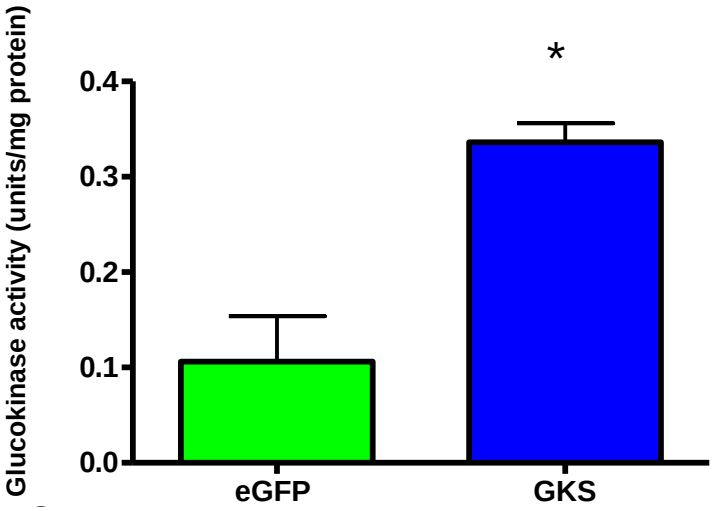


Figure 2.8 Effect of* GKS-pTR-CGW *plasmid transfection on GK activity in HEK293T cells: *GKS activity in HEK293T cells 48hr after transfection with either* GKS-pTR-CGW *plasmid (blue bar) or* pTR-CGW *plasmid (green bar). Values are shown in units of enzymatic activity per mg of protein +/- SEM n=4 * P<0.05.*

2.4.7 Effect of GKAS-pTR-CGW plasmid transfection on GK activity in HEPG2 cells

Transfection of HEPG2 cells with GKAS-pTR-CGW plasmid resulted in decreased GK activity compared to controls (control 0.31 ± 0.024 vs. GKAS 0.19 ± 0.011 units/mg protein, n=4, P<0.05**)** (figure 2.9).

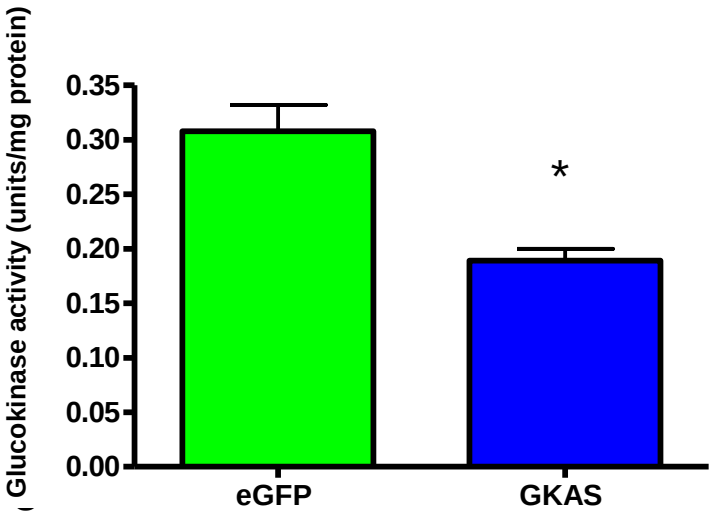


Figure 2.9 Effect of GKAS-pTR-CGW plasmid transfection on GK activity in HEPG2 cells: *GK activity in HEPG2 cells 48hr after transfection with either GKAS-pTR-CGW plasmid (blue bar) or pTR-CGW plasmid (green bar). Values are shown in units of enzymatic activity per mg of protein +/- SEM n=4 * P<0.05.*

2.5 Discussion

Prior to the production of GK and GKAS AAV particles, the efficacy of the plasmids was tested *in vitro*. At present, there is no assay that directly measures GK activity. The assays used in this thesis estimate the activity of GK based on two coupled reactions. The first reaction, glucose to glucose-6-phosphate, is catalysed by GK. In the next reaction glucose-6-phosphate dehydrogenase catalyses the conversion of glucose-6-phosphate to 6-phospho-D-gluconate with the production of NADPH which is measured spectrophotometrically.

However, GK is not the only enzyme expressed in the rat brain that phosphorylates glucose to give G-6-P. The rat brain expresses a variety of hexokinases, with hexokinase I being expressed at high levels (Shinohara *et al*, 1991). As such, the production of G-6-P cannot be fully attributed to GK. This in turn means that NADPH production during the assay is also not fully attributable to GK. To ensure that the AAV plasmids were having a specific effect on GK expression I first had to choose an assay that was sufficiently sensitive and accurate.

In the standard GK assay, the interfering effect of hexokinases is partially controlled for based on the known enzymatic properties of GK and other hexokinases. GK has a low affinity and high Km for glucose compared to other hexokinases (Meglasson & Matschinsky, 1984). This means that it is possible to partially differentiate between the effect of GK and other hexokinases by altering the glucose concentration in the reaction media. At glucose concentrations of 0.5mmol/l glucose hexokinase activity is near maximal whereas glucokinase activity is low (Liu *et al*, 1991). At glucose concentrations of 100mmol/l the activity of both enzymes should be maximal. To calculate GK activity in a sample the assay is performed in both 0.5mmol/l and 100mmol/l glucose and the result of the former is subtracted from the latter.

The optimized GK assay utilizes enzymatic inhibition to control for hexokinase interference. 5-thio-D-glucose is a structural analogue of glucose that inhibits others hexokinases but not GK (Wilson & Chung, 1989). 3-O-methyl-*N*-acetylglucosamine inhibits *N*-acetylglucosamine kinase which catalyses the reaction *N*-acetylglucosamine to *N*-acetylglucosamine-6-phosphate. At high glucose concentrations, *N*-

acetylglucosamine kinase will also phosphorylate glucose to give G-6-P (Miwa *et al*, 1995). For this reason, it is also necessary to inhibit the actions of *N*-acetylglucosamine kinase in the GK assay.

To test the efficacy of the GK assay methods I performed the GK assays on HEK293T cell lysate. HEK293T cells express hexokinase but do not express GK. Since there is no GK in HEK293T cells GK activity and NADPH production should be zero.

Using the standard assay method, the production of NADPH was 0.057mmol/l. This suggests that the standard GK assay does not accurately measure GK activity. It is possible that one of the reasons this assay is unreliable is that it does not control for the activity of *N*- acetylglucosamine kinase at high glucose concentrations.

Using the optimized GK assay NADPH production was 0.025mmol/l. While this method did not give a perfect result it is a significant improvement on the standard method. For this reason, the optimized GK assay was chosen for subsequent analysis of GK activity.

Next it was necessary to investigate the efficacy of pTR-CGW-GKS plasmid *in vitro*. To do this, HEK293T cells were transiently transfected with the plasmid. After 48 hours, cells were lysed and assayed for GK activity using the optimized method. Following transfection with pTR-CGW-GKS plasmid GK activity in HEK293T cells was increased three-fold compared to controls. Thus, demonstrating the efficacy of the GKS -pTR-CGW plasmid *in vitro*.

A similar protocol was used to investigate the efficacy of the antisense plasmid. In this case HEPG2 cells, which express GK, were transfected with GKAS-pTR-CGW. Transfection of HEPG2 cells with the antisense plasmid decreased GK activity by approximately one third compared to controls. This level of knockdown is comparable to the results of Gardiner et al who reported approximately 50% knockdown of NPY expression from cultured RIN 56 NPY cells using antisense AAV (Gardiner *et al*, 2005).

Having established the efficacy of both plasmids the AAV viral particles were produced and *in vivo* experiments commenced.

Chapter 3

Effect of iArc rAAV-GKS administration on food intake and body weight

3.1 Introduction

3.1.1 The Glucostatic hypothesis

Jean Mayer's 1953 "Glucostatic hypothesis" proposed that short-term food intake was regulated by glucose metabolism in critical brain regions. At the centre of the hypothesis was the concept that a reduction in arteriovenous (AV) difference in blood glucose is met with hunger and feeding, with an increase in AV glucose difference having the opposite effect. As part of the hypothesis, Mayer predicted the existence of glucose-sensing neurones (which were not discovered until 1961) and predicted that glucose-sensing neurones in the ventromedial hypothalamus would be of importance in the regulation of feeding (Mayer, 1955;Mayer, 1953).

Mayer argued that glucose-sensing was the likely mechanism that regulated short-term feeding because a) glucose is utilized preferentially by most tissues and in the fed state the CNS uses it exclusively b) glucose is usually the first substrate to become depleted (bodily stores being very low) and c) prevention of low level of glucose is necessary to avoid "death through incapacitation of the central nervous system"(Mayer, 1953).

3.1.2 Experimental evidence

In the years following the publication of the glucostatic hypothesis a number of investigators attempted to demonstrate the hypothesis experimentally. Manipulation of glucose levels in various regions of the body including the general circulation (Smith & Epstein, 1969) and portal circulation (Tordoff *et al*, 1989) have been shown to alter feeding behaviour. However, some investigators have found that manipulation of plasma glucose does not influence feeding behaviour. For example, in an experiment conducted by Bernstein *et al*, hyperglycemia was shown to have no effect on feeding behaviour in humans. Nine healthy men received a glucose solution either intravenously or intragastrically in a dose sufficient to induce hyperglycemia. The study was run in a cross over design with each participant acting as his own control on separate days. Thirty minutes following treatment subjects were offered *ad libitum* access to a buffet meal and food intake and appetite (via questionnaire) were recorded. Treatment with

glucose was not shown to alter food intake or appetite significantly compared with intravenous or intragastric saline treatment (Bernstein & Grossman, 1956).

By contrast in rodents, glucose and 2-deoxy-glucose (2DG) have been shown to alter feeding when administered i.p., ICV and or intra-VMH. Pre-prandial ICV infusion of glucose at doses of 6 to 24μmol/l decreases subsequent meal size in a dose dependent manner in rats (Kurata *et al*, 1986). While infusion of glucose directly into the VMH for a period of 6 days results in decreased food intake and bodyweight gain (Panksepp & Rossi III, 1981).

ICV infusion of 2DG, which specifically inhibits glucose metabolism, results in a potent increase in food intake (Tsujii & Bray, 1990). This effect is also observed when 2DG is infused directly into the VMH (Lenin Kamatchi *et al*, 1986). Interestingly, infusion of glucose epimers including D-mannose, D-allose and D-galactose does not affect food intake or bodyweight (Kurata *et al*, 1986). Taken together, these data suggest a specific role for VMH glucose-sensing in the regulation of short-term feeding, as predicted by Mayer.

3.1.3 Mechanism of glucose-induced regulation of feeding

The mechanism by which hypothalamic glucose-sensing affects feeding behaviour is not well characterised although it is thought to involve the POMC/CART and NPY/AgRP expressing neurones of the ARC. It is well accepted that POMC/CART and NPY/AgRP neurones are glucose sensitive. However, there is a degree of disagreement regarding their exact electrophysiological characteristics. For example, subpopulations of NPY expressing neurones have been shown to be GI by Fioramonti et al and GE by Claret et al (Fioramonti *et al*, 2007 ;Claret *et al*, 2007).

In support of the results of Fioramonti et al, systemic glucoprivation caused by i.p. administration of 2DG has been shown to increase mRNA levels of both NPY and AGRP (Sergeyev *et al*, 2000). A decrease in plasma glucose would be expected to activate GI neurones and increase their peptide release. Thus, the increase in NPY with glucoprivation suggests that at least some NPY neurones are GI. Intraperitoneal 2DG administration has also been shown to increase NPY peptide levels in the ARC

(Akabayashi *et al*, 1993). Interestingly, glucoprivic feeding as a result of i.p. 2DG is largely attenuated in rats that are pre-treated with NPY-antiserum in the PVN (He *et al*, 1998). Feeding response to 2DG is also attenuated in NPY KO mice and food intake in these mice is not significantly increased by insulin-induced hypoglycaemia (Sindelar *et al*, 2004). This suggests that an NPY-dependent mechanism underlies at least part of the feeding response to hypoglycaemia and also that NPY neurones are responsive to decreasing plasma glucose.

Glucose-sensing in POMC neurones might also be important in the regulation of feeding behaviour. POMC mRNA is decreased in streptozotocin (STZ)-induced diabetes. POMC levels are normalised with insulin treatment and normalisation of plasma glucose levels (Kim *et al*, 1999).

Glucose has been shown to increase POMC release in a dose dependent manner from hypothalamic explants taken from lean mice. This effect, is absent in explants taken from diet-induced obese mice (Parton *et al*, 2007), suggesting that glucose-sensing in POMC neurones is lost in obesity. In addition, the sensitivity of POMC neurones to leptin appears to be dependent on local glucose concentration. At high glucose levels (11mM) leptin excites POMC neurones and increases their firing rate. At low glucose concentrations (5mM) leptin has the opposite effect, hyperpolarising POMC neurones and decreasing their action potential firing rate (Ma *et al*, 2008).

3.1.4 Blood glucose and spontaneous feeding

Despite the preponderance of evidence linking neuronal glucose-sensing with the regulation of food intake it has been difficult to demonstrate a role for VMH glucose-sensing in spontaneous feeding. It has also been suggested that many of the experiments linking neural glucose-sensing to food intake do so using supraphysiological glucose concentrations. For example in the experiments of Parton *et al*, glucose concentration of 5mM and 11mM were used to alter the sensitivity of POMC neurones to leptin *ex vivo* (Parton *et al*, 2007). Glucose levels in the VMH have been recorded over a range of 0.73-4.23mM with ambient concentrations of 1.43mM in fed rats (Mayer *et al*, 2006;de Vries *et al*, 2005). Since the “low” glucose concentration used by Parton *et al* is above

the highest physiological level recorded in the VMH it is possible that the results achieved do not reflect normal physiology.

In both humans and rats, a high proportion of spontaneous meals are preceded by a 5-12% decrease in plasma glucose levels (Campfield *et al*, 1985;Melanson *et al*, 1999). In a recent study conducted by Dunn-Meynell *et al*, the pre-prandial decrease in plasma glucose was confirmed. However, there was no consistent relationship between changes in VMH glucose levels and spontaneous feeding. Altering VMH glucose-sensing, by decreasing mRNA, caused a reduction in glucoprivic feeding but had no effect on spontaneous feeding, bodyweight or adiposity (Dunn-Meynell *et al*, 2009). Thus, the results of this study would appear to suggest that VMH glucose-sensing is important in glucoprivic feeding but not in the day to day regulation of energy balance. In addition, spontaneous feeding is associated with a decrease in plasma glucose but not a decrease in VMH glucose. This raises the possibility that feeding behaviour may be regulated by glucose-sensing in a region of the body other than the VMH, perhaps in the periphery. This is also in opposition to the "Glucostatic hypothesis" since Mayer predicted that VMH glucose sensors regulate feeding behaviour.

3.2 Hypothesis and Aims

3.2.1 Hypothesis

GK is expressed in a number of hypothalamic nuclei and an important step in this work is to establish which nucleus/nuclei are quantitatively most important in feeding behaviour. Fasting has been shown to increase GK mRNA expression in the ARC. It is hypothesised that fasting will also increase GK enzymatic activity in a nucleus specific manner. Based on the results of the fasting studies I will choose a hypothalamic nucleus as the primary target for rAAV induced increase in GK. It is hypothesised that intranuclear injection of rAAV-GKS will increase GK activity local to the injection site and will affect food intake, bodyweight and glucose homeostasis.

3.2.2 Aims and Objectives

I aim to investigate the role of hypothalamic glucose-sensing neurones in the regulation of energy intake and glucose homeostasis. In order to do this I will:

1. Measure the effect of fasting on GK activity in the ARC, PVN and VMN to establish which nuclei are quantitatively most important in the regulation of glucose homeostasis and feeding behaviour
2. Examine the physiological effect of up regulation of GK mRNA in specific hypothalamic nuclei on food intake and glucose homeostasis
3. Examine the effect of up regulation of GK mRNA on hypothalamic gene expression

3.3 Methods

3.3.1 Animals

Male Wistar rats (specific pathogen free, Charles River UK Ltd, Margate, Kent, UK) were maintained under a controlled environment (temperature 21-23ºC, 12 hour light-dark cycle, lights on at 07:00) with *ad libitum* access to food (RM1 diet, Special Diet Services UK Ltd, Witham, Essex, UK) and water. All animal procedures were approved under the British Home Office Animals (Scientific Procedures) Act 1986 (Project licence no. 70/6377). Prior to all experiments animals were acclimatised to the Imperial College animal unit for 7 days. In all experiments animals were randomised to treatment and control groups as described in appendix III.

3.3.2 Isolation of specific hypothalamic nuclei by punch biopsy from coronal sections

Rats were killed by decapitation, and brains removed. Brains were then placed on filter paper with the ventral surface facing upwards so that the hypothalamus was visible, and sections caudal and rostral to the hypothalamus were cut away using a razorblade. The brain was then frozen using isopentane cooled on dry ice. Frozen brains were then mounted upon a freezing sled microtome (Shandon Southern Products Ltd, Runcorn, UK). Eight hundred micrometre sections from the rostro-caudal extent of the hypothalamus were then cut and mounted on poly-lysine slides. Slides were kept on dry ice to re-freeze sections and the ARC, PVN and VMN were identified using a rat brain atlas (Paxinos & Watson C, 2007) and removed using a 22 gauge neuropunch (Fine Science Tools, Linton, UK).

3.3.3 Isolation of specific hypothalamic nuclei by punch biopsy from sagittal sections

Rats were killed by decapitation, and brains removed. Brains were then placed on filter paper with the ventral surface facing upwards so that the hypothalamus was visible, and sections lateral to the hypothalamus on either side were cut away using a razorblade. The remaining block of brain was then frozen using isopentane cooled on dry ice. Frozen brains were mounted upon a freezing sled microtome (Shandon Southern Products Ltd). Sagittal sections of 1.2mm containing the ARC, VMH and PVN were then cut and mounted on slides. Slides were kept on dry ice to re-freeze sections and nuclei were identified and removed using a 22 gauge neuropunch (Fine Science Tools).

3.3.4 Quantification of glucokinase activity in the hypothalamic nuclei of fed and fasted rats

Punch biopsies from the ARC, VMN and PVN were taken from three groups of rats; group 1 (n=8) was allowed *ad libitum* access to standard chow during a 48 hour period, group 2 (n=8) was fasted for 24 hours and group 3 (n=9) fasted for 48 hours. Animals were killed by decapitation 2 hours after lights-on on the final day of the study and hypothalamic nuclei were isolated (as in section 3.3.2) and optimized glucokinase assay was performed on homogenised hypothalamic nuclei (as described in 2.3.5.2).

3.3.5 Protein assay on punch biopsy samples

There is inherent variability in the amount of hypothalamic tissue collected by punch biopsy. In order to compensate for this the protein content of the punch biopsy homogenate must be calculated in order to standardise the results of the GK activity assay.

Homogenate protein content was measured using a well-established modified Lowry protein assay. This method involves reaction of proteins with cupric sulphate and tartrate in an alkaline solution to form tetradentate copper-protein complexes. These copper-protein complexes produce a peak in absorbance at 750nm and can be measured spectrophotometrically to quantify the amount of protein in a sample.

Materials

Lowry protein assay kit (Pierce, Rockford, IL, USA)
Bovine serum alblumin (BSA) stock solution
2X Folin-Ciocalteu reagent

Method

BSA stock solution was diluted in GDW to make up nine standard solutions of 1, 5, 25, 125, 250, 500, 750, 1,000, and 1,500 µg/ml. One times Folin-Ciocalteu reagent was prepared by diluting the supplied 2X reagent 1:1 with ultra-pure water. All other reagents were supplied ready to use.

Fifty microlitres of BSA standard and 50µl of sample were added to microfuge tubes. One millilitre of modified Lowry reagent was then added to each tube at 15 second intervals, mixed, and incubated for 10 minutes. One hundred microlitres of the prepared 1X Folin-Ciocalteu reagent was then added and the solution was vortexed. The tubes were covered and incubated at room temperature for 30 minutes. The A750 of the samples was then measured in a spectrophotometer. Absorbance values of the blank readings were subtracted from the absorbance readings of all samples and a standard curve plotted. The protein concentration of each of the unknown samples was determined by comparison to the standard curve.

3.3.6 Injection of GKS-AAV in the rat brain

Adult male Wistar rats were anaesthetized by intraperitoneal (i.p.) injection of ketamine 60mg/kg (Parke-Davis, Pontypool, UK) and xylazine 12mg/kg (Bayer UK Ltd, Bury St. Edmunds, UK) and immobilised on a stereotaxic frame (David Kopf Instraments, California, USA). The incisor bar was set at 3.0mm below the interaural plane. The surgical area was shaved, and cleaned with 10% w/v povidine-iodine solution (Betadine). A small (<2cm) rostro-caudal incision was made in the scalp. Animals were injected bilaterally into the ARC using coordinates -3.4mm caudal, +/-0.5mm lateral to the bregma, and 10.5mm below the skull, determined from the rat brain atlas of Paxinos and Watson (Paxinos & Watson C, 2007). A stereotaxically mounted drill, was used to make a 0.65mm burr hole in the skull. Each animal was injected via a 33 gauge steel injector (Plastics-One, Roanoke, Virginia, USA) inserted into, and projecting 1mm below, the tip of a guide cannula. Animals received either 1µl rAAV-GKS at a titre of $2.96x10^{12}$ genome particles/ml or 1µl rAAV-eGFP at a titre of $5.04x10^{12}$ genome particles/ml injected bilaterally into the ARC. The pressure was removed from the injector and the cannula/injector unit was maintained *in situ* for 5 minutes before being slowly extracted to minimise backflow. The incision was sutured with two mattress sutures with 6.0 proline thread. The animal was removed from the frame, re-hydrated with 5ml normal saline, revived with 50µl antisedan (Animalcare Ltd, Dunnington, UK) and placed in a heated box for recovery. Once the rat had regained the righting reflex it was housed individually and monitored for a recovery period of 7 days. The animals were given *ad libitum* access to food (unless pair fed to another group) and food intake and body weight were measured at least 3 times per week following the 7 day post-operative recovery period.

3.3.7 Confirmation of gene transfer by in situ hybridisation

In situ hybridisation is a method for the detection and quantification of mRNA whilst maintaining the structural integrity of the tissue. It relies on the hybridisation of a complementary probe, usually radiolabelled RNA, to the target mRNA in tissue mounted on poly-lysine slides.

Following rAAV-GKS injections transgene expression was confirmed in brains taken from three animals using an ^{35}S labelled riboprobe specific for GK. The ^{35}S GK riboprobe was labelled as described below using pBluescript-GK as a template. The pBluescript-GK plasmid was created by endonuclease digestions of pBluescript and full length GK using BamHI and PstI (as described in 2.3.2.1). Following endonuclease digestion pBluescript and GK were ligated and the plasmid was amplified and purified.

3.3.7.1 **Production of radiolabelled RNA probe for in situ hybridisation**

Materials

Linearised template (pBluescript-GK (200ng/µl) linearised by digestion with BamHI for antisense probe)
100M DTT
RNase inhibitor, 30U/µl
10x nucleotide mix: 10mM of each ATP, UTP, GTP;
T7 RNA polymerase, 20U/µl (Promega)
10x RNApolymerase buffer (Promega)
DNase I, 7.5 U/µl (GE Healthcare)
10x DNase buffer
5M Ammonium acetate (appendix I)
[^{35}S]CTPαS, 30TBq/mmol, 1.5GBq/ml (GE Healthcare)

Method

Radioactively labelled RNA was produced using an *in vitro* transcription reaction. Two hundred nanograms of template were added to a reaction buffer containing 10mM DTT, 1x nucleotide mix, 1x polymerase buffer, 30U RNase inhibitor and 3.75MBq [^{35}S]CTPαS in a total volume of 9µl. To this 20U of T7 RNA polymerase was added and the reaction incubated for at least 2 hours at 37ºC. After incubation, 6µl GDW, 1µl DNase I and 3µl DNase buffer was added. This was followed by a 15 minute incubation at 37ºC. Ammonium acetate was added to a final concentration of 2M and 2.5volumes ice cold absolute ethanol was added and the mixture left at -20ºC for at least an hour for the RNA to precipitate. RNA was recovered by centrifugation at 8,000xg for 7 minutes and the pellet was dissolved in 100µl GDW. To measure the activity or the radiolabelled probe, 1µl was counted on a microbeta counter (Wallac, Waltham, MA).

3.3.7.2 **In situ hybridisation**

Materials

4% (v/v) formaldehyde in 0.1M phosphate buffered solution (PBS)
100% acetic anhydride (VWR)
0.1M triethanolamine pH 8.0
20x SSC (appendix I)
70% ethanol in distilled water
Chloroform (VWR)
Hybridisation buffer (appendix I)
- 50% (v/v) Formamide
- 600mM sodium chloride
- 80mM Tris-HCl, pH 7.5
- 4mM EDTA
- 100mM DTT
- 0.1 mg/ml yeast tRNA
- 2% (w/v) Dextran sulphate, mw ~500,000

1x RNase buffer
10mM Tris pH 8
1mM EDTA
0.5M sodium chloride

Method

Twelve micrometre brain sections were cut on a cryostat at -25ºC (Bright instrument Company, Huntingdon, Cambridgeshire, UK). The sections were mounted onto poly-lysine coated slides and stored at -20ºC until hybridisation. *In situ* hybridisation was carried out on every third slide. The sections were fixed in 4% (v/v) formaldehyde in 0.1M PBS for 20 minutes. Slides were washed twice in 0.1MPBS, for 5 minutes. Sections were then incubated in 0.1M TEA for 2 minutes and acetylated in 0.25% (v/v) acetic acid anhydride in 0.1M TEA for 10 minutes. Sections were washed twice in 0.01M PBS for 2 minutes and then dehydrated by immersion in 70% ethanol for 3

minutes. Finally, slides were delipidated in chloroform for 5 minutes and allowed to air dry. All steps were performed at room temperature unless otherwise stated.

Hybridisation buffer was supplemented with the ^{35}S labelled probe (1 x 10^6 Bq) and 80µl added to each slide. A coverslip was placed over each slide and the slides were hybridised at 60ºC overnight. Next, the slides were washed in 4x SSC with gentle agitation to remove coverslips and then washed four times in 4x SSC for 5 minutes. Slides were then RNase treated by incubation for 30 minutes at 37ºC in 1x RNase buffer containing 100µg/ml RNase A. This was followed by two 5 minute washes in 10mM DTT/2x SSC at room temperature. Slides were washed in 10mM DTT/1x SSC followed by 10mM DTT/0.5x SSC for 10 minutes each. Slides were then washed in 10mM DTT/0.1x SSC at 60ºC for 30 minutes. Finally, slides were rinsed in 10mM DTT/0.1x SSC and dehydrated in 70% ethanol for 3 minutes before being allowed to air dry. After washing and dehydration, the slides were exposed to Bio-Max film (Kodak, Hemel Hempstead, Herts, UK) at room temperature. After three days exposure the film was developed and transgene expression determined by observation of specific hybridisation.

3.3.8 Cohort One

3.3.8.1 **Effect of iARC rAAV-GKS on food intake and bodyweight**

Male Wistar rats were injected bilaterally into the ARC with 1µl of either rAAV-GKS (n=25) or rAAV-eGFP (n=16). Intake of RM1 diet (standard chow) and body weight were measured three times per week for a period of 40 days. Three rats from the rAAV-GKS group were killed 3 week post injection and brains were removed and used for *in situ* hybridization.

3.3.8.2 **Effect of iARC rAAV-GKS on GK activity in the ARC and PVN**

On day 40 animals were killed by decapitation and the ARC and PVN were isolated and homogenized (as described in 3.3.3). Optimized glucokinase assay was then performed on homogenised hypothalamic nuclei (as described in 2.3.5.2).

3.3.8.3 **Effect of iARC rAAV-GKS on body composition**

Body composition analysis was required to establish the ratio of fat mass to lean body mass. The principle behind this practice involves dissolving the carcass in a saponification reaction using a strong alkali. The component fats and proteins from the resultant solution can then be analysed using standard assay procedures. To determine carcass protein content a modified Lowry protein assay was performed (as described in 3.3.5). Fat mass was determined by glycerol assay (as described in 3.3.8.4). Rats had previously been decapitated and brains had been collected for GK assay. Heads and remaining brain matter where returned to the carcasses before saponification.

Carcasses were weighed and placed into separate containers. Carcasses were dissolved using 3M KOH in 65% ethanol (appendix I) in equal volumes to carcass weight. The carcasses were incubated in the alkali solution at 70˚C for five days. The resultant liquid was made up to 1L with absolute ethanol and stored at room temperature until required.

3.3.8.4 **Glycerol assay**

In order to determine the total fat mass of rats, a glycerol assay was used. Glycerol concentrations were determined using reagents and methods from Randox Laboratories Ltd, UK. All buffers were supplied ready to use with the exception of reagent 2 which was reconstituted with 15ml of buffer 1. 1M glycerol stock solution was diluted in GDW to provide standard glycerol concentrations of 5mM, 2mM, 1mM, 0.5mM, 0.2mM, 0.1mM, and 0.05mM. Ten microlitres dissolved carcass sample was diluted 1:100 with GDW. To start the assay, 1ml reagent 2 was transferred into fresh eppendorf tubes. To this 30µl of sample, standard, or buffer (for blank value) was added and left to incubate at room temperature for 10 minutes. Two hundred microlitres from each tube was transferred into a well on a 96-well. The glycerol concentration of each sample was determined by measuring absorbance at 520nm and reading from the standard curve.

3.3.9 Cohort 2

3.3.9.1 Effect of iARC rAAV-GKS on food intake and bodyweight, effect of pair feeding

Male Wistar rats were injected iARC with 1µl rAAV-GKS (n=30) or rAAV-eGFP (n=15). Following recovery rats injected with rAAV-GKS were divided into two group; Group 1 (n=15) received *ad libitum* access to standard chow. Group 2 (n=15) were pair fed standard chow to the food intake of the rAAV-eGFP (n=16) of the previous day. Food intake and bodyweight were recorded at 2-3day intervals for a period of 33days. The food hoppers of the pair fed GKS group were refilled daily.

3.3.9.2 Effect of iARC rAAV-GKS on 24hr food intake following fast

To further elucidate the role of ARC GK in feeding behaviour rAAV-GKS (n=12), rAAV-eGFP (n=14) and rAAV GKS rats pair fed to rAAV-eGFP (n=10) were fasted for 24hr hours after which time they were allowed *ad libitum* access to standard chow. Body weight was measure before fasting, after 24hr fast and 24hr post re-feed starting on day 35. Food intake was measure at 1,2,4,8 and 24hr post re-feed. Chow was returned at the onset of the dark phase.

3.3.9.3 Body composition

At the termination of the study (day 40) rats were killed by decapitation. Trunk blood was collected and assayed for insulin and glucose. Epididymal WAT and interscapular BAT were removed and weighed. Brains were removed and hypothalami were dissected, frozen in liquid nitrogen and stored at -80°C.

3.3.9.4 **Glucose homeostasis**

Following decapitation trunk blood was collected in tubes coated with heparin and 200µl aprotinin (Trasylol). Plasma was separated by centrifugation and frozen on liquid nitrogen. Plasma insulin was assayed by ELISA. Plasma glucose was assayed using an enzymatic oxidation reaction (described below).

3.3.9.5 **Glucose assay**

Materials

Glucose assay kit (Randox Laboratories Ltd. UK)

Methods

Plasma glucose concentrations were determined using reagents and methods from Randox Laboratories Ltd. This assay involves two linked reactions which are shown below. In the first reaction glucose is oxidised by glucose oxidase (GOD) to give gluconic acid and hydrogen peroxide. In the second reaction hydrogen peroxide reacts with 4-aminophenazone and phenol under catalysis of peroxidise (POD). The products of the second reaction are water and quinoneimine.

$$\text{Glucose} + O_2 + H_2O \xrightarrow{\text{GOD}} \text{gluconic acid} + H_2O_2$$

$$2\,H_2O_2 + \text{4-aminophenazone} + \text{phenol} \xrightarrow{\text{POD}} \text{quinoneimine} + 4\,H_2O$$

All buffers were supplied ready to use and the GOD-PAP reagent was reconstituted using one vial R1b buffer. Plasma samples were thawed on wet ice and diluted 1:5 in normal saline. Standard glucose concentrations were produced using standard glucose solution and methods provided by Randox. On a 96 well plate 5µl of sample or standard was mixed with 280µl of reconstituted GOD-PAP reagent and incubated for 10

minutes at 37˚C. The A500 of the samples was then measured in a spectrophotometer. Absorbance values of the blank readings were subtracted from the absorbance readings of all samples and standards, and a standard curve plotted. The glucose concentration of each of the unknown samples was determined by comparison to the standard curve. For full calculations see appendix III.

3.3.9.6 **Plasma insulin ELISA**

Material

Rat insulin ELISA kit (Linco Research, Missouri, USA)

Methods

Plasma insulin concentrations were determined using reagents and methods from Linco Research. All reagents were provided ready to use with the exception of 10X wash buffer that was diluted 1:10 in GDW. Prior to setting up the reaction all wells were washed three times with 300µl of 1X wash buffer and residual buffer was removed by tapping the plate on absorbent towels. Ten microlitres of sample, premixed rat insulin standard or quality control were added to wells followed by 80µl detection antibody (pre-titered biotinylatd anti-insulin antibody). Plates were sealed and incubated at room temperature for 2 hours on a plate shaker at 400rpm. Following incubation, solution was decanted from wells as previously described and wells washed three times with 300µl wash buffer. Next, 100µl of enzyme solution containing streptavidin-horseradish peroxidise was added and the plate was sealed and agitated for 30 minutes at 400rpm. Following incubation solution was decanted and wells washed six times with wash buffer. One hundred microlitres of substrate reagent was added, containing 3,3',5,5'-tetramethylbenzidine, and was incubated for 15 minute. The A590 of the samples was then measured in a spectrophotometer. Absorbance values of the blank readings were subtracted from the absorbance readings of all samples and standards, and a standard curve plotted. The insulin concentration of each of the unknown samples was determined by comparison to the standard curve.

3.3.9.7 **Quantification of Hypothalamic mRNA by QPCR**

Quantitative PCR (QPCR) was used to analyse the expression of a range of mRNA species in order to assess their involvement in the perceived phenotype.

3.3.9.7.1 RNA Extraction

Materials

Tri-reagent (Helena Biosciences, Sunderland, UK)

Method

RNA was extracted from whole hypothalami using the Tri-reagent method according to the manufacturer's protocol. Hypothalamic tissue was ground under liquid nitrogen with a pestle and mortar before being homogenised in 1ml Tri-reagent and subsequently transferred to 1.5ml eppendorfs to incubate at room temperature for 5 minutes.

3.3.9.7.2 RNA Purification

In order to accurately analyse mRNA levels by TaqMan assay sample RNA must not be contaminated with DNA. To achieve this, RNA samples were treated with DNase solution.

Materials

Purelink RNA Mini kit (Invitrogen)
Purelink DNase

Method

Chloroform was added to each sample in a ratio of 0.2ml:1ml of Tri-reagent before vigorous agitation by hand and incubation at room temperature for 3 minutes. Samples were subjected to centrifugation at 12000xg for 15 minutes at 4°C to facilitated phase separation. The upper aqueous phase of each sample was transferred to a fresh tube and an equal volume of 70% ethanol added. Seven hundred microlitres of the resulting mixture was transferred to a spin cartridge before centrifugation at 12000xg for 15 seconds at room temperature. This was repeated until the total sample volume had been processed. The sample RNA was now bound to the spin cartridge, which was subjected to centrifugation at 12000xg for 15 seconds at room temperature with 350µl of wash buffer 1. Eighty microlitres of Purelink DNase was then added directly to the spin cartridge membrane the cartridge incubated at room temperature for 15 minutes. The centrifugation step using wash buffer I was repeated before washing twice with wash buffer II and subsequent centrifugation at 12000xg for 15 minutes. The RNA was then dissolved in RNase-free GDW and stored before its yield was determined spectrophotometrically according to the following equation:

RNA (µg) = dilution factor x 40 x 260nm

3.3.9.7.3 Reverse Transcription of Hypothalamic mRNA

RNA was converted into its complementary cDNA sequence by reverse transcription in order to allow its amplification by PCR. The High Capacity cDNA Reverse Transcription Kit uses the random primer scheme for initiating cDNA synthesis.

Materials

RNA Samples
High Capacity cDNA Reverse Transcription Kit (Applied Biosystems)
96 Well Assay Plate

Method

Ten microlitres of each RNA sample was added in triplicate to reaction wells containing 1X RT buffer, 4mM dNTP mix, 1X RT random primers, and Multiscribe reverse transcriptase. The plate was then foil-sealed before being incubated in a thermal cycler programmed to the following conditions: 25°C for 10 minutes, 37°C for 120 minutes, 85°C for 5 minutes. Following cycle completion, cDNA templates were stored at -20°C.

3.3.9.7.4 QPCR Analysis of Hypothalamic cDNA

TaqMan QPCR assay allows accurate quantification of gene expression by incorporating a fluorescent reporter-tagged probe into the amplification reaction. During PCR, the probe anneals to its complementary sequence, however fluorescence of the tagged reporter is suppressed by the presence of a quencher dye. Taq DNA polymerase cleaves only probes that are hybridised to the target. This separates the quencher from the reporter, producing fluorescence. The increase in fluorescence is relative to the concentration of the target gene in the sample.

Materials

Sample cDNA template (50µg/ml)
Endogenous control cDNA template (5µg/ml)
TaqMan Gene Expression Assay (Applied Biosystems)
TaqMan Gene Expression Master Mix
384 Well Assay Plate

Method

Each QPCR reaction contained: 50ng of the target gene assay, 1µl of cDNA template, 10µl master mix, and GDW to give a final volume of 20µl. To quantify total RNA, a gene expression assay targeting the 18S ribosomal subunit and 10ng target gene were used. cDNA was diluted 1:10 prior to use. Each reaction was mixed and the plate was sealed.

The sealed plate was loaded onto a thermal cycler and processed under the following conditions: 50°C for 2 minutes, 95°C for 10 minutes, 95°C for 15 seconds and 60°C for 1 minute. The cycle was repeated for 40 cycles. The amplification data for each sample was corrected against its respective endogenous control.

3.3.10 Cohort 3

3.3.10.1 Effect of iARC rAAV-GKS on food intake and bodyweight: High energy diet

Male Wistar rats were injected iARC with 1µl rAAV-GKS (n=15) or rAAV-eGFP (n=15). Prior to surgery animals were given *ad libitum* access to high energy chow (D12266B, Research Diets Inc., New Brunswick, USA) for a 3 day acclimatisation period. Following surgery, rats were allowed to recover for a period of 7 days and were given *ad libitum* access to high energy chow. Intake of high energy chow and bodyweight were measured three times per week for a period of 37 days.

3.3.11 Statistical analysis

All longitudinal data (growth curves/cumulative food intake) were analysed using the population-averaged general estimating equation (GEE). For all other data, unpaired t-test was used for experiments with two groups and analysis of variance (ANOVA) followed by Bonferroni post hoc analysis was used for experiments with more than two groups. $P<0.05$ was considered statistically significant throughout. Data analysis was performed using GraphPad Prism 4 software (CA, USA) and Stata 9.

3.4 Results

3.4.1 Glucokinase activity in the hypothalamic nuclei of fed and fasted rats

Glucokinase activity was significantly increased in the ARC of rats fasted for 24hr and 48hr compared to controls (controls 0.0059+/-0.0011 vs 24hr fast 0.0087+/-0.0001 units/mg protein, n=8, P=<0.05; 48hr fast 0.009+/-0.0001 units/mg protein**,** P=<0.05 n=9)(figure 3.1). In the PVN glucokinase activity was unchanged following 24hr and 48hr fast compared to controls (controls 0.01+/-0.0013 vs 24hr fast 0.011+/-0.0008 arbitrary units, n=8; 48hr fast 0.01+/-0.001 units/mg protein, n=9)(figure 3.2). In the VMN glucokinase activity was unchanged following 24hr fast and 48hr fast compared to controls (controls 0.011+/-0.0012 vs 24hr fast 0.009+/-0.0008 units/mg protein, n=8**;** 48hr fast 0.01+/-0.001 units/mg protein, n=9) (figure 3.3).

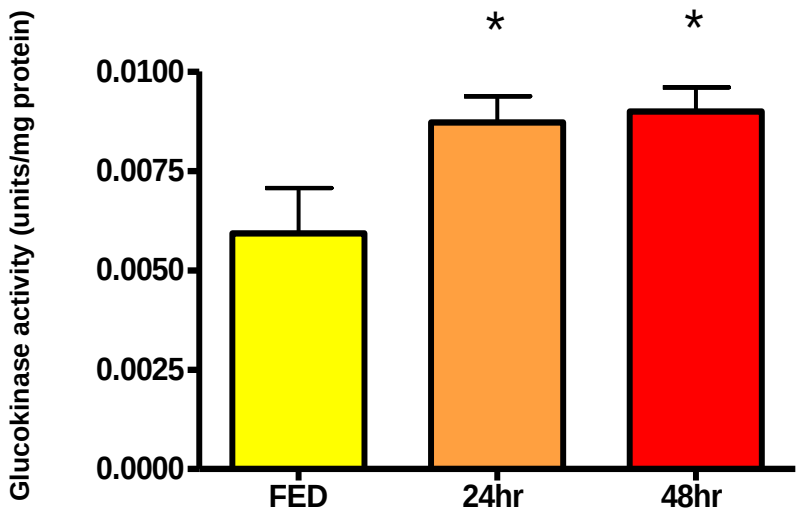


Figure 3.1 Glucokinase activity in ARC of fed and fasted rats: *GK activity in ARC of fed (yellow bar), 24hr fasted (orange bar) and 48hr fasted (red bar) male Wistar rats. Data are expressed as mean units of enzymatic activity per mg protein +/- SEM, n=8-9, *=P<0.05 vs fed.*

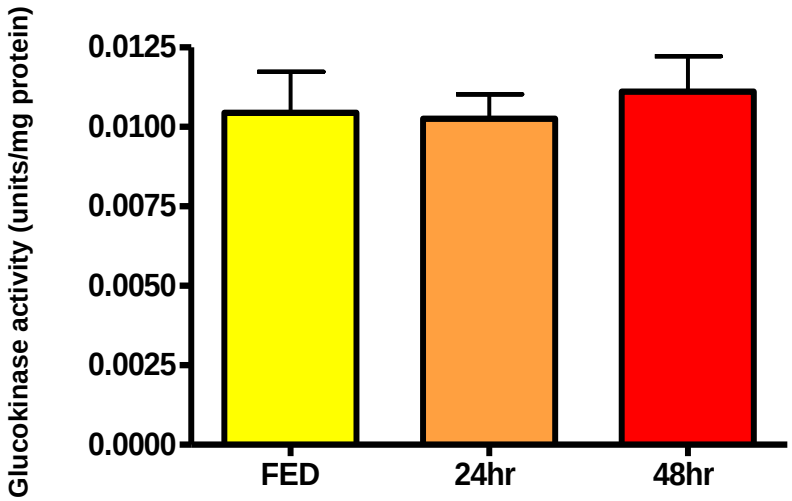


Figure 3.2 Glucokinase activity in the PVN of fed and fasted rats: *GK activity in PVN of fed (yellow bar), 24hr fasted (orange bar) and 48hr fasted (red bar) male Wistar rats. Data are expressed as mean units of enzymatic activity per mg protein +/- SEM, n=8-9.*

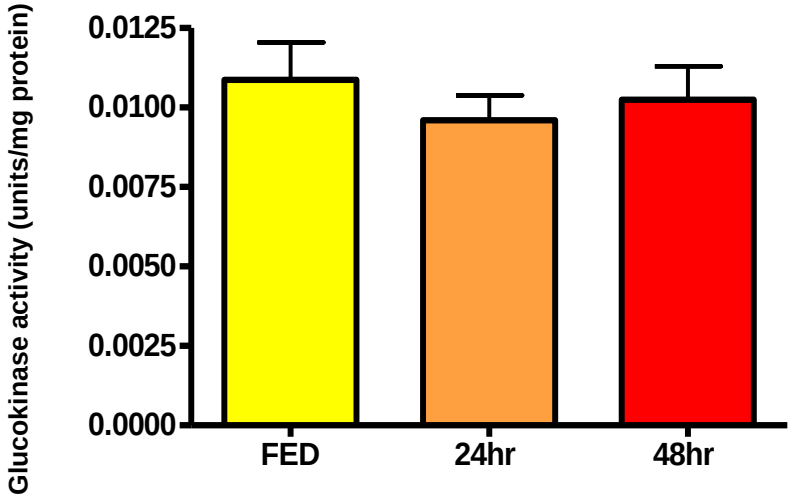


Figure 3.3 Glucokinase activity in the VMN of fed and fasted rats: *GK activity in VMN of fed (yellow bar), 24hr fasted (orange bar) and 48hr fasted (red bar) male Wistar rats. Data are expressed as mean units of enzymatic activity per mg protein +/- SEM, n=8-9.*

3.4.2 Cohort 1: Effect of iARC rAAV-GKS on food intake and bodyweight

3.4.2.1 Confirmation of gene transfer by in situ hybridisation

Three weeks post injection three rats from the GKS group were killed and *in situ* hybridisation was performed to confirm transgene expression. Transgene expression was demonstrated in all three brains and was localized to the ARC. For a representative image of *in situ* hybridisation see figure 3.4.

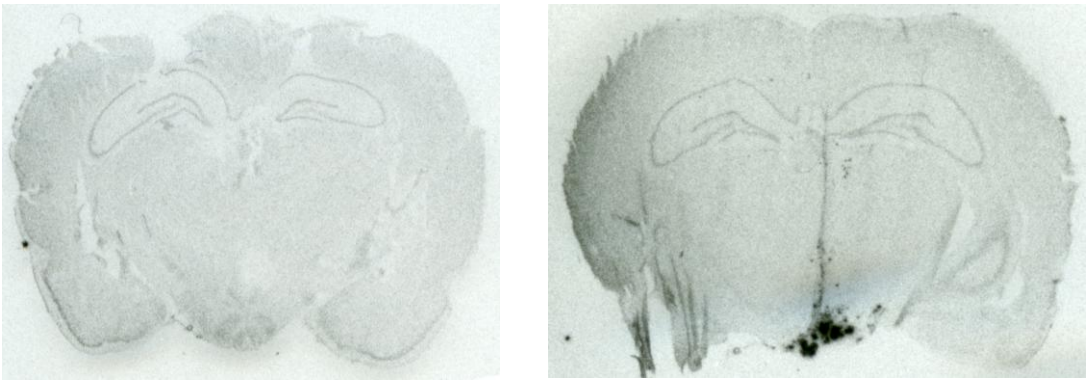
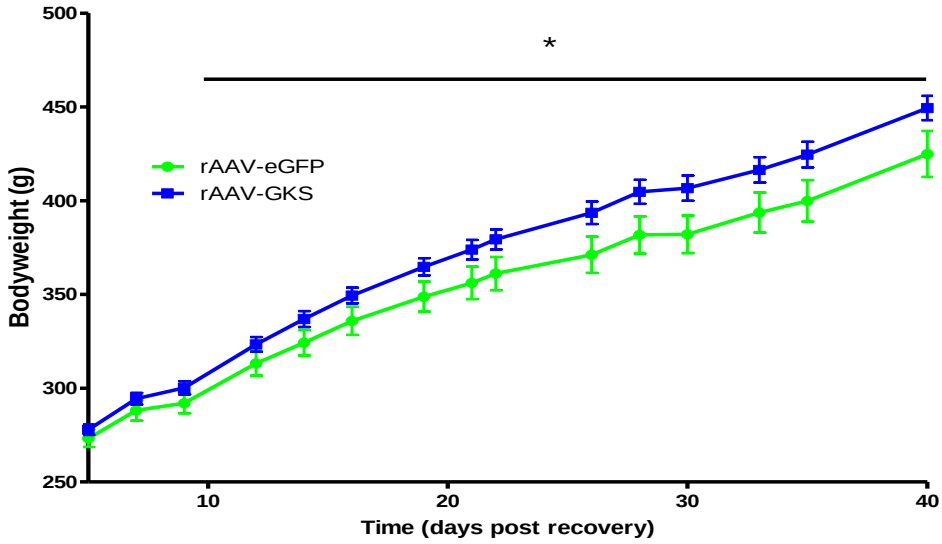


Figure 3.4 Confirmation of gene transfer by in situ hybridisation*: GK mRNA expression in brains of male Wistar rats a) endogenous expression b) GK expression in the ARC 3 weeks post injection with rAAV-GKS.*

3.4.2.2 **Effect on bodyweight and bodyweight gain**

At the termination of the experiment (day 40 post recovery), there was a pronounced and significant difference in bodyweight (eGFP 424.9 +/- 12.9g vs GKS 449.4 +/- 6.5g, n=12-16, P=<0.05) and bodyweight gain (eGFP 151.7 +/- 8.9g vs GKS 171.6 +/- 5.9g, n=12-16, P=<0.05) between the eGFP group and the GKS group (figure 3.5).

a)



b)

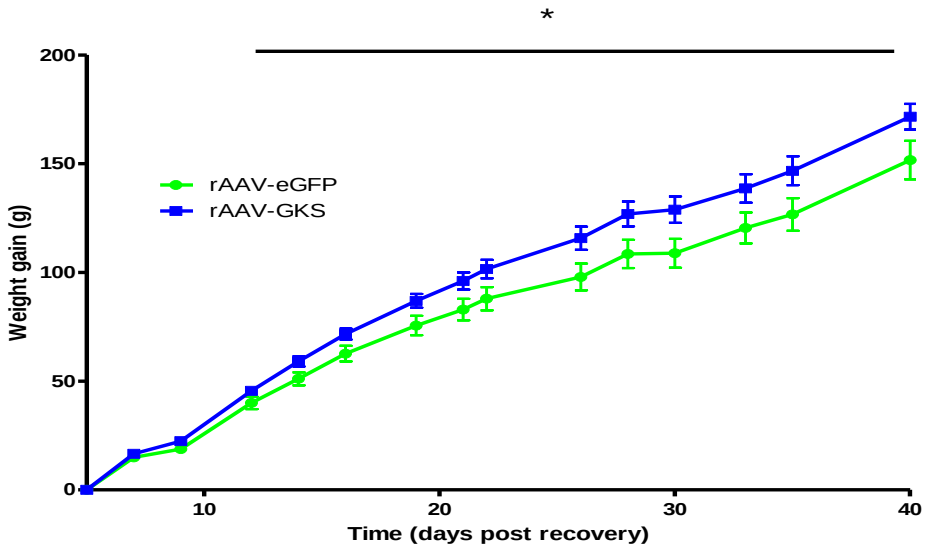


Figure 3.5 Effect of iARC rAAV-GKS on bodyweight and bodyweight gain: *a) Bodyweight and b) bodyweight gain following bilateral injection of 1ul rAAV-eGFP (green line) or 1ul rAAV-GKS (blue line). Male Wistar rats were fed normal chow. Data are expressed as mean +/- SEM for both groups, n=12-16, *=P<0.05.*

3.4.2.3 **Effect on food intake**

At day 40, when the experiment was terminated, there was a significant increase in cumulative food intake in the GKS group compared to the eGFP group (eGFP 1094.3+/- 22.4g vs GKS 1183.2 +/- 25.7g, n=12-16, P=<0.01) (figure 3.6).

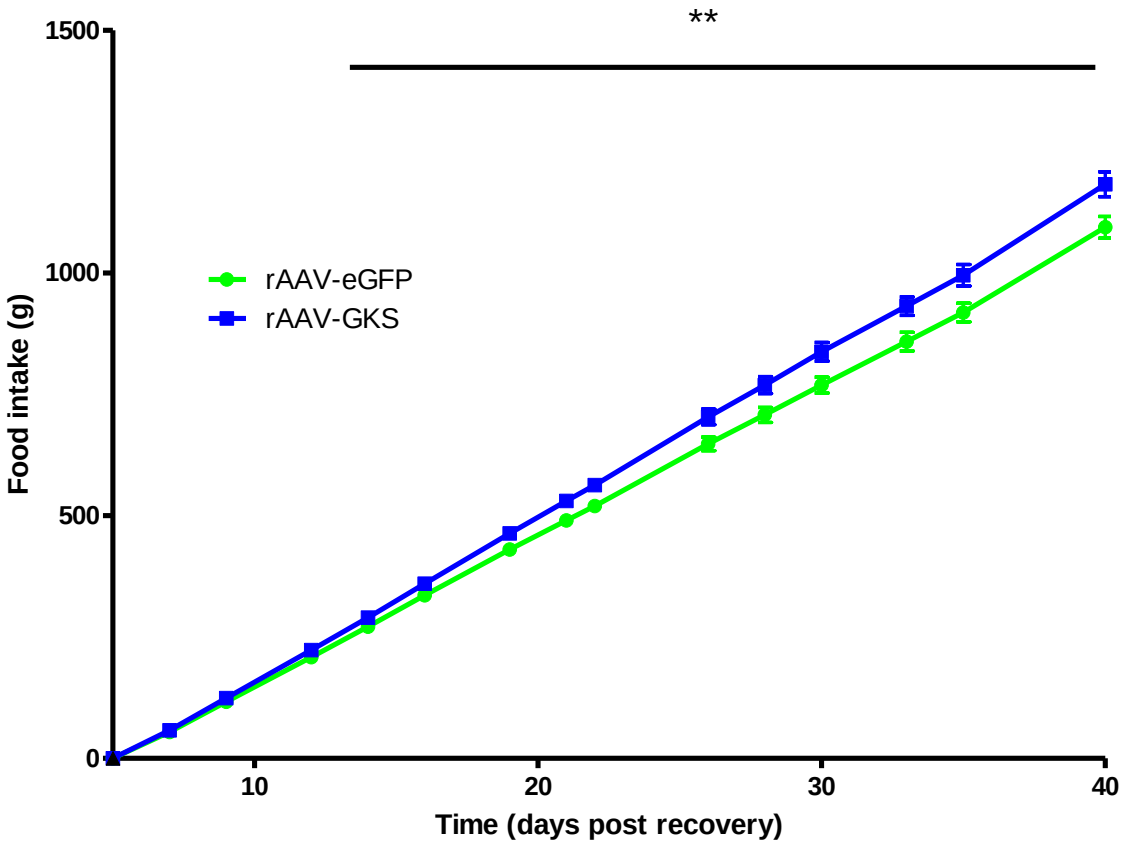


Figure 3.6 Effect of iARC rAAV-GKS on food intake*: Food intake following bilateral injection of 1ul rAAV-eGFP (green line) or 1ul rAAV-GKS (blue line). Male Wistar rats were fed normal chow. Data are expressed as mean +/- SEM for both groups, n=12-16, **=P<0.01.*

3.4.2.4 **Body composition**

At the termination of the study (day 40) body composition was analysed by carcass dissolution followed by protein and glycerol assays. Glycerol concentration was significantly higher in samples taken from GKS animals compared to controls (eGFP 0.66+/-0.05mM vs. GKS 0.88+/-0.07mM, n=12-16, P=<0.05) and body fat percentage was 4.8% higher in GKS animals (eGFP 23.2+/-1.7% vs. GKS 27.9+/-1.6%, n=12-16) (figure 3.7). There was no difference in mean protein concentration of samples (eGFP 71.1+/-2.1mg/ml vs. GKS 75.9+/-2.7mg/ml, n=12-16) or percentage bodyweight as protein (eGFP 16.9 +/-0.4% vs. GKS 16.9+/-0.5%, n=12-16) (figure 3.7).

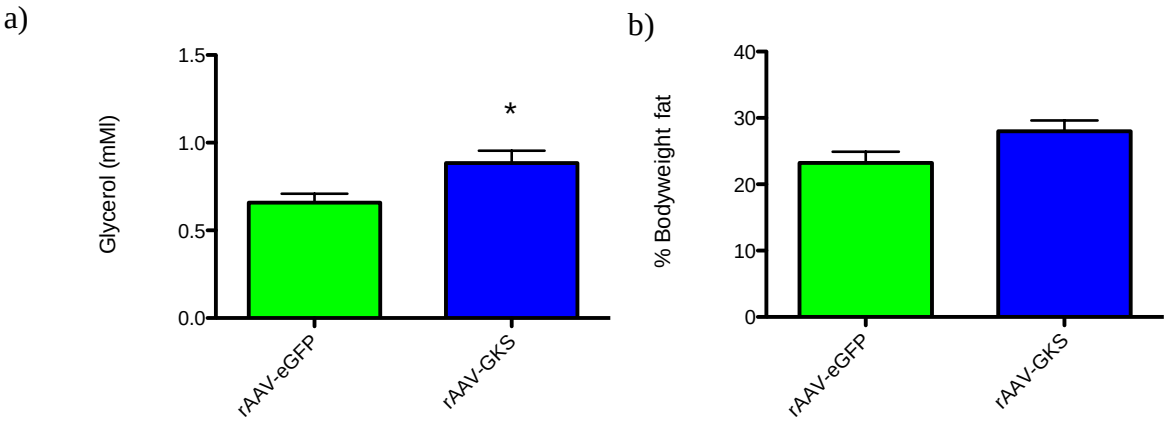


Figure 3.7 Effect of iARC rAAV-GKS on glycerol concentration and adiposity*: (a) Glycerol concentration of saponification reaction samples and (b) body fat percentage of male Wistar rats after bilateral injection with either 1ul rAAV-eGFP (green bars) or 1ul rAAV-GKS (blue bars) 40 days post surgical recovery. Data are expressed as mean +/- SEM for both groups, n=12-16, *=P<0.05.*

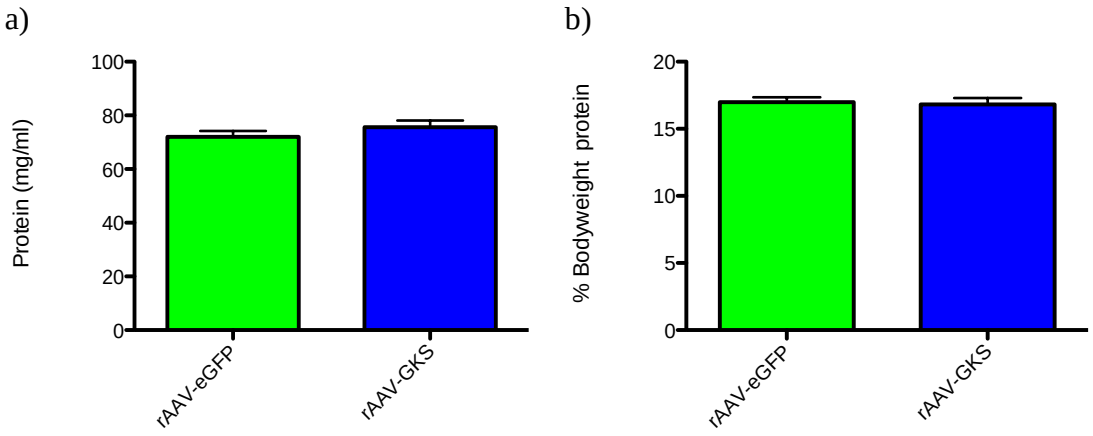


Figure 3.8 Effect of iARC rAAV-GKS on protein concentration and lean body mass*: (a) Protein concentration of saponification reaction samples and (b) percentage bodyweight as protein of male Wistar rats injected with either 1ul rAAV-eGFP (green bar) or 1ul rAAV-GKS (blue bar) 40 days post surgical recovery. Data are expressed as mean +/- SEM for both groups, n=12-16.*

3.4.2.5 **Effect of iARC rAAV-GKS on GK activity in the ARC and PVN**

Punch biopsies from the ARC and PVN of animals in the study group were homogenised and optimised GK assay was performed. GK activity increased slightly but not significantly in the GKS group compared to eGFP controls (eGFP 0.0048+/-0.0007 vs GKS 0.0056+/-0.0006 units/mg protein, n=8-11) (figure 3.9a). In the PVN there was no difference between the groups (eGFP 0.0052+/-0.0011 vs GK 0.0052+/-0.0004 units/mg protein, n=8-11) (figure 3.9b).

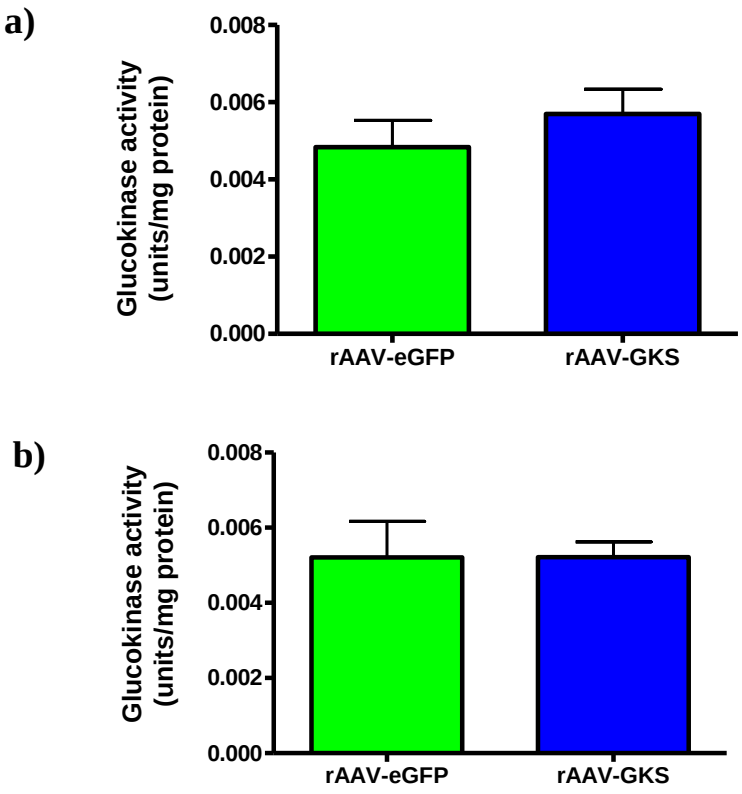


Figure 3.9 Effect of iARC rAAV-GKS on GK activity in the ARC and PVN*: GK activity in the a) ARC and b) PVN of male Wistar rats 40 days post surgical recovery following iARC injection of either 1ul rAAV-eGFP (green bars) or 1ul rAAV-GKS (blue bars). Data are expressed as mean units of enzymatic activity per mg protein +/- SEM, n=8-9, n=8-11.*

3.4.3 Cohort 2: Effect of iARC rAAV-GKS on food intake and bodyweight, effect of pair feeding

3.4.3.1 Effect on bodyweight and weight gain

At the termination of the experiment (day 33 post recovery) there was a significant difference in bodyweight (eGFP 399.4 +/- 4.7g vs GKS 419.0 +/- 5.5g, n=11-13, P=<0.01 and weight gain (eGFP 123.4 +/- 2.6g vs GKS 145.5 +/- 6.5g, n=11-13, P=<0.01) in the GKS compared to the eGFP group. There was also a significant difference between the bodyweight (GKS 419.0 +/- 5.5g vs GKPF 393.2 +/- 5.5g, n=13-15, P=<0.001) and weight gain (GKS 145.5 +/- 6.5g vs GKPF 114.5 +/- 5.9g, n=13-15, P=<0.001) of the GKS group and the GKPF group. There was no significant difference between the bodyweight or weight gain of the eGFP group and the GKPF group (figure 3.10).

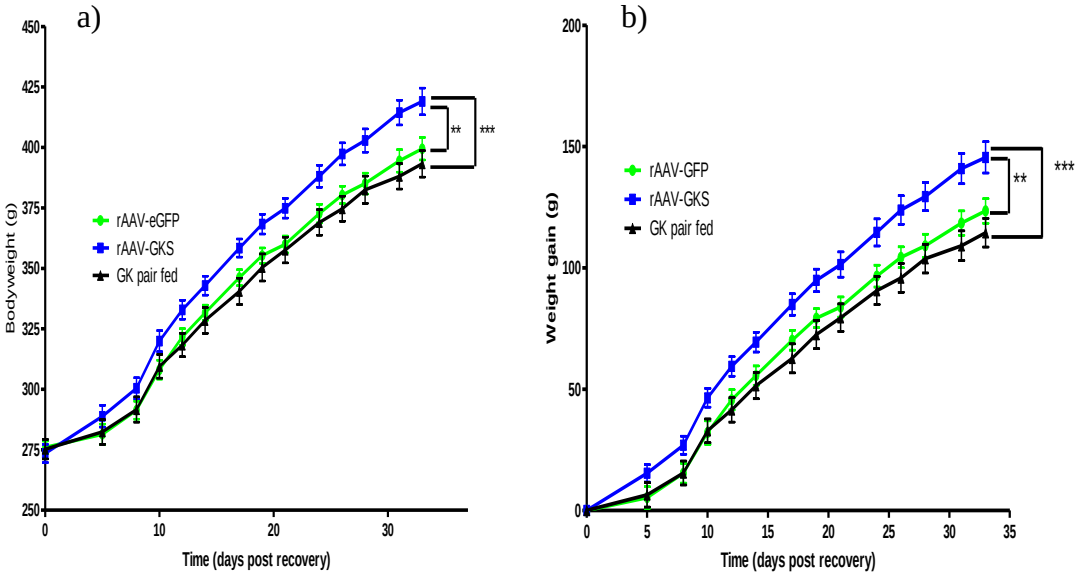


Figure 3.10 Effect of iARC rAAV-GKS on bodyweight and weight gain; effect of pair feeding*: a) Bodyweight and b) weight gain following bilateral injection of 1ul rAAV-eGFP (green line) or 1ul rAAV-GKS (blue line) and animals receiving 1ul rAAV-GKS pair fed to rAAV-eGFP (black line). Male Wistar rats were fed normal chow. Data are expressed as mean +/- SEM for all groups, n=11-15,**=P<0.01, ***=P<0.001.*

3.4.3.2 **Effect on food intake**

At the termination of the experiment (day 33) there was a small difference between the food intake of the GKS group (963.0 +/-13.9g, n=13) and the eGFP group (932.0 +/-6.4g, n=11) but this did not reach significance (figure 3.11).

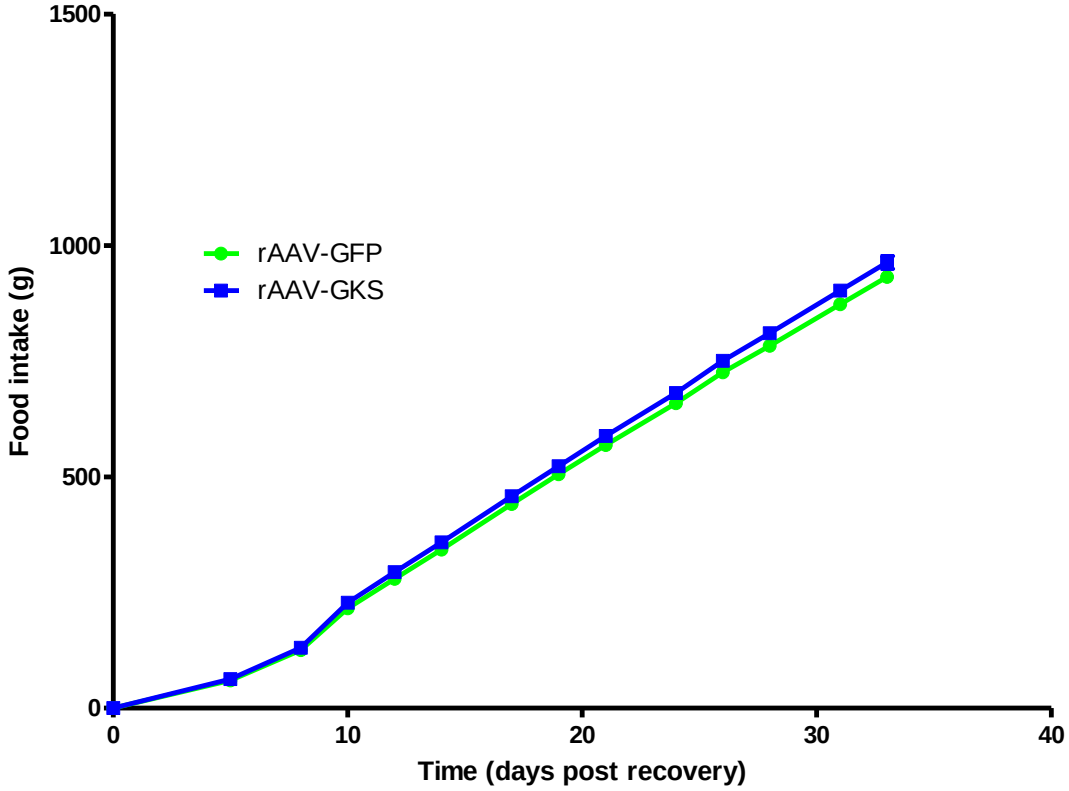


Figure 3.11 *Effect of iARC rAAV-GKS on food intake, effect of pair feeding: Food intake following bilateral injection of 1ul rAAV-eGFP (green line) or 1ul rAAV-GKS (blue line). Male Wistar rats were fed normal chow. Data are expressed as mean +/- SEM for both groups, n=11-13.*

3.4.3.3 **Effect of iARC rAAV-GKS on 24hr food intake and bodyweight following 24hr fast**

3.4.3.3.1 Food intake

Food intake was not different between the groups until the 8-24hr period post re-feeding when the GKPF group and the GKS group consumed significantly more chow compared to the eGFP group (eGFP 9.6+/-0.82g vs GKPF 14.9 +/- 0.87g, n=10-14, P=<0.001; GKS 12.5+/- 0.64g, n=12**,** P=<0.05 vs eGFP) (figure 3.12e). Cumulative 24hr food intake was significantly different between the GKPF group and the eGFP group (eGFP 35.5+/- 0.59g vs rAAV-GKPF 39.9 +/-1.38g, n=10-14, P=<0.05) but neither were significantly different from the rAAV-GKS groups (36.7+/- 0.75g, n=12) (figure 3.12f).

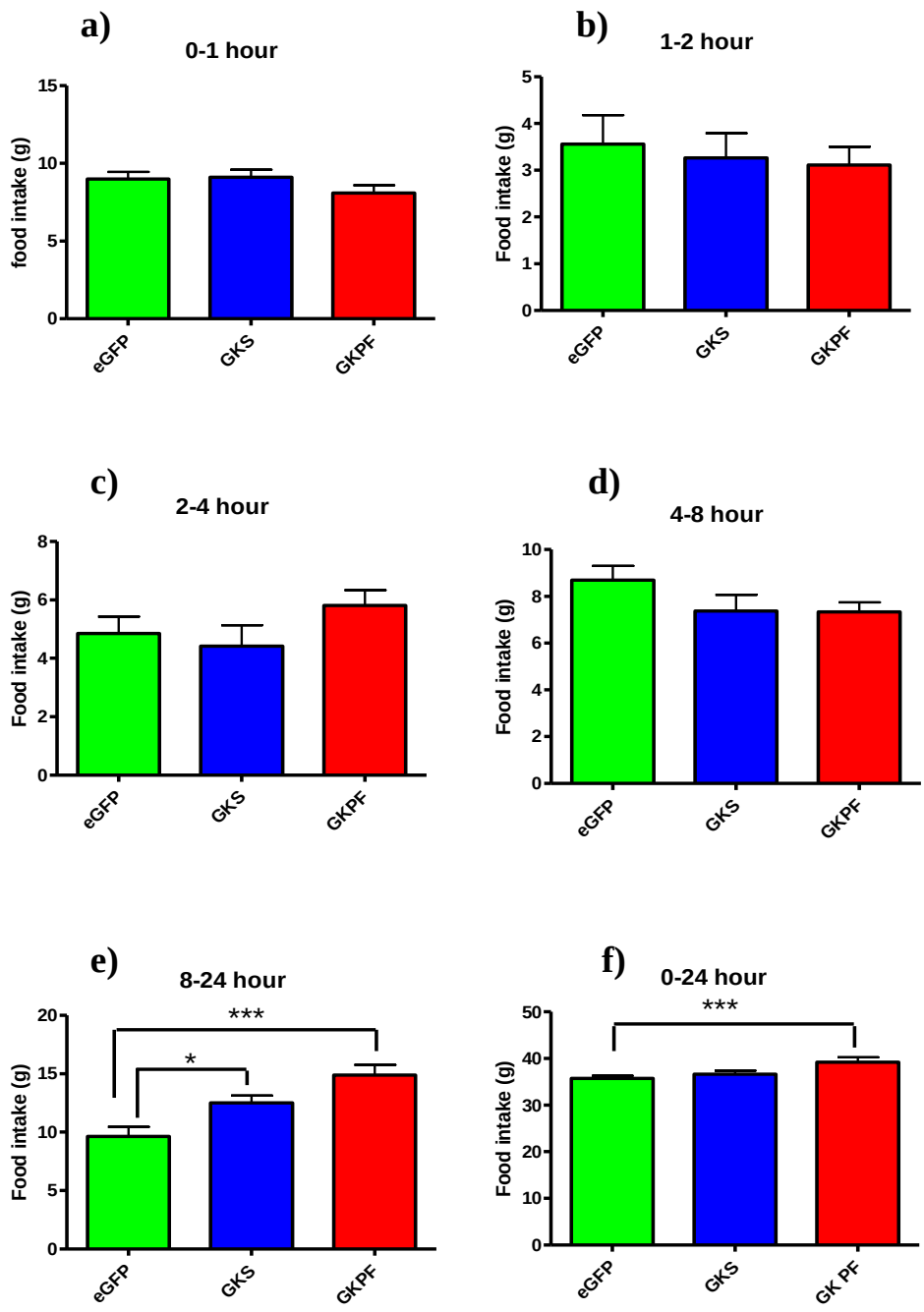


Figure 3.12 Effect of iARC rAAV-GKS on 24hr food intake following 24hr fast: 24hr food intake of male Wistar rats injected with 1ul rAAV-eGFP (green bars), 1ul rAAV-GKS (blue bars) and rats injected with 1ul rAAV-GKS and pair fed to rAAV-eGFP animals throughout life (red bars). All groups were fasted for 24hr and allowed *ad libitum* access to standard chow for a 24hr period at the start of the dark phase day 35 post recovery. Data are expressed as mean +/- SEM for all groups, n=10-14,*=P<0.05, ***=P<0.001.

3.4.3.3.2 Bodyweight

Following 24hr fast the GKPF group lost significantly less weight (16.7 +/-0.7g, n=14) than the GKS group (24.9+/-0.68g, n=12, P=<0.05) and eGFP group (23.1+/-0.67g, n=10, P=<0.05) (figure 3.13a). Following 24hr re-feed the GKS group gained significantly more weight than the eGFP group (eGFP 16.6+/- 1.22g vs GKS 19.5+/-0.46g, n=10-12,P=<0.05), as did the GKPF group (20.9 +/-1.61g, n=14, P=<0.05). The GKPF group gained significantly more weight than the GKS group (P=<0.05) (figure 3.13b).

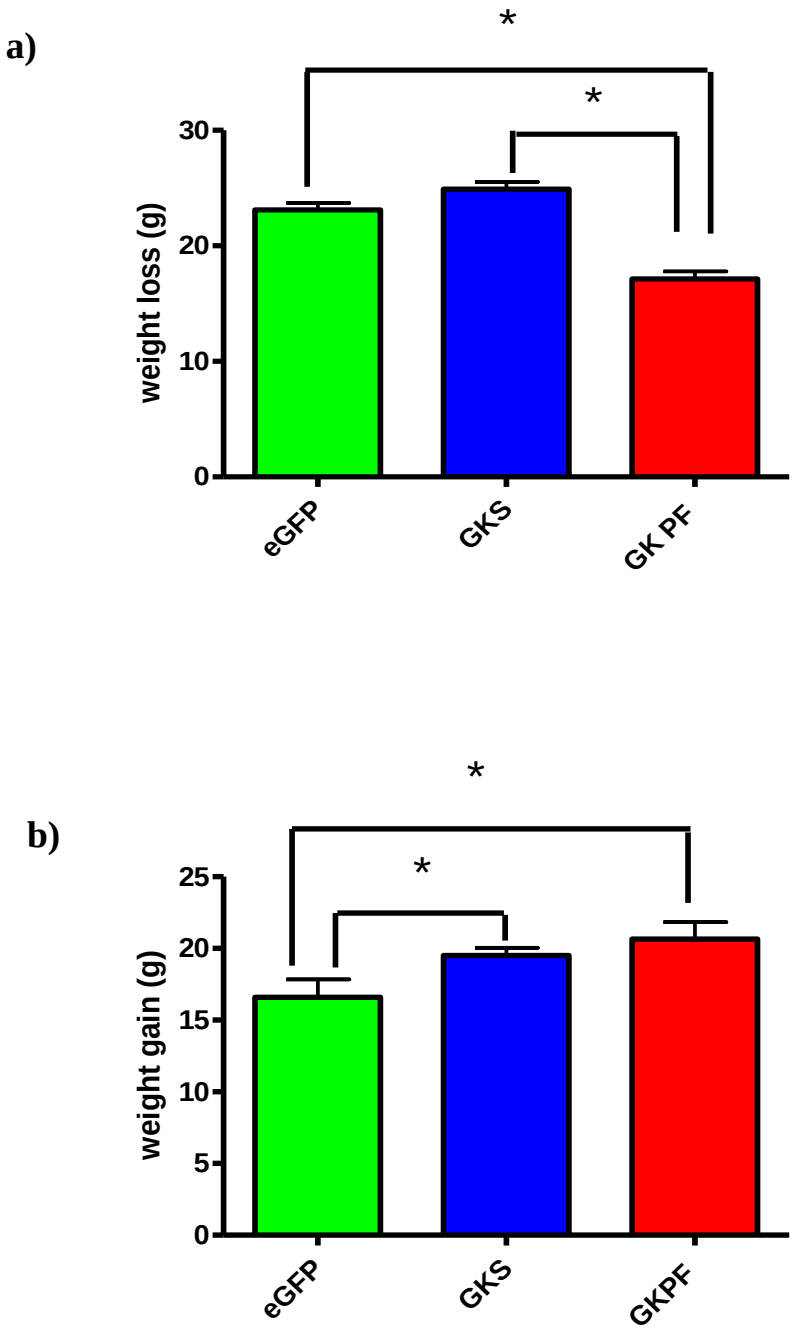


Figure 3.13 **Effect of iARC rAAV-GKS on 24hr weight gain following 24hr fast and re-fed:** *24hr a) bodyweight loss and b) bodyweight gain of male Wistar rats injected with 1ul rAAV-eGFP (green bar), 1ul rAAV-GKS (blue bar) and rats injected bilaterally with 1ul rAAV-GKS and pair fed to rAAV-eGFP animals throughout life (red bar). All groups were fasted for 24hr and allowed ad libitum access to standard chow for a 24hr period at the start of the dark phase on day 35 post recovery. Bodyweight was measured post 24hr fast (a) and 24hr after re-feeding (b). Data are expressed as mean +/- SEM for all groups, n=10-14, *=P<0.05*

3.4.3.4 **Effect of iARC rAAV-GKS on body composition and plasma hormones**

At the termination of the study (day 40 post recovery) rats were killed by decapitation and tissues were collected.

3.4.3.4.1 BAT weight

Intrascapular brown adipose tissue (BAT) was removed and weighed. BAT weight was not different between the GKS group and the eGFP group (eGFP 0.55+/- 0.03g vs GKS 0.62+/-0.04g, n=10-12). BAT weight was lower in the GKPF group compared to GKS (GKS 0.62+/-0.04g vs GKPF 0.47+/-0.03g, n=10-14, P=<0.05). BAT weight was also lower in the GKPF group compared to the eGFP but this did not reach significance (eGFP 0.55+/- 0.03g vs GKPF 0.47+/-0.03g, n=10-14) (figure 3.14).

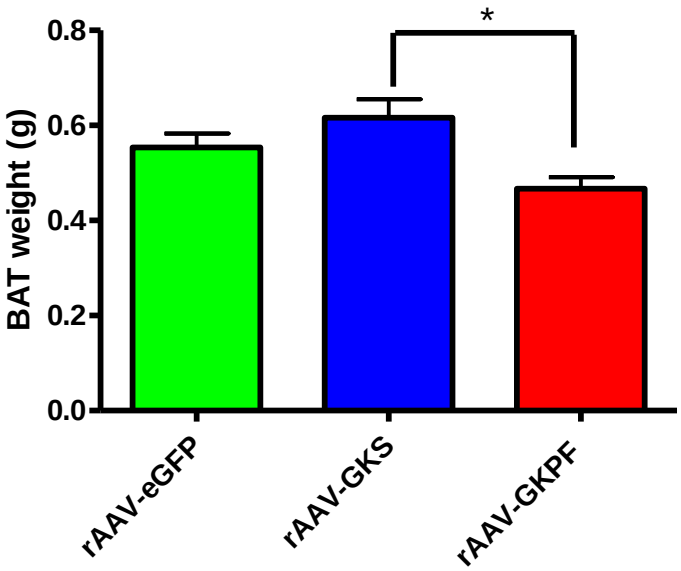


Figure 3.14 **Effect of iARC rAAV-GKS on BAT weight:** *BAT weight of male Wistar rats injected bilaterally with 1ul rAAV-eGFP (green bar), 1ul rAAV-GKS (blue bar) and rats injected with 1ul rAAV-GKS and pair fed to rAAV-eGFP animals throughout life (red bar). Data are expressed as mean +/- SEM for all groups, n=10-14, *=P<0.05.*

3.4.3.4.2 Epididymal WAT weight

Epididymal white adipose tissue (WAT) was removed and weighed. Epididymal WAT weight was not significantly different between the groups (eGFP 6.89+/- 0.44g vs GKS 8.38+/-0.84g vs GKPF 7.64+/- 0.53 n=10-14) (figure 3.15).

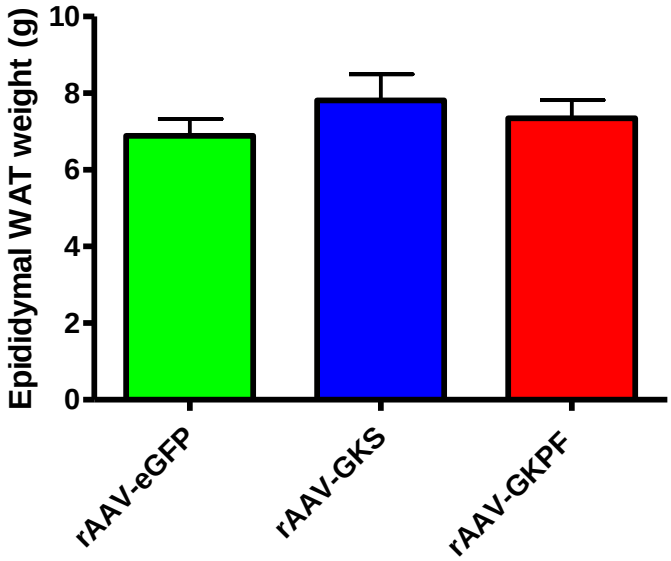


Figure 3.15 **Effect of iARC rAAV-GKS on epididymal WAT weight:** *Epididymal WAT weight of male Wistar rats injected bilaterally with 1ul rAAV-eGFP (green bar), 1ul rAAV-GKS (blue bar) and rats injected with 1ul rAAV-GKS and pair fed to rAAV-eGFP animals throughout life (red bar). Data are expressed as mean +/- SEM for all groups, n=10-14.*

3.4.3.4.3 Fed blood glucose

In the fed state blood glucose levels were not different between the groups (eGFP 4.7+/-0.2g vs GKS 4.7+/-0.1g vs GKPF 4.8+/- 0.1 n=10-14) (figure 3.16).

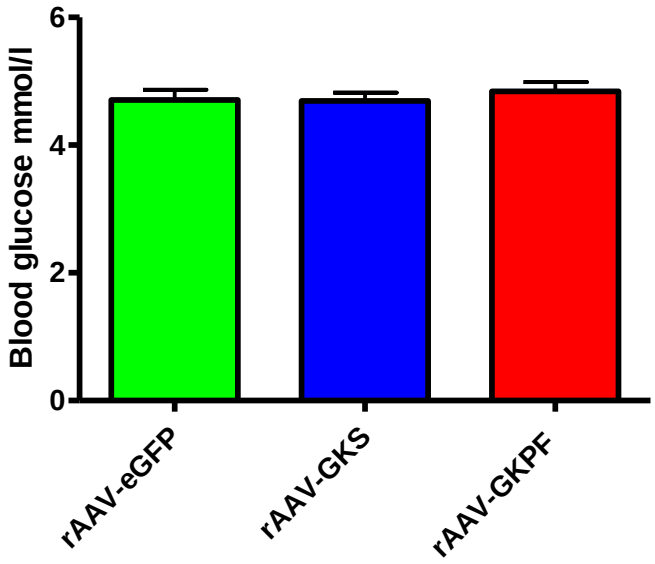


Figure 3.16 **Effect of iARC rAAV-GKS on fed blood glucose:** *Blood glucose measured in fed male Wistar rats injected bilaterally with 1ul rAAV-eGFP (green bar), 1ul rAAV-GKS (blue bar) and rats injected with 1ul rAAV-GKS and pair fed to rAAV-eGFP animals throughout life (red bar). Data are expressed as mean +/- SEM for all groups, n=10-14.*

3.4.3.4.4 Fed plasma insulin

In the fed state plasma insulin was significantly higher in the GKS group compared to eGFP controls (eGFP 301.2+/- 16.7pmol/l vs GKS 388.0+/-40.8pmol/l, n=10-12, P=<0.05) and compared to GK animals pair fed to controls **(**GKS 388.0+/-40.8pmol/l vs GKPF 254.8+/-13.9pmol/l, n=10-14, P=<0.01**)** (figure 3.17).

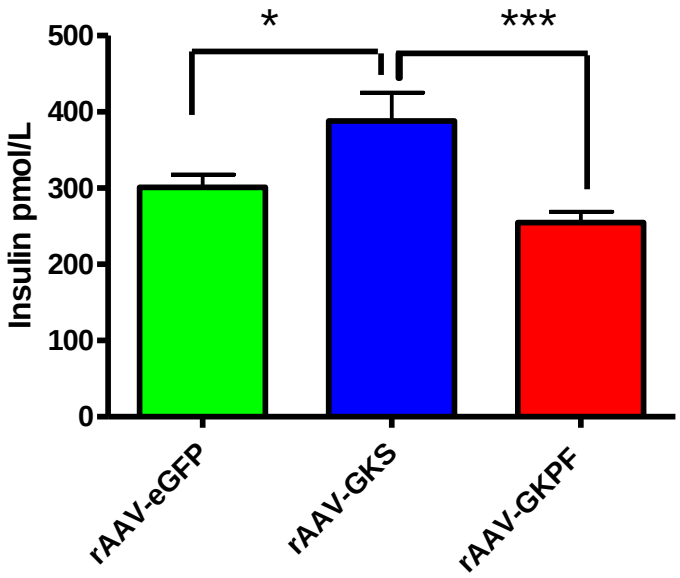


Figure 3.17 **Effect of iARC rAAV-GKS on fed plasma insulin:** *Plasma insulin measured in fed male Wistar rats injected bilaterally with 1ul rAAV-eGFP (green bar), 1ul rAAV-GKS (blue bar) and rats injected with 1ul rAAV-GKS and pair fed to rAAV-eGFP animals throughout life (red bar). Data are expressed as mean +/- SEM for all groups, n=10-14, *=P<0.05, **=P<0.01.*

3.4.3.5 **Hypothalamic gene expression**

3.4.3.5.1 GK

Hypothalamic GK mRNA expression was significantly increased in GKS treated animals compared to control at the termination of the study **(**eGFP 3.93+/- 1.19 vs GKS 53.9+/-12.16 arbitrary units, n=10-12, P=<0.05). Hypothalamic GK mRNA was also significantly increased in the pair fed GK group compared to controls **(**eGFP 3.93+/- 1.19 vs GKPF 58.47+/- 14.6 arbitrary units, n=10-14, P=<0.01**)** (figure 3.18).

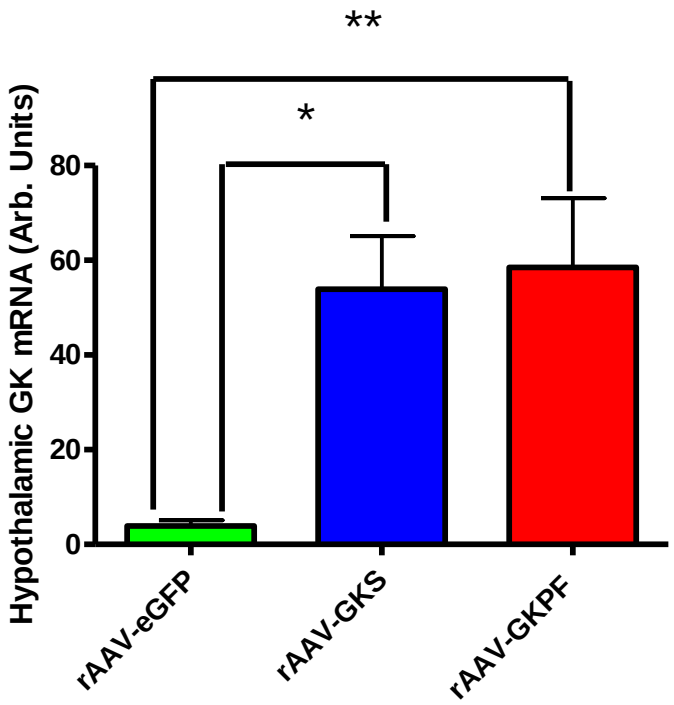


Figure 3.18 **Effect of iARC rAAV-GKS on hypothalamic GK mRNA expression:** *GK mRNA expression measured in whole hypothalami from fed male Wistar rats injected bilaterally with 1ul rAAV-eGFP (green bar), 1ul rAAV-GKS (blue bar) and rats injected with 1ul rAAV-GKS and pair fed to rAAV-eGFP animals throughout life (red bar). Data are expressed as mean +/- SEM for all groups, n=10-14, *=P<0.05, **=P<0.01.*

3.4.3.5.2 AMPK

Hypothalamic AMPK mRNA expression was not significantly different between the groups (eGFP 0.66+/- 0.09 vs GKS 0.64+/-0.08 arbitrary units, n=10-12) (figure 3.19).

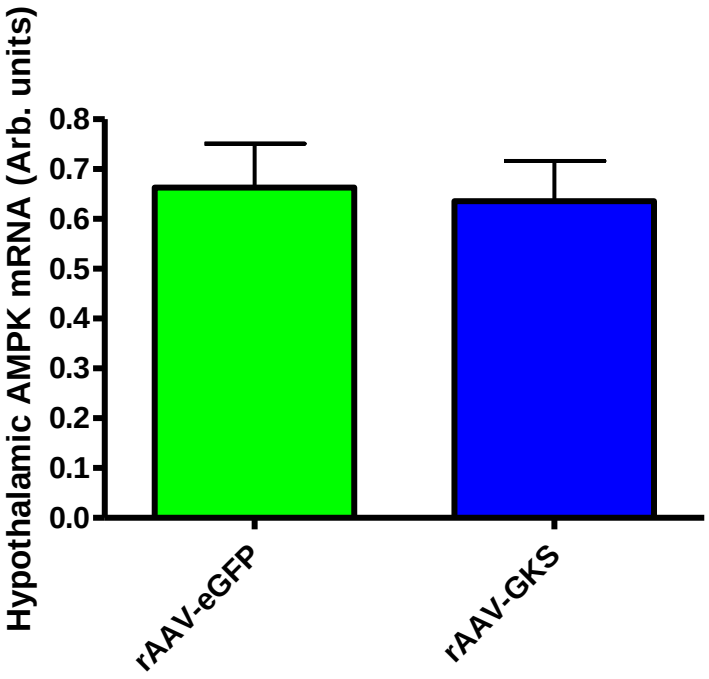


Figure 3.19 **Effect of iARC rAAV-GKS on hypothalamic AMPK mRNA expression:** *AMPK mRNA expression measured in whole hypothalami from fed male Wistar rats injected bilaterally with 1ul rAAV-eGFP (green bar)or 1ul rAAV-GKS (blue bar). Data are expressed as mean +/- SEM for all groups, n=10-12.*

3.4.3.5.3 CART

Hypothalamic CART mRNA expression was not significantly different between the groups (eGFP 0.59+/-0.09 vs GKS 0.52+/-0.06 arbitrary units, n=10-14) (figure 3.20).

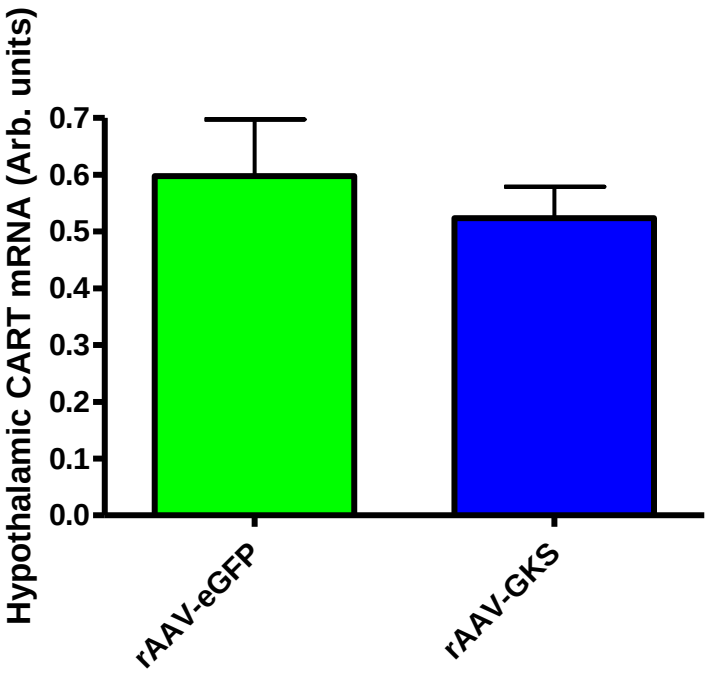


Figure 3.20 **Effect of iARC rAAV-GKS on hypothalamic CART mRNA expression:** *CART mRNA expression measured in whole hypothalami from fed male Wistar rats injected bilaterally with 1ul rAAV-eGFP (green bar)or 1ul rAAV-GKS (blue bar). Data are expressed as mean +/- SEM for all groups, n=10-12.*

3.4.3.5.4 FAS

Hypothalamic FAS mRNA expression was not significantly different between the groups (eGFP 0.45+/-0.09 vs GKS 0.58+/-0.08 arbitrary units, n=10-12) (figure 3.21).

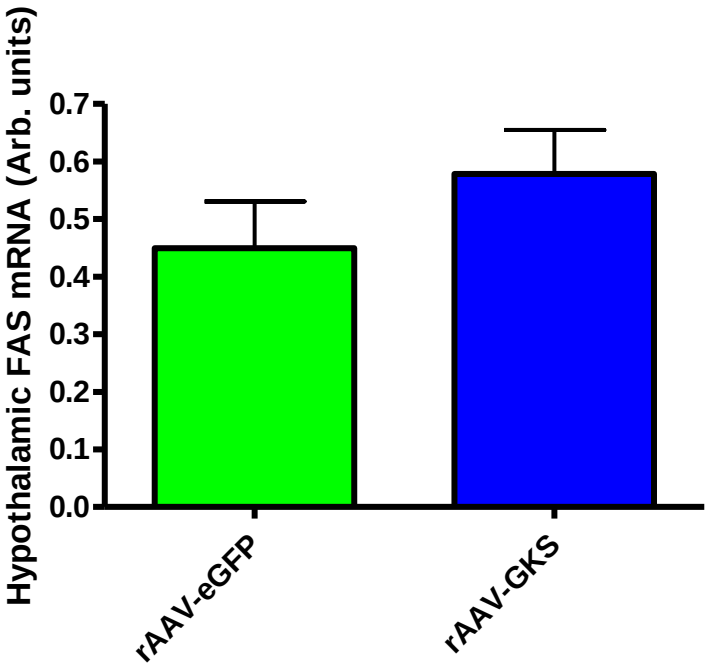


Figure 3.21 **Effect of iARC rAAV-GKS on hypothalamic FAS mRNA expression:** *FAS mRNA expression measured in whole hypothalami from fed male Wistar rats injected bilaterally with 1ul rAAV-eGFP (green bar)or 1ul rAAV-GKS (blue bar). Data are expressed as mean +/- SEM for all groups, n=10-12.*

3.4.3.5.5 NPY

Hypothalamic NPY mRNA expression was not significantly different between the groups (eGFP 0.66+/-0.1 vs GKS 0.63+/-0.04 arbitrary units, n=10-12) (figure 3.22).

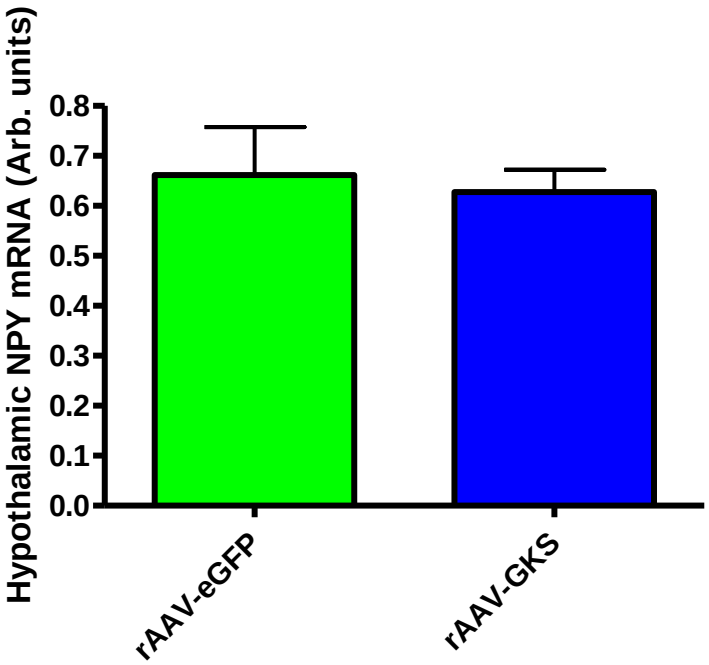


Figure 3.22 **Effect of iARC rAAV-GKS on hypothalamic NPY mRNA expression:** *NPY mRNA expression measured in whole hypothalami from fed male Wistar rats injected bilaterally with 1ul rAAV-eGFP (green bar)or 1ul rAAV-GKS (blue bar). Data are expressed as mean +/- SEM for all groups, n=10-12.*

3.4.3.5.6 POMC

Hypothalamic POMC mRNA expression was not significantly different between the groups (eGFP 0.59+/-0.11 vs GKS 0.64+/-0.11 arbitrary units, n=10-12) (figure 3.23).

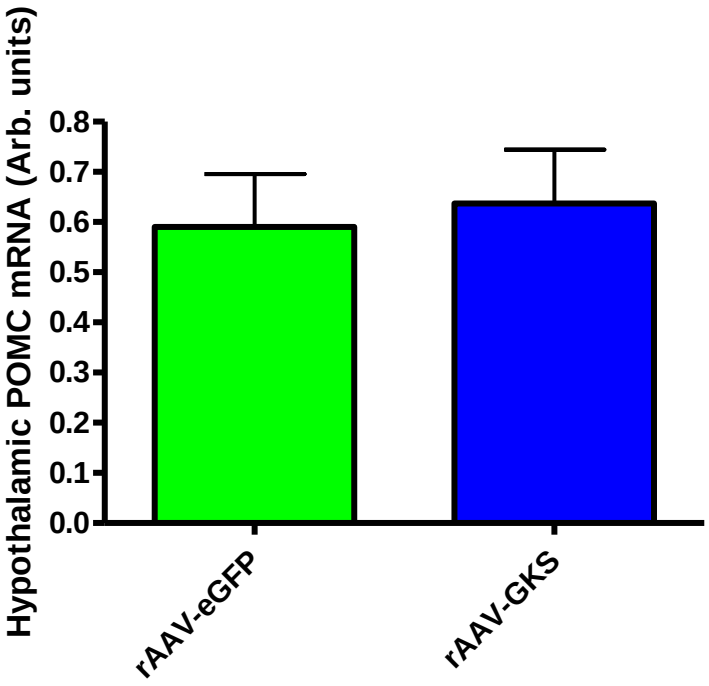


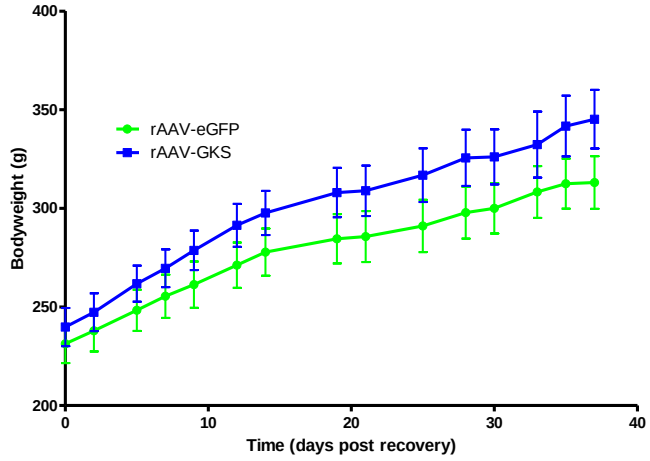
Figure 3.23 **Effect of iARC rAAV-GKS on hypothalamic POMC mRNA expression:** *POMC mRNA expression measured in whole hypothalami from fed male Wistar rats injected bilaterally with 1ul rAAV-eGFP (green bar)or 1ul rAAV-GKS (blue bar). Data are expressed as mean +/- SEM for all groups, n=10-12.*

3.4.4 Cohort 3: Effect of iARC rAAV-GKS on food intake and bodyweight: High energy diet

3.4.4.1 Effect on bodyweight gain

At the termination of the experiment (day 37), there was no significant difference between the mean bodyweights of the groups (eGFP 313.1+/-13.3g vs GKS 345.2+/-14.8g, n=9-11). However, weight gain was significantly different between the eGFP group and the GKS group (eGFP 81.8+/-5.5g vs GKS 105.4+/- 7.4g, n=9-11, P=<0.05) (figure 3.24).

a)



b)

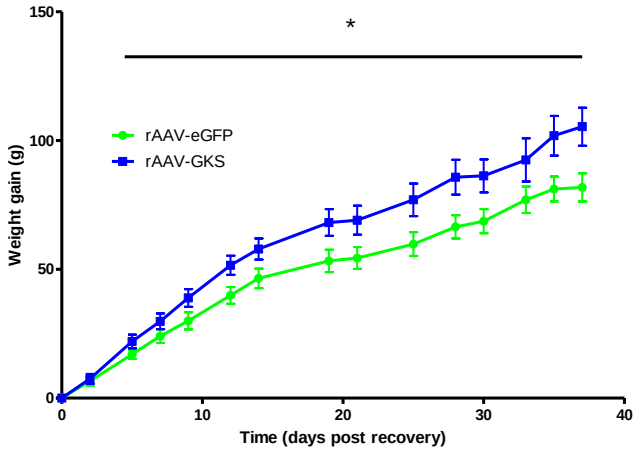


Figure 3.24 Effect of iARC rAAV-GKS on bodyweight and weight gain; high energy diet: *a) bodyweight and b) weight gain following bilateral injection of 1ul rAAV-eGFP (green line) or 1ul rAAV-GKS (blue line). Male Wistar rats were fed a high energy diet for 37 days. Data are expressed as mean +/- SEM for both groups, n=9-11, *=P<0.05.*

3.4.4.2 **Effect on food intake**

At the termination of the study (day 37) food intake was significantly higher in the GKS group compared to controls (eGFP 803.5+/-14.6g vs GKS 887.0+/- 25.8g, n=9-11, P=<0.05) (figure 3.25).

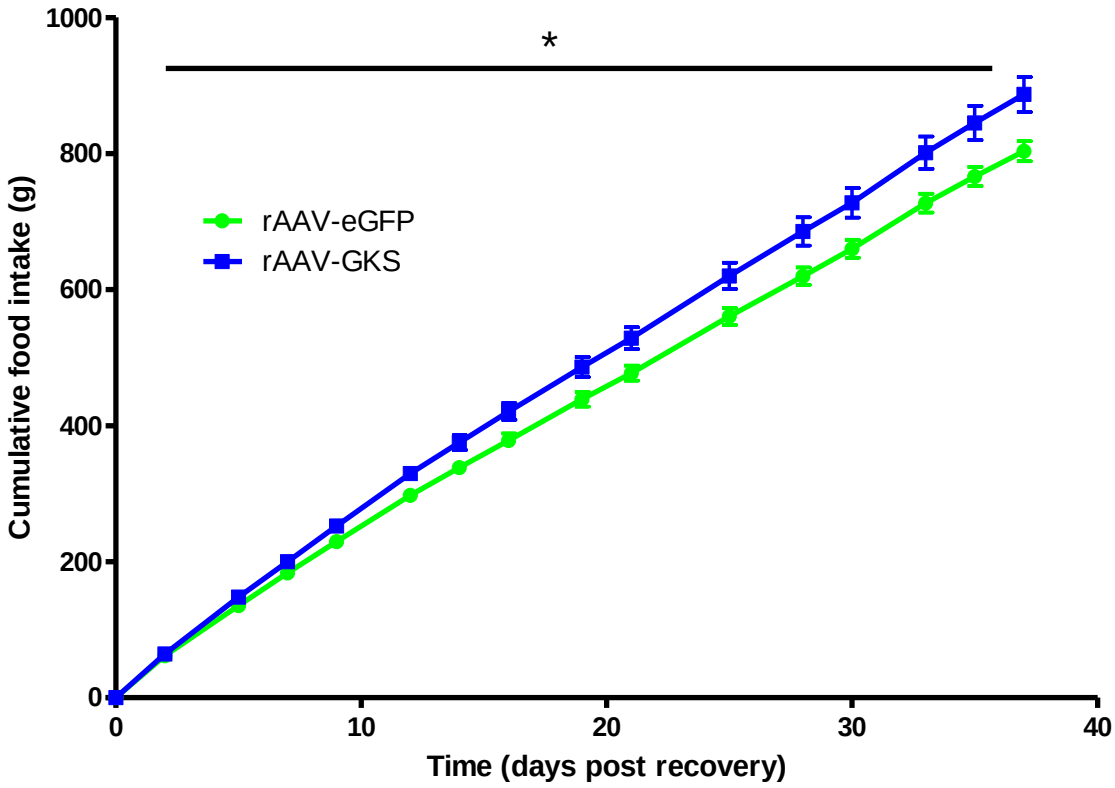


Figure 3.25 Effect of iARC rAAV-GKS on intake of high energy diet: *Food intake following bilateral injection of 1ul rAAV-eGFP (green line) or 1ul rAAV-GKS (blue line). Male Wistar rats were fed a high energy diet for 37 days. Data are expressed as mean +/- SEM for both groups, n=9-11, *=P<0.05.*

3.5 Discussion

3.5.1 Identifying a primary target for rAAV-GKS injection

Glucose-sensing neurones are found in numerous hypothalamic nuclei including the ARC, PVN, LHA and VMN (Lynch *et al*, 2000). For this reason, the first task was to identify which nucleus/nuclei might be quantitatively most important in feeding behaviour. To achieve this GK assay was performed on punch biopsies taken from the ARC, PVN and VMN of fed rats and rats subjected to a fast of either 24 or 48 hours. Fasting, for 24 or 48 hours, resulted in an increase in GK activity in the ARC compared to fed controls with no difference observed in the VMN or PVN. This finding is in line with previously published material which shows that GK mRNA is increased with fasting (Kang *et al*, 2008). These findings are also in agreement with a large body of evidence which shows that insulin induced hypoglycaemia results in increased GK mRNA expression and activity in the VMH (which comprises the ARC and VMN) (Dunn-Meynell *et al*, 2002;Kang *et al*, 2008;Tkacs *et al*, 2000).

The ARC is located at the base of the hypothalamus and possesses a highly fenestrated blood brain barrier. This allows access to circulating factors including glucose, fatty acids, leptin and ghrelin (Cone *et al*, 2001). It is likely that the supply of glucose to the ARC, and perhaps the VMN, is greater than in deeper regions of the brain (Mountjoy & Rutter, 2007). Furthermore, the ARC contains the orexigenic NPY/ AgRP neurones and the anorexic POMC/CART neurones, some of which are believed to be glucose sensitive (Cone *et al*, 2001;Ibrahim *et al*, 2003;Muroya *et al*, 1999). As such, ARC glucose-sensing neurones are well placed to act as primary central "metabolic sensors" and it is also possible that due to their co-localisation and/or close proximity to NPY/AgRP and POMC/CART neurones glucose sensing neurones may also act as "metabolic effectors" by influencing feeding behaviour and glucose homeostasis. Taken together with the results of the fasting study, these data suggest that ARC glucose sensing may be of particular importance in the regulation of energy balance. For this reason, the ARC was chosen as the primary target for rAAV-GKS microinjection.

3.5.2 *Ex-vivo* GK assay

In testing the efficacy of the plasmids used in the production of the rAAV-GKS, it was found that treating HEK293T cells with pTR-CGW-GKS increased NADPH production 3-fold in the GK assay. In this assay, GK activity is linked to the production of NADPH (described in 2.3.5.2). The increase in NADPH production suggests that the sense plasmid (pTR-CGW-GKS) was producing functioning GK enzyme that was able to phosphorylate glucose and initiate glycolysis via the GK pathway.

The primary objective of this work has been to alter the sensitivity of hypothalamic glucose-sensing neurones by increasing GK activity via rAAV mediated gene transfer. While *in situ* hybridisation confirmed increased GK mRNA in the GKS treated animals the GK activity assay failed to show a significant increase in activity in the GK group compared to eGFP controls. This may have occurred for a number of reasons. Firstly, it is possible that the GK assay was not sufficiently sensitive to detect the changes in activity resulting from treatment. In testing this assay *in vitro*, a cell type was selected that does not express GK therefore, no NADPH should be produced during the reaction. Since the cell lysate was highly diluted in the reaction mixture NADPH produced by the cell prior to the reaction should be minimal. In light of this, the fact that NADPH was detected suggests that hexokinase activity may not have been fully inhibited; this would interfere with the results of the assay and could reduce its sensitivity.

It is also possible that the punching technique used was inaccurate. In the study investigating the effect of fasting on ARC GK activity a difference was observed between GK activity in the fasted and fed states. During this study, brains were sliced in the coronal plane and each nucleus was excised bilaterally by two punch biopsies. In the study investigating the effect of iARC rAAV-GKS treatment an alternative method was used. In the rAAV studies the brains were sliced in the sagittal plain and both sides of the desired nucleus were excised by a single punch. During this study, the nuclei of interest were identified using land marks on the brain in the sagittal plain.

The majority of work conducted on the rat brain by this group has dealt with brain slices in the coronal plane and numerous anatomical markers are available for identification of specific hypothalamic nuclei. In slicing the brains in the sagittal plain, I hoped to isolate a greater proportion of the desired nucleus than would be possible in the coronal plain.

Unfortunately, preparing sagittal brain sections and identifying nuclei using sagittal markers proved to be challenging. It is possible that the failure to observe a difference in GK activity using this method may have resulted from inaccuracy in the localisation of biopsies taken.

3.5.3 Effect of iARC rAAV-GKS; Cohort one

In the initial feeding study, injection of rAAV-GKS into the ARC resulted in a significant increase in food intake accompanied by significantly increased bodyweight. The divergence in food intake between the treatment group and control group began early (approximately 9 days post injection) and continued to diverge until the termination of the study. The increase in bodyweight gain in the GKS group also began early but reached a plateau at day 22. After this time the difference in bodyweight between the groups was maintained such that at the termination of the study the GKS group were 6% heavier than controls. At the termination of the study carcass analysis was performed. Carcass analysis revealed that the difference in bodyweight observed between the groups resulted from a significant increase in percentage body fat in the GKS group. There was no difference in lean mass between the groups.

The results of the first feeding study were unexpected as they apparently disagreed with available literature. Glucose infusion ICV decreases food intake acutely (Kurata *et al*, 1986). Whereas, ICV infusion of the glucoprivic agent 2DG into the 3rd cerebral ventricle results in increased feeding (Tsujii & Bray, 1990). It could therefore be hypothesized that increasing GK expression in the ARC (which is hypothesised to increase glucose metabolism therein) would result in a reduction in food intake. As this was not the case, the feeding study was repeated in a second cohort of animals with the addition of a GKS group pair-fed to controls to help clarify the role of feeding in the increased bodyweight observed.

3.5.4 Effect of iARC rAAV-GKS; Cohort two

In the second feeding study, the bodyweight gain of the GKS group was again significantly greater than controls. The pair-fed GKS group and the control group were not different in weight, suggesting that the increased bodyweight of the GKS animals in the previous study was primarily due to increased food intake. However, the food intake of the *ad libitum* fed GKS group in cohort two was only slightly, and not significantly, higher than the eGFP controls.

At the termination of the feeding study (day 33) cumulative food intake in the GKS group was 31g higher than controls. This equates to an increase in energy intake of 482kJ across the duration of the study. Approximately 34kJ are required to store 1g of adipose tissue so it is unlikely that the 22g difference in bodyweight between the groups can be accounted for solely by food intake. That said, the 20g difference between the bodyweights of the GKS group and the controls in the first cohort could be explained by the 1,309kj difference in their energy intake.

To further investigate the observed differences between the groups I measured food intake and bodyweight gain for a period of 24 hours following a 24 hour fast. Upon re-feeding, there was no difference in food intake between the groups until the 8-24 hours period when both the GKS group and the pair fed GKS group consumed significantly more chow than eGFP controls. There was no significant difference in cumulative food intake between the *ad libitum* fed GKS group and their controls over the total 24hr period. Interestingly, despite the fact that food intake was not different both GKS groups gained significantly more weight than the eGFP group. Combined with the results of the long term feeding study these data suggest that increasing GK mRNA in the ARC may have additional effects on metabolism beyond those on food intake. For example it is possible that the treatment might decrease energy expenditure.

At the termination of the study, tissues were harvested. BAT weight was not different between the GKS group and the eGFP controls. BAT weight was significantly lower in the pair fed GKS group compared to the *ad libitum* fed GKS group. BAT metabolism and mass are reduced by fasting and this result is likely to reflect the fact that the pair fed GKS group are calorie restricted compared to the *ad libitum* GK group (Rothwell *et al*, 1984). During the 24 hour fast the pair fed GKS group lost significantly less weight

than both other groups. It is possible that this result is related to the reduction in BAT weight observed in this group.

To confirm the successful increase of GK mRNA expression in the treatment groups I harvested whole hypothalami and performed quantitative PCR (QPCR) for GK mRNA. GK mRNA was increased 15-fold in the pair fed GKS group and 14-fold in the *ad libitum* GKS group compared to controls. Taken together with the results of the *in situ* hybridization these data suggest that GK mRNA was successfully increased by treatment. In addition to GK, I performed QPCR for AMPK, CART, FAS, NPY and POMC mRNA. Other than GK, there was no significant difference in mRNA expression of any gene assayed.

Glucose sensing in the VMH has been shown to be involved in the regulation of glucose homeostasis. For this reason, I performed assays for plasma glucose and insulin in non-fasted animals at the termination of the study. There was no significant difference in plasma glucose between the groups. The plasma glucose levels recorded in this experiment are close to values reported in the literature (Dunn-Meynell *et al*, 2009; da Vries *et al*, 2005; Anderson, 2011). This suggests that the assay method used provided an accurate measure of true plasma glucose values. Plasma insulin was significantly higher in the GKS group compared to the pair fed GKS group and compared to the eGFP controls. The fact that the pair fed GKS group had lower plasma insulin compared to the *ad libitum* GKS group again suggests that the pair fed group were calorie restricted because calorie restriction has a well-accepted insulin lowering effect. The increased plasma glucose in the GKS group compared to the eGFP group could be interpreted in a number of ways. Firstly, since the GKS group were larger and more adipose than the controls, it could be suggested that increased insulin is the result of peripheral insulin resistance as observed in type II diabetes mellitus. Another possibility is that the increased GK mRNA expression within the ARC has had a specific effect on pathways that regulate pancreatic insulin release. The release of insulin from the pancreas is under significant neural influence and lesioning of the VMH has been shown to enhance insulin secretion, which suggests that VMH signalling is important in the regulation of insulin secretion (Hahn *et al*, 1981;Gerich *et al*, 1976).

At present, there is considerable interest in the use of GK activators in the treatment of type II diabetes. Oral administration of the GK activator RO-28-1675 has been shown to

decrease plasma glucose and increase plasma insulin levels in mice (Grimsby *et al*, 2003). In addition, it has been hypothesised that a GK activator that could cross the blood brain barrier could be used to reduce food intake and thus treat obesity (Al-Hasani *et al*, 2003). The data presented in this chapter are important because they indicate that increasing GK mRNA in the ARC could have the opposite effect, increase food intake and weight gain.

3.5.5 Effect of iARC rAAV-GKS; High energy diet

The results of my work so far have demonstrated that increasing GK mRNA in the ARC using rAAV results in increased bodyweight gain and food intake. However, the standard chow diet is low in both fat and sugar (see appendix II) and does not contain nutrient levels similar to the diet of westernized human populations. Considering the proposed use of GK activators in the treatment of diabetes and obesity it was important to assess the effect of increased ARC GK mRNA on intake of a high energy western-style diet.

As observed on standard chow, there was a significant increase in both food intake and bodyweight gain in the GKS group compared to controls on the high energy diet. The difference in food intake started early (at day 9) and continue to diverge until the termination of the study at day 37 by which time the GKS group had gain 23.6g more than controls. Despite the difference in weight gain there was no difference in mean bodyweight between the groups.

The work in this chapter demonstrates that increasing GK mRNA expression in the ARC results in a robust and reproducible increase in food intake and bodyweight gain on standard chow and a high energy western style diet. From the results of the 24 hour food intake study it would also appear that feeding patterns are altered by treatment as food intake in the GKS groups was only different in the 8-24 hour period. There was no significant difference in the expression of any of the feeding related hypothalamic genes assayed so at present there is no proposed hypothalamic mechanism of action. Interestingly, plasma insulin levels in the fed state were significantly higher in the GKS group compared to controls despite no difference in plasma glucose levels. Further

experiments including glucose tolerance test and insulin tolerance test are required to assess the effect of treatment on glucose homeostasis.

Chapter 4

Effect iArc rAAV-GKS administration on intake of sugars and glucose homeostasis

4.1 Introduction

4.1.1 The role of sugars in the regulation of food intake

Manipulation of glucose levels in numerous regions of the body have been shown to affect feeding behaviour (see section 1.1.10.1). The effect of manipulation of glucose metabolism on feeding behaviour normally follows a reasonably predictable pattern. Manipulations that increase glucose levels tend to decrease feeding acutely while those that decrease glucose metabolism (such as 2DG infusion) increase feeding. When glucose and other sugars are provided either as a pre load prior to a meal or in addition to chow the effects are less predictable.

In rats, provision of a 32% (w/v) solution of sucrose, fructose or glucose in addition to standard chow results in a significant increase in energy intake and fat pad mass compared to standard chow fed controls. Daily energy intake was greatest in the group provided sucrose, followed by the fructose group with the glucose group consuming the least. In all cases, increased energy intake was a result of intake of sugar solution rather than increased intake of standard chow (Kanarek & Orthen-Gambill, 1982).

Glucose and fructose have also been shown to alter feeding behaviour when consumed as a preload before a meal. However, the results of studies of this nature are inconsistent. Rodin et al 1998, fasted human participants overnight before providing a solution containing 50g of either glucose or fructose. Two and a quarter hours after consumption of the solution participants were presented with a buffet meal and calorie intake was measured. In this study, the fructose preload group consumed fewer calories at the buffet than the glucose preload group suggesting that fructose has a greater inhibitory effect on food intake. Plasma glucose and plasma insulin were significantly increased in the glucose group compared to the fructose group and calorie intake was correlated to plasma insulin levels such that higher plasma insulin was associated with increased food intake. The authors hypothesise that the difference between the groups may have resulted from the rapid storage and utilization of glucose following the glucose load. Two hours after a glucose load, plasma glucose levels have been shown to fall below baseline, an effect not observed with fructose (Rodin *et al*, 1988). It is plausible that a transient fall in plasma glucose following a glucose load may result in

an increased drive to feed. The majority of spontaneous meals in rats and humans are preceded by fall in plasma glucose (Dunn-Meynell *et al*, 2009).

Using a similar study protocol to that of Rodin, Shafer *et al* 1987, found that glucose decreased food intake to a greater extent than fructose when delivered as a preload. In this study, participants were fasted and offered a solution containing either 25g of fructose or glucose 1 hour prior to a buffet meal. Calorie intake was significantly reduced by glucose and fructose compared with water and the glucose group consumed less than the fructose group (Shafer *et al*, 1987).

It is possible that the differences between the results of these studies might involve both the time at which the meal was presented after the preload and the amount of sugar provided in the preload. Although plasma glucose and insulin levels were not recorded during the Shafer study it is likely that the magnitude of the increase in plasma glucose would not be as great as in the Rodin study because the glucose dose was half the size. In addition, in the Shafer study, the buffet meal was provided one hour after the preload, whereas in the Rodin study the meal was provided after two and a quarter hours. One hour after an oral glucose load plasma glucose would be expected to be higher than baseline. Thus, in the Shafer study, it is possible that plasma glucose was increased when the meal was presented. In the Rodin study, plasma glucose was lower than baseline when the meal was presented, this might potentially explain the observed differences.

4.1.2 Fructose metabolism in the brain and food intake

The pathways by which fructose and glucose are metabolised differ; both in the periphery and the central nervous system (CNS). In the CNS, glucose infusion has a well-accepted effect of decreasing food intake. Interestingly, ICV infusion of fructose has been shown to increase food intake (Miller *et al*, 2002). It is believed that the differential effects of ICV fructose and glucose on food intake result from the manner in which they are metabolised.

Glucose and fructose are both ultimately metabolised via glycolysis in the CNS and the liver. However, the early steps in the metabolism of glucose and fructose differ. Glucose

metabolism is regulated by a rate limiting step in which fructose-6-phosphate is converted to fructose-1-6-bisphosphate by phosphofructokinase (PFK). The first step in fructolysis is the phosphorylation of fructose to fructose-1-phosphate by 2-keto-hexokinase. Following this step, fructose enters glycolysis at the triose level and thus fructose metabolism by-passes regulation by PFK. Phosphorylation of fructose by 2-keto-hexokinase is unregulated and rapidly utilizes ATP. Indeed, while ICV infusion of glucose increases hypothalamic ATP levels, infusion of fructose does the opposite and decreases hypothalamic ATP (Cha *et al*, 2008).

Increased ATP as a result of glucose infusion reduces levels of phosphorylated AMPK (pAMPK). This in turn increases the activity of acetyl-CoA carboxylase (ACC) resulting in increased levels of malonyl-CoA. Malonyl-CoA is a potent inhibitor of the mitochondrial transporter CPT-1 and increased levels of malonyl-CoA have been shown to decrease food intake via increased expression of POMC and CART mRNA (Cha *et al*, 2008).

Following ICV fructose infusion, hypothalamic ATP levels fall and levels of pAMK are increased. This decreases the activity of ACC, resulting in a reduction in malonyl-CoA, increased feeding and decreased POMC mRNA (Cha *et al*, 2008).

The majority of dietary fructose is metabolised by the liver before it can enter general circulation. However, at higher doses, dietary fructose increases plasma fructose concentrations. Fasting plasma fructose is usually lower than 1mg/dL. Following ingestions of 18-100g of fructose plasma levels increase in a dose dependent manner from 4.5-13.0mg/dL within 60 minutes (Cook, 1969). Combined with the fact that the CNS expresses enzymes that are specific to fructolysis this suggests that post-prandial fructose metabolism occurs in the CNS. When considered with the results of Cha *et al*, this further suggests the possibility that central fructose metabolism might be an important regulator of food intake.

The effects of sugars on food intake are complex and dependent on a number of factors including type of sugar, size of dose and timing of administration. The fact that central administration of glucose and fructose produces different effects highlights the importance of specific nutrient sensing pathways in the regulation of feeding behaviour. The correlation between plasma insulin and food intake also suggests the intriguing

possibility that at least part of the effect of sugars on food intake might be secondary to their effect on glucose homeostasis.

4.2 Hypothesis and Aims

4.2.1 Hypothesis

In earlier chapters, increasing GK mRNA in the ARC was shown to increase food intake and bodyweight gain. It is hypothesised that increasing GK mRNA in the ARC will also alter the intake of sugar solutions and intake of standard chow when a sugar solution is available. Furthermore, it is hypothesised that increasing GK mRNA in the ARC will affect glucose homeostasis.

4.2.2 Aims and Objectives

The aims of this chapter are to

1. Examine the effect of up regulation of ARC GK mRNA on intake of sugars
2. Examine the effect of up regulation of ARC GK mRNA on preference to sugars or standard chow
3. Examine the effect of up regulation of ARC GK mRNA on glucose homeostasis

4.3 Methods

4.3.1 Cohort 4: Effect of iARC rAAV-GKS on food intake, intake of glucose and bodyweight gain

4.3.1.1 Energy intake calculation

In studies in which food intake and intake of glucose solution were measured, total energy intake in kcal was calculated as follows:

kcal from standard chow= food intake in g x 3.523kcal/g standard chow

kcal from glucose solution= (glucose solution consumed ml x concentration of glucose g/ml)x 4kcal/g glucose

Total energy intake= kcal from glucose solution + kcal from standard chow

4.3.1.2 Effect of iARC-GKS on intake sugars and standard chow

Animals were maintained as described in 3.3.1 and were randomised to control and treatment groups as described in appendix

Adult male Wistar rats were bilaterally injected in the ARC with either 1ul rAAV-GKS (n=10) or rAAV-eGFP (n=10) and allowed to recover for 7 days (as described in 3.3.6). Twenty-one days later they were fasted for 4hr. Following 4hr fast animals were given *ad libitum* access to a solution containing 10% (w/v) glucose at the onset of the dark phase. Intake of the glucose solution was measured at 1,2,4,8,12,16 and 24hr. In all experiments described in this thesis animals had *ad libitum* access to water.

On day 24 post injection male Wistar rats injected iARC with either 1ul rAAV-GKS (n=10) or rAAV-eGFP (n=10) were fasted for 4hr. Following 4hr fast animals were given *ad libitum* access to a solution containing 10% (w/v) fructose at the onset of the dark phase. Intake of the fructose solution was measured at 1,2,4,8,12,16 and 24hr.

On day 28 post injection male Wistar rats injected iARC with either 1ul rAAV-GKS (n=10) or rAAV-eGFP (n=10) were fasted for 4hr. Following 4hr fast standard chow

was returned at the onset of the dark phase and food was weighed at 1,2,4,8,12,16 and 24hr.

4.3.1.3 **Effect of iARC rAAV-GKS on 24hr intake of standard chow and 2% glucose solution**

On day 31 post injection male Wistar rats injected iARC with either 1ul rAAV-GKS (n=10) or rAAV-eGFP (n=10) were fasted for 4hr. Following 4hr fast standard chow was returned and animals were given *ad libitum* access to a 2% (w/v) glucose solution at the onset of the dark phase. Intake of standard chow and glucose solution were measured at 1,2,4,8,12,16 and 24hr. Total kcal intake was calculated as described in 4.3.1.1.

4.3.1.4 **Effect of iARC rAAV-GKS on 24hr intake of standard chow and 10% glucose solution**

On day 40 post injection male Wistar rats injected iARC with either 1ul rAAV-GKS (n=10) or rAAV-eGFP (n=10) were fasted for 4hr. Following 4hr fast standard chow was returned and animals were given *ad libitum* access to a 10% (w/v) glucose solution at the onset of the dark phase. Intake of standard chow and glucose solution were measured at 1,2,4,8,12,16 and 24hr. Total kcal intake was calculated as described in 4.3.1.1.

4.3.1.5 **Effect of iARC rAAV-GKS on 24hr intake of standard chow and 20% glucose solution**

On day 44 post injection male Wistar rats injected iARC with either 1ul rAAV-GKS (n=10) or rAAV-eGFP (n=10) were fasted for 4hr. Following 4hr fast standard chow was returned and animals were given *ad libitum* access to a 20% (w/v) glucose solution at the onset of the dark phase. Intake of standard chow and glucose solution were measured at 1,2,4,8,12,16 and 24hr. Total kcal intake was calculated as described in 4.3.1.1.

4.3.1.6 **Effect of iARC rAAV-GKS on 24hr intake of standard chow and 40% glucose solution**

On day 50 post injection male Wistar rats injected iARC with either 1ul rAAV-GKS (n=10) or rAAV-eGFP (n=10) were fasted for 4hr. Following 4hr fast standard chow was returned and animals were given *ad libitum* access to a 40% (w/v) glucose solution at the onset of the dark phase. Intake of standard chow and glucose solution were measured at 1,2,4,8,12,16 and 24hr. Total kcal intake was calculated as 4.3.1.1.

4.3.1.7 **Effect of iARC rAAV-GKS on intake of standard chow and 10% glucose solution: long term study**

54 days post injection male Wistar rats injected iARC with either 1ul rAAV-GKS (n=10) or rAAV-eGFP (n=10) were maintained with *ad libitum* access to RM1 diet (standard chow) and a solution containing 10% (w/v) glucose with free access to water. Food intake, intake of 10% glucose solution and bodyweight were measured for a period of 31 days. In addition, total energy intake from glucose and chow was calculated.

4.3.1.8 **Effect of iARC rAAV-GKS on plasma glucose following oral glucose challenge**

At day 85 post injection male Wistar rats injected iARC with either 1ul rAAV-GKS (n=10) or rAAV-eGFP (n=10) were fasted over night with free access to water. At the onset of the light phase animals were offered a 20% (w/v) D-glucose solution providing 2.5g/kg glucose which was consumed within 10 minutes. Thirty minutes after the glucose solution had been consumed animals were killed by decapitation and trunk blood was collected in lithium heparin tubes (Microvette, Sarstedt, Nümbrecht, Germany). Plasma was separated by centrifugation at 2,400xg for 5minutes at 4˚C and frozen on liquid nitrogen. Plasma glucose was assayed as described in 3.3.9.5 and plasma insulin was assayed as described in 3.3.9.6.

4.3.2 Group 5

4.3.2.1 **Oral glucose tolerance test by gavage (oGTT)**

Materials

20% (w/v) glucose solution (Clintech, Dublin, Ireland)
Lithium heparin tubes (Microvette)

Method

Adult male wistar rats were bilaterally injected in the ARC with either 1ul rAAV-GKS (n=10) or rAAV-eGFP (n=10) and allowed to recover for 7 days (as described in section 3.3.6) On day 20 post recovery oGTT was performed. Male Wistar rats injected iARC with either 1ul rAAV-GKS (n=10) or rAAV-eGFP (n=9) were fasted over night with free access to water. On the day of the procedure rats were cannulated into the lateral tail vein (as described in 4.3.3.2). After all rats had been cannulated and cannulae checked, baseline blood samples were collected. Rats received glucose (2.5g/kg) via oral gavage and blood samples were collected at 15, 30, 60 and 120 minutes post gavage. Between blood sampling rats were returned to the home cage with free access to water. Blood samples of approximately 120µl were collected at each time point in lithium heparin tubes and plasma was separated by centrifugation at 2,400xg for 5 minutes at 4˚C. Plasma was frozen on liquid nitrogen and plasma glucose was assayed as described in 3.3.9.5.

4.3.2.2 **Tail vein cannulation**

Materials

Warming cabinet (Vet Tech Solutions Ltd, Cheshire,UK)

Restraining tube (Vet Tech Solutions Ltd)

25 gauge needles (Tyco Healthcare Ltd, Hampshire, UK)

24 gauge/19mm Cannulae (Millpledge Veterinary, Nottinghamshire, UK)

Zinc Oxide surgical adhesive tape (Millpledge Veterinary)

Ethyl chloride liquid spray (L.E. West, Barking, UK)

Heparin sodium diluted 1:10 in normal saline (Heparin sodium 1000IU/ml, LEO Pharma Ltd, Bucks, UK)

Method

Tail vein cannulation is a technique that allows multiple blood sampling with minimal discomfort to the animal. Prior to cannulation rats were warmed in a 39˚C warming cabinet for 10 minutes to dilate blood vessels. Next, rats were immobilised in a restraining tube and ethyl chloride was sprayed on the area of the tail that was to be cannulated. The lateral tail vein was visualised and an indwelling cannula inserted. The cannula was fixed in place using surgical tape and the cannula covered to prevent its removal. Blood flow was confirmed and 100µl of diluted heparin was injected into the cannula to prevent clotting. Following cannulation rats were returned to the home cage for 45 minutes prior to further procedures to reduce the influence of stress responses on experimental results. Blood was collected by inserting a 25 gauge needle into the cannula and gently massaging the tail. In all experiments 120µl of fluid was discarded prior to collection of blood to decrease sample contamination with heparin. Following each sample collection 100µl of diluted heparin was injected into the cannula to prevent clotting. After the final sample collection rats were placed in the restraint tube, cannula was removed and the animal returned to its home cage.

4.3.2.3 **Insulin tolerance test**

Materials

Human insulin, diluted 1:100. (Humulin S, soluble insulin 100 IU/ml, Eli Lilly & Co. Ltd, Basingstoke, UK)
Lithium heparin tubes (Microvette)

Method

On day 35 post recovery male Wistar rats injected iARC with either 1ul rAAV-GKS (n=10) or rAAV-eGFP (n=9) were fasted for 4 hours with free access to water. Following fast rats were cannulated into the lateral tail vein (as described in 4.3.3.2). After all rats had been cannulated and cannulae checked, baseline blood samples were collected. Rats then received an i.p. injection of insulin (2 IU/kg), and blood samples were collected at 15, 30, 90, and 150 minutes post-injection. Between sampling rats were returned to the home cage with free access to water. Blood samples of approximately 120 µl were collected in lithium heparin tubes and plasma was separated by centrifugation at 2,400xg for 5 minutes at 4˚C. Plasma was frozen on liquid nitrogen and plasma insulin was assayed as described in 3.3.9.6.

4.3.2.4 **Voluntary oral glucose tolerance test (vGTT)**

Materials

20% glucose solution (Clintech)
Lithium heparin tubes (Microvette, Sarstedt)

Method

On 48 post recovery vGTT was performed. Male Wistar rats injected iARC with either 1ul rAAV-GKS (n=10) or rAAV-eGFP (n=9) were fasted over night with free access to water. Following fast rats were cannulated into the lateral tail vein (as described in 4.3.3.2). After all rats had been cannulated and cannulae checked, baseline blood

samples were collected. Next, animals were offered a 20% (w/v) D-glucose solution providing 2.5g/kg glucose which was consumed within 10 minutes. Blood samples were collected at 15, 30, 60, and 120 minutes post-glucose. Between sampling rats were returned to the home cage with free access to water. Blood samples of approximately 120µl were collected at each time point in lithium heparin tubes and plasma was separated by centrifugation at 2,400xg for 5 minutes at 4˚C. Plasma was frozen on liquid nitrogen and plasma glucose was assayed as described in 3.3.9.5.

4.3.2.5 **Effect of iARC rAAV-GKS on glucose stimulated insulin release**

Materials

Rat insulin ELISA kit (Linco Research)

Method

Plasma collected during the vGTT on day 48 post injection was assayed for insulin as described in 3.3.9.6.

4.3.3 Statistical analysis

Longitudinal data (growth curves, cumulative food and glucose intake) was analysed using the population-averaged general estimating equation (GEE). For all other data, unpaired t-test was used to analyse individual time points and to analyse AUC in glucose and insulin tolerance tests. $P<0.05$ was considered statistically significant throughout. Data analysis was performed using GraphPad Prism 4 software (CA, USA) and Stata 9.

4.4 Results

4.4.1 Cohort 4

4.4.1.1 **24 hour intake of 10% glucose**

Intake of a 10% glucose solution was measured for 24hr starting at the onset of the dark phase (day 21). Intake of 10% glucose solution was significantly greater in the GKS animals compared to controls in the 0-2hr period (eGFP 22.3+/- 1.0ml vs GKS 27.0+/- 1.7ml, n=10, p=<0.05) , the 0-4hr period (eGFP 43.1+/- 1.4ml vs GKS 50.5+/-1.8ml, n=10, p=<0.05), the 0-8hr period (eGFP 81.5+/- 3.8ml vs GKS 92.8+/-3.3ml, n=10, p=<0.05), the 0-12hr period (eGFP 135.0+/- 4.6ml vs GKS 154.1+/-5.3ml, n=10, p=<0.05) and the 0-16hr period (eGFP 143.6+/- 4.9ml vs GKS 164.0+/-7.5ml, n=10, p=<0.05) (figure 4.1)

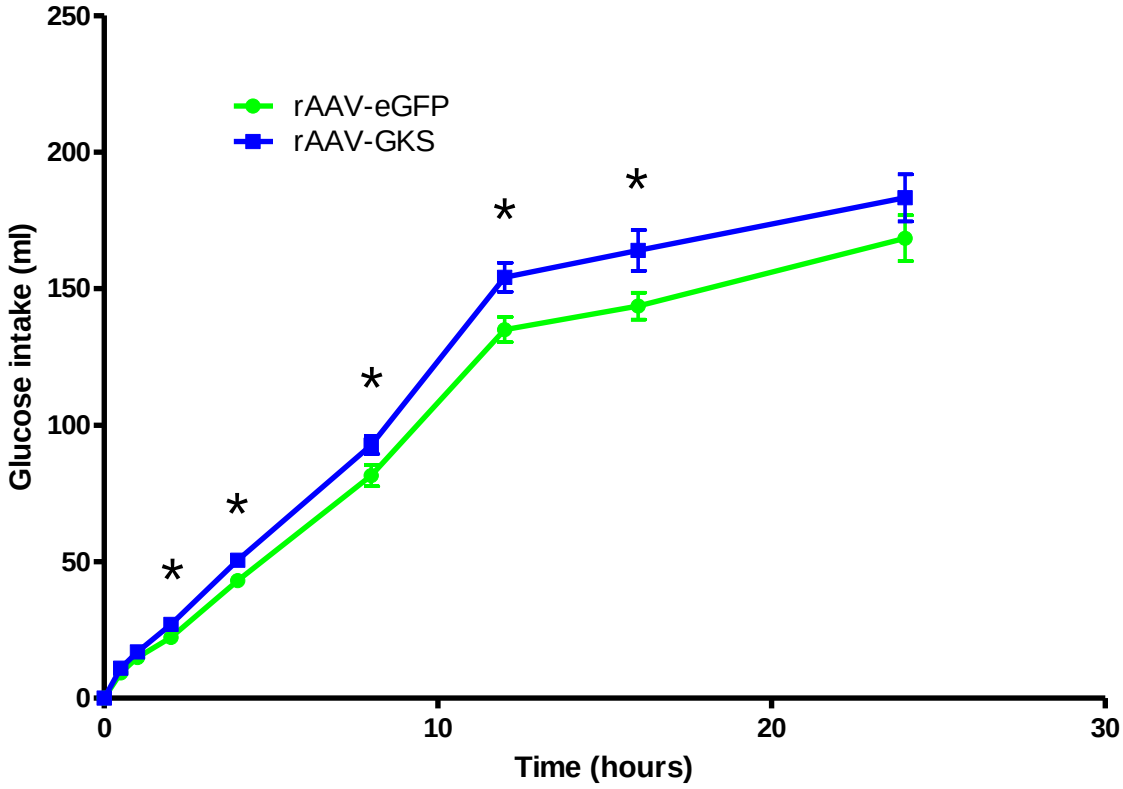


Figure 4.1 Effect of iARC rAAV-GKS on 24hr intake of 10% glucose solution: *24hr intake of 10% glucose solution in male Wistar rats bilaterally injected with 1ul rAAV-eGFP (green line) or 1ul rAAV-GKS (blue line). Rats were given ad libitum access to a 10% glucose solution at the onset of the dark phase (day 21). Data are expressed as mean +/- SEM for both groups, n=10, *=P<0.05.*

4.4.1.2 **24 hour intake of 10% fructose**

Intake of a 10% fructose solution was measured for 24hr starting at the onset of the dark phase (day 24). There was no significant difference in the intake of 10% fructose solution at any time point. (figure 4.2)

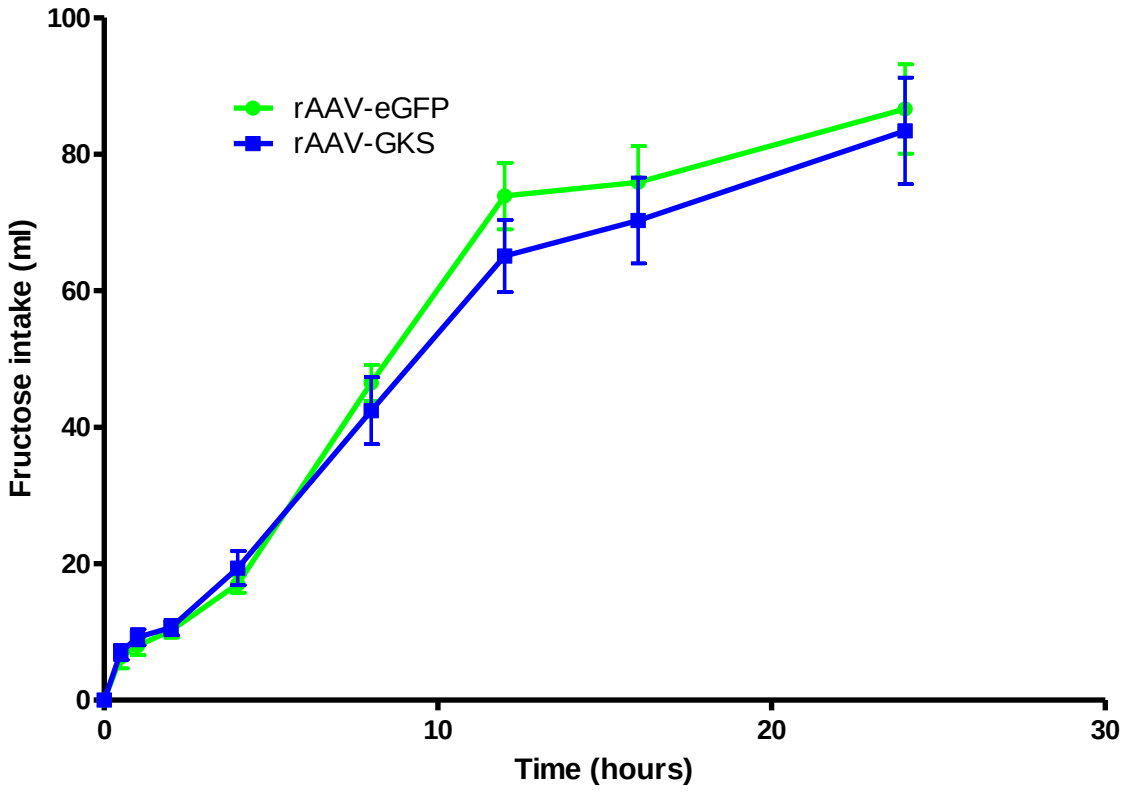


Figure 4.2 Effect of iARC rAAV-GKS on 24hr intake of 10% fructose solution: *24hr intake of 10% fructose solution in male Wistar rats bilaterally injected with 1ul rAAV-eGFP (green line) or 1ul rAAV-GKS (blue line). Rats were given ad libitum access to a 10% fructose solution at the onset of the dark phase (day 24). Data are expressed as mean +/- SEM for both groups, n=10, *=P<0.05.*

4.4.1.3 **24 hour food intake without glucose solution**

To establish that the feeding pattern of cohort four was similar to that of previous GKS groups food intake was measured for 24hr starting at the onset of the dark phase (day 28). Food intake was significantly higher in GKS animals compared to controls in the 0-8hr period (eGFP 12.8+/- 1.2g vs GKS 16.0+/-0.6g, n=10, p=<0.05), the 0-12hr period (eGFP 20.5+/- 0.6g vs GKS 22.7+/-0.9g, n=10, p=<0.05) and the 0-16hr period (eGFP 21.3+/-0.7g vs GKS 23.8+/-0.8g, n=10, p=<0.05). Food intake was higher over 24hr but this did not reach significance (eGFP 26.4+/- 1.1g vs GKS 29.21+/-1.3g, n=10, p=<0.12) (figure 4.3).

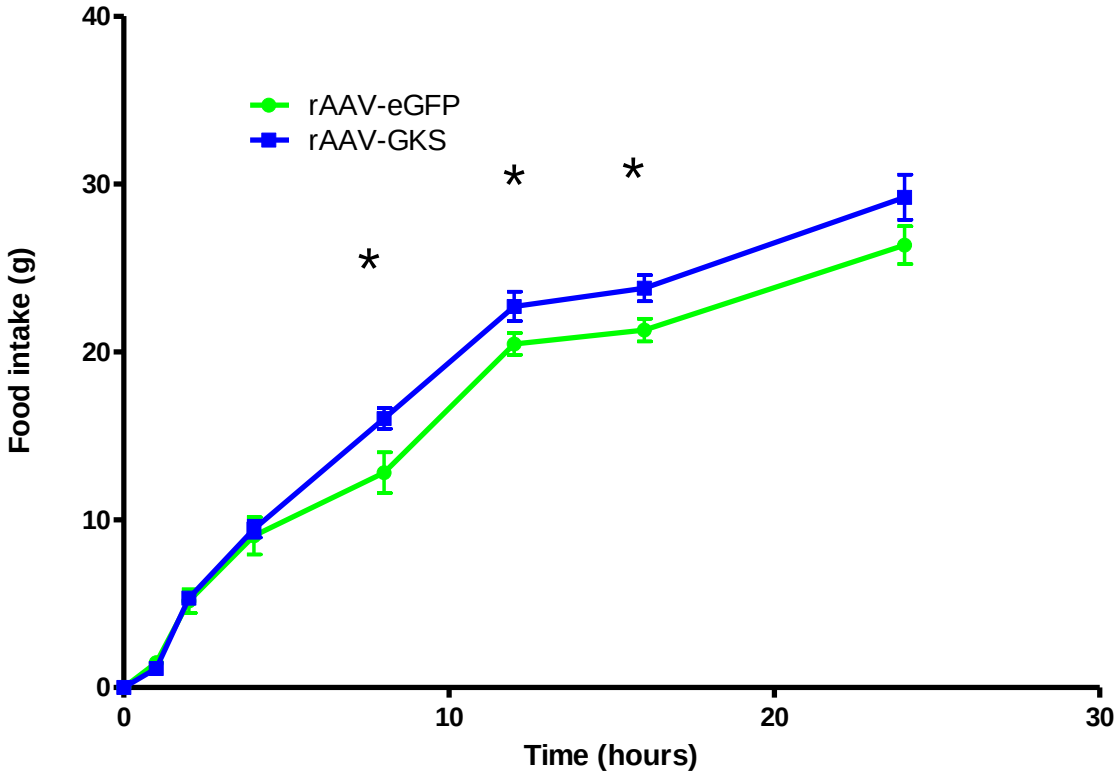


Figure 4.3 Effect of iARC rAAV-GKS on 24hr food intake without glucose solution: *24hr food intake of male Wistar rats bilaterally injected with 1ul rAAV-eGFP (green line) or 1ul rAAV-GKS (blue line). Rats were fed normal chow at the onset of the dark phase (day 28). Data are expressed as mean +/- SEM for both groups, n=10, *=P<0.05.*

4.4.1.4 **24 hour intake of standard chow and 2% glucose solution**

Intake of standard chow and a 2% glucose solution were measured in GKS animals and their controls over a 24hr period starting at the onset of the dark phase (day 31). Food intake was not different between the groups at any time point (figure 4.4).

Intake of 2% glucose solution was greater in the GKS group compared to controls in the 0-1hr period (eGFP 8.1+/- 2.7ml vs GKS 18.6+/-1.5ml, n=10, p=<0.01), 0-2hr period (eGFP 18.6+/-3.7ml vs GKS 34.7+/-3.4ml, n=10, p=<0.01), 0-4hr period (eGFP 31.6+/-3.3ml vs GKS 61.1+/-5.3ml, n=10, p=<0.001), 0-8hr period (eGFP 59.4+/-8.5ml vs GKS 110.3+/-8.3ml, n=10, p=<0.001), 0-12hr period (eGFP 82.1+/-11.8ml vs GKS 134.6+/-9.6ml, n=10, p=<0.01), 0-16hr period (eGFP 84.3+/-11.9ml vs GKS 140.0+/-11.3ml, n=10, p=<0.01), and 0-24hr period (eGFP 86.3+/-12.9ml vs GKS 145.4+/-11.3ml, n=10, p=<0.01) (figure 4.5).

Total energy intake was not different between the groups at any time point (figure 4.6).

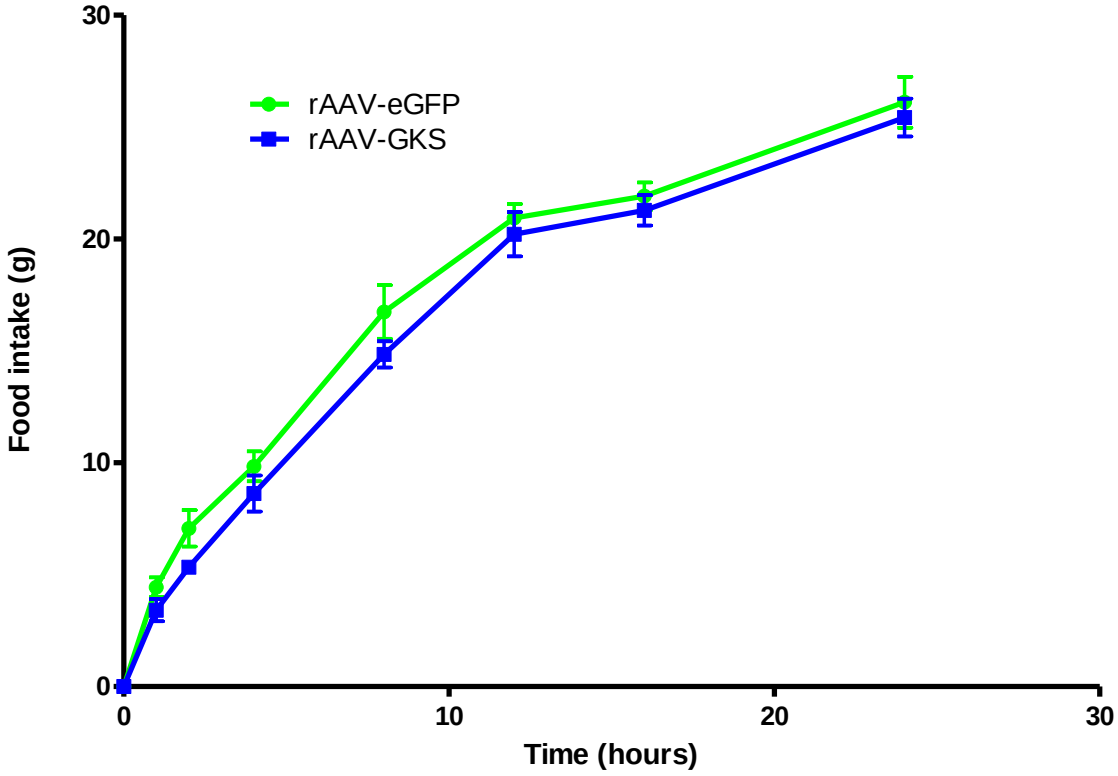


Figure 4.4 Effect of iARC rAAV-GKS on 24hr food intake (with 2% glucose solution): *24hr food intake of male Wistar rats bilaterally injected with 1ul rAAV-eGFP (green line) or 1ul rAAV-GKS (blue line). Rats were fed normal chow with ad libitum access to a 2% glucose solution at the onset of the dark phase (day 31). Data are expressed as mean +/- SEM for both groups, n=10.*

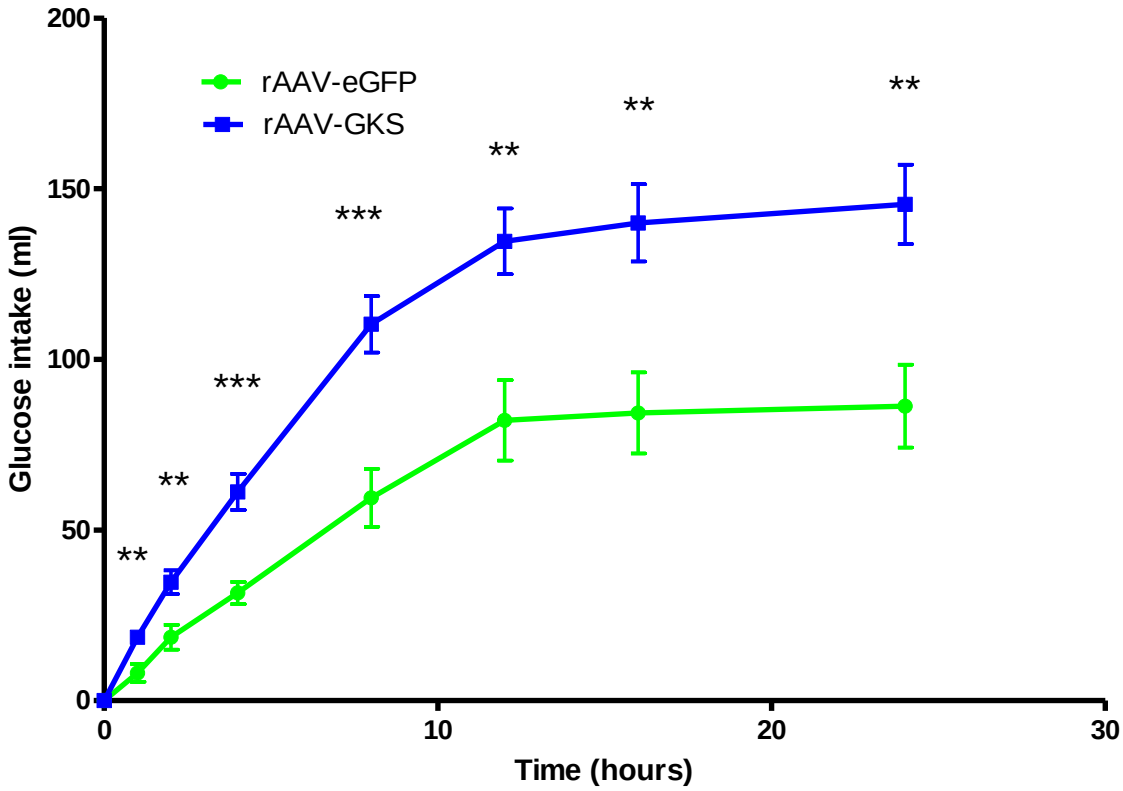


Figure 4.5 Effect of iARC rAAV-GKS on 24hr intake of a 2% glucose solution: *24hr intake of 2% glucose solution of male Wistar rats bilaterally injected with 1ul rAAV-eGFP (green line) or 1ul rAAV-GKS (blue line). Rats were fed normal chow with ad libitum access to a 2% glucose solution at the onset of the dark phase (day 31). Data are expressed as mean +/- SEM for both groups, n=10, **=P<0.01, ***=P<0.001.*

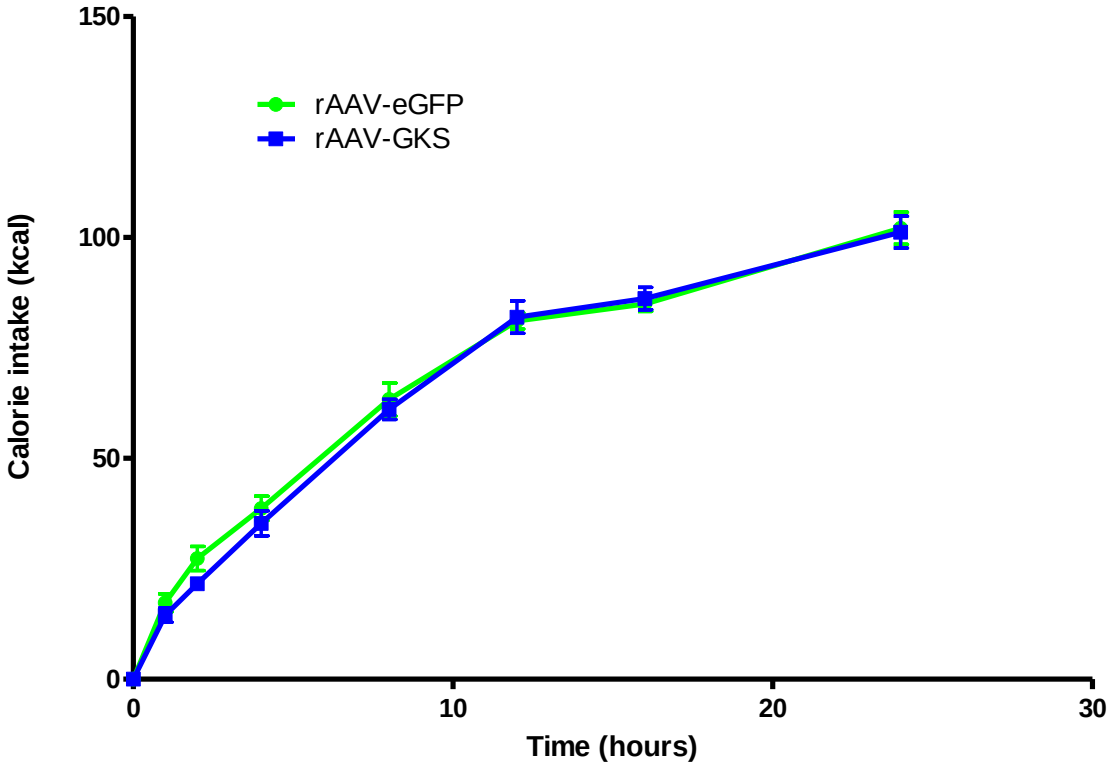


Figure 4.6 Effect of iARC rAAV-GKS on total energy intake over a 24hr period (2% glucose): *Total 24hr energy intake of male Wistar rats bilaterally injected with 1ul rAAV-eGFP (green line) or 1ul rAAV-GKS (blue line). Rats were fed normal chow with ad libitum access to a 2% glucose solution at the onset of the dark phase (day 31). Data are expressed as mean +/- SEM for both groups, n=10.*

4.4.1.5 **24 hour intake of standard chow and 10% glucose solution**

Intake of standard chow and a 10% glucose solution were measured in GKS animals and their controls over a 24hr period starting at the onset of the dark phase (day 40). Food intake was not different between the groups at any time point (figure 4.7).

Intake of 10% glucose solution was greater in the GKS group compared to controls in the 0-8 hour period (eGFP 55.9+/- 2.4ml vs GKS 65.8+/-3.2ml, n=10, p=<0.05) and the 0-24hr period (eGFP 88.0+/- 6.4ml vs GKS 107.6+/-4.4ml, n=10, p=<0.05) (figure 4.8).

Total energy intake was not different between the groups at any time point (figure 4.9).

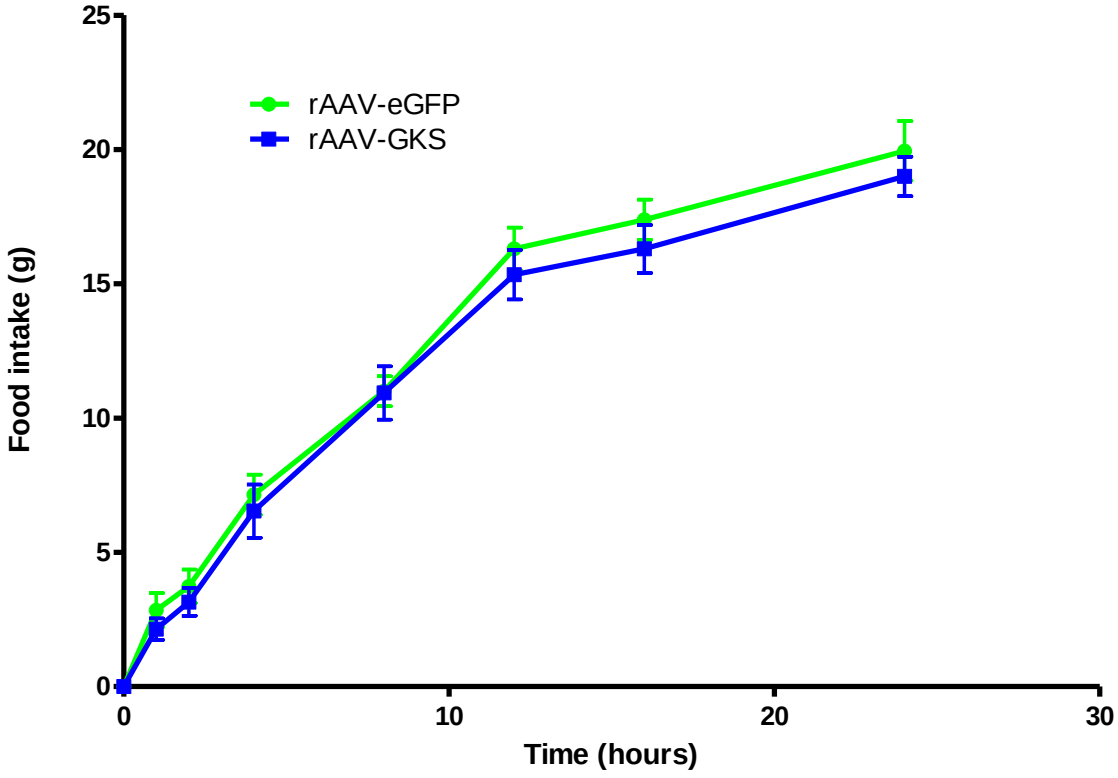


Figure 4.7 Effect of iARC rAAV-GKS on 24hr food intake (with 10% glucose solution): *24hr food intake of male Wistar rats bilaterally injected with 1ul rAAV-eGFP (green line) or 1ul rAAV-GKS (blue line). Rats were fed normal chow with ad libitum access to a 10% glucose solution at the onset of the dark phase (day 40). Data are expressed as mean +/- SEM for both groups, n=10.*

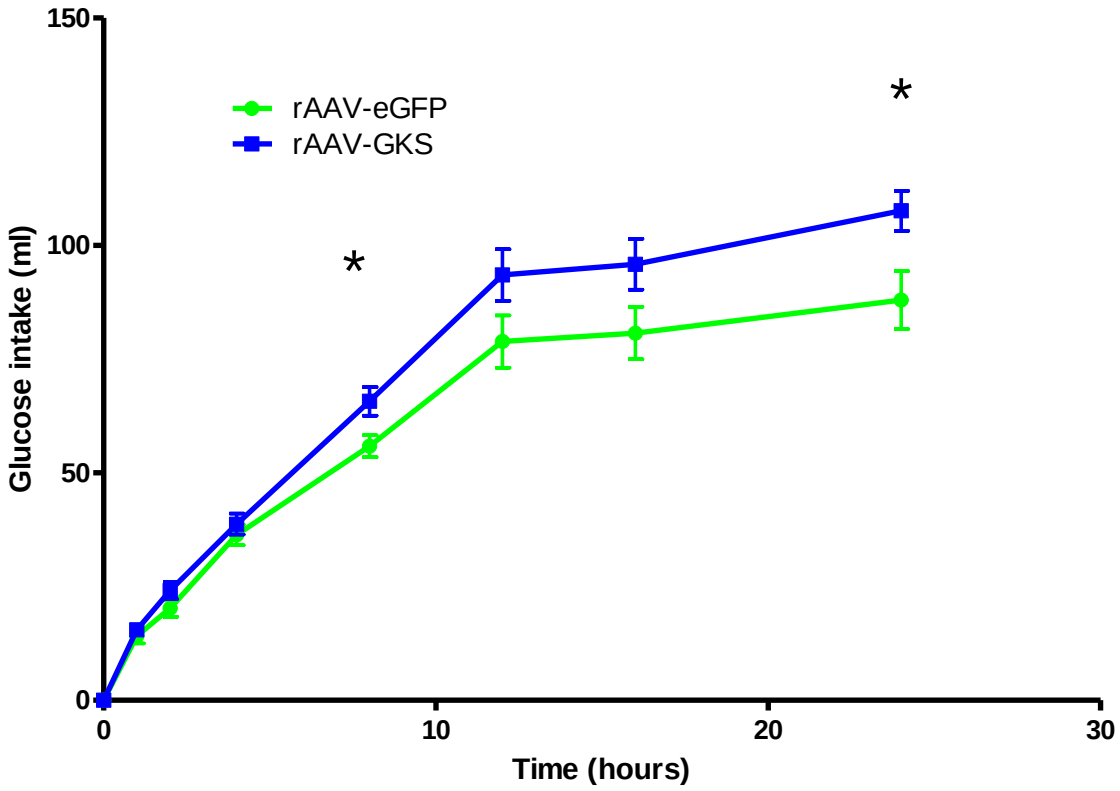


Figure 4.8 Effect of iARC rAAV-GKS on 24hr intake of a 10% glucose solution: *24hr intake of 10% glucose of male Wistar rats bilaterally injected with 1ul rAAV-eGFP (green line) or 1ul rAAV-GKS (blue line). Rats were fed normal chow with ad libitum access to a 10% glucose solution at the onset of the dark phase (day 40). Data are expressed as mean +/- SEM for both groups, n=10, *=P<0.05.*

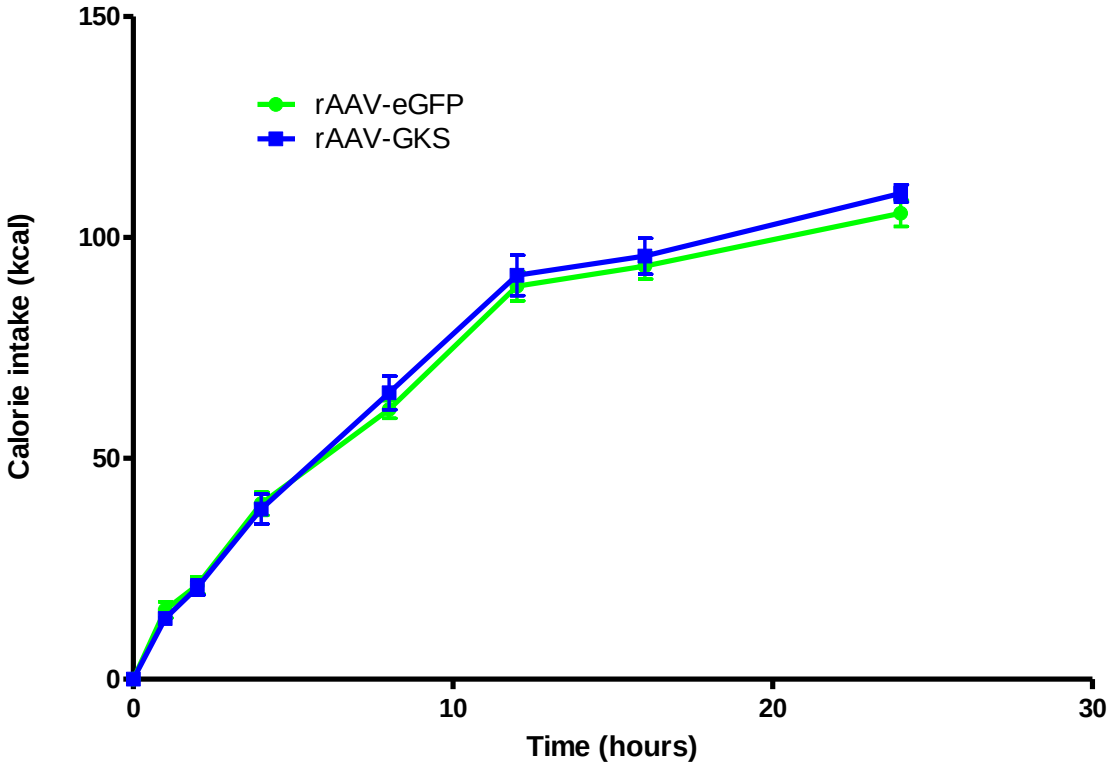


Figure 4.9 Effect of iARC rAAV-GKS on total energy intake over a 24hr period (10% glucose): *Total 24hr energy intake of male Wistar rats bilaterally injected with 1ul rAAV-eGFP (green line) or 1ul rAAV-GKS (blue line). Rats were fed normal chow with ad libitum access to a 10% glucose solution at the onset of the dark phase (day 40). Data are expressed as mean +/- SEM for both groups, n=10.*

4.4.1.6 **24 hour intake of standard chow and 20% glucose solution**

Intake of standard chow and a 20% glucose solution were measured in GKS animals and their controls over a 24hr period starting at the onset of the dark phase (day 44). Food intake was not different between the groups at any time point (figure 4.10).

Intake of 20% glucose solution was greater in the GKS group compared to controls in the 0-1hr period (eGFP 8.8+/- 0.7ml vs GKS 14.6+/-1.9ml, n=10, p=<0.05), 0-16hr period (eGFP 62.5+/- 2.9ml vs GKS 71.4+/-2.8ml, n=10, p=<0.05) and the 0-24hr period (eGFP 75.3+/-3.8ml vs GKS 88.5+/-3.6ml, n=10, p=<0.05) (figure 4.11).

Total energy intake was not different between the groups at any time point (figure 4.12).

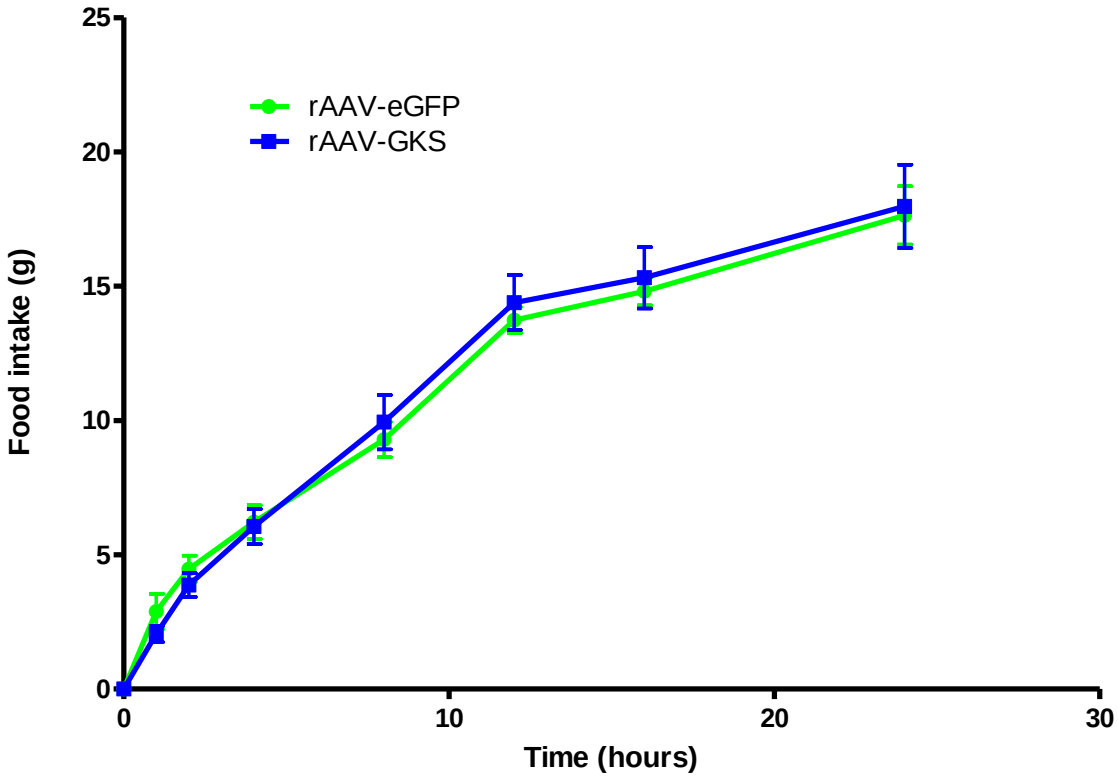


Figure 4.10 Effect of iARC rAAV-GKS on 24hr food intake (with 20% glucose solution): *24hr food intake of male Wistar rats bilaterally injected with 1ul rAAV-eGFP (green line) or 1ul rAAV-GKS (blue line). Rats were fed normal chow with ad libitum access to a 20% glucose solution at the onset of the dark phase (day 44). Data are expressed as mean +/- SEM for both groups, n=10.*

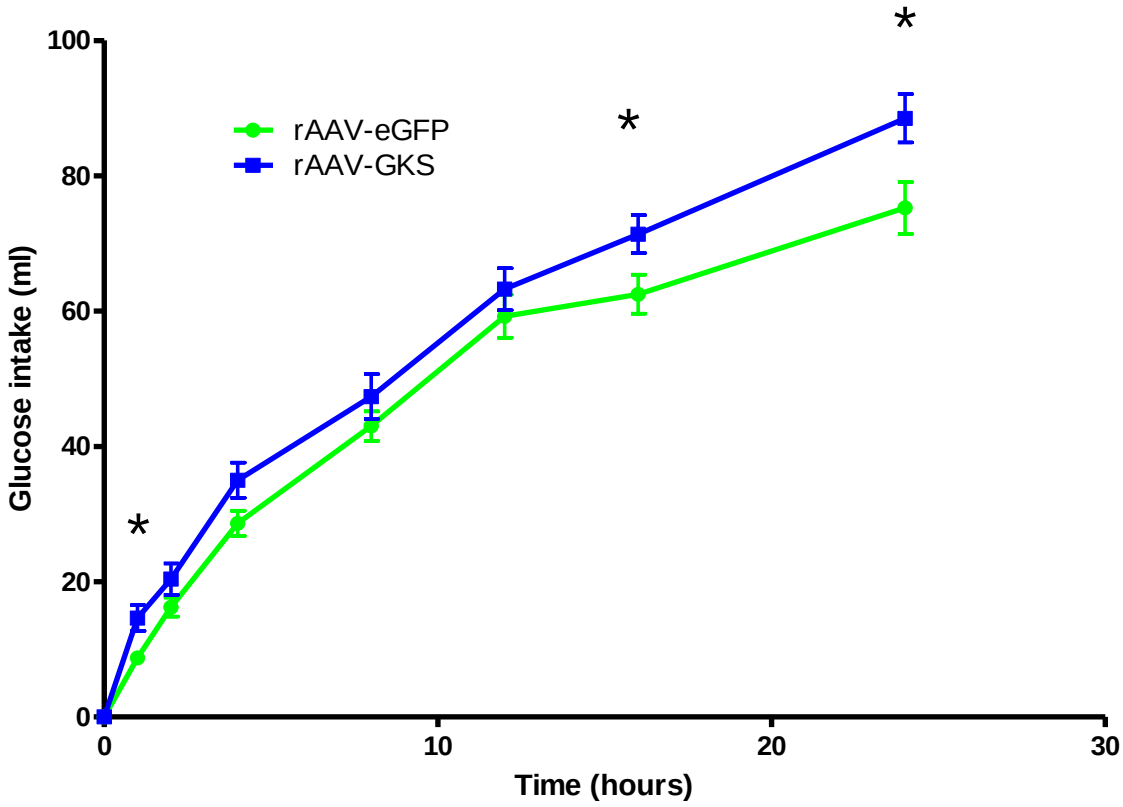


Figure 4.11 Effect of iARC rAAV-GKS on 24hr intake of a 20% glucose solution: *24hr intake of 20% glucose of male Wistar rats bilaterally injected with 1ul rAAV-eGFP (green line) or 1ul rAAV-GKS (blue line). Rats were fed normal chow with ad libitum access to a 20% glucose solution at the onset of the dark phase (day 44). Data are expressed as mean +/- SEM for both groups, n=10, *=P<0.05.*

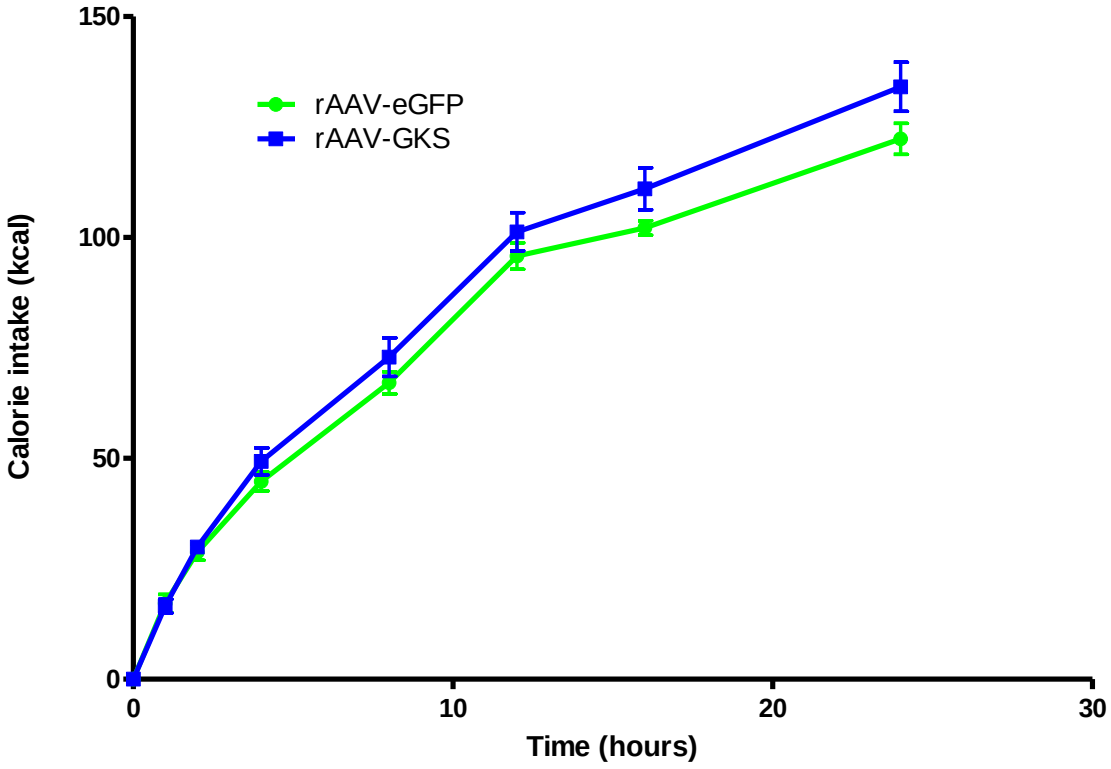


Figure 4.12 Effect of iARC rAAV-GKS on total energy intake over a 24hr period (20% glucose): *Total 24hr energy intake of male Wistar rats bilaterally injected with 1ul rAAV-eGFP (green line) or 1ul rAAV-GKS (blue line). Rats were fed normal chow with ad libitum access to a 20% glucose solution at the onset of the dark phase (day 44). Data are expressed as mean +/- SEM for both groups, n=10.*

4.4.1.7 **24 hour intake of standard chow and 40% glucose solution**

Intake of standard chow and a 40% glucose solution were measured in GKS animals and their controls over a 24hr period starting at the onset of the dark phase (day 50). Food intake was not different between the groups at any time point (figure 4.13).

Intake of 40% glucose solution was not different between the groups at any time point (figure 4.14).

Total energy intake was greater in the GKS animals compared to controls in the 0-16hr period (eGFP 100.0+/-1.7kcal vs GKS 112.0+/-4.9kcal, n=10, p=<0.05) and the 0-24hr period (eGFP 125.4+/-2.3kcal vs GKS 137.5+/-5.0kcal, n=10, p=<0.05) (figure 4.15).

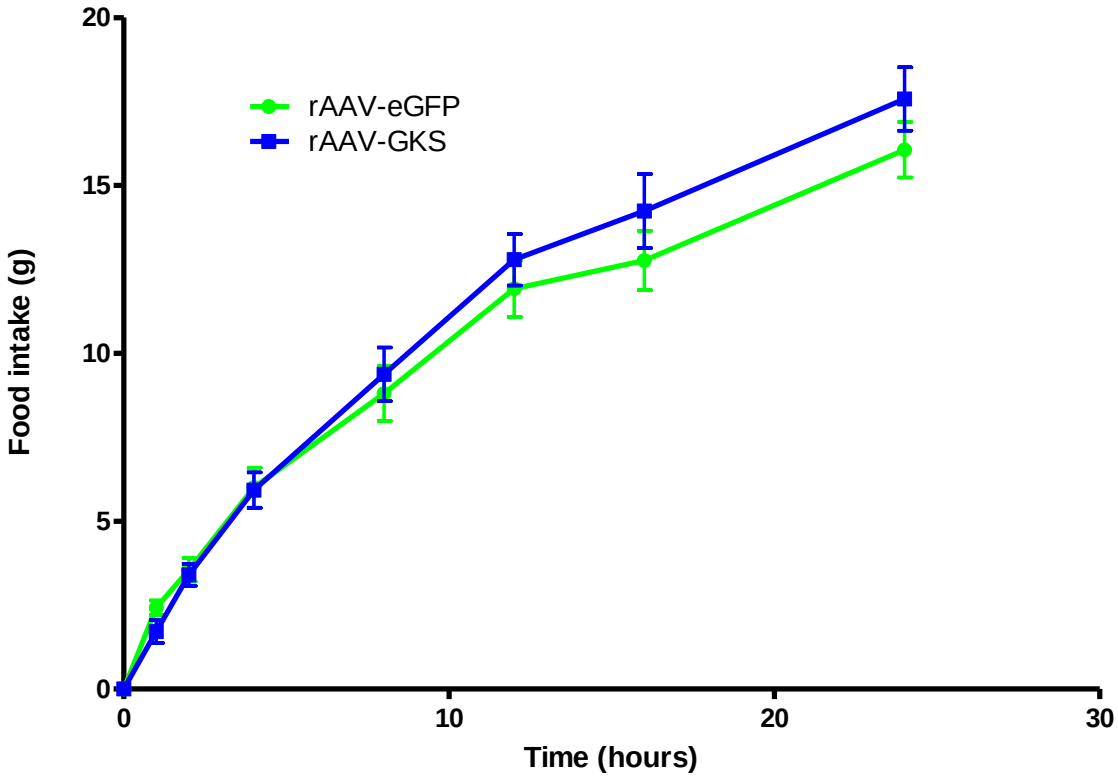


Figure 4.13 Effect of iARC rAAV-GKS on 24hr food intake (with 40% glucose solution): *24hr food intake of male Wistar rats bilaterally injected with 1ul rAAV-eGFP (green line) or 1ul rAAV-GKS (blue line). Rats were fed normal chow with ad libitum access to a 40% glucose solution at the onset of the dark phase (day 50). Data are expressed as mean +/- SEM for both groups, n=10.*

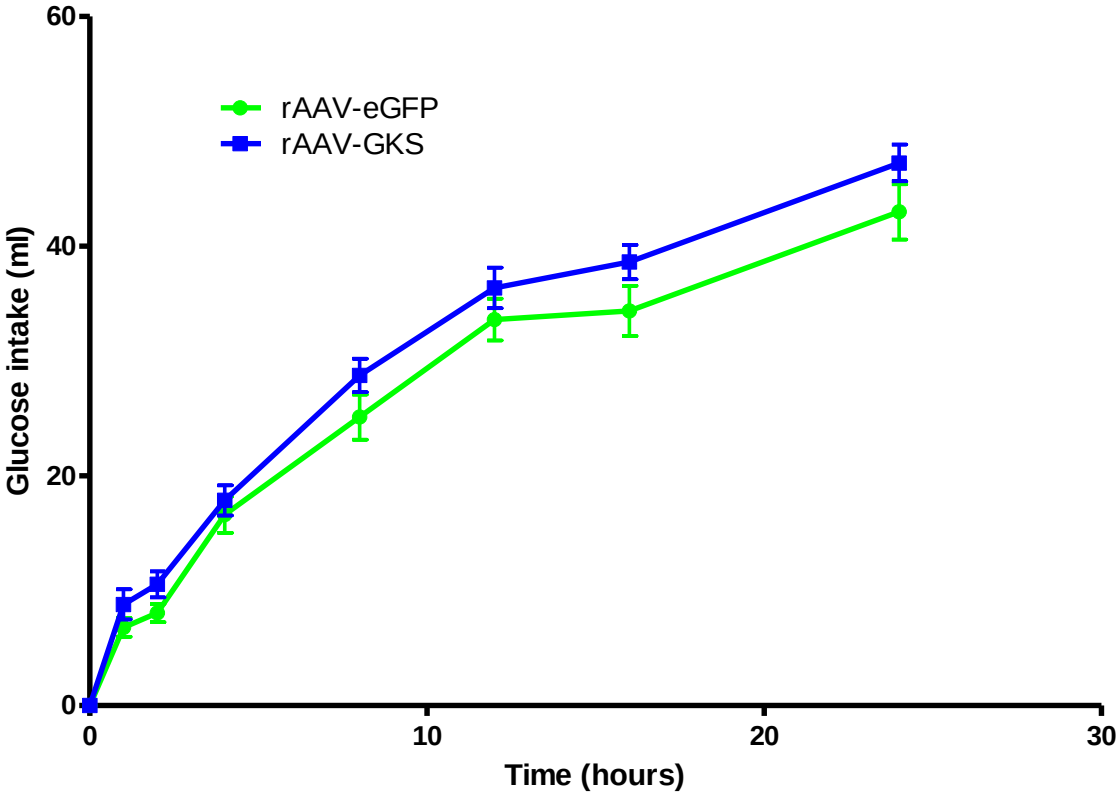


Figure 4.14 Effect of iARC rAAV-GKS on 24hr intake of a 40% glucose solution: *24hr intake of 40% glucose of male Wistar rats bilaterally injected with 1ul rAAV-eGFP (green line) or 1ul rAAV-GKS (blue line). Rats were fed normal chow with ad libitum access to a 40% glucose solution at the onset of the dark phase (day 50). Data are expressed as mean +/- SEM for both groups, n=10.*

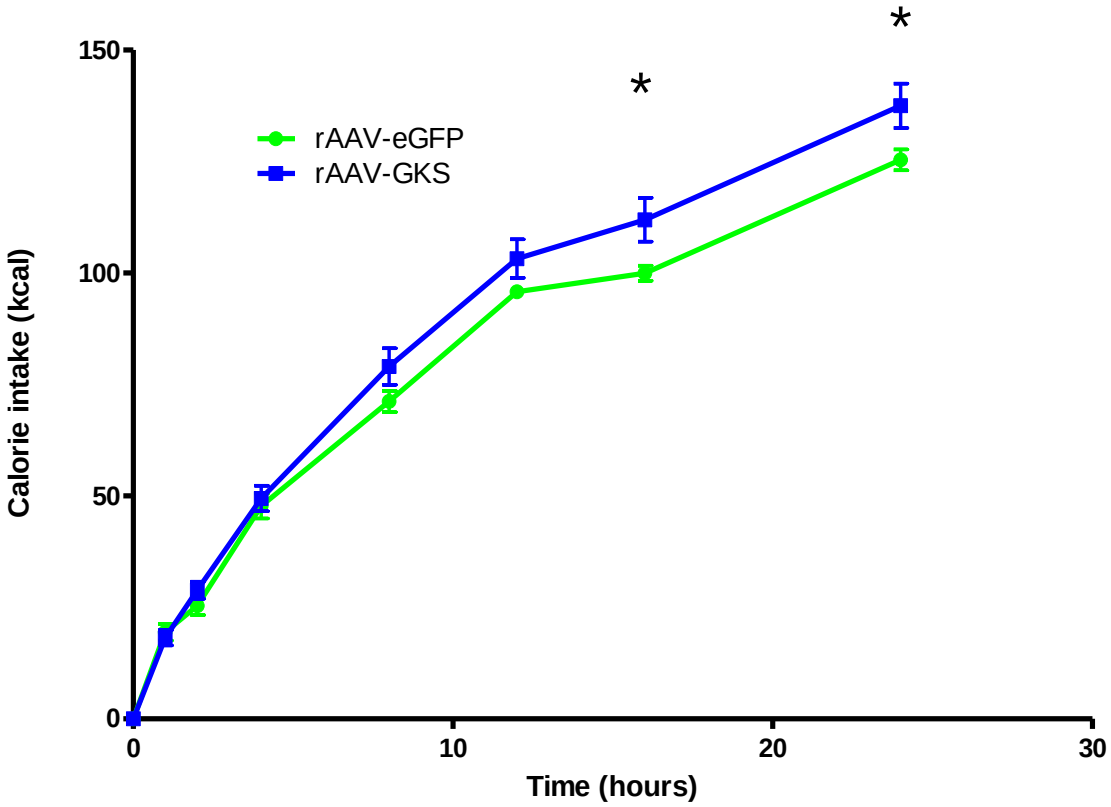
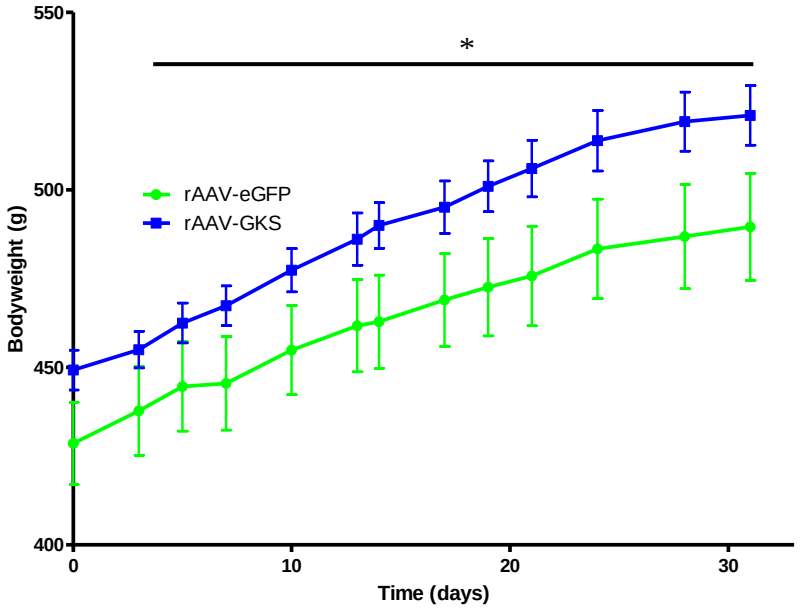


Figure 4.15 Effect of iARC rAAV-GKS on total energy intake over a 24hr period (40% glucose): *Total 24hr energy intake of male Wistar rats bilaterally injected with 1ul rAAV-eGFP (green line) or 1ul rAAV-GKS (blue line). Rats were fed normal chow with ad libitum access to a 40% glucose solution at the onset of the dark phase (day 50). Data are expressed as mean +/- SEM for both groups, n=10, *=P<0.05.*

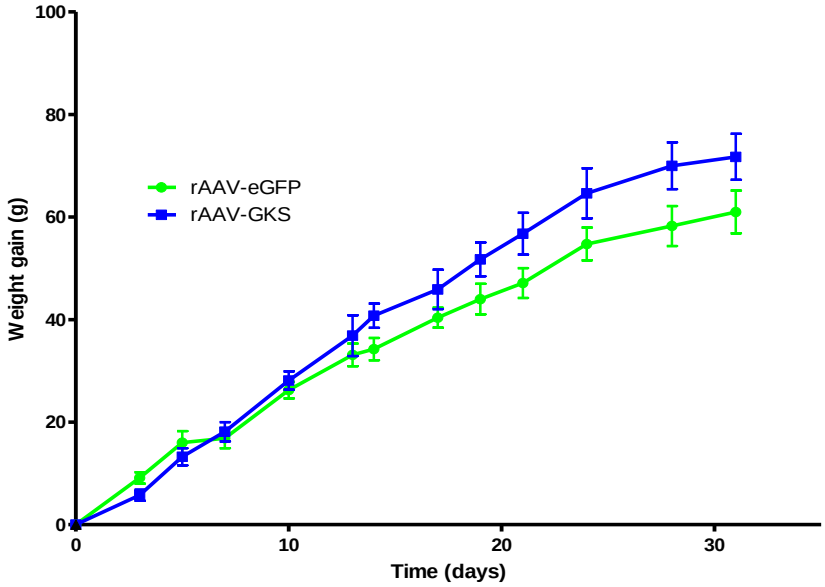
4.4.1.8 **Effect of iARC rAAV-GKS on food intake, intake of glucose and bodyweight gain**

Animals were maintained with *ad libitum* access to standard chow and a 10% glucose solution for 31 days from day 54 post recovery. Mean bodyweights of the rAAV-eGFP group and rAAV-GKS group on day 54 were 428.6g and 449.3g respectively. This difference was not statistically significant (p=0.13). At the termination of the experiment there was a significant difference in bodyweight between the groups (eGFP 489.6 +/- 15.1g vs GKS 521.0 +/- 8.39g, n=10, p=<0.05). Weight gain was not different between the groups (eGFP 61.0 +/- 4.2g vs GKS 71.8 +/- 4.5g, n=10) (figure 4.16). There was no significant difference in intake of standard chow between the groups (eGFP 691.9+/- 19.4g vs GKS 682.1+/-22.8g, n=10) (figure 4.17).The GKS group consumed a significantly greater volume of 10% glucose solution than their controls (eGFP 691.9+/- 19.4ml vs GKS 682.1+/-22.8ml, n=10, p=<0.05) (figure 4.18). There was no significant difference in total energy intake from standard chow and 10% glucose solution between the groups (eGFP 3456.9+/- 78.6g vs GKS 3615+/-100.4g, n=10) (figure 4.19).

a)



b)



b)

Figure 4.16 Effect of iARC rAAV-GKS on bodyweight and bodyweight gain: *a) bodyweight and b) weight gain following bilateral injection of 1ul rAAV-eGFP (green line) or 1ul rAAV-GKS (blue line). Male Wistar rats were fed normal chow with ad libitum access to a 10% glucose solution. Data are expressed as mean +/- SEM for both groups, n=10.*

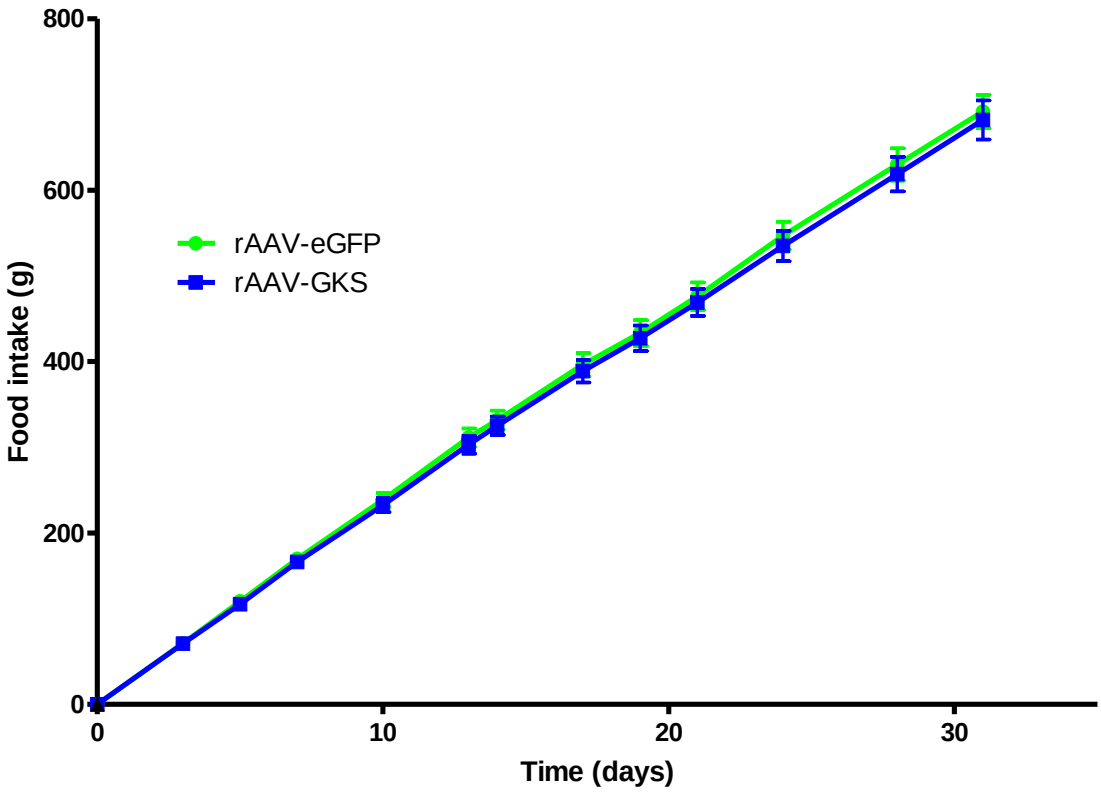


Figure 4.17 Effect of iARC rAAV-GKS on food intake: *Food intake following bilateral injection of 1ul rAAV-eGFP (green line) or 1ul rAAV-GKS (blue line). Male Wistar rats were fed normal chow with ad libitum access to a 10% glucose solution. Data are expressed as mean +/- SEM for both groups, n=10.*

4.4.1.9 **Effect on intake of 10% glucose solution**

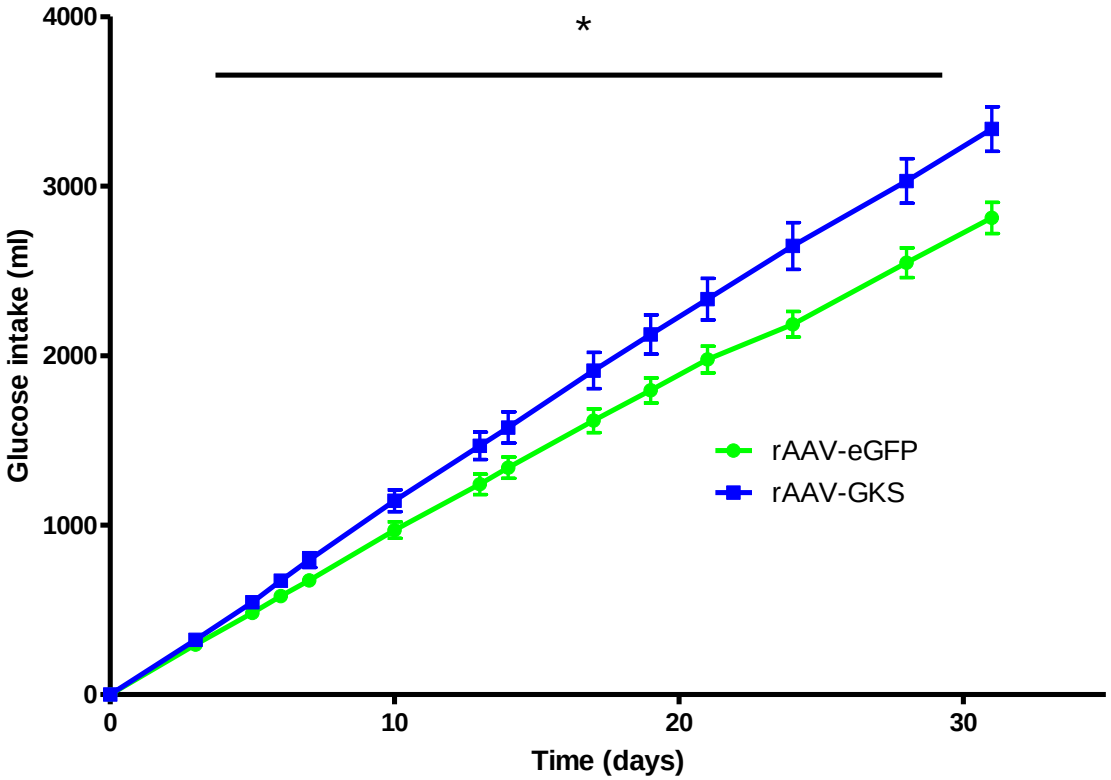


Figure 4.18 Effect of iARC rAAV-GKS on intake of 10% glucose solution: *Intake of 10% glucose solution following bilateral injection of 1ul rAAV-eGFP (green line) or 1ul rAAV-GKS (blue line). Male Wistar rats were fed normal chow with ad libitum access to a 10% glucose solution. Data are expressed as mean +/- SEM for both groups, n=10, *=P<0.05.*

4.4.1.10 **Effect on total energy intake**

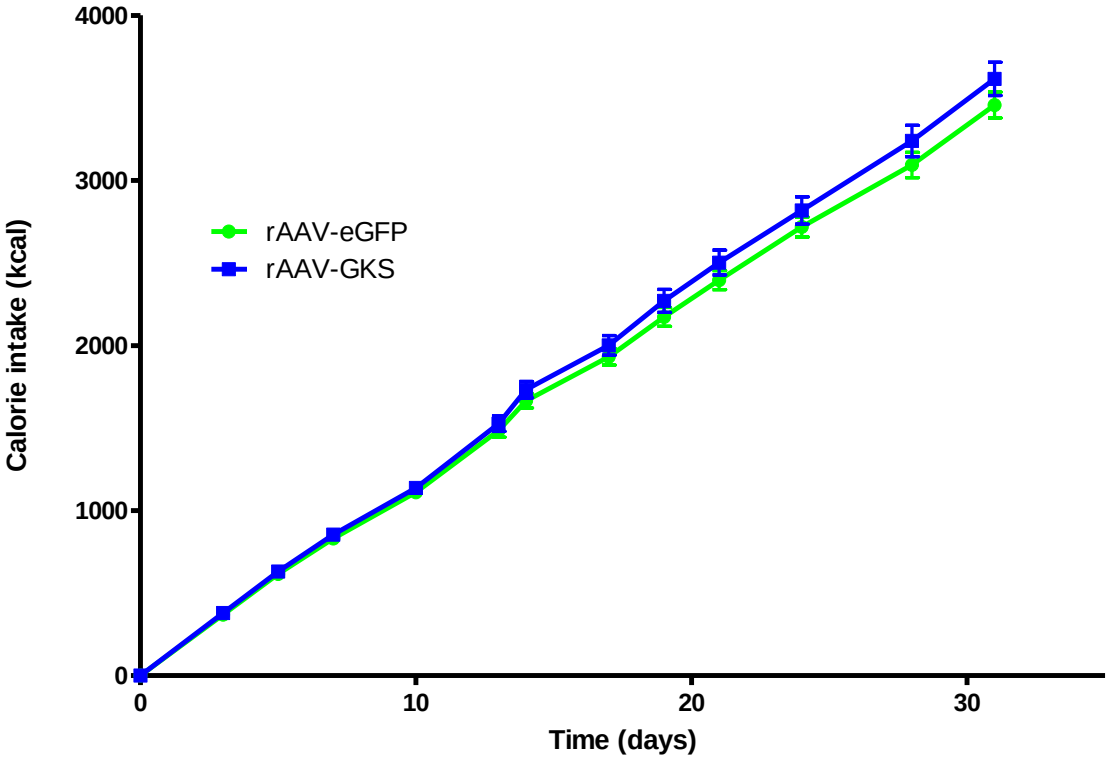


Figure 4.19 Effect of iARC rAAV-GKS on total energy intake: *Total energy intake following bilateral injection of 1ul rAAV-eGFP (green line) or 1ul rAAV-GKS (blue line). Male Wistar rats were fed normal chow with ad libitum access to a 10% glucose solution. Data are expressed as mean +/- SEM for both groups, n=10.*

4.4.1.11 **Effect of iARC rAAV-GKS on plasma glucose following oral glucose challenge**

At the termination of the study (day 85) GKS animals and controls received a solution containing 2.5mg of glucose per kg of bodyweight. The solution was consumed voluntarily in less than 10 minutes. Blood glucose levels were measured prior to consumption of glucose and at 30 minutes after consumption when animals were euthanized by CO_2 inhalation. Plasma glucose prior to consumption of glucose was not different between the groups **(**eGFP 4.2+/-0.2mmol/L vs GKS 4.0+/-0.2mmol/L, n=10). At 30 minutes plasma glucose was significantly lower in the GKS group compared to controls (eGFP 6.9+/-0.3mmol/L vs GKS 5.0+/-0.2mmol/L, n=10, p=<0.001) (figure 4.20).

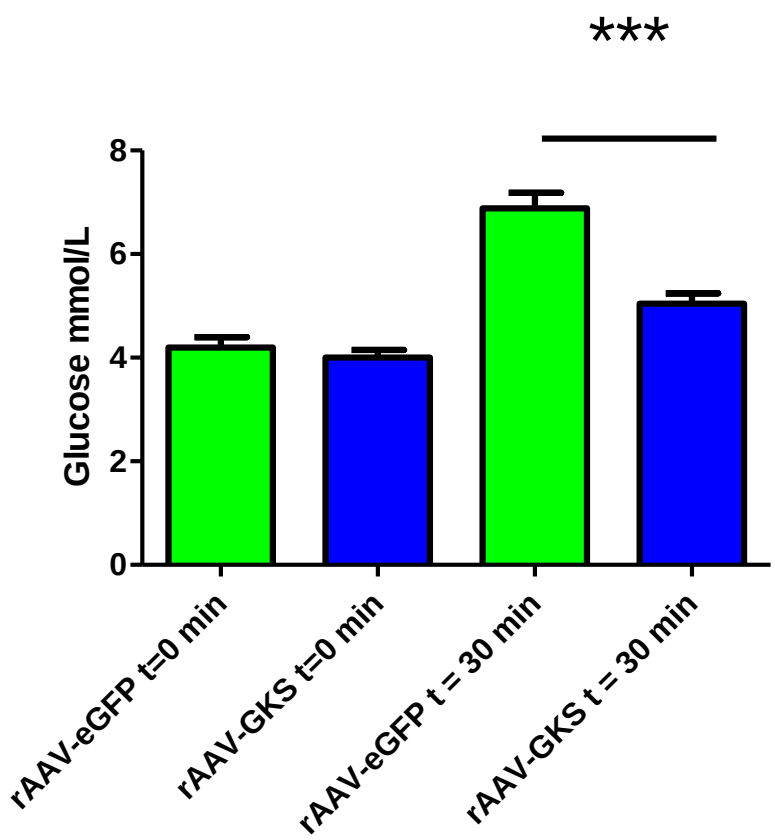


Figure 4.20 Effect of iARC rAAV-GKS on plasma glucose response to oral glucose challenge: *GKS animals and controls received a solution containing 2.5mg/kg of glucose. Plasma glucose levels were measured prior to consumption of glucose and 30 minutes after. Data are expressed as mean +/- SEM for both groups, n=10, ***=P<0.001.*

4.4.2 Cohort 5: Glucose homeostasis

4.4.2.1 **Oral glucose tolerance test**

To assess the role of GK in the ARC in the regulation glucose homeostasis GKS animals and their controls were subjected to oral glucose tolerance test at 20 days post recovery. Glucose was delivered by oral gavage. Glucose clearance at 30 minutes was significantly improved in the GKS group compared to controls (eGFP 7.7+/-0.6mmol/L vs GKS 4.6+/-0.3mmol/L, n=9-10, p=<0.001)**.** There was no significant difference at any other time point (figure 4.21). Area under the curve (AUC) was significantly lower in the GKS group compared to controls (eGFP 614.4+/-21.5 vs GKS 522.4+/-26.3, n=9-10, p=<0.05).

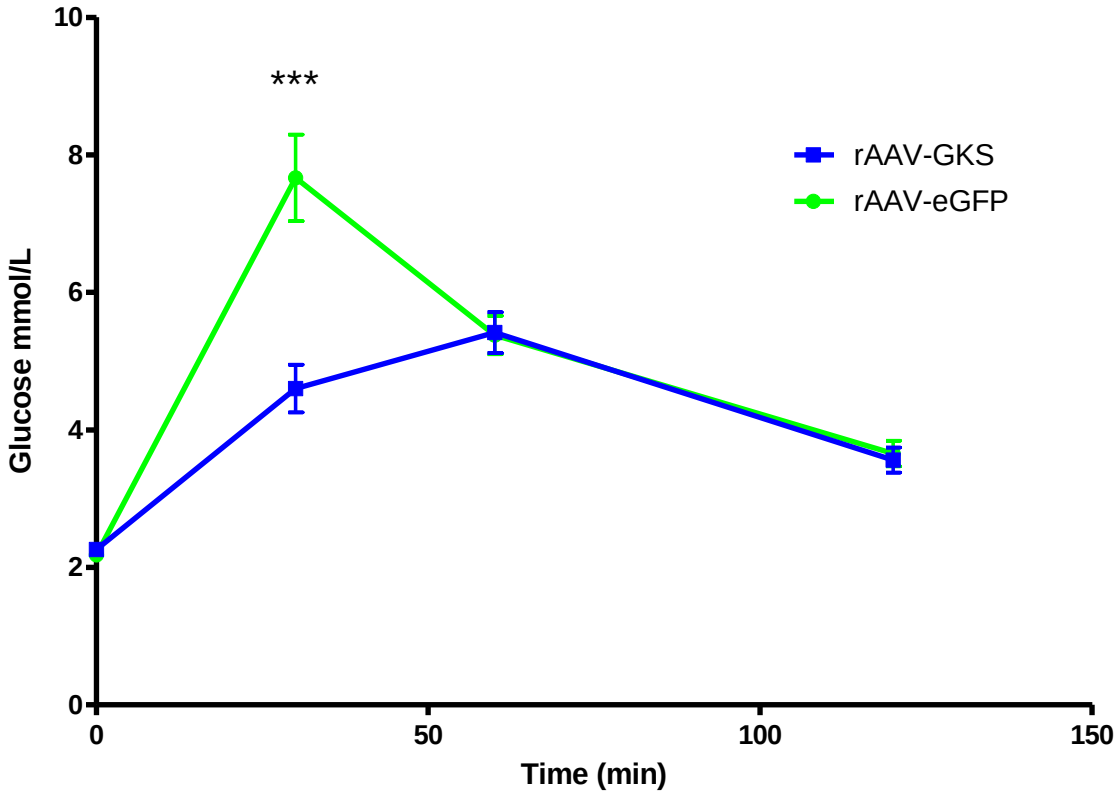


Figure 4.21 Oral glucose tolerance test via gavage: *GKS animals and controls received a bolus glucose dose (2.5g/kg body weight) via oral gavage and their blood glucose response was measured over the course of 2 hours (day 20) .Data are expressed as mean +/- SEM for both groups, n=9-10, ***=P<0.001.*

4.4.2.2 **Insulin tolerance test**

At 35 days post recovery insulin tolerance test was performed. Plasma glucose was significantly lower in the GKS group compared to controls at the 60 minute time point (eGFP 2.9+/-0.1mmol/L vs GKS 2.5+/-0.2mmol/L, n=9-10, p=<0.05) and at the 120 minute time point (eGFP 2.0+/-0.1mmol/L vs GKS 1.7+/-0.1mmol/L, n=9-10, p=<0.05) (figure 4.22)**.** AUC was not significantly different between the groups (eGFP 394.3+/-11.1 vs GKS 370.5+/-13.5, n=9-10).

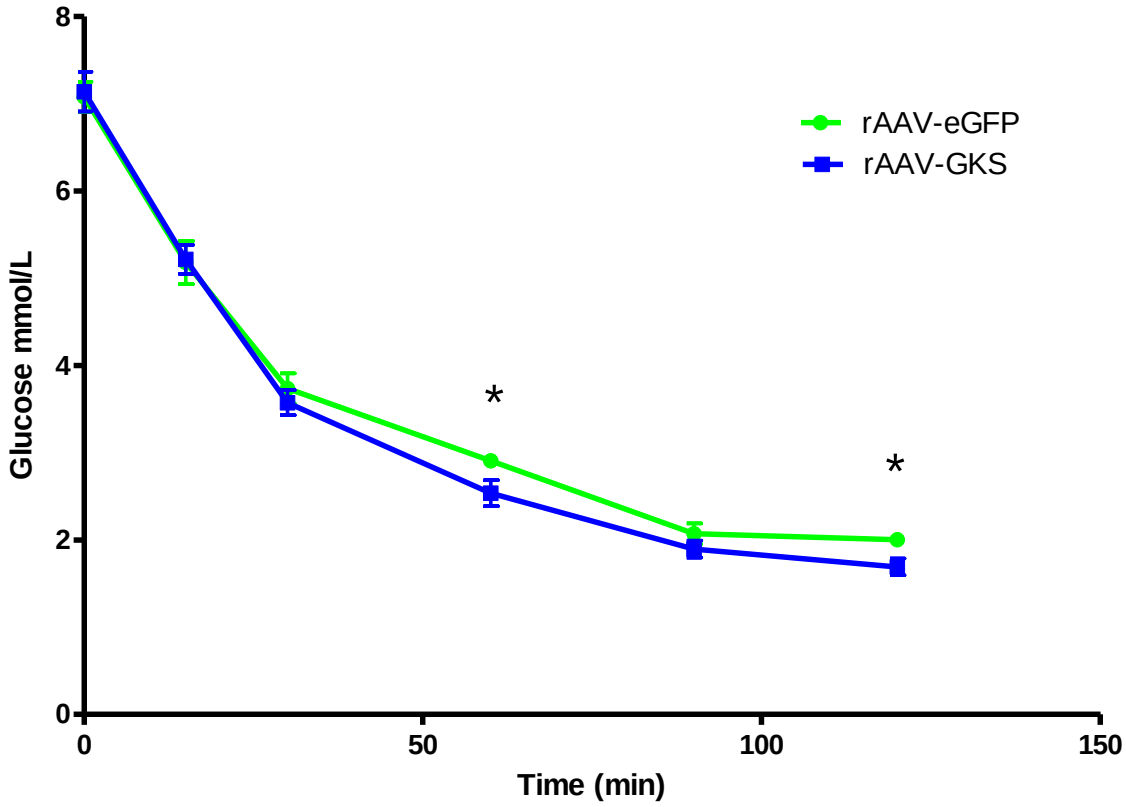


Figure 4.22 Insulin tolerance test: *GKS animals and controls received a bolus i.p. insulin dose (2.0IU/kg body weight) and their blood glucose response was measured over the course of 2.5 hours (day 35) .Data are expressed as mean +/- SEM for both groups, n=9-10, *=P<0.05.*

4.4.2.3 **Voluntary oral glucose tolerance test group 5**

GKS animals and their controls were subjected to vGTT at 48 days post recovery. Plasma glucose was significantly lower in the GKS group compared to controls at the 15 minute time point (eGFP 7.4+/-0.2mmol/L vs GKS 6.4+/-0.3mmol/L, n=9-10, p=<0.05) and the 30 minute time point (eGFP 7.8+/-0.2mmol/L vs GKS 6.9+/-0.3mmol/L, n=9-10, p=<0.05**).** There was no significant difference between the groups at any other time point (figure 4.23). AUC was not significantly different between the groups (eGFP 849.1+/-15.5 vs GKS 805.1+/-23.9, n=9-10).

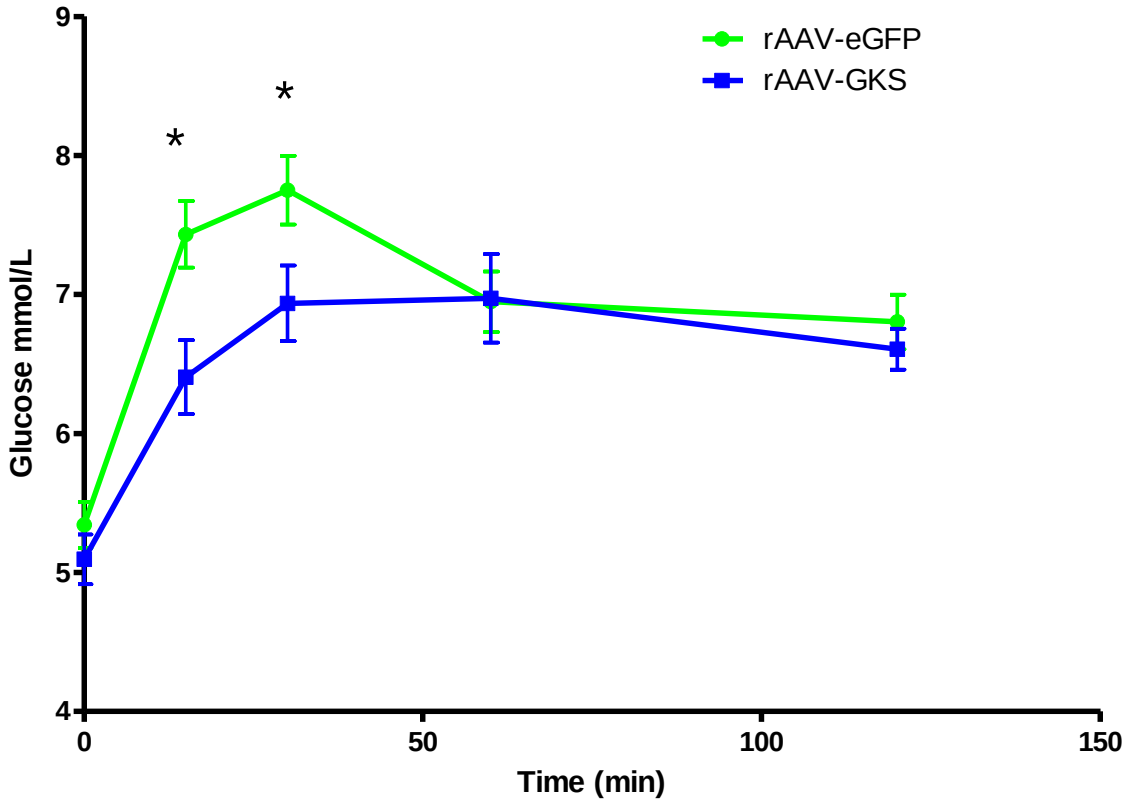


Figure 4.23 Voluntary oral glucose tolerance test: *GKS animals and controls voluntarily consumed a glucose solution containing 2.5g/kg body weight and their blood glucose response was measured over the course of 2 hours (day 48) .Data are expressed as mean +/- SEM for both groups, n=9-10, *=P<0.05.*

4.4.2.4 **Plasma insulin during voluntary oral glucose tolerance test**

During the vGTT on day 48, plasma was collected at 0,15,30 and 60 minutes and was subsequently assayed for insulin. Plasma insulin was significantly higher in the GKS group compared to controls at 30 minute (eGFP 0.71+/-0.2ng/mL vs GKS 1.64+/-0.4g/mL, n=8-9, p=<0.05)**.** There was no significant difference at any other time point (figure 4.24). AUC was not significantly different between the groups (eGFP 92.2+/-20.9 vs GKS 140.7+/-28.4, n=9-10).

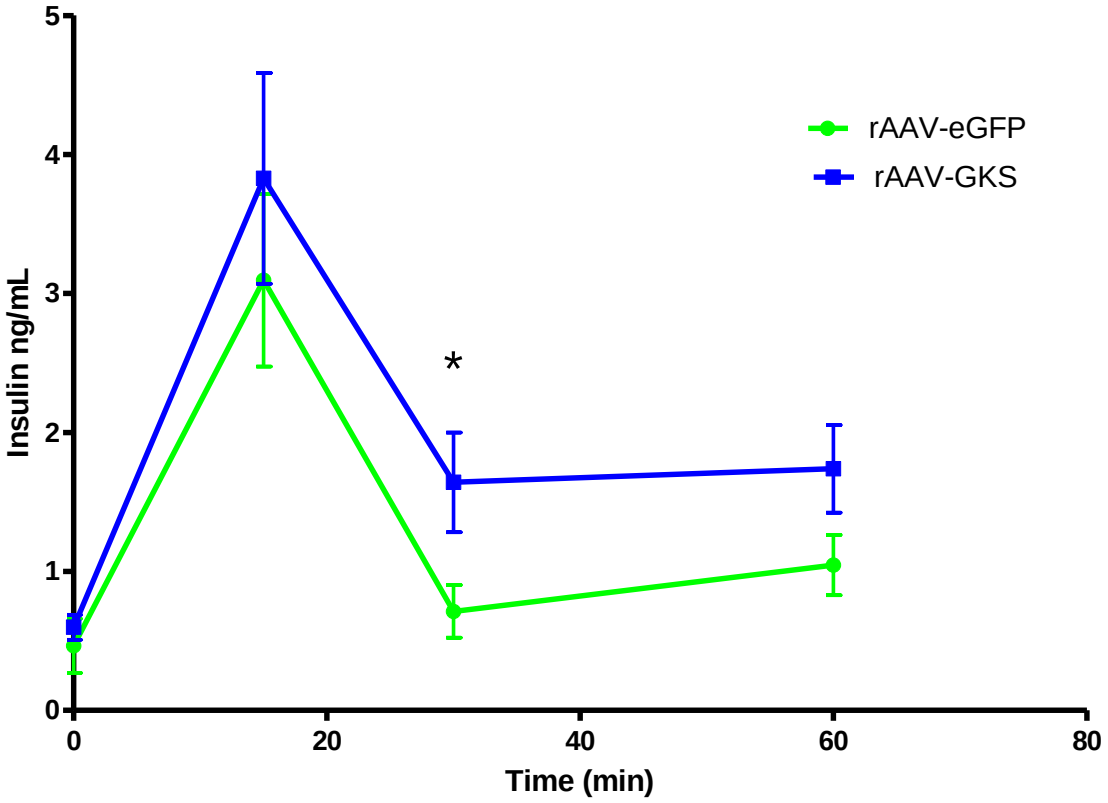


Figure 4.24 Plasma insulin during voluntary oral glucose tolerance test: *GKS animals and controls voluntarily consumed a glucose solution containing 2.5g/kg body weight and their plasma insulin response was measured for 1hour .Data are expressed as mean +/- SEM for both groups, n=8-9, *=P<0.05.*

4.5 Discussion

In the last chapter, increasing GK mRNA in the ARC was shown to increase food intake and bodyweight gain on both standard chow and high calorie western style diet. In addition, the increased fasting plasma insulin in the GKS group suggested that the treatment might also affect glucose homeostasis. In this chapter I investigated the effect of increased GK mRNA in the ARC on intake of sugars and on glucose homeostasis.

In the first experiment, rats were offered a solution containing 10% (w/v) D-glucose for a period of 24 hours. Intake of the glucose solution was significantly higher in the GKS group compared to the controls at all-time points between 0-2 hour and 0-16 hour but was not significantly different over 24 hours.

In contrast, fructose intake between the groups was not different at any time point. Fructose enters glycolysis downstream of GK so it would not be expected to be sensed via the GK pathway. In addition, fructose intake does not influence plasma glucose levels in the fed state (Lee & Wolever, 1998). Taken together with the results of the glucose intake study, these data suggest that increasing GK mRNA in the ARC alters feeding behaviour via its effect on glucose-sensing rather than causing indiscriminate hyperphagia. It is important to note that while the standard chow diet does not contain high levels of glucose, it does contain high levels of starch (see appendix II). Starch is formed of large numbers of glucose molecules linked by glucosidic bonds. Thus, post digestion, the standard chow diet provides a high proportion of its energy from glucose, which would be sensed via the GK pathway in ARC neurones.

The 24 hour intake of standard chow was also measured in the current cohort to ensure that food intake followed a similar pattern to that of previous groups. Food intake was significantly greater in the GKS group compared to control in the 0-8, 0-12 and 0-16 hour time points. In cohort two, the GKS group consumed significantly more standard chow than the controls in the 8-24 hour period. In both cohorts, the GKS group consumed more chow than controls over the full 24 hour period but this did not reach significance in either study. Thus, the feeding patterns of the current cohort were comparable to those of previous groups.

Next, I examined the effect of increased ARC GK mRNA on preference to glucose over standard chow. In separate experiments, rats were given *ad libitum* access to solutions of 2%, 10%, 20% or 40% glucose in addition to standard chow.

At glucose concentrations of 2% and 10%, intake of glucose was significantly higher in the GKS group compared to controls over 24 hours. Interestingly, the increased intake of glucose in the GKS groups led to a normalisation of food intake and total energy intake compared to controls. These results are striking because, for the first time, energy intake was not different between the groups at any time point.

At 20% glucose, a similar pattern was observed. Food intake was not different between the groups and glucose intake was significantly higher in the GKS group compared to controls over 24 hours. Total calorie intake was also not different but at the later time points (16 and 24 hours) there was a non-significant divergence such that at 24 hours the GKS group had consumed 13.8kcal more than controls. At 40% glucose, neither food nor glucose intake was significantly different. However, both were non-significantly higher in the GKS group and this resulted in a significant increase in total energy intake at the 0-16 and 0-24 hour time points in the GKS group.

The fact that low concentration glucose solutions normalised the total energy intake of the groups may be due to the energy density of the solutions. In all experiments, the GKS group consumed a greater proportion of their total energy intake from glucose compared to the controls. This suggests an increased preference for glucose over standard chow compared to the control group.

In the 2% glucose study, the GKS group consumed 59.1ml more glucose solution than the controls over 24 hours. However, this equates to a difference in energy intake of only 4.7kcal. In the same study, the controls consumed 0.7g more chow than the GKS group, this equates to a difference in energy intake of 2.1kcal. Thus, it does not appear that the addition of the glucose solution reduced the appetite of the GKS group. Rather, it appears that the increased drive to consume glucose caused the GKS group to preferentially consume a vast quantity of a very low energy-density food stuff (the 2% glucose solution being 98% water). Gastric dissention has a well-accepted effect of reducing appetite (Geliebter *et al*, 1988), considering the fact that the GKS group consumed nearly 60ml more water than the controls, this is likely to be a factor in this study. A similar pattern was observed in the 10% glucose study.

With increasing glucose concentrations, the difference in total energy intake between the groups increased. At 2% glucose the controls consumed 98% of the total energy intake of the GKS group over 24 hours. This decreased to 96% in the 10% glucose study, 91% in the 20% glucose study and 90% in the 40% glucose study. During the study measuring intake of standard chow alone, the 24 hour food intake of the controls was also 90% of the GKS group. Thus, during the 40% glucose study the difference in energy intake between the groups is the same as it was on standard chow alone. This suggests that the effect of the glucose solution on reducing the energy intake of the GKS group is concentration dependent. That said, it is of interest that increased ARC GK mRNA would increase the drive to consume glucose.

I was next interested to see whether the effect of a low concentration glucose solution on food intake contained beyond 24 hours. To investigate this, the GKS group and controls were maintained on standard chow with *ad libitum* access to a 10% glucose solution for a period of 31 days. As was observed during the 24 hour studies glucose intake was higher in the GKS groups compared to controls and there was no difference in food intake or total energy intake. In addition, bodyweight gain was not different between the groups although the weight gain of the groups did appear to be diverging towards the end of the study. The bodyweight of the GKS group was significantly higher than controls at the termination of the study. However, the mean bodyweight of the GKS group was 20g greater than the controls at the beginning of the study. This difference in starting bodyweight will have contributed to the difference in bodyweight observed at the termination of the study.

The results of the sugar feeding studies suggest that 1) GK animals have an increased drive to consume glucose compared to controls and 2) when offered standard chow and glucose GK animals have an increased preference for glucose over standard chow compared to controls. As discussed in the introduction to this chapter, the effect of sugars on food intake is complex and dependent on many factors including dosage, timing of administration and effect on plasma glucose and insulin. At present, it is not possible to determine whether the increased intake of glucose in the GK group is the result of increased meal size or increased meal number. Accurate analysis of feeding patterns might help to elucidate the mechanisms involved in the perceived phenotype.

It is also unclear why increasing GK mRNA in the ARC would increase an animal's preference to glucose over standard chow. Changes in plasma insulin and glucose have been shown to influence intake of glucose and to increase the palatability of sweet tasting foods (Rodin *et al*, 1985;Jacobs, 1958). Considering the effects of iARC rAAV-GKS on glucose homeostasis (discussed below) it is possible that the effects on food and glucose intake might be secondary to changes in glucose homeostasis.

In cohort two, plasma insulin in the fed state was significantly higher in the GKS group compared to controls, suggesting that treatment might be affecting glucose homeostasis.

To investigate this further, rats were offered a glucose solution containing 2.5g/kg glucose which was consumed in less than 10 minutes. Plasma was collected prior to ingestion of glucose and 30 minutes afterward. The purpose of this experiment was to assess the effect of increased GKS on glucose disposal. At baseline, there was no difference in plasma glucose between the groups. Thirty minutes after the oral glucose load, plasma glucose levels were significantly lower in the GKS group compared to controls, demonstrating enhanced post-prandial glucose clearance.

To further investigate the effect of increased ARC GK mRNA on glucose homeostasis, GTTs and ITTs were performed. During GTTs, glucose was delivered using two methods. The first method utilized oral gavage to deliver glucose as is commonly practised. The second method was novel and involved training rats to voluntarily consume a solution containing the desired glucose dose. After a brief period of training, all animals consumed the solution within 10 minutes with most doing so in less than 5 minutes.

The voluntary oral glucose tolerance test holds a number of advantages over the gavage method. Firstly, because the voluntary method is less invasive and requires less animals handling, it is likely that levels of stress in the study animals will be decreased. Handling animals and oral gavage have both been shown to cause stress to laboratory animals and both result in increased plasma glucose (Balcombe *et al*, 2004). Secondly, glucose sensing in the oral cavity is involved in cephalic phase insulin secretion (Berthoud *et al*, 1980;Berthoud & Powley, 1990). The cephalic phase insulin response is only responsible for 1-3% of postprandial insulin secretion (Teff & Engelman, 1996). Despite this, the small rise in plasma insulin has been shown to be important in post prandial glucose tolerance. In an early experiment, rats received a carbohydrate rich

meal voluntarily or via an indwelling intragastric cannula. Direct infusion of the meal into the stomach resulted in a significant reduction in glucose tolerance compared to voluntary feeding suggesting that cephalic phase insulin release is important in the regulation of post prandial plasma glucose (Steffens, 1976).

During the GTT using the oral gavage method, glucose tolerance was significantly increased in the GKS group compared to controls. The results of this experiment must be interpreted with some caution. At the 0min time point, fasted plasma glucose in both groups was close to 2mmol/l. This value is lower than levels reported in the literature in similar conditions (Fragloudakis *et al*, 2008; Dias *et al*, 2009; Xu *et al*, 1999). A possible explanation for these values is human error. During sample collection, the first 120µl of fluid must be discarded to avoid contamination with heparin. If this step were missed, the concentration of glucose in the collected fluid would be lower than the true concentration in the blood.

Increased glucose disposal during GTT can be the result of either increased peripheral insulin sensitivity or increased glucose stimulated insulin release. To help identify the source of the increased glucose tolerance in the GKS group I subsequently performed an insulin tolerance test (ITT). ITT revealed a small but significant difference in plasma glucose at the 60 minute and 120 minute time points. The fact that there was no difference in plasma glucose prior to the 60 minute time point suggests that the insulin sensitivity of peripheral tissues was not different between the groups.

The enhanced glucose disposal of the GKS group was confirmed by the voluntary GTT. Post prandial plasma glucose levels were significantly lower in the GKS group compared to controls at the 15 and 30 minute time points. Plasma collected at the 15, 30 and 60 minute time points was also assayed for insulin to establish the effect of treatment on glucose stimulated insulin release. Plasma insulin was significantly higher in the GKS group compared to the controls at 30 minutes. Taken together with the result of the ITT, these data suggest that increasing GK mRNA in the ARC results in improved glucose tolerance via increased glucose stimulated insulin release.

ICV glucose infusion has been shown to increase plasma insulin levels, suggesting that insulin secretion is regulated by the CNS (Schultz-Klarr *et al*, 1994). The fact that increasing GK mRNA in the ARC resulted in increased plasma insulin in the fed state and increased glucose stimulated insulin release is in agreement with this data.

Furthermore, it suggests that manipulation of glucose metabolism specifically in the ARC is sufficient to alter whole body glucose homeostasis. Ablation of the VMH (which contain the ARC) causes hyperinsulinemia, which is reversed by severing the vagus nerve (Inoue *et al*, 1991). This suggests that signals from the VMH and relayed via the vagus are important in the regulation of pancreatic insulin secretion. It is possible that the effect of increased ARC GK mRNA might also be dependent on relay via the vagus nerve. This could be tested in vagotomised rats injected iARC with rAAV-GKS.

In the last chapter, I showed that increasing GK mRNA in the ARC results in increased food intake and bodyweight gain on both standard chow and western style diet. In this chapter, I have shown that the effect of treatment on food intake and bodyweight gain can be ameliorated by offering animals a solution containing a low concentration of glucose; both in the short term and during longitudinal studies. It appears that the GKS group have a greater drive to consume glucose than the controls and that increased intake of glucose inhibits calorie intake from standard chow. In addition, the effect of treatment on glucose sensing seems to be specific because intake of fructose was not different between the groups.

I have also shown that the glucose tolerance of GKS animals is significantly increased due to an increase in glucose stimulated insulin release. The increased glucose tolerance of the GKS group is of particular interest considering the fact that they are heavier and more adipose than the controls. In mice, rats and humans, increased adiposity is usually associated with decreased glucose tolerance (Surwit *et al*, 1988;Martin *et al*, 2006;Hayashi *et al*, 2003).

Chapter 5

General discussion and plan of future work

Numerous lines of evidence suggest a role for hypothalamic glucose-sensing neurones in energy balance and glucose homeostasis. It is becoming increasingly clear that functions that had previously been thought to be controlled peripherally are also subject to central regulation (Andersson *et al*, 2004;Borg *et al*, 1997;Borg *et al*, 1995;Burdakov *et al*, 2005b;Daly, 2004;Hardie *et al*, 1998;Levin *et al*, 2004). Furthermore, recent evidence suggests strong interaction between nutrient sensing in the periphery and nutrient sensing in the CNS in the regulation of energy balance. For example, Wang et al have shown that intraduodenal lipid infusion decreases hepatic glucose output and increases insulin sensitivity. Interestingly, this pathway was shown to involve a gut-brain-liver axis, which is on signal relay in the CNS (Wang *et al*, 2008). Glucose-sensing neurones in the ARC are ideally placed to integrate central and peripheral information. Equally, their action potential firing rates are affected by numerous nutrient and nutrient derived signals (Lam *et al*, 2005b;Tsujii & Bray, 1990;Wang *et al*, 2004;Wang *et al*, 2006). As such, glucose-sensing neurones in the ARC are well placed and functionally capable of playing an important role in energy balance and glucose homeostasis. The aim of this work was to investigate the physiological function of glucose-sensing neurones in the ARC via manipulation of GK using rAAV.

GK is one of the rate limiting steps in glycolysis and manipulation of GK has been shown to alter the electrophysiological properties of glucose-sensing neurones in the hypothalamus (Kang *et al*, 2006). For this reason, GK was chosen as a tool to manipulate glucose-sensing neurones during these studies. Glucose-sensing neurones are found in numerous hypothalamic nuclei that are implicated in the regulation of feeding behaviour and glucose homeostasis. Thus, before commencing rAAV studies, it was important to identify which glucose sensing region of the hypothalamus was most likely to be involved in the regulation of food intake.

To do this, rats were fasted for 24 or 48 hours and subsequently GK activity assay was performed on punch biopsy taken from the ARC, VMN and PVN. Fasting, for either 24 or 48 hours, resulted in a significant increase in GK activity in the ARC with no effect observed in either the PVN or the VMN. For this reason, the ARC was chosen as the primary target for rAAV induced up-regulation of GK.

5.1.1 Summary of rAAV results

Injection of rAAV-GKS into the ARC resulted in a significant increase in food intake and bodyweight gain compared to rAAV-eGFP injected controls. The increase in bodyweight was subsequently found to result from a specific increase in adipose tissue with no difference in lean mass between the groups.

In the second cohort I included an additional GKS group that were pair fed to the control group in order to assess the role of food intake in the observed differences in bodyweight gain. In this study, there was no difference in bodyweight gain between the GKS animals that were pair fed to the control and the control group. This would suggest that the difference in bodyweight gain between the GKS group and controls in the previous study could be attributed to the increased food intake of the GKS group. However, during this study, the food intake of the *ad libitum* fed GKS group was not significantly greater than controls, despite their increased bodyweight gain. Thus, increasing GK mRNA in the ARC appears to result in complex metabolic changes which require further investigation.

In the next study, GKS animals and their controls were fed a high calorie "western style" diet. In this study, as was the case with previous cohorts, the GKS group gained significantly more weight than the controls and food intake was significantly increased. This study was important because the constitution of the standard chow does not closely match that of westernised humans; being high in starch and low in fat (see appendix II).

Next, I investigated the effect of increased ARC GK mRNA on intake of sugars by offering animals a 10% w/v glucose solution for 24 hours. GKS animals consumed a greater volume of the glucose containing solution throughout much of the recorded 24 hour period. Interestingly, there was no difference in the intake of a fructose containing solution at any time point. Fructose is not directly sensed via the GK pathway in glucose-sensing neurones, this result suggests that treatment had a specific effect on glucose metabolism.

In experiments in which rats were offered a glucose solution in addition to standard chow the GKS group displayed an increased preference to glucose over standard chow

compared to controls. At glucose concentrations below 40% the increased intake of glucose in the GKS group resulted in a normalisation of food intake, and total energy intake was not different between the groups. This effect was also observed in a longitudinal study lasting 31days, in which total energy intake (from standard chow and glucose) and weight gain were not different between the groups. This was the first longitudinal study in which the GKS group did not gain significantly more weight than controls.

In addition to its effects on food intake, increasing GK mRNA in the ARC produced profound effects on glucose homeostasis. GKS animals were considerably more glucose tolerant than controls despite their increased adiposity. The improved glucose tolerance of GKS animals was associated with increased glucose-stimulated insulin release.

Next I performed an insulin tolerance test to assess the effect of increased ARC GK mRNA on insulin sensitivity. There was no difference between the groups during the early time points of the insulin tolerance test, this suggests that treatment does not affect peripheral insulin sensitivity. However, the fact that plasma glucose was different at later time points could suggest dampening of the hormonal counter regulatory response to hypoglycaemia (discussed below).

5.1.2 Mechanism of action

Increasing GK in the ARC is hypothesised to increase the sensitivity of glucose-sensing neurones to a given quantity of glucose. In this model, neurones would essentially "perceive" local glucose concentrations to be higher than they actually are due to increased glycolysis. The results of the glucose and insulin tolerance tests are consistent with this hypothesis.

During the glucose tolerance test plasma glucose did not increase to the same degree in the GKS group compared to controls. The lower plasma glucose in the GKS group was the result of increased glucose-stimulated insulin release. Insulin release is regulated both autonomously at the level of the pancreatic β-cell and neurally. It has been suggested that glucose sensing in the CNS may predominate over pancreatic glucose sensing in the regulation of insulin secretion. Indeed, ICV glucose infusion has been

shown to increase plasma insulin independent of changes in plasma glucose (Schultz-Klarr *et al*, 1994).

The enhanced insulin release of the GKS animals in this study is interesting for two reasons. Firstly, this data suggests that ARC glucose sensing may be important in the regulation of insulin secretion. Secondly, it supports the hypothesis that increasing GK causes neurones to 'perceive' local glucose concentrations to be higher than they actually are. In this case, leading to a hypersensitivity of the system and exaggerated insulin secretion following glucose administration. This is also likely to occur following food intake.

During the insulin tolerance test, plasma glucose was lower in the GKS group compared to control at the later time points. One explanation for this finding may be a dampening of the hormonal counter regulatory response to hypoglycaemia (CRR).

The CRR involves a reduction in plasma insulin combined with increased plasma glucagon, noradrenaline and adrenaline, as well as increased sympathetic and parasympathetic outflow from the CNS (Cryer, 1993). The CRR increases plasma glucose in the absence of food by increasing glycolysis and gluconeogenesis in the liver while simultaneously decreasing peripheral glucose utilization.

In type I diabetes, the CRR is dampened by repeated hypoglycaemia, such that a lower blood glucose threshold must be met before it is initiated (Cryer, 1997).This in turn leads to an increase in both the frequency and severity of hypoglycaemic events experienced. It has been estimated that 2-10% of deaths in type I diabetic patients are the result of severe hypoglycaemia related to hypoglycaemia unawareness and a dampening of the CRR (Cryer, 2009;Skrivarhaug *et al*, 2006).

In a recent paper, Levin *et al* tested the hypothesis that alterations in VMH GK expression affect the CRR to hypoglycaemia. Bilateral injection of Compound A (a GK activator) blunted the CRR to insulin-induced hypoglycaemia causing reductions in glucagon, noradrenaline and adrenaline compared to controls (Levin *et al*, 2008). Conversely, both acute and chronic down regulation of GK, via alloxan and short hairpin RNA, results in an increase in adrenaline response to hypoglycaemia (Sanders *et al*, 2004). Thus, increasing GK activity in the VMH appears to blunt the CRR while decreasing GK activity may heighten it.

In this work, I increased GK mRNA in the ARC using rAAV-GKS. During the ITT, there was no difference between the groups before 60 minutes. However, at 60 and 120 minutes plasma glucose was significantly lower in the GKS group compared to controls. Increasing GK mRNA in the VMH has been shown to decrease the release of counter regulatory hormones in response to insulin-induced hypoglycaemia. The fact that the GKS animals had lower plasma glucose at later time points is consistent with this finding. This is also consistent with the hypothesis that GK mRNA over-expression in the ARC alters the sensitivity of glucose sensing neurones. In this case, because neurones would 'perceive' local glucose levels to be higher than they were, plasma glucose would have to fall to a lower level before the CRR was initiated.

What is not immediately clear is why increasing GK mRNA in the ARC would increase food intake and bodyweight gain. Glucose has been shown to have an inhibitory effect on food intake when administered to the VMH. It could therefore be hypothesised that increasing GK in the ARC, which is believed to increase glucose metabolism, would also inhibit food intake rather than increasing it. One potential explanation for this finding is that the effect of treatment on food intake could be secondary to its effects on glucose homeostasis.

As discussed previously, hypoglycaemia can increase food intake. Interestingly, repeated insulin-induced hypoglycaemia decreases the hormonal CRR but increases the drive to feed (Sanders *et al*, 2006). This suggests that these two aspects of the glucostatic mechanism might be differently regulated. It is also possible that in the face of a decreased hormonal CRR the drive to feed could be increased in order to maintain plasma glucose.

If the CRR of the GKS group is decreased (as suggested by the results of the ITT) it is possible that they may need to consume a greater quantity of food in order to maintain their plasma glucose levels.

It is also possible, that following food intake, the enhanced glucose-stimulated insulin release of the GKS group might lead to more rapid storage of incoming glucose (as is suggested by the GTT results). It has been shown that most spontaneous meals are preceded by a small dip in blood sugar (Dunn-Meynell *et al*, 2009). If blood sugar falls more quickly in the GKS animals after every meal, it is feasible that the frequency of

these small dips in blood sugar would be increased, especially if the CRR is defective. This in turn might increase meal frequency.

The phenotype of the GKS group is similar to that of rats in which the VMH has been lesioned in that both display hyperphagia associated with hyperinsulinemia (Hustvedt & Lovo, 1972). Furthermore, in both models, hyperinsulinemia occurs as a result of manipulation of the VMH, albeit by entirely different methods. Lesioning the VMH results in hyperinsulinemia within 20 minutes (Berthoud & Jeanrenaud, 1979). This shows that hyperinsulinemia precedes hyperphagia in this model. Interestingly, celiac vagotomy of VMH lesioned rats results in normalisation of plasma insulin levels and food intake (Inoue *et al*, 1991). This suggests that hyperinsulinemia may underlie the changes observed in food intake and that hyperinsulinemia *per se* may be sufficient to increase food intake; a concept further supported by the fact that intensive insulin therapy and Glibenclamide treatment in diabetic patients are associated with weight gain (UK Prospective Diabetes Study (UKPDS) Group, 1998).

Mild hyperinsulinemia might also explain why the GKS group consumed more glucose than the controls. Anecdotally, hypoglycaemia is associated with an increased drive to consume sugary foods (Hunt *et al*, 1990;Smith & Sauder, 1969). In humans, high plasma insulin has been shown to increase food intake and also to increase the palatability of sweet tasting foods (Rodin *et al*, 1985). A study investigating glucose intake in rats showed that rats normally preferentially consume a 10% glucose solution over a 35% glucose solution. However, following an insulin injection, the preference shifted and rats consumed a greater quantity of the 35% glucose solution (Jacobs, 1958). Taken together, this suggests that certain deviations in plasma glucose and insulin are able to influence food preference in a manner that helps to restore normoglycaemia. The high insulin levels of the GKS group might therefore explain why they showed a preference for glucose over standard chow compared to controls.

It is also possible that increasing GK mRNA in the ARC could directly increase the drive to consume foods containing glucose. A number of cell types with mammalian biology are dependent on glucose including erythrocytes. Despite this, storage of glucose is extremely limited. It might therefore be advantageous for mammals to be able to detect food sources that are high in glucose, especially during fast. In support of this notion, it has recently been shown that chronic food restriction increases sweet taste

receptor mRNA on rat taste buds. In addition, fasting has been shown to enhance the preference for a high concentration saccharin solution which suggests nutritional state can influence preference for sweet tasting foods (Chen *et al*, 2010). In early experiments in this work, fasting was shown to increase GK activity in the ARC of wild type animals suggesting that GK expression is influenced by nutritional state. When GK mRNA was artificially increased in the ARC using rAAV animals showed a clear preference for glucose containing solutions compared to the controls. It is perhaps possible that GK in the ARC might also be involved in modulating preference to sweet food in response to nutritional status.

5.1.3 The significance of this work

This work is of significance for a number of reasons. Firstly, this is the first study to chronically increase hypothalamic GK mRNA. Secondly, the effects of this treatment have revealed interesting and in some cases unexpected results which have broader significance.

At present, a number of pharmaceutical companies are investigating the application of small molecule GK activators in the treatment of type II diabetes mellitus. GK activators have been shown to act on β-pancreatic cells to increase glucose-stimulated insulin release and on the liver to increase glucose uptake (Grimsby *et al*, 2003). In a recent review, it was hypothesised that GK activators might represent a "magic bullet" in the treatment of diabetes because, in addition to their effects on glucose homeostasis, they might also reduce food intake if they are able to cross the blood brain barrier (Al-Hasani *et al*, 2003).

The results of this work support and extend the notion that increased GK activity would have beneficial effects on glucose stimulated insulin release. Indeed, while much focus has been placed on the effect of GK activation in the pancreas this work has shown that increasing GK mRNA in the ARC alone is sufficient to increase glucose stimulated insulin release and glucose tolerance. If GK activators do cross the blood brain barrier it is likely that they would increase glucose-stimulated insulin release both locally at the pancreas and via their effects in the hypothalamus.

The suggestion that GK activators would decrease food intake is not supported by this work. In fact, the opposite was observed; increased ARC GK mRNA resulted in hyperphagia and obesity. Obesity and increased adiposity underlie the great majority of type II diabetes cases (Bloomgarden, 2000). If GK activators increase food intake and weight gain in a similar fashion to rAAV-GKS this could negatively influence their efficacy as a treatment for type II diabetes. That said, increased weight gain is a common side effect in type II diabetic patients treated with intensive insulin therapy or sulfonylureas such as Glibenclamide (UK Prospective Diabetes Study (UKPDS) Group, 1998). These treatments are sufficiently efficacious despite their effect on weight gain and it is possible that this would also be true of GK activators.

The results of this thesis also partially support Jean Mayer's 1954 "Glucostatic hypothesis." Mayer correctly predicted the existence of glucose-sensing neurones in the VMH. However, his prediction that glucose-sensing neurones would be involved in the regulation of feeding behaviour has remained unsubstantiated despite significant research effort. This work is the first to show that chronic alteration of hypothalamic GK mRNA influences food intake and adiposity. Since up-regulation of GK is hypothesised to increase the sensitivity of glucose sensing neurones this work supports Mayer's prediction that these cells are involved in the regulation of food intake. However, it is presently unclear whether this is a direct effect on feeding behaviour or a consequence of the treatments effect on glucose homeostasis.

5.1.4 Future work

At the outset of this work, I sought to investigate the physiological function of glucose-sensing neurones in the hypothalamus by manipulating GK expression. The results of this thesis suggest that regulation of energy balance and glucose homeostasis are among the primary physiological roles of glucose-sensing neurones in the ARC. However, further investigation is required to resolve a number of issues.

Having chosen the ARC as a target for this study, the primary objective was to increase GK activity by stereotaxic injection of rAAV-GKS. Despite the observed phenotypic differences between the groups, I was unable to show that rAAV-GKS injection had

increased GK activity in the ARC of the treatment group compared to controls. Increased GK mRNA expression in the hypothalamus was established using QPCR and was confirmed by *in situ* hybridization. Furthermore, I showed that transfection of HEK 293T cells with GKS-pTR-CGW (the plasmid from which the rAAV-GKS was produced) resulted in increased GK activity. Taken together, these data support the notion that injection of rAAV-GKS into the ARC increases GK activity therein. However, this has not been confirmed experimentally.

In order to fully validate the results of these studies it will be necessary to increase the accuracy of the punch biopsy technique used. During the early studies on the effect of fasting on GK activity, punch biopsies were taken from coronal brain sections and positive results were achieved. During the studies investigating the effect of iARC rAAV-GKS injection, punch biopsies were taken from sagittal sections and this failed to show a change in GK activity. Future GK assays should be performed on punches taken from coronal sections. Considering the magnitude of the increase in GK mRNA expression it is possible that this would be sufficient to confirm increased GK activity. If this were not sufficient, it would be necessary to investigate methods to improve the GK assay such as the addition of a GK activator to the assay as described by Zelent *et al* (Zelent *et al*, 2006).

Altering GK expression has been shown (by other investigators) to influence the electrophysiological properties of glucose-sensing neurones. However, in the present study I have been unable to investigate the effect of rAAV-GKS on the electrophysiological properties of glucose-sensing neurones. To investigate the electrophysiological properties of neurones it would be necessary to collaborate with a group that has expertise in performing this technique. rAAV does not infect 100% of neurones at the injection site. To improve the results of electrophysiological analysis, it would be advantageous to introduce to a method to detect neurones that had been infected. One option would be to alter the GKS-pTR-CGW cassette to include the eGFP gene. This would allow the identification of rAAV infected neurones using florescent microscopy.

One of the major findings of this work was that increasing GK mRNA in the ARC results in increased feeding and subsequently increased adiposity. I have hypothesised that the effect on feeding behaviour could be secondary to the effect of treatment on

glucose homeostasis. However, this hypothesis does not exclude the possibility that the treatment might also be affecting gene expression and peptide release at the level of the hypothalamus.

QPCR analysis of hypothalami taken from animals in cohort two revealed no difference in the expression of any feeding related genes assayed. The brains used in this experiment were harvested from rats in the early light phase and rats had not been fasted overnight so food intake in the hours prior to harvest was almost certainly variable. Hypothalamic gene expression and the activity of glucose-sensing neurones are dynamic and dependent on feeding state. It is therefore possible that any changes brought about by over expression of GK mRNA may also be dependent on the nutritional status of the animal. In order to investigate this possibility, I would repeat the QPCR in two further groups. Brains from the first group would be harvested following an overnight fast and brains from the second group after consumption of a controlled quantity of glucose; to assess the effect of treatment during hyperglycemia and hypoglycaemia.

It would also be interesting to investigate the effect of increased ARC GK mRNA on the release of hypothalamic neuropeptides such as α-MSH and NPY using ex-vivo hypothalamic explants. This method has been used successfully by Parton *et al* who showed that glucose-sensing of POMC neurones is lost following high fat feeding (Parton *et al*, 2007). In this study, α-MSH release from explants was shown to increase as glucose concentrations in the assay media were increased; an effect lost in the brains of obese mice. Since increased GK is hypothesised to increase the sensitivity of neurones to a given quantity of glucose, it is possible that it might also affect the release of α-MSH and NPY from explants incubated in a glucose-containing media. This might help to explain the effect of treatment on food intake.

Another issue that is unresolved is whether increasing GK in the ARC has effects on energy balance beyond its effects on food intake. In most studies, GKS animals consumed significantly more chow than control and gained significantly more weight. In cohort two, the GKS group gained significantly more weight than the controls but their food intake was not significantly higher. It is possible that this finding is purely anomalous. Equally, this finding could suggest that treatment has decreased energy expenditure. NPY expressing neurones of the hypothalamus have been shown to be

sensitive to glucose. In addition, NPY has a well-accepted role in the regulation of energy balance in rodents via it effects on brown adipose tissue (Egawa *et al*, 1991). If rAAV-GKS influences NPY release, it is also possible that it would affect brown adipose tissue metabolism and energy balance. For these reasons, it would be advantageous to observe a future cohort in the comprehensive laboratory animal monitoring system (CLAMS). CLAMS allows for accurate and detailed observation of numerous parameters including food intake, physical activity, carbon dioxide production and oxygen consumption.

Increasing GK mRNA in the ARC had profound and repeatable effects on glucose homeostasis. The increased glucose tolerance of the GKS group was shown to be due to an increase in glucose-stimulated insulin release. However, the physiological mechanism by which this occurs was not investigated.

As discussed above, lesioning of the VMH results in obesity and hyperinsulinemia, mainly due to disinhibition of pancreatic insulin secretion (Hustvedt & Lovo, 1972;Inoue *et al*, 1991). This model shares the main phenotypic characteristics of the rAAV-GKS group in this study; being both hyperphagic and hyperinsulinemic. Selective vagotomy of the efferent celiac (pancreatic) branch of the vagus decreases plasma insulin and food intake in VMH lesioned rats (Inoue *et al*, 1991).

To extrapolate the involvement of the celiac vagus branch in the mild hyperinsulinemia of GKS animals, glucose tolerance test could be performed in GKS animals that had been subjected to celiac vagotomy. This procedure might also influence the food intake and adiposity of the GKS group (as it does in VMH lesioned rats) and could provide further clues as to the source of their observed hyperphagia.

Finally, it will be important to investigate the effect of down-regulation of GK mRNA in the ARC using anti-sense rAAV. In the present study, GK mRNA expression was increased 14-fold following rAAV-GKS injection into the ARC. While this may not necessarily equate to a 14-fold increase in enzymatic activity, it is possible that treatment may have increased GK activity to supraphysiological levels. It is therefore possible that the effects observed in this work are pharmacological rather than physiological. Decreasing GK expression using anti-sense rAAV would add weight to this study because down-regulation of gene expression tends to be more suggestive of a physiological role.

References

Afione,S.A., Wang,J., Walsh,S., Guggino,W.B., & Flotte,T.R. (2000) Delayed expression of adeno-associated virus vector DNA. *Intervirology*, **42**, 213-220.

Akabayashi,A., Zaia,C.T.B.V., Silva,I., Chae,H.J., & Leibowitz,S.F. (1993) Neuropeptide Y in the arcuate nucleus is modulated by alterations in glucose utilization. *Brain research*, **621**, 343-348.

Al-Hasani,H., Tschop,M.H., & Cushman,S.W. (2003) Two birds with one stone: novel glucokinase activator stimulates glucose-induced pancreatic insulin secretion and augments hepatic glucose metabolism. *Molecular Interventions*, **3**, 367.

American Diabetes Association (2011) Diagnosis and Classification of Diabetes Mellitus. *Diabetes Care*, **34**, S62.

Anand,B.K. & Brobeck,J.R. (1951) Localization of a" feeding center" in the hypothalamus of the rat. p.323.

Anand,B.K., Chhina,G.S., Sharma,K.N., Dua,S., & Singh,B. (1964) Activity of single neurons in the hypothalamic feeding centers: effect of glucose. *American Journal of Physiology*, **207**, 1146.

Anderson ML. (2011) The Effect of a Dietary Carbohydrase Enzyme System on Blood Glucose Levels When Combined with Foods of Varying Glycemic Index in Male Sprague-Dawley Rats. *Journal of Medicinal Food*,[Epub ahead of print].

Andersson,U., Filipsson,K., Abbott,C.R., Woods,A., Smith,K., Bloom,S.R., Carling,D., & Small,C.J. (2004) AMP-activated protein kinase plays a role in the control of food intake. *Journal of Biological Chemistry*, **279**, 12005.

Atchison,R.W. & Casto,B.C. (1965) Adenovirus-associated defective virus particles. *Science*, **149**, 754-756.

Balcombe,J.P., Barnard,N.D., & Sandusky,C. (2004) Laboratory routines cause animal stress. *Journal of the American Association for Laboratory Animal Science*, **43**, 42-51.

Balkan,B. & Li,X. (2000) Portal GLP-1 administration in rats augments the insulin response to glucose via neuronal mechanisms. *American Journal of Physiology-Regulatory, Integrative and Comparative Physiology*, **279**, 1449.

Barcia,C., Jimenez-Dalmaroni,M., Kroeger,K.M., Puntel,M., Rapaport,A.J., Larocque,D., King,G.D., Johnson,S.A., Liu,C., & Xiong,W. (2007) One-year expression from high-capacity adenoviral vectors in the brains of animals with pre-existing anti-adenoviral immunity: clinical implications. *Molecular Therapy*, **15**, 2154-2163.

Baron,V., Kaliman,P., Gautier,N., & Van Obberghen,E. (1992) The insulin receptor activation process involves localized conformational changes. *Journal of Biological Chemistry*, **267**, 23290.

Berns,K.I. & Adler,S. (1972) Separation of two types of adeno-associated virus particles containing complementary polynucleotide chains. *Journal of Virology*, **9**, 394.

Bernstein,L.M. & Grossman,M.I. (1956) An experimental test of the glucostatic theory of regulation of food intake. *Journal of Clinical Investigation*, **35**, 627.

Berthoud,H.R. & Jeanrenaud,B. (1979) Acute hyperinsulinemia and its reversal by vagotomy after lesions of the ventromedial hypothalamus in anesthetized rats. *Endocrinology*, **105**, 146.

Berthoud,H.R. & Powley,T.L. (1990) Identification of vagal preganglionics that mediate cephalic phase insulin response. *American Journal of Physiology-Regulatory, Integrative and Comparative Physiology*, **258**, 523.

Berthoud,H.R., Trimble,E.R., Siegel,E.G., Bereiter,D.A., & Jeanrenaud,B. (1980) Cephalic-phase insulin secretion in normal and pancreatic islet-transplanted rats. *American Journal of Physiology- Endocrinology And Metabolism*, **238**, E336.

Biggers,D.W., Myers,S.R., Neal,D., Stinson,R., Cooper,N.B., Jaspan,J.B., Williams,P.E., Cherrington,A.D., & Frizzell,R.T. (1989) Role of brain in counterregulation of insulin-induced hypoglycemia in dogs. *Diabetes*, **38**, 7.

Bloomgarden,Z.T. (2000) American Diabetes Association Annual Meeting, 1999: diabetes and obesity. *Diabetes Care*, **23**, 118-124.

Bohenzky,R.A., Lefebvre,R.B., & Berns,K.I. (1988) Sequence and symmetry requirements within the internal palindromic sequences of the adeno-associated virus terminal repeat. *Virology*, **166**, 316-327.

Borg,M.A., Sherwin,R.S., Borg,W.P., Tamborlane,W.V., & Shulman,G.I. (1997) Local ventromedial hypothalamus glucose perfusion blocks counterregulation during systemic hypoglycemia in awake rats. *Journal of Clinical Investigation*, **99**, 361.

Borg,W.P., Sherwin,R.S., During,M.J., Borg,M.A., & Shulman,G.I. (1995) Local ventromedial hypothalamus glucopenia triggers counterregulatory hormone release. *Diabetes*, **44**, 180.

Broberger,C., De Lecea,L., & Sutcliffe,J.G. Hypocretin/orexin-and melanin-concentrating hormone-expressing cells form distinct populations in the rodent lateral hypothalamus: relationship to the neuropeptide Y and agouti gene-related protein systems.

Bronk,J.R. (1999) *Human Metabolism*, Addison Wesley Longman Limited, London.

Burcelin,R., Dolci,W., & Thorens,B. (2000a) Portal glucose infusion in the mouse induces hypoglycemia: evidence that the hepatoportal glucose sensor stimulates glucose utilization. *Diabetes*, **49**, 1635.

Burcelin,R., Dolci,W., & Thorens,B. (2000b) Glucose sensing by the hepatoportal sensor is GLUT2-dependent: in vivo analysis in GLUT2-null mice. *Diabetes*, **49**, 1643.

Burdakov,D., Gerasimenko,O., & Verkhratsky,A. (2005a) Physiological changes in glucose differentially modulate the excitability of hypothalamic melanin-concentrating hormone and orexin neurons in situ. *Journal of Neuroscience*, **25**, 2429.

Burdakov,D., Luckman,S.M., & Verkhratsky,A. (2005b) Glucose-sensing neurons of the hypothalamus. *Philosophical Transactions of the Royal Society B: Biological Sciences*, **360**, 2227.

Campfield,L.A., Brandon,P., & Smith,F.J. (1985) On-line continuous measurement of blood glucose and meal pattern in free-feeding rats: the role of glucose in meal initiation. *Brain research bulletin*, **14**, 605-616.

Cha,S.H., Wolfgang,M., Tokutake,Y., Chohnan,S., & Lane,M.D. (2008) Differential effects of central fructose and glucose on hypothalamic malonylûCoA and food intake. *Proceedings of the National Academy of Sciences*, **105**, 16871.

Chen,K., Yan,J., Suo,Y., Li,J., Wang,Q., & Lv,B. (2010) Nutritional status alters saccharin intake and sweet receptor mRNA expression in rat taste buds. *Brain research*, **1325**, 53-62.

Claret,M., Smith,M.A., Batterham,R.L., Selman,C., Choudhury,A.I., Fryer,L.G.D., Clements,M., Al Qassab,H., Heffron,H., & Xu,A.W. (2007) AMPK is essential for energy homeostasis regulation and glucose sensing by POMC and AgRP neurons. *Journal of Clinical Investigation*, **117**, 2325-2336.

Cone,R.D., Cowley,M.A., Butler,A.A., Fan,W., Marks,D.L., & Low,M.J. (2001) The arcuate nucleus as a conduit for diverse signals relevant to energy homeostasis. *International journal of obesity and related metabolic disorders: journal of the International Association for the Study of Obesity*, **25**, S63.

Cook,G.C. (1969) Absorption products of D (-) fructose in man. *Clinical science*, **37**, 675.

Cryer,P.E. (1997) *Hypoglycemia: pathophysiology, diagnosis, and treatment*, Oxford University Press, USA.

Cryer,P.E. (2009) *Hypoglycemia in Diabetes: Pathophysiology, Prevalence, and Prevention*, American Diabetes Association.

Cryer,P.E. (1993) Glucose counterregulation: prevention and correction of hypoglycemia in humans. *American Journal of Physiology- Endocrinology And Metabolism*, **264**, E149.

Daly,T.M. (2004) Overview of adeno-associated viral vectors. *Methods Mol Biol*, **246**, 157-165.

Davis,J.D., Wirtshafter,D., Asin,K.E., & Brief,D. (1981) Sustained intracerebroventricular infusion of brain fuels reduces body weight and food intake in rats. *Science*, **212**, 81.

De Jong,A., Strubbe,J.H., & Steffens,A.B. (1977) Hypothalamic influence on insulin and glucagon release in the rat. *American Journal of Physiology- Endocrinology And Metabolism*, **233**, E380.

De Lecea,L., Kilduff,T.S., Peyron,C., Gao,X.B., Foye,P.E., Danielson,P.E., Fukuhara,C., Battenberg,E.L.F., Gautvik,V.T., & Bartlett,F.S. (1998) The hypocretins: hypothalamus-specific peptides with neuroexcitatory activity. *Proceedings of the National Academy of Sciences of the United States of America*, **95**, 322.

de Vries,M.G., Lawson,M.A., & Beverly,J.L. (2005) Hypoglycemia-induced noradrenergic activation in the VMH is a result of decreased ambient glucose. *American Journal of Physiology- Regulatory, Integrative and Comparative Physiology*, **289**, R977.

Dhillon,H., Zigman,J.M., Ye,C., Lee,C.E., McGovern,R.A., Tang,V., Kenny,C.D., Christiansen,L.M., White,R.D., & Edelstein,E.A. (2006) Leptin directly activates SF1 neurons in the VMH, and this action by leptin is required for normal body-weight homeostasis. *Neuron*, **49**, 191-203.

Dias T, Mota-Filipe H, Liu B, Jones P, Houghton PJ, Paulo A. (2009). Recovery of oral glucose tolerance by wistar rats after treatment with *Coreopsis tinctoria* infusion. *Phytotherapy Research*,**24**, 699-705.

Drucker,D.J. (2007) The role of gut hormones in glucose homeostasis. *Journal of Clinical Investigation*, **117**, 24-32.

Duan,D., Sharma,P., Yang,J., Yue,Y., Dudus,L., Zhang,Y., Fisher,K.J., & Engelhardt,J.F. (1998) Circular intermediates of recombinant adeno-associated virus have defined structural characteristics responsible for long-term episomal persistence in muscle tissue. *Journal of Virology*, **72**, 8568.

Dunn-Meynell,A.A., Routh,V.H., Kang,L., Gaspers,L., & Levin,B.E. (2002) Glucokinase is the likely mediator of glucosensing in both glucose-excited and glucose-inhibited central neurons. *DIABETES-NEW YORK-*, **51**, 2056-2065.

Dunn-Meynell,A.A., Sanders,N.M., Compton,D., Becker,T.C., Eiki,J., Zhang,B.B., & Levin,B.E. (2009) Relationship among brain and blood glucose levels and spontaneous and glucoprivic feeding. *Journal of Neuroscience*, **29**, 7015.

Egawa,M., Yoshimatsu,H., & Bray,G.A. (1991) Neuropeptide Y suppresses sympathetic activity to interscapular brown adipose tissue in rats. *The American journal of physiology*, **260**, R328.

Elayat,A.A. (1995) An immunocytochemical and morphometric study of the rat pancreatic islets. *Journal of anatomy*, **186**, 629.

Evans,M.L., McCrimmon,R.J., Flanagan,D.E., Keshavarz,T., Fan,X., McNay,E.C., Jacob,R.J., & Sherwin,R.S. (2004) Hypothalamic ATP-sensitive K+ channels play a key role in sensing hypoglycemia and triggering counterregulatory epinephrine and glucagon responses. *Diabetes*, **53**, 2542.

Falb,M. & Muller,K. (2008) Metabolism of halophilic archaea. *Extremophiles*, **12**, 117-196

Ferrari,F.K., Samulski,T., Shenk,T., & Samulski,R.J. (1996) Second-strand synthesis is a rate-limiting step for efficient transduction by recombinant adeno-associated virus vectors. *Journal of Virology*, **70**, 3227.

Fioramonti,X.Contio, S, Song,Z., Routh, V. H., Lorsignol,A.,& Ponivsuf,L. (2007) Characterization of glucosensing neuron subpopulations in the Arcuate nucleus. *Diabetes*, **56**, 1219

Frangloudakis G, Gyte AC, Loxham SJG, Poucher SM. (2008). The intravenous glucose tolerance test in cannulated Wistar rats: A robust method for the *in vivo* assessment of glucose-stimulated insulin secetion.*Journal of Pharmacological and Toxicological Methods.* **57** 106-113.

Gardiner,J.V., Kong,W.M., Ward,H., Murphy,K.G., Dhillo,W.S., & Bloom,S.R. (2005) AAV mediated expression of anti-sense neuropeptide Y cRNA in the arcuate nucleus of rats results in decreased weight gain and food intake. *Biochemical and biophysical research communications*, **327**, 1088-1093.

Geary,N. (1990) Pancreatic glucagon signals postprandial satiety. *Neuroscience & Biobehavioral Reviews*, **14**, 323-338.

Geary,N. & Smith,G.P. (1983) Selective hepatic vagotomy blocks pancreatic glucagon's satiety effect. *Physiology & Behavior*, **31**, 391-394.

Geliebter,A., Westreich,S., & Gage,D. (1988) Gastric distention by balloon and test-meal intake in obese and lean subjects. *American Journal of Clinical Nutrition*, **48**, 592.

Gerich,J.E., Charles,M.A., & Grodsky,G.M. (1976) Regulation of pancreatic insulin and glucagon secretion. *Annual review of physiology*, **38**, 353.

Gordon,J.W., Scangos,G.A., Plotkin,D.J., Barbosa,J.A., & Ruddle,F.H. (1980) Genetic transformation of mouse embryos by microinjection of purified DNA. *Proceedings of the National Academy of Sciences of the United States of America*, **77**, 7380.

Grabauskas,G., Song,I., Zhou,S.Y., & Owyang,C. (2010) Electrophysiological identification of glucose-sensing neurons in rat nodose ganglia. *The Journal of Physiology*, **588**, 617-632.

Grimsby,J., Sarabu,R., Corbett,W.L., Haynes,N.E., Bizzarro,F.T., Coffey,J.W., Guertin,K.R., Hilliard,D.W., Kester,R.F., & Mahaney,P.E. (2003) Allosteric activators of glucokinase: potential role in diabetes therapy. *Science*, **301**, 370.

Grupe,A., Hultgren,B., Ryan,A., Ma,Y.H., Bauer,M., & Stewart,T.A. (1995) Transgenic knockouts reveal a critical requirement for pancreatic beta cell glucokinase in maintaining glucose homeostasis. *Cell*, **83**, 69-78.

Gutzwiller,J.P., Guke, B., Drewe,J., Hildebrand,P., Ketterer,S., Handschin,D., Winterhalder,R., Conen,D., & Beglinger,C. (1999) Glucagon-like peptide-1: a potent regulator of food intake in humans. *Gut* **44**, 81.

Haffner,S.M. & Miettinen,H. (1997) Insulin resistance implications for type II diabetes mellitus and coronary heart disease. *The American journal of medicine*, **103**, 152-162.

Hahn,H.J., Bierwolf,B., Blech,W., Weiss,I., Besch,W., Wulfert,P., Hartmann,K., & Voss,C. (1981) Enhanced insulin secretion in vitro as a consequence of ventromedial hypothalamic lesions in the rat. *Upsala Journal of Medical Sciences*, **86**, 197-205.

Hardie,D.G., Carling,D., & Carlson,M. (1998) The AMP-activated/SNF1 protein kinase subfamily: metabolic sensors of the eukaryotic cell? *Annual Review of Biochemistry*, **67**, 821-855.

Hauner,H., Glatting,G., Kaminska,D., & Pfeiffer,E.F. (1988) Effects of gastric inhibitory polypeptide on glucose and lipid metabolism of isolated rat adipocytes. *Annals of Nutrition and Metabolism*, **32**, 282-288.

Havrankova,J., Roth,J., & Brownstein,M. (1978) Insulin receptors are widely distributed in the central nervous system of the rat. *Nature*

Hayashi,T., Boyko,E.J., Leonetti,D.L., McNeely,M.J., Newell-Morris,L., Kahn,S.E., & Fujimoto,W.Y. (2003) Visceral adiposity and the risk of impaired glucose tolerance. *Diabetes Care*, **26**, 650.

He,B., White,B.D., Edwards,G.L., & Martin,R.J. (1998) Neuropeptide Y antibody attenuates 2-deoxy--glucose induced feeding in rats. *Brain research*, **781**, 348-350.

Henquin,J.C. (2000) Triggering and amplifying pathways of regulation of insulin secretion by glucose. *Diabetes*, **49**, 1751.

Horvath,T.L., Diano,S., & van den Pol,A.N. (1999) Synaptic interaction between hypocretin (orexin) and neuropeptide Y cells in the rodent and primate hypothalamus: a novel circuit implicated in metabolic and endocrine regulations. *Journal of Neuroscience*, **19**, 1072.

Hunt,L.M., Browner,C.H., & Jordan,B. (1990) Hypoglycemia: Portrait of an illness construct in everyday use. *Medical Anthropology Quarterly*, **4**, 191-210.

Hustvedt,B.E. & Lovo,A. (1972) Correlation between hyperinsulinemia and hyperphagia in rats with ventromedial hypothalamic lesions. *Acta Physiologica Scandinavica*, **84**, 29-33.

Ibrahim,N., Bosch,M.A., Smart,J.L., Qiu,J., Rubinstein,M., Ronnekleiv,O.K., Low,M.J., & Kelly,M.J. (2003) Hypothalamic proopiomelanocortin neurons are glucose responsive and express KATP channels. *Endocrinology*, **144**, 1331.

Im,D.S. & Muzyczka,N. (1990) The AAV origin binding protein Rep68 is an ATP-dependent site-specific endonuclease with DNA helicase activity. *Cell*, **61**, 447-457.

Inoue,S., Nagase,H., Satom,S., Saito,M., Egawa,M., Tanaka,K., & Takamura,Y. (1991) Role of the efferent and afferent vagus nerve in the development of ventromedial hypothalamic (VMH) obesity. *Brain research bulletin*, **27**, 511-515.

Ishihara,H., Maechler,P., Gjinovci,A., Herrera,P.L., & Wollheim,C.B. (2003) Islet -cell secretion determines glucagon release from neighbouring -cells. *Nature Cell Biology*, **5**, 330-335.

Iynedjian,P.B. (2009) Molecular physiology of mammalian glucokinase. *Cellular and Molecular Life Sciences*, **66**, 27-42.

Iynedjian,P.B., Mubius,G., Seitz,H.J., Wollheim,C.B., & Renold,A.E. (1986) Tissue-specific expression of glucokinase: identification of the gene product in liver and pancreatic islets. *Proceedings of the National Academy of Sciences*,**83**, 1998

Iynedjian,P.B. (1993) Mammalian glucokinase and its gene. *Biochemical Journal*, **293**, 1.

Iynedjian,P.B., Gjinovci,A., & Renold,A.E. (1988) Stimulation by insulin of glucokinase gene transcription in liver of diabetic rats. *Journal of Biological Chemistry*, **263**, 740.

Jacobs,H.L. (1958) Studies on sugar preference: I. The preference for glucose solutions and its modification by injections of insulin. *Journal of Comparative and Physiological Psychology*, **51**, 304-310.

Jay,F.T., Laughlin,C.A., & Carter,B.J. (1981) Eukaryotic translational control: adeno-associated virus protein synthesis is affected by a mutation in the adenovirus DNA-binding protein. *Proceedings of the National Academy of Sciences of the United States of America*, **78**, 2927.

Kanarek,R.B. & Orthen-Gambill,N. (1982) Differential effects of sucrose, fructose and glucose on carbohydrate-induced obesity in rats. *Journal of Nutrition*, **112**, 1546.

Kang,L., Dunn-Meynell,A.A., Routh,V.H., Gaspers,L.D., Nagata,Y., Nishimura,T., Eiki,J., Zhang,B.B., & Levin,B.E. (2006) Glucokinase is a critical regulator of ventromedial hypothalamic neuronal glucosensing. *Diabetes*, **55**, 412.

Kang,L., Routh,V.H., Kuzhikandathil,E.V., Gaspers,L.D., & Levin,B.E. (2004) Physiological and molecular characteristics of rat hypothalamic ventromedial nucleus glucosensing neurons. *Diabetes*, **53**, 549.

Kang,L., Sanders,N.M., Dunn-Meynell,A.A., Gaspers,L.D., Routh,V.H., Thomas,A.P., & Levin,B.E. (2008) Prior hypoglycemia enhances glucose responsiveness in some ventromedial hypothalamic glucosensing neurons. *American Journal of Physiology- Regulatory, Integrative and Comparative Physiology*, **294**, R784.

Kaplan,J.M., Armentano,D., Sparer,T.E., Wynn,S.G., Peterson,P.A., Wadsworth,S.C., Couture,K.K., Pennington,S.E., George,J.A., & Gooding,L.R. (1997) Characterization of factors involved in modulating persistence of transgene expression from recombinant adenovirus in the mouse lung. *Human gene therapy*, **8**, 45-56.

Kim,E.M., Grace,M.K., Welch,C.C., Billington,C.J., & Levine,A.S. (1999) STZ-induced diabetes decreases and insulin normalizes POMC mRNA in arcuate nucleus and pituitary in rats. *American Journal of Physiology- Regulatory, Integrative and Comparative Physiology*, **276**, 1320.

Klip, A. & Paquet, M. (1990) Glucose transport and glucose transporters in the muscle and their metabolic regulation. *Diabetes Care, **13**, 228-243*

Kurata,K., Fujimoto,K., Sakata,T., Etou,H., & Fukagawa,K. (1986) D-glucose suppression of eating after intra-third ventricle infusion in rat. *Physiology & Behavior*, **37**, 615-620.

Kyostio,S.R., Owens,R.A., Weitzman,M.D., Antoni,B.A., Chejanovsky,N., & Carter,B.J. (1994) Analysis of adeno-associated virus (AAV) wild-type and mutant Rep proteins for their abilities to negatively regulate AAV p5 and p19 mRNA levels. *Journal of Virology*, **68**, 2947.

Lam,T.K.T., Gutierrez-Juarez,R., Pocai,A., Bhanot,S., Tso,P., Schwartz,G.J., & Rossetti,L. (2007) Brain glucose metabolism controls the hepatic secretion of triglyceride-rich lipoproteins. *Nature medicine*, **13**, 171-180.

Lam,T.K.T., Gutierrez-Juarez,R., Pocai,A., & Rossetti,L. (2005a) Regulation of blood glucose by hypothalamic pyruvate metabolism. *Science*, **309**, 943.

Lam,T.K.T., Schwartz,G.J., & Rossetti,L. (2005b) Hypothalamic sensing of fatty acids. *Nature neuroscience*, **8**, 579-584.

Lee,B.M. & Wolever,T.M. (1998) Effect of glucose, sucrose and fructose on plasma glucose and insulin responses in normal humans: comparison with white bread. *European journal of clinical nutrition*, **52**, 924.

Leloup,C., Arluison,M., Lepetit,N., Cartier,N., Marfaing-Jallat,P., Ferro,P., & Ponicaud,L. (1994) Glucose transporter 2 (GLUT 2): expression in specific brain nuclei. *Brain research*, **638**, 221-226.

Lenin Kamatchi,G., Veeraragavan,K., Chandra,D., & Bapna,J.S. (1986) Antagonism of acute feeding response to 2-deoxyglucose and 5-thioglucose by GABA antagonists: the relative role of ventromedial and lateral hypothalamus. *Pharmacology Biochemistry and Behavior*, **25**, 59-62.

Levin,B.E., Becker,T.C., Eiki,J., Zhang,B.B., & Dunn-Meynell,A.A. (2008) Ventromedial hypothalamic glucokinase is an important mediator of the counterregulatory response to insulin-induced hypoglycemia. *Diabetes*, **57**, 1371.

Levin,B.E., Dunn-Meynell,A.A., & Routh,V.H. (1999) Brain glucose sensing and body energy homeostasis: role in obesity and diabetes. *American Journal of Physiology- Regulatory, Integrative and Comparative Physiology*, **276**, 1223.

Levin,B.E., Routh,V.H., Kang,L., Sanders,N.M., & Dunn-Meynell,A.A. (2004) Neuronal glucosensing: what do we know after 50 years? *Diabetes*, **53**, 2521.

Liu,F., Dong,Q., Myers,A.M., & Fromm,H.J. (1991) Expression of human brain hexokinase in: Purification and characterization of the expressed enzyme* 1. *Biochemical and biophysical research communications*, **177**, 305-311.

Loftus,T.M., Jaworsky,D.E., Frehywot,G.L., Townsend,C.A., Ronnett,G.V., Lane,M.D., & Kuhajda,F.P. (2000) Reduced food intake and body weight in mice treated with fatty acid synthase inhibitors. *Science*, **288**, 2379.

Lu,M., Wheeler,M.B., Leng,X.H., & Boyd,A.E. (1993) The role of the free cytosolic calcium level in beta-cell signal transduction by gastric inhibitory polypeptide and glucagon-like peptide I (7-37). *Endocrinology*, **132**, 94.

Luquet,S., Perez,F.A., Hnasko,T.S., & Palmiter,R.D. (2005) NPY/AgRP neurons are essential for feeding in adult mice but can be ablated in neonates. *Science*, **310**, 683.

Lusby,E., Fife,K.H., & Berns,K.I. (1980) Nucleotide sequence of the inverted terminal repetition in adeno-associated virus DNA. *Journal of Virology*, **34**, 402.

Lynch,R.M., Tompkins,L.S., Brooks,H.L., Dunn-Meynell,A.A., & Levin,B.E. (2000) Localization of glucokinase gene expression in the rat brain. *Diabetes*, **49**, 693.

Ma,X., Zubcevic,L., & Ashcroft,F.M. (2008) Glucose regulates the effects of leptin on hypothalamic POMC neurons. *Proceedings of the National Academy of Sciences*, **105**, 9811.

Magee,M.F. & Bhatt,B.A. (2001) Management of Decompensated Diabetes:: Diabetic Ketoacidosis and Hyperglycemic Hyperosmolar Syndrome. *Critical care clinics*, **17**, 75-106.

Mandel,R.J., Rendahl,K.G., Spratt,S.K., Snyder,R.O., Cohen,L.K., & Leff,S.E. (1998) Characterization of intrastriatal recombinant adeno-associated virus-mediated gene transfer of human tyrosine hydroxylase and human GTP-cyclohydrolase I in a rat model of Parkinson's disease. *Journal of Neuroscience*, **18**, 4271.

Martin,T.L., Alquier,T., Asakura,K., Furukawa,N., Preitner,F., & Kahn,B.B. (2006) Diet-induced obesity alters AMP kinase activity in hypothalamus and skeletal muscle. *Journal of Biological Chemistry*, **281**, 18933.

Matschinsky,F., Liang,Y., Kesavan,P., Wang,L., Froguel,P., Velho,G., Cohen,D., Permutt,M.A., Tanizawa,Y., & Jetton,T.L. (1993) Glucokinase as pancreatic beta cell glucose sensor and diabetes gene. *Journal of Clinical Investigation*, **92**, 2092.

Matschinsky,F.M. (1990) Glucokinase as glucose sensor and metabolic signal generator in pancreatic beta-cells and hepatocytes. *Diabetes*, **39**, 647.

Mayer,C.H., Fink,H., Rex,A., & Voigt,J.P. (2006) Changes in extracellular hypothalamic glucose in relation to feeding. *European Journal of Neuroscience*, **24**, 1695-1701.

Mayer,J. (1953) Glucostatic mechanism of regulation of food intake. *New England Journal of Medicine*, **249**, 13-16.

Mayer,J. (1955) Regulation of energy intake and the body weight: the glucostatic theory and the lipostatic hypothesis. *Annals of the New York Academy of sciences*, **63**, 15-43.

Mayer,J. (1952) The glucostatic theory of regulation of food intake and the problem of obesity. *Bull.New Engl.Med.Cent.*, **14**, 43-49.

McAulay,V., Deary,I.J., & Frier,B.M. (2001) Symptoms of hypoglycaemia in people with diabetes. *Diabetic Medicine*, **18**, 690-705.

McCrimmon,R. (2008) The mechanisms that underlie glucose sensing during hypoglycaemia in diabetes. *Diabetic Medicine*, **25**, 513-522.

Meglasson,M.D. & Matschinsky,F.M. (1984) New perspectives on pancreatic islet glucokinase. *American Journal of Physiology- Endocrinology And Metabolism*, **246**, E1.

Melanson,K.J., Westerterp-Plantenga,M.S., Saris,W.H.M., Smith,F.J., & Campfield,L.A. (1999) Blood glucose patterns and appetite in time-blinded humans: carbohydrate versus fat. *American Journal of Physiology- Regulatory, Integrative and Comparative Physiology*, **277**, 337.

Miller,C.C., Martin,R.J., Whitney,M.L., & Edwards,G.L. (2002) Intracerebroventricular injection of fructose stimulates feeding in rats. *Nutritional Neuroscience*, **5**, 359-362.

Miller,D.G., Adam,M.A., & Miller,A.D. (1990) Gene transfer by retrovirus vectors occurs only in cells that are actively replicating at the time of infection. *Molecular and cellular biology*, **10**, 4239.

Minokoshi,Y., Alquier,T., Furukawa,N., Kim,Y.B., Lee,A., Xue,B., Mu,J., Foufelle,F., Ferri,P., & Birnbaum,M.J. (2004) AMP-kinase regulates food intake by responding to hormonal and nutrient signals in the hypothalamus. *Nature*, **428**, 569-574.

Miwa,I., Mita,Y., Murata,T., Okuda,J., Sugiura,M., Hamada,Y., & Chiba,T. (1995) UTILITY OF 3-O-METHYL-N-ACETYL-D-GLUCOSAMINE, AN N-

ACETYLGLUCOSAMINE KINASE INHIBITOR, FOR ACCURATE ASSAY OF GLUCOKINASE IN PANCREATIC ISLETS AND LIVE R. *Enzyme & protein*, **48**, 135-142.

Miyoshi,H., Takahashi,M., Gage,F.H., & Verma,I.M. (1997) Stable and efficient gene transfer into the retina using an HIV-based lentiviral vector. *Proceedings of the National Academy of Sciences of the United States of America*, **94**, 10319.

Mokan,M., Mitrakou,A., Veneman,T., Ryan,C., Korytkowski,M., Cryer,P., & Gerich,J. (1994) Hypoglycemia unawareness in IDDM. *Diabetes Care*, **17**, 1397.

Mountjoy,P.D. & Rutter,G.A. (2007) Glucose sensing by hypothalamic neurones and pancreatic islet cells: AMPle evidence for common mechanisms? *Experimental Physiology*, **92**, 311.

Muroya,S., Yada,T., Shioda,S., & Takigawa,M. (1999) Glucose-sensitive neurons in the rat arcuate nucleus contain neuropeptide Y. *Neuroscience letters*, **264**, 113-116.

Naldini,L., Blomer,U., Gallay,P., Ory,D., Mulligan,R., Gage,F.H., Verma,I.M., & Trono,D. (1996) In vivo gene delivery and stable transduction of nondividing cells by a lentiviral vector. *Science*, **272**, 263.

Nelson,G., Hoon,M.A., Chandrashekar,J., Zhang,Y., Ryba,N.J.P., & Zuker,C.S. (2001) Mammalian sweet taste receptors. *Cell*, **106**, 381-390.

Niemann,H. & Kues,W.A. (2003) Application of transgenesis in livestock for agriculture and biomedicine. *Animal reproduction science*, **79**, 291-317.

Nilsson,G. & Uvnas Wallensten,K. (1977) Effect of teasing and sham feeding on plasma glucagon concentration in dogs. *Acta Physiologica Scandinavica*, **100**, 298-302.

Nishimura,H., Pallardo,F.V., Seidner,G.A., Vannucci,S., Simpson,I.A., & Birnbaum,M.J. (1993) Kinetics of GLUT1 and GLUT4 glucose transporters expressed in Xenopus oocytes. *Journal of Biological Chemistry*, **268**, 8514.

Nishiyama,Y. (2004) Herpes simplex virus gene products: the accessories reflect her lifestyle well. *Reviews in medical virology*, **14**, 33-46.

Nishizawa,M., Moore,M.C., Shiota,M., Gustavson,S.M., Snead,W.L., Neal,D.W., & Cherrington,A.D. (2003) Effect of intraportal glucagon-like peptide-1 on glucose metabolism in conscious dogs. *American Journal of Physiology-Endocrinology And Metabolism*, **284**, E1027.

Obici,S., Zhang,B.B., Karkanias,G., & Rossetti,L. (2002) Hypothalamic insulin signaling is required for inhibition of glucose production. *Nature medicine*, **8**, 1376-1382.

Oomura,Y., Kimura,K., Ooyama,H., Maeno,T., Iki,M., & Kuniyoshi,M. (1964) Reciprocal activities of the ventromedial and lateral hypothalamic areas of cats. *Science*, **143**, 484-485.

Panksepp,J. & Rossi III,J. (1981) d-Glucose infusions into the basal ventromedial hypothalamus and feeding. *Behavioural Brain Research*, **3**, 381-392.

Park,K., Kim,W.J., Cho,Y.H., Lee,Y.I., Lee,H., Jeong,S., Cho,E.S., Chang,S.I., Moon,S.K., & Kang,B.S. (2008) Cancer gene therapy using adeno-associated virus vectors. *Frontiers in bioscience: a journal and virtual library*, **13**, 2653.

Parker,H.E., Habib,A.M., Rogers,G.J., Gribble,F.M., & Reimann,F. (2009) Nutrient-dependent secretion of glucose-dependent insulinotropic polypeptide from primary murine K cells. *Diabetologia*, **52**, 289-298.

Parton,L.E., Ye,C.P., Coppari,R., Enriori,P.J., Choi,B., Zhang,C.Y., Xu,C., Vianna,C.R., Balthasar,N., & Lee,C.E. (2007) Glucose sensing by POMC neurons regulates glucose homeostasis and is impaired in obesity. *Nature*, **449**, 228-232.

Paxinos,G. & Watson C (2007) *The Rat Brain in Stereotaxic Coordinates*, Sixth edn, Academic Press, London.

Pellerin,L., Pellegri,G., Bittar,P.G., Charnay,Y., Bouras,C., Martin,J.L., Stella,N., & Magistretti,P.J. (2000) Evidence supporting the existence of an activity-dependent astrocyte-neuron lactate shuttle. *Developmental neuroscience*, **20**, 291-299.

Penicaud,L., Leloup,C., Fioramonti,X., Lorsignol,A., & Benani,A. (2006) Brain glucose sensing: a subtle mechanism. *Current Opinion in Clinical Nutrition & Metabolic Care*, **9**, 458.

Postic,C., Shiota,M., & Magnuson,M.A. (2001) Cell-specific roles of glucokinase in glucose homeostasis. *Recent Progress in Hormone Research*, **56**, 195.

Pyke,D.A. (1979) Diabetes: the genetic connections. *Diabetologia*, **17**, 333-343.

Qian,S., Chen,H., Weingarth,D., Trumbauer,M.E., Novi,D.E., Guan,X., Yu,H., Shen,Z., Feng,Y., & Frazier,E. (2002) Neither agouti-related protein nor neuropeptide Y is critically required for the regulation of energy homeostasis in mice. *Molecular and cellular biology*, **22**, 5027.

Qing,K., Mah,C., Hansen,J., Zhou,S., Dwarki,V., & Srivastava,A. (1999) Human fibroblast growth factor receptor 1 is a co-receptor for infection by adeno-associated virus 2. *Nature medicine*, **5**, 71-77.

Qiu,J. & Brown,K.E. (1999) Integrin [alpha] V [beta] 5 Is Not Involved in Adeno-Associated Virus Type 2 (AAV2) Infection. *Virology*, **264**, 436-440.

Reimann,F., Habib,A.M., Tolhurst,G., Parker,H.E., Rogers,G.J., & Gribble,F.M. (2008) Glucose sensing in L cells: a primary cell study. *Cell metabolism*, **8**, 532-539.

Ren,X., Zhou,L., Terwilliger,R., Newton,S.S., & De Araujo,I.E. (2009) Sweet taste signaling functions as a hypothalamic glucose sensor. *Frontiers in Integrative Neuroscience*, **3**.

Rodin,J., Reed,D., & Jamner,L. (1988) Metabolic effects of fructose and glucose: implications for food intake. *American Journal of Clinical Nutrition*, **47**, 683.

Rodin,J., Wack,J., Ferrannini,E., & DeFronzo,R.A. (1985) Effect of insulin and glucose on feeding behavior. *Metabolism*, **34**, 826-831.

Roncero,I., Alvarez,E., Vβzquez,P., & Blozquez,E. (2000) Functional glucokinase isoforms are expressed in rat brain. *Journal of neurochemistry*, **74**, 1848-1857.

Rose,J.A., Maizel Jr,J.V., Inman,J.K., & Shatkin,A.J. (1971) Structural proteins of adenovirus-associated viruses. *Journal of Virology*, **8**, 766.

Rosenbloom,A.L. & Hanas,R. (1996) Diabetic ketoacidosis (DKA): treatment guidelines. *Clinical pediatrics*, **35**, 261.

Rothwell,N.J., Saville,M.E., & Stock,M.J. (1984) Brown fat activity in fasted and refed rats. *Bioscience Reports*, **4**, 351-357.

Russek,M. (1970) Demonstration of the influence of an hepatic glucosensitive mechanism on food-intake. *Physiology & Behavior*, **5**, 1207-1209.

Sacchi,T. & Bani,D. (1985) New views on the identification of the various cell types in the pancreatic islets of the rat. *Cells Tissues Organs*, **122**, 1-17.

Sambrook,J., Fritsch,E.F., & Maniatis,T. (1989) Molecular Cloning: A Laboratory Manual Cold Spring Harbor Laboratory Press. *New York*, **5**.

Samulski,R.J., Chang,L.S., & Shenk,T. (1989) Helper-free stocks of recombinant adeno-associated viruses: normal integration does not require viral gene expression. *Journal of Virology*, **63**, 3822.

Sanders,N.M., Dunn-Meynell,A.A., & Levin,B.E. (2004) Third ventricular alloxan reversibly impairs glucose counterregulatory responses. *Diabetes*, **53**, 1230.

Sanders,N.M., Figlewicz,D.P., & Taborsky,G.J. (2006) Feeding and neuroendocrine responses after recurrent insulin-induced hypoglycemia. *Physiology & Behavior*, **87**, 700-706.

Schultz-Klarr,S., Wright-Richey,J., & Dunbar,J.C. (1994) Plasma glucose, insulin and cardiovascular responses after intravenous intracerebroventricular injections of insulin, 2-deoxyglucose and glucose in rats. *Diabetes research and clinical practice*, **26**, 81-89.

Schwartz,M.W., Woods,S.C., Porte,D., Seeley,R.J., & Baskin,D.G. (2000) Central nervous system control of food intake. *Nature*, **404**, 661-671.

Seaquist,E.R., Damberg,G.S., Tkac,I., & Gruetter,R. (2001) The effect of insulin on in vivo cerebral glucose concentrations and rates of glucose transport/metabolism in humans. *Diabetes*, **50**, 2203.

Sergeyev,V., Broberger,C., Gorbatyuk,O., & H÷kfelt,T. (2000) Effect of 2-mercaptoacetate and 2-deoxy-D-glucose administration on the expression of

NPY, AGRP, POMC, MCH and hypocretin/orexin in the rat hypothalamus. *Neuroreport*, **11**, 117.

Shafer,R.B., Levine,A.S., Marlette,J.M., & Morley,J.E. (1987) Effects of xylitol on gastric emptying and food intake. *American Journal of Clinical Nutrition*, **45**, 744.

Shinohara,Y., Ichihara,J., & Terada,H. (1991) Remarkably enhanced expression of the type II hexokinase in rat hepatoma cell line AH130. *FEBS letters*, **291**, 55-57.

Siegel,E.G. & Creutzfeldt,W. (1985) Stimulation of insulin release in isolated rat islets by GIP in physiological concentrations and its relation to islet cyclic AMP content. *Diabetologia*, **28**, 857-861.

Simpson,I.A., Dwyer,D., Malide,D., Moley,K.H., Travis,A., & Vannucci,S.J. (2008) The facilitative glucose transporter GLUT3: 20 years of distinction. *American Journal of Physiology- Endocrinology And Metabolism*, **295**, E242.

Sindelar,D.K., Marie,L.K., Miura,G., Palmiter,R.D., & Schwartz,M.W. (2004) Neuropeptide Y is required for hyperphagic feeding in response to neuroglucopenia. *Endocrinology*, **145**, 3363.

Skrivarhaug,T., Bangstad,H.J., Stene,L.C., Sandvik,L., Hanssen,K.F., & Joner,G. (2006) Long-term mortality in a nationwide cohort of childhood-onset type 1 diabetic patients in Norway. *Diabetologia*, **49**, 298-305.

Smith,G.P. & Epstein,A.N. (1969) Increased feeding in response to decreased glucose utilization in the rat and monkey. *American Journal of Physiology*, **217**, 1083.

Smith,S.L. & Sauder,C. (1969) Food cravings, depression, and premenstrual problems. *Psychosomatic medicine*, **31**, 281.

Snyder,B.R., Boulis,N.M., & Federici,T. (2010) Viral vector-mediated gene transfer for CNS disease. *Expert Opinion on Biological Therapy*, **10**, 381-394.

Srivastava,A., Lusby,E.W., & Berns,K.I. (1983) Nucleotide sequence and organization of the adeno-associated virus 2 genome. *Journal of Virology*, **45**, 555.

Steffens,A.B. (1976) Influence of the oral cavity on insulin release in the rat. *American Journal of Physiology*, **230**, 1411.

Stempel,F. & Jungermann,K. (1997) Sensing by intrahepatic muscarinic nerves of a portal-arterial glucose concentration gradient as a signal for insulin-dependent glucose uptake in the perfused rat liver. *FEBS letters*, **406**, 119-122.

Stolarczyk,E., Guissard,C., Michau,A., Even,P.C., Grosfeld,A., Serradas,P., Lorsignol,A., Penicaud,L., Brot-Laroche,E., & Leturque,A. (2010) Detection of extracellular glucose by GLUT2 contributes to hypothalamic control of food intake. *American Journal of Physiology- Endocrinology And Metabolism*, **298**, E1078.

Summerford,C., Bartlett,J.S., & Samulski,R.J. (1999) V 5 integrin: a co-receptor for adeno-associated virus type 2 infection. *Nature medicine*, **5**, 78-82.

Summerford,C. & Samulski,R.J. (1998) Membrane-associated heparan sulfate proteoglycan is a receptor for adeno-associated virus type 2 virions. *Journal of Virology*, **72**, 1438.

Surwit,R.S., Kuhn,C.M., Cochrane,C., McCubbin,J.A., & Feinglos,M.N. (1988) Diet-induced type II diabetes in C57BL/6J mice. *Diabetes*, **37**, 1163.

Szabo,A.J., Iguchi,A., Burleson,P.D., & Szabo,O. (1983) Vagotomy or atropine blocks hypoglycemic effect of insulin injected into ventromedial hypothalamic nucleus. *American Journal of Physiology- Endocrinology And Metabolism*, **244**, E467.

Tang-Christensen,M., Larsen,P.J., Goke,R., Fink-Jensen,A., Jessop,D.S., Moller,M., & Sheikh,S.P. (1996) Central administration of GLP-1-(7-36) amide inhibits food and water intake in rats. *American Journal of Physiology- Regulatory, Integrative and Comparative Physiology*, **271**, 848.

Teff,K.L. & Engelman,K. (1996) Oral sensory stimulation improves glucose tolerance in humans: effects on insulin, C-peptide, and glucagon. *American Journal of Physiology- Regulatory, Integrative and Comparative Physiology*, **270**, 1371.

Temin,H.M. & Baltimore,D. (1972) RNA-directed DNA synthesis and RNA tumor viruses. *Adv Virus Res*, **17**, 129-186.

Thorens,B. (1992) Molecular and Cellular Physiology of GLUT-2, a High-Jfm Facilitated Diffusion Glucose Transporter. *Molecular Biology of Receptors and Transporters: Bacterial and glucose transporters*, **137**, 209.

Tkacs,N.C., Dunn-Meynell,A.A., & Levin,B.E. (2000) Presumed Apoptosis and Reduced Arcuate Nucleus Neuropeptide Y and Pro-Opiomelanocortin mRNA in Non-Coma Hypoglycemia. *Diabetes*, **49**, 821.

Tordoff,M.G., Tluczek,J.P., & Friedman,M.I. (1989) Effect of hepatic portal glucose concentration on food intake and metabolism. *American Journal of Physiology-Regulatory, Integrative and Comparative Physiology*, **257**, 1474.

Tsujii,S. & Bray,G.A. (1990) Effects of glucose, 2-deoxyglucose, phlorizin, and insulin on food intake of lean and fatty rats. *American Journal of Physiology-Endocrinology And Metabolism*, **258**, E476.

UK Prospective Diabetes Study (UKPDS) Group (1998) Intensive blood-glucose control with sulphonylureas or insulin compared with conventional treatment and risk of complications in patients with type 2 diabetes (UKPDS 33). *Lancet*, **352**, 837-853.

Vannucci,S.J., Koehler-Stec,E.M., Li,K., Reynolds,T.H., Clark,R., & Simpson,I.A. (1998) GLUT4 glucose transporter expression in rodent brain: effect of diabetes. *Brain research*, **797**, 1-11.

Wang,P.Y.T., Caspi,L., Lam,C.K.L., Chari,M., Li,X., Light,P.E., Gutierrez-Juarez,R., Ang,M., Schwartz,G.J., & Lam,T.K.T. (2008) Upper intestinal lipids trigger a gut-brain-liver axis to regulate glucose production. *NATURE-LONDON-*, **452**, 1012.

Wang,R., Cruciani-Guglielmacci,C., Migrenne,S., Magnan,C., Cotero,V.E., & Routh,V.H. (2006) Effects of oleic acid on distinct populations of neurons in the hypothalamic arcuate nucleus are dependent on extracellular glucose levels. *Journal of neurophysiology*, **95**, 1491.

Wang,R., Liu,X., Hentges,S.T., Dunn-Meynell,A.A., Levin,B.E., Wang,W., & Routh,V.H. (2004) The regulation of glucose-excited neurons in the hypothalamic arcuate nucleus by glucose and feeding-relevant peptides. *Diabetes*, **53**, 1959.

Weatherford,S.C. & Ritter,S. (1988) Lesion of vagal afferent terminals impairs glucagon-induced suppression of food intake. *Physiology & Behavior*, **43**, 645-650.

Weitzman,M.D., Kyistii,S.R., Kotin,R.M., & Owens,R.A. (1994) Adeno-associated virus (AAV) Rep proteins mediate complex formation between AAV DNA and its integration site in human DNA. *Proceedings of the National Academy of Sciences of the United States of America*, **91**, 5808.

Wells,D.J. (2004) Gene therapy progress and prospects: electroporation and other physical methods. *Gene therapy*, **11**, 1363-1369.

Wilson,J.E. & Chung,V. (1989) Rat brain hexokinase: Further studies on the specificity of the hexose and hexose 6-phosphate binding sites* 1. *Archives of biochemistry and biophysics*, **269**, 517-525.

Wolfe,D., Mata,M., & Fink,D.J. (2009) A human trial of HSV-mediated gene transfer for the treatment of chronic pain. *Gene therapy*, **16**, 455-460.

Wong,G.T., Gannon,K.S., & Margolskee,R.F. (1996) Transduction of bitter and sweet taste by gustducin.

Xu G, Stoffers DA, Hanemer JF, Bonner-Weir S. (1999). Exendin-4 Stimulates both beta-cell reblication and neogenesis, resulting in increased beta-cell mass and improved glucose tolerance in diabetic rats. *Diabetes*, **48**, 2270-2276.

Yang,X., Mastaitis,J., Mizuno,T., & Mobbs,C.V. (2007) Glucokinase regulates reproductive function, glucocorticoid secretion, food intake, and hypothalamic gene expression. *Endocrinology*, **148**, 1928.

Zaiss,A.K. & Muruve,D.A. (2005) Immune responses to adeno-associated virus vectors. *Current gene therapy*, **5**, 323-331.

Zarjevski,N., Cusin,I., Vettor,R., Rohner-Jeanrenaud,F., & Jeanrenaud,B. (1993) Chronic intracerebroventricular neuropeptide-Y administration to normal rats mimics hormonal and metabolic changes of obesity. *Endocrinology*, **133**, 1753.

Zelent,D., Golson,M.L., Koeberlein,B., Quintens,R., Van Lommel,L., Buettger,C., Weik-Collins,H., Taub,R., Grimsby,J., & Schuit,F. (2006) A glucose sensor role for glucokinase in anterior pituitary cells. *Diabetes*, **55**, 1923.

Zhang,J., Li,C., Chen,K., Zhu,W., Shen,X., & Jiang,H. (2006) Conformational transition pathway in the allosteric process of human glucokinase. *Proceedings of the National Academy of Sciences*, **103**, 13368.

1. Appendix I – Solutions

aCSF (K+ = 5.9mM)

$NaHCO_3$	20mM
NaCl	126mM
Na_2HPO_4	0.9mM
KCL	5.9mM
$CaCl_2$	1mM
$MgSO_4$	0.09mM
Glucose	5mM
Trasylol	10ml/L
Ascorbic Acid	176mg/L
Distilled H_2O	540ml/L

3M Alcoholic KOH solution:

Add 39g KOH pastels to 200 ml 65% ethanol

5M ammonium acetate

Dissolve 385g CH3.COONH4 in 600ml autoclaved distilled water, then make up to 1l.

2M Calcium chloride:

10.8g $CaCl_2.6H_2O$ was dissolved in 20ml GDW and sterilise by filtration through 0.22µm filter and store in 1ml aliquots at -20˚C

Caesium chloride-saturated propan-2-ol:

Mix 100g $CsCl_2$, 100ml GDW and 100ml propan-2-ol and leave to settle.

0.5M ethylenediaminetetra-acetic acid (EDTA):

In 800ml autoclaved water dissolve 186.1g $C_{10}H_{14}H_2O_8Na_2.2H_2O$ and adjust to pH 8.0 with 1M NaOH. Make up to 1L with water

Gel loading buffer:

Mix 3.125ml 80% glycerol, 50µl 0.5M EDTA, and 10mg orange G in 6.075ml of autoclaved distilled water.

Glucokinase extraction buffer:

Dissolve 0.508g $MgCl_2$, 0.913g Sodium ethylenediamine tetraacetate, 5.591g KCl and 0.35ml 2-mercaptoethanol in 500ml GDW. Use 1M KOH to alter the pH of the solution to 7.3.

Gly- Gly:

Dissolve 6.6g Gly –gly in 500ml. Use 5M KOH to alter pH to 8.

GTE

Mix 2.5ml 1M Tris-HCl, pH 8.0, 2ml 0.5M $C_{10}H_{14}H_2O_8Na_2.2H_2O$ and 5ml 18% glucose and top up to 100ml. Sterilise by passing through a 0.2µm filter.

HEPES-buffered saline (HBS)

280mM NaCl, 10mM KCl, 1.5mM Na_2HPO_4, 12mM dextrose, 50mM HEPES (Sigma) pH7.07. Sterilise by filtration through 0.22µm filter and store in 5ml aliquots at -20˚C

Hybridisation buffer

Dissolve 0.5g dried milk powder in 48ml GDW and 0.5ml 500mM EDTA. Add 25ml 1M Na phosphate, 25 ml 20 % SDS, 2.5mM ATA.

LB culture media

Dissolve 5g sodium chloride, 10g tryptone and 5g yeast extract to 1l of distilled water. Adjust to pH 7.5 with 10M sodium hydroxide and sterilise by autoclaving.

Lysis buffer

Add 8.765g NaCl, 6.055g Tris, make up to 1l with GDW and adjust to pH8.5.

1M magnesium chloride

Dissolve 203.3g $MgCl_2$ in 1L GDW.

3M potassium acetate

Dissolve 294.4g CH_3COOK in 500ml water, add 115ml glacial acetic acid and water up to 1L.

2M sodium acetate

pH 5.2: Dissolve 164.1g CH_3COONa in 800ml a/c water, adjust to pH 5.2 with glacial acetic acid and make up to 1L with water

5M sodium chloride

Dissolve 292.2 g NaCl in 1L GDW.

20% sodium dodecyl sulphate (SDS)

Add 200g SDS to 800ml a/c water, heat to 60˚C while stirring. Allow to cool and make up to 1L with water.

0.2% sodium hydroxide 1% SDS

Add 3ml 10M NaOH to 140ml GDW, mix and add 7.5ml 20% SDS.

20xSSC

Dissolve 1.753g NaCl, 14.2g Na_2HPO4 and 7.4g $C_{10}H_{14}H_2O_8Na_2.2H_2O$ in 700ml GDW, adjust to pH 7.7 with 10M NaOH and make up to 1L with GDW.

50 x TAE

Dissolve 242g Trizma base in 843ml water and mix in 57ml glacial acetic acid and 100ml 0.5M $C_{10}H_{14}H_2O_8Na_2.2H_2O$.

0.1 x TE

1mM Tris-HCl, pH 0.8 and 0.1mM EDTA, pH 0.8

2M Tris-HCl, pH 8.0:

dissolve 121.1g Trizma base in 450ml GDW and adjust to pH 8.0 with HCl. Make up to 500ml.

Versene

2.7mM KCl, 0.14M NaCl 1.5mM KH_2PO_4, 8mM $Na_2HPO_4.2H_2O$, 3mM EDTA, 0.1% phenol red.

2. Appendix II - Figures

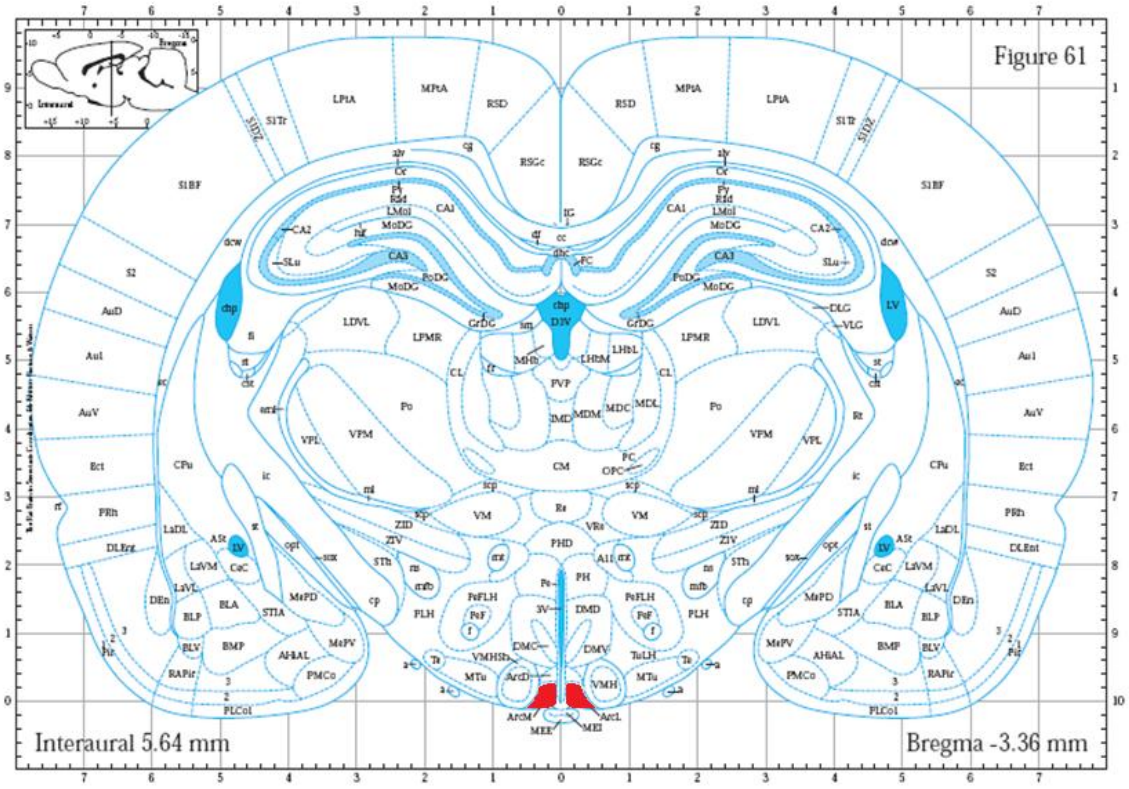


Figure 0.1 Schematic of a coronal section of the rat brain

Reproduced from "The Rat Brain in Stereotaxic Co-ordinates" (Paxinos & Watson C, 2007). The level is 3.36mm posterior to bregma, which corresponds approximately to the co-ordinates used to target the ARC in this work (-3.4 from bregma). The ARC is highlighted in red.

NUTRIENTS		Total	Supp (9)
Proximate Analysis			
Moisture (1)	%	10.00	
Crude Oil	%	2.71	
Crude Protein	%	14.38	
Crude Fibre	%	4.65	
Ash	%	6.00	
Nitrogen Free Extract	%	61.73	
Digestibility Co-Efficients (7)			
Digestible Crude Oil	%	2.47	
Digestible Crude Protein	%	12.92	
Carbohydrates, Fibre and Non Starch Polysaccharides (NSP)			
Total Dietary Fibre	%	17.05	
Pectin	%	1.52	
Hemicellulose	%	10.17	
Cellulose	%	4.32	
Lignin	%	1.68	
Starch	%	44.97	
Sugar	%	4.05	
Energy (5)			
Gross Energy	MJ/kg	14.74	
Digestible Energy (15)	MJ/kg	11.90	
Metabolisable Energy (15)	MJ/kg	10.74	
Atwater Fuel Energy (AFE)(8)	MJ/kg	13.75	
AFE from Oil	%	7.42	
AFE from Protein	%	17.49	
AFE from Carbohydrate	%	75.09	
Fatty Acids			
Saturated Fatty Acids			
C12:0 Lauric	%	0.02	
C14:0 Myristic	%	0.14	
C16:0 Palmitic	%	0.31	
C18:0 Stearic	%	0.04	
Monounsaturated Fatty Acids			
C14:1 Myristoleic	%	0.02	
C16:1 Palmitoleic	%	0.09	
C18:1 Oleic	%	0.77	
Polyunsaturated Fatty Acids			
C18:2(ω6) Linoleic	%	0.69	
C18:3(ω3) Linolenic	%	0.06	
C20:4(ω6) Arachidonic	%	0.13	
C22:5(ω3) Clupanodonic	%		
Amino Acids			
Arginine	%	0.91	
Lysine (6)	%	0.66	0.07
Methionine	%	0.22	0.04
Cystine	%	0.24	
Tryptophan	%	0.18	
Histidine	%	0.35	
Threonine	%	0.49	
Isoleucine	%	0.54	
Leucine	%	0.98	
Phenylalanine	%	0.66	
Valine	%	0.69	
Tyrosine	%	0.49	
Taurine	%		
Glycine	%	1.11	
Aspartic Acid	%	0.67	

NUTRIENTS		Total	Supp (9)
Glutamic Acid	%	3.17	
Proline	%	1.20	
Serine	%	0.56	
Hydroxyproline	%		
Hydroxylysine	%		
Alanine	%	0.16	
Macro Minerals			
Calcium	%	0.73	0.63
Total Phosphorus	%	0.52	0.04
Phytate Phosphorus	%	0.24	
Available Phosphorus	%	0.28	0.04
Sodium	%	0.25	0.19
Chloride	%	0.38	0.32
Potassium	%	0.67	
Magnesium	%	0.23	
Micro Minerals			
Iron	mg/kg	159.30	82.50
Copper	mg/kg	11.50	1.94
Manganese	mg/kg	72.44	19.22
Zinc	mg/kg	35.75	
Cobalt	µg/kg	634.10	550.00
Iodine	µg/kg	1202.69	1085.00
Selenium	µg/kg	298.99	100.00
Fluorine	mg/kg	10.49	
Vitamins			
β-Carotene (2)	mg/kg	0.16	
Retinol (2)	µg/kg	2566.38	2400.00
Vitamin A (2)	iu/kg	8554.27	8000.00
Cholecalciferol (3)	µg/kg	15.54	15.00
Vitamin D (3)	iu/kg	621.70	600.00
α-Tocopherol (4)	mg/kg	76.45	56.82
Vitamin E (4)	iu/kg	84.10	62.50
Vitamin B_1 (Thiamine)	mg/kg	8.58	1.96
Vitamin B_2 (Riboflavin)	mg/kg	4.33	2.94
Vitamin B_6 (Pyridoxine)	mg/kg	4.81	0.98
Vitamin B_{12} (Cyanocobalamine)	µg/kg	7.49	6.00
Vitamin C (Ascorbic Acid)	mg/kg	2.59	
Vitamin K (Menadione)	mg/kg	10.17	9.36
Folic Acid (Vitamin B_9)	mg/kg	0.79	
Nicotinic Acid (Vitamin PP) (6)	mg/kg	61.32	2.45
Pantothenic Acid (Vitamin $B_{3/5}$)	mg/kg	20.17	5.80
Choline (Vitamin $B_{4/7}$)	mg/kg	1080.14	366.60
Inositol	mg/kg	2369.59	
Biotin (Vitamin H) (6)	µg/kg	277.13	

Notes

1. All values are calculated using a moisture basis of 10%.
   Typical moisture levels will range between 9.5 - 11.5%.
2. a. Vitamin A includes Retinol and the Retinol equivalents of β-carotene
   b. Retinol includes the Retinol equivalents of β-Carotene.
   c. 0.48 µg Retinol = 1 µg β-carotene = 1.6 iu Vitamin A activity
   d. 1 µg Retinol = 3.33* iu Vitamin A activity
   e. 1 iu Vitamin A = 0.3 µg Retinol = 0.6 µg β-carotene
   f. The standard analysis for Vitamin A does not detect β-carotene
3. 1 µg Cholecalciferol (D_3) = 40.0 iu Vitamin D
4. 1 mg all-rac-α-tocopherol = 1.1 iu Vitamin E activity
   1 mg all-rac-α-tocopherol acetate = 1.0 iu Vitamin E activity
5. 1 MJ = 239.23 Kcalories = 239.23 Calories = 239,230 calories
6. These nutrients coming from natural raw materials such as cereals may have low availabilities due to the interactions with other compounds.
7. Based on in-vitro digestibility analysis.
8. AF Energy = Atwater Fuel Energy = (((CO%/100)*9000)+(((CP%/100)*4000)+(((NFE%/100)*4000)/239.23
9. Supplemented nutrients from manufactured and mined sources.
15. Calculated.

Table 0.1 Nutritional information for RM1 normal chow diet

Product Data

D12266B

OpenSource DIETS™

Description

Condensed milk diet. Purified match to C11024.

Used in Research

Obesity
Diabetes
Hypertension

Packaging

Product is packed in 12.5 kg box. Each box is identified with the product name, description, lot number and expiration date.

Lead Time

IN-STOCK. Ready for next day shipment.

Gamma-Irradiation

Yes. Add 10 days to delivery time.

Form

Pellet, Powder, Liquid

Shelf Life

Most diets require storage in a cool dry environment. Stored correctly they should last 3-6 months.

Control Diets

D12489B
D10001

Formula

Product #		D12266B	
		gm%	kcal%
Protein		18.5	16.8
Carbohydrate		56.7	51.4
Fat		15.6	31.8
	Total		100.0
	kcal/gm	4.41	

Ingredient	gm	kcal
Casein, 80 Mesh	190	760
DL-Methionine	3	12
Corn Starch	215	860
Maltodextrin 10	75	300
Sucrose	290	1160
Cellulose, BW200	30	0
Butter Fat	44.2	397.8
Corn Oil	118	1062
Mineral Mix S10001	40	0
Calcium Carbonate	5.5	0
Sodium Chloride	5.5	0
Potassium Citrate, 1 H2O	13.5	0
Vitamin Mix V10001	11	44
Choline Bitartrate	2	0
FD&C Yellow Dye #5	0	0
FD&C Red Dye #40	0.1	0
Total	1042.8	4595.8

RESEARCH DIETS INC.
www.ResearchDiets.com

Research Diets, Inc.
20 Jules Lane
New Brunswick, NJ 08901
Tel: 732.247.2390
Fax: 732.247.2340
info@researchdiets.com

Copyright © 2006 Research Diets, Inc. All rights reserved. D12266B

Table 0.2 Nutritional information for high energy diet (Research Diets Inc, USA)

3. Appendix III- Randomisation method and calculations

Randomisation

In all experiments, rats were randomised into groups of equal mean bodyweight as described below.

Animals were weighed on the day before surgery. Bodyweights were entered into a Microsoft Excel spread sheet and sorted from the highest to lowest. The column to the right of bodyweight data was labelled “Group”. In the group column the number “1” or “2” was inserted next to each bodyweight in the following order from lowest to highest “1,2,2,1,1,2,2,1,1,2”. Next, the data was sorted by group and the mean for both groups calculated. If there was less than a 2g difference between the mean of both groups, no further action was taken. If this was not the case, animals were randomly moved between groups until the means were within 2g.

Glucose assay

Plasma glucose concentration was determined using reagents and methods from Randox Laboratories Ltd (see 3.3.9.5). Following incubation, the A500 of the samples was measured in a spectrophotometer. The A500 of samples was compared to a standard curve to give the glucose concentration in the reaction. Prior to the assay samples were diluted by a factor of 1 in 5 in normal saline. To calculate plasma glucose concentration the concentration of glucose in the assay reaction was multiplied by five.

Example:

Cohort: Two

Group: rAAV-GKS

Rat I.D: 5

A500: 0.4627

Assay reaction glucose concentration from standard curve: 0.952mmol/l

Plasma glucose= assay reaction glucose concentration x dilution factor

Plasma glucose: 0.952mmol/l x 5 = 4.76mmol/l

Glucokinase activity assay

The glucokinase activity assay was performed as described in 2.3.5.2. Following incubation, the A340 of the samples was measured in a spectrophotometer. The A340 of samples was compared to a standard curve for glucokinase activity (units of enzymatic activity). To correct for variation in the size of samples collected the results of the GK activity assays were corrected to sample protein concentration.

Example:

Cohort: One

Group: rAAV-eGFP

Rat ID: 29

Nucleus: ARC

A340: 0.347

Sample GK activity from standard curve: 0.028units

Sample protein concentration: 0.352mg/ml

GK activity units/mg protein = sample GK activity/sample protein concentration

GK activity: 0.028units/0.352mg/ml = 0.079units/mg protein

4. Appendix IV – List of suppliers

Advanced Biotechnology Centre, Imperial College, London, UK

Animalcare Limited, Dunnington, York, UK

Applied Biosystems, Warrington, UK

ATCC, Middlesex, UK

Bayer UK Ltd, Bury St Edmunds, UK

Beckman Coulter (U.K.), Buckinghamshire, UK

Bright Instrument Company, Huntingdon, Cambridgeshire, UK

Boehringer Ingelheim, Berkshire, UK

Charles River, Bicester, UK

Clintech, Dublin, Ireland

David Kofp Instruments, Tujunga, CA, USA

Du Pont, Bristol, UK

Eli Lilly & Co.Ltd, Basingstoke, UK

Eppendorf, Hamburg, Germany

Fine Science Tools, Linton, UK

Fisher Scientific UK, Loughborough, Leicestershire, UK

GE Healthcare, Buckinghamshire, UK

Genomics Core Laboratory, Imperial College London, UK

Graphpad Prism, Graphpad Sorfware, San Diego, CA, USA

Helena biosciences, Sunderland, UK

Invitrogen Life Technologies, Paisley, UK

Kodak, Hemel Hempstead, Hertfordshire, UK

LEO Pharma, Buckinghamshire, UK

L.E West, Barking, UK

Life Sciences Technology, Eggenstein, Germany

Linco Research, Missouri, USA

Microvette, Sarstedt, Numbrecht, Germany

Millipore, Watford, Hertfordshire, UK

Millpledge Veterinary, Nottinghamshire, UK

New England Biolabs (UK) Ltd, Hitchin, Hertfordshire, UK

Novagen, Nottingham, UK

Oswell DNA Services, Southampton, UK

Parke-Davis, Pontypool, UK

Plastics-One, Roanoke, Virginia, USA

Pierce, Rockford, IL, USA

Promega, Madison, WI, USA

Randox Laboratories Ltd, County Antrim, UK

Research Diets Inc, New Brunswick, NJ, USA

Shandon Southern Products Ltd, Runcorn, UK

Sigma Ltd, Poole, Dorset, UK

Special Diet Services, Witham, Essex, UK

ThermoFisher Leicestershire, UK

Tyco Healthcare, Hampshire, UK

Vet Tech Solutions Ltd, Cheshire, UK

VWR International Ltd, Poole, UK

Wallac, Waltham, MA, USA

WPA, Cambridgeshire, UK